Exploring cell-type and single cell specific responses in plants to environmental stimuli

by

Cantug Bar

Thesis

Submitted to the University of Warwick

for the degree of

Doctor of Philosophy

Dr. Miriam Gifford

Dr. Steve Jackson

School of Life Sciences

Jan 2020

TABLE OF CONTENTS

LIST OF FIGURES

LIST OF TABLES

ACKNOWLEDGEMENTS

This thesis was made possible by influence of many individuals. During this process some had larger impact than the others and I wish to acknowledge their support and guidance in this section. These people made me grow not just as an academic but also as a person through the span of my research.

Guidance of my supervisors Dr. Miriam Gifford and Dr. Vardis Ntoukakis was invaluable through this journey. Their perspectives in research has shaped mine and given me new visions towards the future I would otherwise not possess. For that, I will be forever grateful. I would also like to thank my secondary supervisor Dr. Steve Jackson and my advisory panel members Prof. Patrick Schafer, Prof. Murray Grant and Prof. George Bassel for their advice in shaping my research through my studies.

I would like to thank Dr. Beatriz Lagunas, Dr Silke Lehmann, Dr. Ruth Schafer, Dr. Daniela Sueldo, Dr. Sophie Piquerez, Dr. Ana Domingues Ferreras, Dr. Alonso Javier Pardall Bermejo, Dr. Sarah Taubman and Ian Hands-Portman for their unending patience in my struggles with technical equipment and experimental optimization processes. Your mentorship provided the sustenance required for this work. I appreciate every minute you have taken from your work to indulge my questions.

I would like to share my appreciation with my colleagues and friends who had similar struggles in their academic endeavours yet still helped me overcome the obstacles on my path. I would like to share my deepest gratitude with Natassa Kanali, Dr. Estelle Dacheux, Dr. Mark Walsh and Dr. Eri Tsukamoto for making the four years I spent in the UK the most fantastical years so far and bringing laughter, and imagination to my life. If I stood standing at the end, know that you had a big part in it.

I would like to acknowledge Breagha Magill and Alex Sokolnik for their help in experimental procedures and producing results. Their presence made my days of chaos more manageable.

I would also like to thank my family. For all they have given so much from themselves to make me who I am today. No words exist in any language to define my gratitude to them. I will forever strive to reach the high bar they have set.

Finally, I want to thank the kingfisher who showed me the way when I was lost. Thank you all… Truly

DECLARATIONS

This thesis is written and submitted to University of Warwick in accordance with the regulations towards the completion of my degree as a Doctor of Philosophy. It has been written by me and was not submitted for previous consideration towards completion of another degree. The work in this thesis has been performed by me except otherwise stated.

ABBREVIATIONS

$^1O_2$	Singlet Oxygen
ABA	Abscisic acid
ABRC	Arabidopsis Biological Resource Centre
AFB3	*AUXIN SIGNALLING F-BOX 3*
APX	Ascorbate peroxidase
AU	Arbitrary unit
BASTA	Glufosinate
BR	Brassinosteroid
CAT	Catalase
cDNA	complementary deoxyribonucleic acid
CDPK	Calcium dependent protein kinase
cHATS	Constitutive high-affinity transporter system
ChIP	Chromatin immunoprecipitation
CK	Cytokinin
CM	Chorismate mutase
co	Cortex
COBL8	*COBRA-LIKE 9*
COI1	*CORONATINE INSENSITIVE 1*
CTR1	*CONSTITUTIVE TRIPLE RESPONSE 1*
DE	Differentially expressed
dH2O	Distilled water
DNA	Deoxyribonucleic acid
dpt	Days post transformation
DR	Downregulated
EFR	*ELONGATION FACTOR-TU RECEPTOR*
EIN2	*ETHYLENE INSENSITIVE 2*
ep	Epidermis
ES	Enzyme solution
ET	Ethylene
ETI	Effector triggered immunity
ETR1	*ETHYLENE RESPONSE 1*
ETS	Effector triggered susceptibility

EXT1	*EXTENSIN 1*
EXTPA7	*EXPANSIN A7*
FACS	Fluorescence activated cell sorting
FDA	Fluorescein diacetate
FLARE	Flagellin rapidly elicited
FLS2	*FLAGELLIN SENSING 2*
FRK1	*FLG22-INDUCED RECEPTOR-LIKE KINASE 1*
FS	Forward scatter
GB	Gibberellin
GFP	Green fluorescence protein
GID1	*GA INSENSITIVE DWARF 1A*
GMO	Genetically modified organism
GO	Gene ontology
GPI	Glycosylphosphatidylinositol
GPX	Glutathione peroxidase
GUS	B-Glucuronidase
H2O2	Hydrogen peroxide
HATS	High-affinity transporter system
HF	High relative fluorescence
HR	Hypersensitive response
HSFA1A	*HEAT SHOCK FACTOR A1A*
iHATS	Inducible high-affinity transporter system
INTACT	Isolation of nuclei in tagged in specific cell types
JA	Jasmonic acid
JAZ	*JASMONATE-JIM-DOMAIN*
JIN1/MYC2	*JASMONATE INSENSITIVE/MYC2*
LATS	Low-affinity transporter system
LB	Luria-Bertani
LF	Low relative fluorescence
LR	Lateral root
LR-FC	Lateral root founder cell
MAPK	Mitogen activated protein kinase
MAPKK	Mitogen activated protein kinase kinase

MAPKKK	Mitogen activated protein kinase kinase kinase
MFM	Modified Fahräeus media
mRNA	Messenger ribonucleic acid
MS	Murashige and Skoog
N	Nitrogen
NAC	*NAM/ATAF/CUC*
NASC	Nottingham Arabidopsis Stock Centre
NB-LRR	Nucleotide binding-leucine rich repeat
Next	External nitrogen concentration
NF	Nod factor
NHL10	*NDR/HIN1-LIKE 10*
NLS	Nuclear localization signal
NPF6.3	*NITRATE TRANSPORTER 1.1*
NPR1	*NONEXPRESSOR OF PATHOGENESIS RELATED GENE 1*
NRT1.1	*NITRATE TRANSPORTER 1.1*
NRT1.3	*NITRATE TRANSPORTER 1.3*
$O^{\bullet -}_2$	Superoxide radical
OD	Optical density
OH.	Hydroxyl radical
PAMP	Pathogen associated molecular pattern
PCD	Programmed cell death
PCR	Polymerase chain reaction
PEP	*ENDOPEPTIDASE*
PHI1	*PHOSPHATE INDUCED 1*
PI	Propidium iodide
PIF	*PHYTOCHROME INTERACTING FACTOR*
PIM	Protoplast induction media
PLC	Phospholipase C
PLT	*PLETHORA*
PP	Protoplast
PR	Pathogenesis related
PR	Primary root

pr	Pericycle
PRR	Pathogen recognition receptor
PrxR	Peroxiredoxin
Pst	*Pseudomonas. syringae* pv. tomato
PTI	PAMP triggered immunity
qPCR	Quantitative polymerase chain reaction
R genes	Resistance genes
RAP2.4A	*RELATED TO APETALA 2.4A*
RF	Relative fluorescence
RF-CoT	Relative fluorescence change over time
RH	Root hair
RLK	Receptor like kinase
RNA	Ribonucleic acid
RNAP	RNA polymerase
ROS	Reactive oxygen species
RSA	Root system architecture
RuBisCO	Ribulose-1,5-bisphosphate carboxylase/oxygenase
SA	Salicylic acid
SAR	Systemic acquired resistance
SASSC	Sendai Arabidopsis Seed Stock Centre
SLY1	*SLEEPY 1*
SOD	Superoxide dismutase
TF	Transcription factor
TGA	TGACG sequence specific binding proteins
TY	Tryptone-yeast extract
UR	Upregulated
WER	*WEREWOLF*
YFP	Yellow fluorescence protein

ABSTRACT

Organisms are in constant interaction with their environment where they respond to abiotic and biotic changes, and in turn affect their surroundings. During these interactions, they undergo molecular, physiological and developmental changes in order to adapt to the dynamic circumstances. As our understanding of organism-environment interactions has grown it was found that multicellular organisms not only have cell-type specific responses, but these responses are not uniform amongst cells of that cell type types. Studying environmental responses at a whole organism level is thus a challenge, whereby using mixed cell samples can mask the detection of specific effects. In this thesis, the aim was therefore to investigate cell-type and single-cell specific responses towards environmental stress conditions in plants.

In Chapter 3, materials for researching nitrogen responses in root tissue types of the model legume plant *Medicago truncatula* were generated. Vector constructs were assembled using promoter sequences with known epidermis, cortex or pericycle tissue-specific expression activity to drive reporter proteins. Tissue specific expression for two out of six constructs was confirmed using transient transformation, paving the way for stable transformation of *M. truncatula* to study tissue-specific expression in legume root systems. In Chapter 4, cell-specific variability in perception of the bacterial pathogen *Pseudomonas syringae* in *Arabidopsis thaliana* was investigated using an inducible reporter line. High variability in reporter protein expression was observed amongst genetically identical leaf spongy mesophyll cells. This variation was found to be highly correlated with nuclear size, which has been shown previously to be an indication of ploidy number. Transcriptomic work in this chapter led to the conclusion that cells exhibiting high reporter protein expression possessed an overall higher transcription capacity. In Chapter 5, potential methods of exploiting the cellular variability identified in Chapter 4 were investigated, with the purpose of regenerating a whole plant from a single cell exhibiting higher expression capabilities. To that end, fluorescent activated cell sorting for isolating live protoplasts was optimised, increasing the efficiency from 0.01% to 30%. Low-density protoplast regeneration trials proved challenging, but this method development paves the way for future work.

1. INTRODUCTION

1.1. ABIOTIC AND BIOTIC ENVIRONMENTAL FACTORS INFLUENCING PLANT GROWTH AND DEVELOPMENT

Ecosystems are made up of non-living (abiotic) and living (biotic) factors. Interactions of these factors with and within each other is what creates the self-sustaining ecosystem we call Earth. Plants are major contributors in our ecosystem and necessary organisms to sustain life as producers of oxygen, food, and many more plant-based products. As all organisms, plants are influenced by their environment and have to respond to the environmental cues they perceive. Efficiency and communication of this perception as well as timing and precision of the response contribute to the overall fitness of plants within that ecosystem.

Abiotic factors affecting plant life are comprised of chemical and physical properties. These factors include but are not limited to; soil nutrient content, soil texture, pH, water availability, light availability and ambient temperature. In a natural environment they are in constant flux due to phenomena such as; seasonal changes, storms, fires, volcanic eruptions and daily modulations. But these factors can also be influenced by human intervention. In agricultural practices, this presents as fertilization, irrigation, pollution and modification of the natural environment through tilling or excavation. Within such dynamic environment, successful development of an organism, depends on these abiotic factors to remain within a certain range. This is defined as the "sufficiency range" and is different for every organism and every environmental factor (Driessche, 1998). Below and above this range, an organism will have impaired development due to deficiency or toxicity effects, respectively (Figure 1.1).

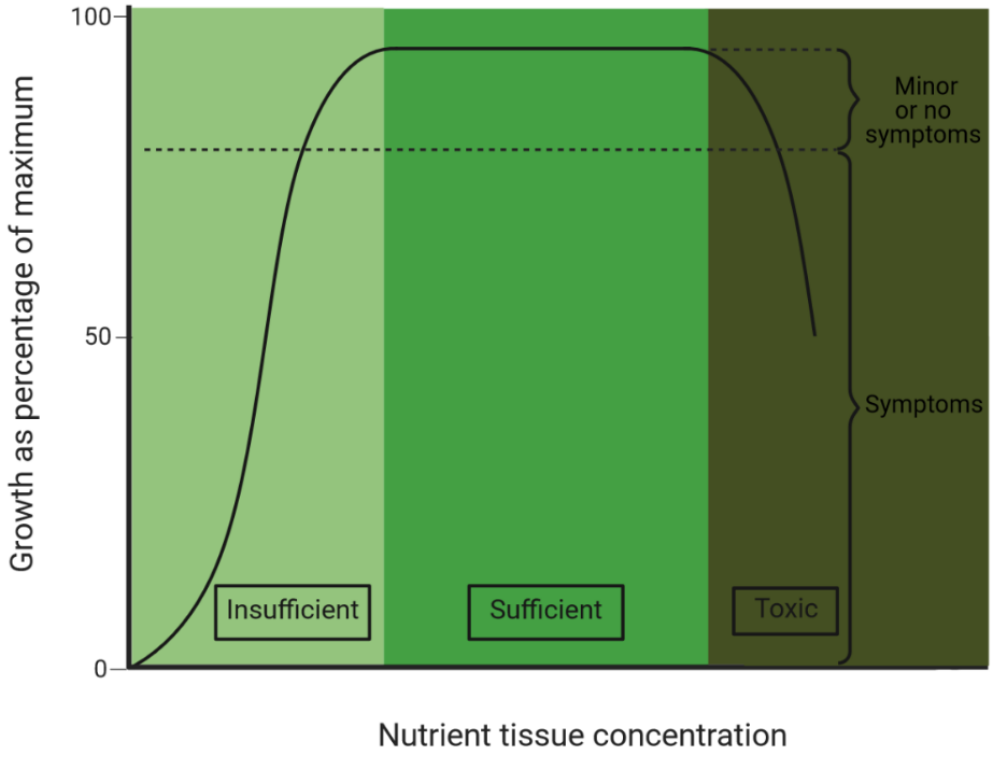

Figure 1.1. Simplified graphical representation of relationship between plant growth and health with environmental nutrient availabilty. Optimal plant growth requires environmental factors to be within a certain range. This range is called the adequate zone. Below or above this range the growth rate starts decreasing exponentially, resulting in symptoms of deficiency or toxicity. Skewness and kurtosis of the graph can change depending on the environmental factor and plant, however deficiency, adequte, and toxicity zones are present for all factors (adapted from Miller, 2014).

Biotic factors include all living organisms (bacterial, fungal, plant and animal populations etc) contained within a defined ecosystem. Just like abiotic factors, they can be influenced by naturally occurring events as well as human intervention. However, their interaction with the environment and each other is even more complex due to symbiosis and competition events occurring between these organisms. As a part of the biotic factors, plants are no exception to these events. With a focus on plant-bacteria symbiosis, nodules are a good example for the interaction between legume plants and nitrogen fixing organisms. In this mutualistic relationship, the plant gains a steady supply of nitrogen from the nitrogen fixing bacteria while the bacteria obtain a niche, carbon fixed in the leaves and other nutrients (Ledgard and Steele, 1992). Plants can also have a parasitic relationship with bacteria in the form of pathogenesis. In order to defend against invading pathogens, plants evolved over time to possess an innate immune system (Jones and Dangl, 2006).

1.2. COMMUNICATION OF STRESS PERCEPTION IN PLANTS

Upon recognition of an environmental stimulus that is disadvantageous or poses a threat, many organisms can migrate to a more advantageous location (taxis) to increase their chances of survival. Plants can adjust their growth and development direction but remain sessile. Their inability to be mobile in the face of negative or positive stimuli results in high selective pressure. It is this type of pressure that drove evolution of plants to possess extremely flexible mechanisms for rapid perception, communication and response to environmental stimuli.

One of the most crucial steps in producing a response to environmental stress is the ability to rapidly recognize and communicate the triggering stimuli before the stress becomes unmanageable. To that end, plants employ specialized receptors that are able to recognize specific types of stress and activate corresponding signalling mechanisms. Most common mechanisms for communication of stress recognition include opening of ion channels, activation of mitogen-activated protein kinase (MAPK) cascades (Latrasse et al., 2017) or cytoplasmic accumulation of signalling molecules such as reactive oxygen species (ROS) (Laloi et al., 2004) and phytohormones (Verma et al., 2016). Each stress type will trigger a unique combination of signalling pathways. In turn, this activates specific transcription factors to remodel the chromatin for regulating expression of relevant genes depending on the triggering stress type (Figure 1.2). This mechanism allows generation of highly specific responses and help enable plants allocate resources between maximising growth or ensuring survival (Abuqamar et al., 2009; Chinnusamy et al., 2004).

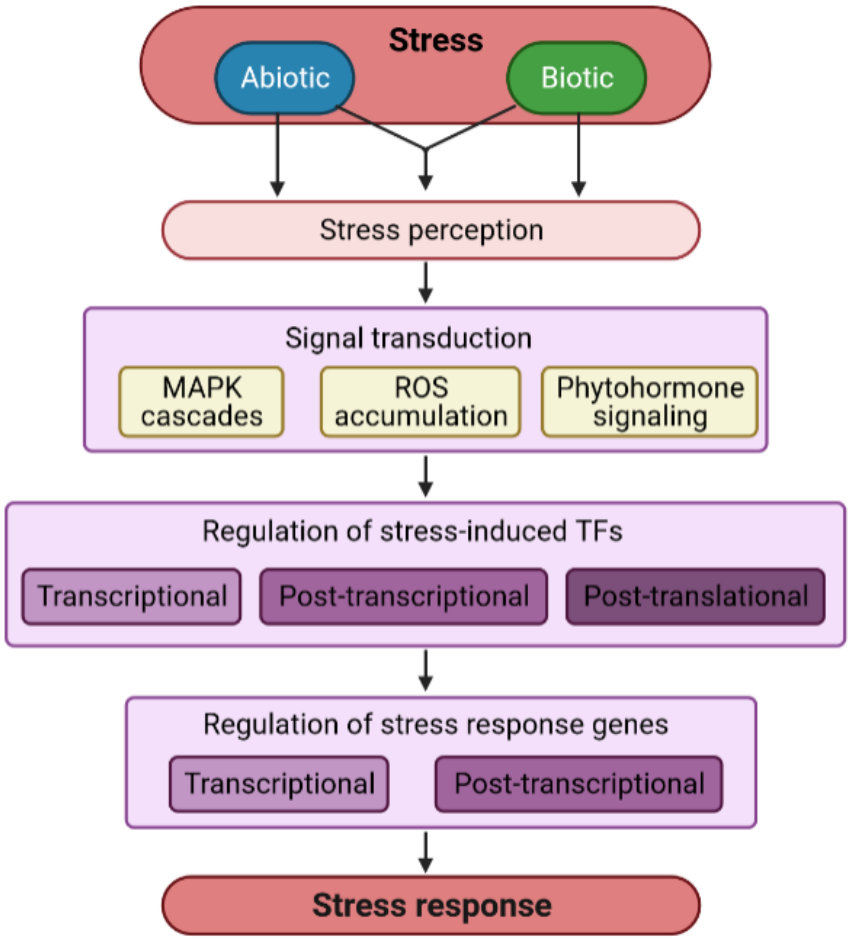

Figure 1.2. Flowchart of events triggered by environmental stimuli leading to response. Plants perceive stress through extracellular or intracellular receptors. Perception of stimuli initiates signal transduction pathways such as MAPK cascades, ROS accumulation and phytohormone production for communication of stimuli. These pathways affect proteins such as transcription factors or regulators of chromatin topology for regulation of specific relevant for producing the appropriate response to the triggering stimuli. (adapted from Atkinson, Lilley and Urwin, 2013)

MAPK signalling cascades enable rapid coordination of responses

Eukaryotes regularly rely on MAPK pathways for transduction of external signals to regulate internal response mechanisms (reviewed in Cristina, Petersen and Mundy, 2010). MAPK pathways minimally consists of three components. These are: MAPK Kinase Kinase (MAPKKK) proteins, which are serine serine/threonine kinases phosphorylating the second component of the pathway, MAPK Kinase (MAPKK). MAPKK proteins are dual-specificity kinases phosphorylating threonine and tyrosine residues on the third component of the pathway; MAPK. Finally, MAPKs are serine/threonine kinases phosphorylating a wide range of targets such as transcription factors and cyto-skeleton associated proteins (Nakagami et al., 2005).

With a need for production of highly specific responses to a wide range of environmental stimuli, high variety of MAPKKK, MAPKK and MAPKs exist. So far, 20 MAPK, 10 MAPKK and 60 MAPKKK proteins were identified so far in *A. thaliana* with most of these genes having orthologues in *M. truncatula*, *O. sativa* and *N. benthamiana* (Ichimura et al., 2002). With so many MAPK proteins available in the cytoplasm, specificity of these cascades was found to be regulated by scaffold proteins that maintain the proximity of MAPK proteins involved in particular pathways through spatio-temporal restrictions (reviewed in Morrison and Davis, 2003). One example of this is found in yeast where the protein Ste5p with no enzymatic activity was found to be required for operation of the yeast mating pheromone pathway. In this example, Ste5p was found to create a signalling module consisting of MAPKKK Ste11p, MAPKK Ste7p, MAPK Fus3p, thus restricting their spatial distribution, increasing their chances of interaction (Widmann et al., 1999). Later, *Arabidopsis* Receptor for Activated C Kinase 1 (RACK1) proteins were discovered to have scaffold functions in MAPK signalling. RACK1 was found to facilitate transduction of biotic stress signalling, triggered by *Pseudomonas aeruginosa* and *Xanthomonas campestris* pathogens in the immune response (Cheng et al., 2015). RACK1 was found to bind MAPKKK, MEKK1; MAPKK, MKK4/5 and MAPK, MAPK3/6 prior to any stimulus to form a signalling module. It was also found that RACK1 interacted with the β subunit of heterotrimeric G module to further increase specificity by restricting spatial distribution of the module to the origin of signal transduction (Cheng et al., 2015). These examples support the existence of scaffold proteins, possibly existing in many different combinations, that are specific for a triggering stimuli.

One of the most widely studied MAPK signalling pathways in plants is for recognition of pathogens. In *A. thaliana,* this pathway initiates with perception of a 22 amino acid conserved motif present on pathogen flagellin structure (flg22) by a transmembrane pathogen recognition receptor Flagellin-sensitive 2 (FLS2) (Chinchilla et al., 2007). Intracellular kinase domain of FLS2 phosphorylates the MAPKKK, MEKK1 which phosphorylates the MAPKKs MKK4 and MKK5. Activated MKK4 and MKK5 proteins phosphorylate MAPK proteins MPK3 and MPK6 however targets of these MAPKs remain unknown. Independent of their targets, it was found that this MAPK pathway results in activation of *WRKY22* and *WRKY29* genes encoding transcription factors responsible for regulation of immune responses (Asai et al., 2002).

With so many members, MAPK pathways also function in transduction of signals from abiotic stress recognition. An example cascade was discovered in *A. thaliana* in communication of cold and salinity stress, consisting of MAPKKK, MEKK1; MAPKK, MKK2 and MAPK MPK4 (Ichimura et al., 2000). In addition to their role in signal transduction, MAPK cascades can also integrate signals from different sources. MAPK proteins can regulate and themselves be regulated by reactive oxygen species (ROS), another molecule with signalling function produced within the cell (Apel and Hirt, 2004; Takahashi et al., 2011; Zhang et al., 2006). This makes MAPK cascades an important mediator of cross-talk between different stresses (Andreasson and Ellis, 2010; Rohila and Yang, 2007).

ROS signalling can modulate abiotic and biotic responses

ROS collectively refers to singlet oxygen ($^1O_2$), hydrogen peroxide (H_2O_2), superoxide radical ($O^{\bullet-}_2$) and hydroxyl radical ($OH^{\bullet}$) molecules constantly produced within a cell in low amounts as a by-product of metabolic activities (Apel and Hirt, 2004). These molecules are highly toxic to the cell itself and can damage protein, DNA and lipid structures (Gill and Tuteja, 2010). To offset their toxic effects, plants constantly produce ROS scavenging enzymes such as superoxide dismutase (SOD), ascorbate peroxidase (APX), catalase (CAT), glutathione peroxidase (GPX) and peroxiredoxin (PrxR) functioning in the removal of H_2O_2 (Mittler et al., 2004).

Plants also produce non-enzymatic molecules called antioxidants. These consist of ascorbic acid, glutathione and flavonoids which are effective in counteracting $OH^{\bullet}$ and $^1O_2$ (Gechev et al., 2006). On top of their antioxidant abilities these molecules also possess signalling properties. Ascorbic acid was found to be involved in regulating cell cycle as well as functioning as coenzyme (reviewed in Hossain et al., 2018) Glutathione was found to have an important role in generation of biotic stress responses, likely through NPR1, via SA-mediated pathway through hormonal crosstalk (Ghanta and Chattopadhyay, 2011). Flavonoids were found to be involved in many pathways including plant fertility, auxin transport (systemic as well as local) and mediation of responses to biotic interactions be it a mutualistic (Nodule formation, mycorrhizal association) or parasitic (pathogenesis) in nature (Peer and Murphy, 2006).

The delicate balance of ROS production and removal is broken upon perception of stress (Apostol et al., 1989). Upon abiotic stress perception, a burst of intracellular

ROS is generated. Following this event, ROS removal mechanisms work to re-establish the balance and reduce elevated ROS levels. In the case of biotic stress perception, an initial ROS burst similar to one produced after abiotic stress perception is produced. If the stress persists, it is followed by a stronger, secondary burst which is maintained over time and leads to events causing programmed cell death (PCD) (Grant and Loake, 2000).

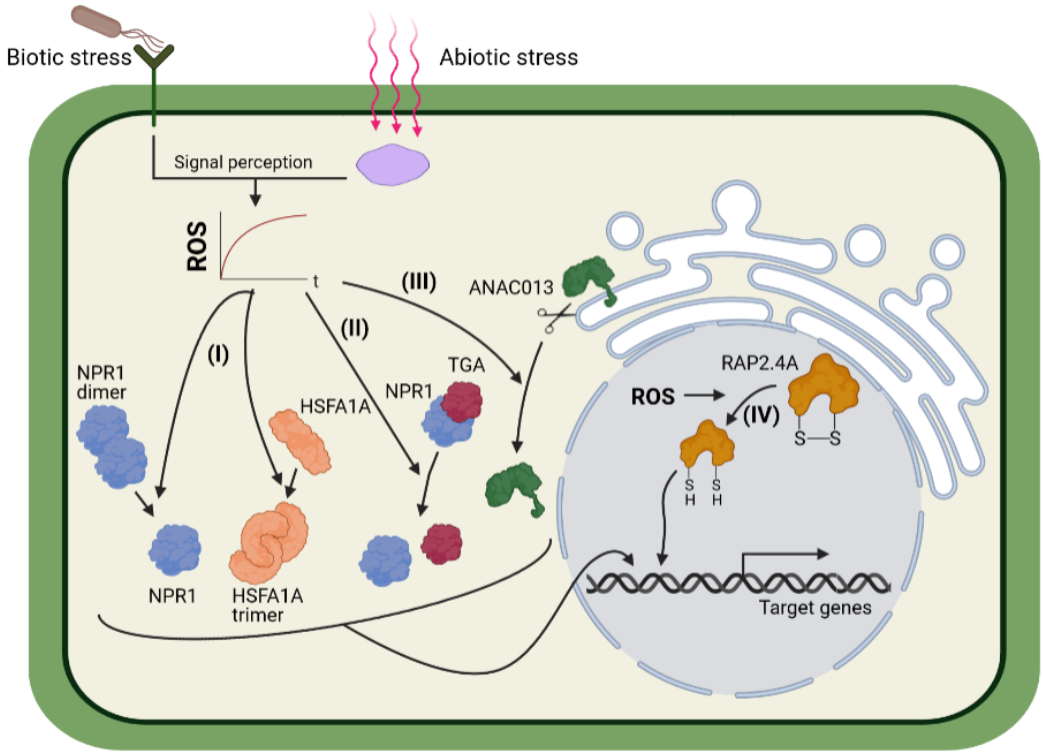

Figure 1.3. Principal effects of intracellular ROS accumulation on redox-sensing mechanisms in regulation of stress specific TF activity. ROS accumulating in the cell after stress perception can lead to **I)** conformational change in quaternary structure inducing or reversing multimer formation; **II)** association/dissociation from a partner/repressor; **III)** proteolytic processing of membrane bound proteins, allowing trans-localization; and **IV)** change in tertiary structure for regulation of DNA binding activity (adapted from He, Van Breusegem and Mhamdi, 2018).

Four different mechanisms have been identified so far for signalling function of ROS in plants. In elevated concentrations, intracellular ROS can alter tertiary or quaternary structure of proteins through modification of disulphide or covalent bonds. The resulting change in conformation can lead to state-switching (active to inactive etc.) for proteins sensitive to ROS. An example of this mechanism was observed in regulation of NONEXPRESSOR OF PATHOGENESIS-RELATED GENE 1 (NPR1).

Normally found in their inactive dimeric state held together by disulphide bonds, increased ROS production reduces these bonds and allows monomerization, leading to activation of the NPR1 (Tada et al., 2008). Another example is HEAT SHOCK FACTOR A1A (HSFA1A), activated through oxidation of its disulphide bonds that allow trimerization and translocation of active form from cytoplasm to nucleus for regulation of gene expression (Figure 1.3.I) (Liu et al., 2013).

Modification of protein conformation also affects interactions of these proteins with their targets (Figure 1.3.II). An example of altered protein-protein interactions was observed between NPR1 and its interacting TGACG sequence-specific binding protein (TGAs) TFs. In order to achieve regulation of gene expression, NPR1 forms a complex with TGAs, however upon reduction with ROS, NPR1 loses its ability to interact with an unmodified TGA (Després et al., 2003).

Changing intracellular ROS concentrations can also lead to proteolytic modification of proteins and transcription factors to alter their states (Figure 1.3.III). An example of this mechanism was observed for NAM/ATAF/CUC (NAC) TF, ANAC013. In its inactive state, this TF is a membrane bound transcription factor with a subcellular localization to ER (He et al., 2018). After treatment of cells with ROS generating agent methyl viologen, ANAC013 was found to switch to an active state through proteolytic cleavage from its anchor on the ER, and translocating to nucleus for regulation of gene expression (De Clercq et al., 2013).

Lastly, ROS can alter affinity of proteins to DNA targets (Figure 1.3.IV). This was observed in the activity of RELATED TO APETALA 2.4A (RAP2.4A) TF. In its active state, RAP2.4A has a homodimeric structure stabilized by an intermolecular disulphide bond. It was found that oxidation or reduction of this stabilizing bond strongly reduces its DNA binding affinity (Shaikhali et al., 2008).

Phytohormone signalling during plant environmental responses

Plants often recognize stresses locally (e.g. at one leaf surface or one lateral root), however in order to overcome them, responses are often required to be mounted globally (at a whole plant level). In order to achieve this, plants utilize hormones for long distance systemic signalling. This way they can regulate developmental processes as well as coordinate stress responses in multiple locations at once, or to multiple stresses at once. Studies show that phytohormones abscisic acid (ABA), salicylic acid

(SA), jasmonates (JA), ethylene (ET), cytokinins (CK), gibberellins (GB), brassinosteroids (BR) and strigolactones play significant roles in control and coordination of these responses against biotic and abiotic stress (Bari and Jones, 2009; Verma et al., 2016).

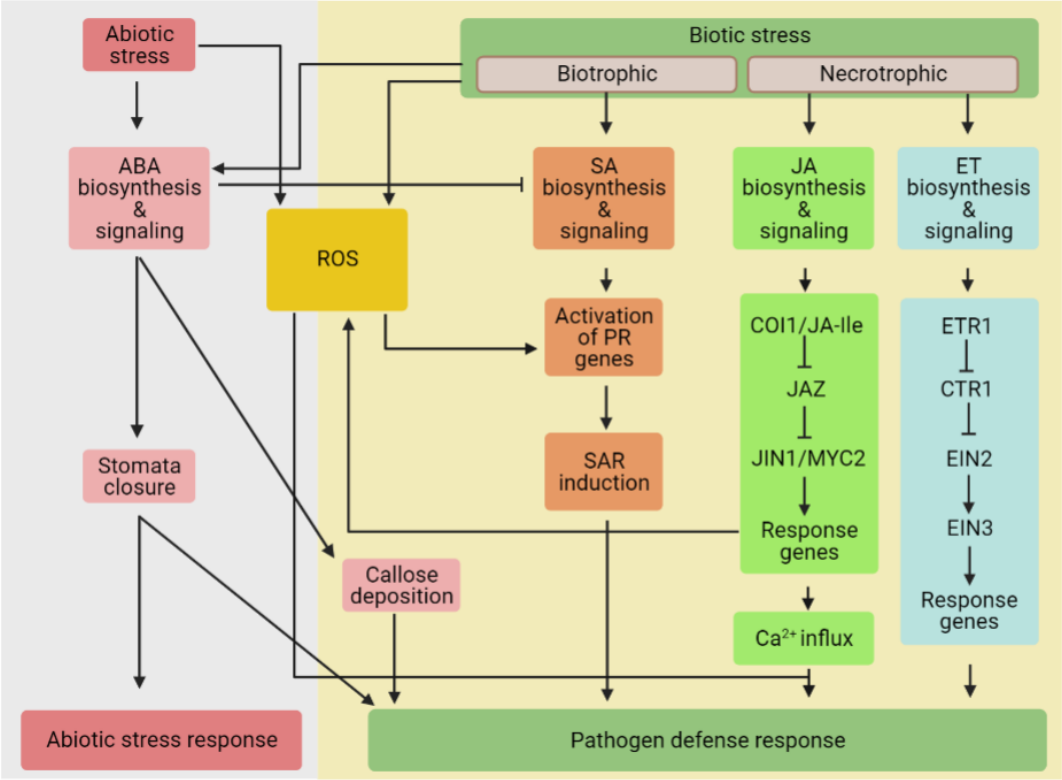

Figure 1.4. Phytohormone signalling pathways in communication of stress perception and production of stress response. Upon salt or drought stress, ABA (Red) pathway is activated which leads to stomatal closure in order to prevent excess water loss. This response also creates a physical barrier for subsequent pathogen attacks. Upon first stages of biotic stress, ABA regulates callose deposition in tissues to slow down pathogen infection further however acts antagonistically if the pathogen stress persists leading to suppression of defence response genes. SA (orange), JA (Green) and ET (Blue) pathways get activated by biotic stress perception. SA signalling pathway is triggered by presence of biotrophic pathogens and through cross talk with ROS, functions in mounting systemic acquired resistance throughout the plant. JA and ET pathways both get activated by necrotrophic pathogen and in both pathways, accumulation of phytohormones lead to repression of transcription factor repressors JAZ and CTR1 respectively that activate transcription factors required for chromatin remodelling to produce the necessary defence responses. (Arrows, positive regulation; Blocked arrows, negative regulation; adapted from Atkinson and Urwin, 2012).

Abscisic Acid (ABA) signalling responses

ABA has a role in communication of both abiotic and biotic stress perception. However, upon biotic stress perception ABA can both activate or repress defences against biotic stresses (Atkinson and Urwin, 2012). It was found that its dual nature is coordinated by the timing of the stress and the state of the host plant. For example, if a plant has previously recognized an abiotic stress such as drought or salinity, the resulting ABA accumulation causes closure of stomata (Figure 1.4-Red). While the plant gains a temporary resistance to drought, it also gains a temporary resistance to pathogen attack by physically restricting pathogen entry to plant tissues (Figure 1.4-Red) (Lee and Luan, 2012). If a plant has not recognized such triggering cues beforehand and does get infected, at early stages of the infection a wild-type ABA pathway can regulate local deposition of callose to prevent further invasion (Figure 1.4-Red) (Ton et al., 2009). However, in later stages of the pathogen infection, ABA acts antagonistically as a negative regulator of defence through modulation of genes involved in the SA pathway (Ton et al., 2009).

Salicylic Acid (SA) pathway interactions

SA production is generally associated with responses against biotrophic and hemi-biotrophic pathogens (Loake and Grant, 2007) such as the oomycete *Peronospora parasitica* or bacterial *Pseudomonas syringae,* respectively (Glazebrook, 2005). Following local perception of pathogen attack, increased biosynthesis and accumulation of SA beyond basal levels allows mounting of systemic acquired resistance (SAR), a state where the plant exhibits global broad-spectrum disease resistance against consecutive infections even from unrelated pathogens to the triggering attack (Gao et al., 2015) (Figure 1.4-Orange). In this mechanism, increased SA concentrations along with high ROS concentrations result in state-switching of NPR1 protein from its inactive oligomeric form to monomeric form and facilitates its translocation to the nucleus (Figure 1.4-Yellow & Orange). Consequently, interaction of NPR1 with TGA transcription factors within the nucleus induces SAR related and pathogenesis related (PR) gene expression to encode a number of proteins with antimicrobial properties that confer resistance to pathogens (Dong, 2004). Studies performed on *Nicotiana benthamiana* showed that once activated, SAR could persist up to 20 days post initial pathogen recognition(Ross, 1961).

Jasmonic Acid (JA) responses

JA is generally responsible for activation of defence in response to necrotrophic pathogens (Wasternack and Hause, 2013) such as fungus *Alternaria brassicicola* (Glazebrook, 2005). JA acts as an internal signalling molecule with active and inactive states. In its active state (JA-Ile) (Fonseca et al., 2009), it interacts with its intracellular receptor Coronatine Insensitive1 (COI1). This interaction leads to degradation of Jasmonate-ZIM-Domain (JAZ) (Chini et al., 2007), a repressor of Jasmonate Insensitive 1/MYC2 (JIN1/MYC2) transcription factor. Once its repressor is eliminated, the JIN1/MYC2 TF can affect chromatin remodelling and activate JA-responsive gene expression, leading to a pathogen recognition response such as a burst of internal ROS production and Ca^{2+} influx (Eulgem and Somssich, 2007) (Figure 1.4-Yellos & Green).

Ethylene (ET) signalling pathway

Similar to JA, ET plays a role in modulating responses against necrotrophic pathogens (Wasternack and Hause, 2013). ET often acts synergistically with JA in the activation of defence related genes upon necrotrophic pathogen recognition (Glazebrook, 2005; Thomma et al., 2001). In the absence of ET, the CONSTITUTIVE TRIPLE RESPONSE (CTR1) protein represses ETHYLENE INSENSITIVE 2 (EIN2), a positive regulator of ET signalling by targeting it for proteasomal degradation. When ET concentration increases in the environment and is perceived by its receptor ETHYLENE RESPONSE 1 (ETR1), the repressor CTR1 is supressed, which in turn allows EIN2 to activate EIN3 family TFs in the nucleus (Ju et al., 2012) (Figure 1.4-Blue). These TFs lead to chromatin remodelling which leads to generation of specific ethylene responses such as accumulation of cell-wall strengthening hydroxyproline rich proteins, production of secondary metabolites such as phytoalexins, and localized cell death, depending on the triggering stimuli (Binder, 2020).

Plant growth and defence trade-off

Energy is a finite and valuable resource for plants and is stored in the form of carbohydrates created through photosynthesis. Because of this, plants require tightly regulated pathways for resource allocation between organs. In optimal conditions, carbohydrate resources are used for growth. However, upon stress recognition, these

resources can be re-allocated for use in defence responses in order to ensure survival. This was illustrated in previous studies, with the use of radiolabelled carbon and nitrogen to trace the synthesis and re-allocation of ribulose-1,5-bisphosphate carboxylase/oxygenase (RuBisCO). RuBisCo functions in production of herbivory defence-related molecules nicotine and phenol amide upon biotic stress perception (Ullmann-Zeunert et al., 2013). In another study, a starch-free mutant was found to have delayed production of SA-related defence responses against a hemi-biotrophic pathogen suggesting requirement for re-allocation of stored energy to mount defence responses (Engelsdorf et al., 2013).

Research into the molecular processes underlying these phenotypes showed plant cells to have altered transcriptome and proteome profiles upon stress recognition in favour of pathways that promote defence responses while inhibiting pathways responsible for growth. This mechanism was termed the growth/defence trade-off and was found to be modulated by transcription factors activated by hormone signalling pathways (Bilgin et al., 2010). Upon recognition of biotic stress, increased intracellular levels of SA and JA were found to lead to downregulation of genes responsible for production of chlorophyll and photosystem components which leads to reduced photosynthetic capacity (SA: Sugano *et al.*, 2010; JA: Jung *et al.*, 2007). Many auxin and GA regulated genes responsible for promoting growth were also found to be downregulated upon pathogen attack as a result of this trade-off (Auxin: Kazan and Manners, 2009; GA: Yang *et al.*, 2012). Another example of this growth/defence trade-off can be seen in the antagonistic relationship between GA and JA signalling pathways (Figure 1.5). Direct interaction of DELLA and JAZ repressor proteins regulated by intracellular GA and JA concentrations, respectively were found to play a crucial role in modulation of this relationship (Hou et al., 2010). Repression of DELLA proteins by JAZ was found to relieve repression of PHYTOCHROME INTERACTING FACTOR (PIF) TFs by DELLA and result in enhanced growth (De Lucas et al., 2008). This cross-talk is suggested to be altered upon pathogen attack with evidence showing JAZ protein degradation after stress perception. This would lead to increased active intracellular DELLA repressor levels and more PIF TF repression that in turn results inhibition of growth (Yang et al., 2012).

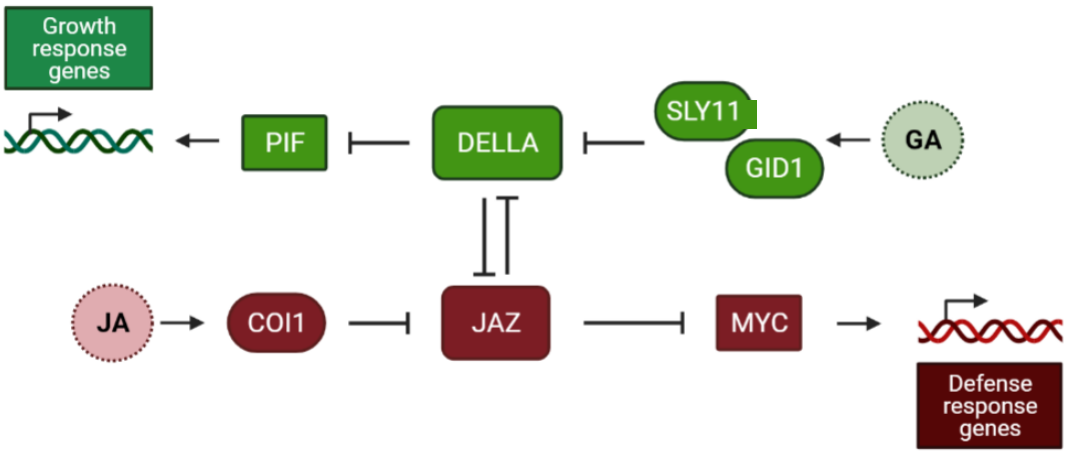

Figure 1.5. Molecular dynamics of Jasmonic acid-Gibberellic acid cross-talk within growth/defence trade-offs. A schematic representing effect of hormones on each other to direct growth or defence in suitable conditions. While GA acts in favour of growth, JA acts towards defence. At the crossroads of this mechanism is DELLA-JAZ interaction. Shapes represent key proteins functioning in hormone pathways, colours represent which hormone pathway each protein functions in. These are: GA pathway, green; JA pathway, Red. (Arrows, positive regulation; Blocked arrows, negative regulation; COI1 (CORONATINE INSENSITIVE 1); JAZ (JASMONATE JIM-DOMAIN); MYC (transcription factor); SLY1 (SLEEPY 1); GID1 (GA INSENSITIVE DWARF 1A); DELLA (repressor protein); PIF; (Huot et al., 2014).

1.3. Enabling solutions towards global food security using modulation of novel molecular mechanisms

Food production and agriculture is a continuously growing industry that is continuously adapting to try to follow the needs of a rising population. The global human population was estimated to be under 6 million before the introduction of agriculture approximately 9000 BC. By the year 1000, this number was already increased to 250 million, and by the year 2000 it stood at 6.1 billion people (Livi-Bacci, 2017). UN projections from 2017 predict the world population will reach 9.8 billion by 2050 (UN, 2017). Analysing this data, it was extrapolated that a 60-70% increase in food production must be achieved between 2005 and 2050 to sustain this exponentially growing population (Fischer, Byerlee and Edmeades, 2014; ELD, 2015). However, even with the increased rate of improvement in food production, it is not possible to sustainably match such exponential growth with conventional methods (Fuglie et al., 2012). This is because changes are not only dependent on the rate of

introduction of new practices stemming from research or availability of resources but also the current state of agricultural land, practices, and policies in place.

Agricultural yields are variable throughout the year due to unpredictable environmental factors throughout the seasons. Focusing on the abiotic factors first, in recent years, loss of arable land (Tian and Niu, 2015) and changing climate trends (Shcherbak et al., 2014) due to global warming have become two extreme examples affecting agriculture. Use of fertilizers and mechanization of agriculture has been among lead practices to increase agricultural yield. However, using these invasive methods, human intervention has rendered 33% of arable land less productive due to leaching, salinization, acidification or contamination (FAO and ITPS, 2015) (Figure 1.6).

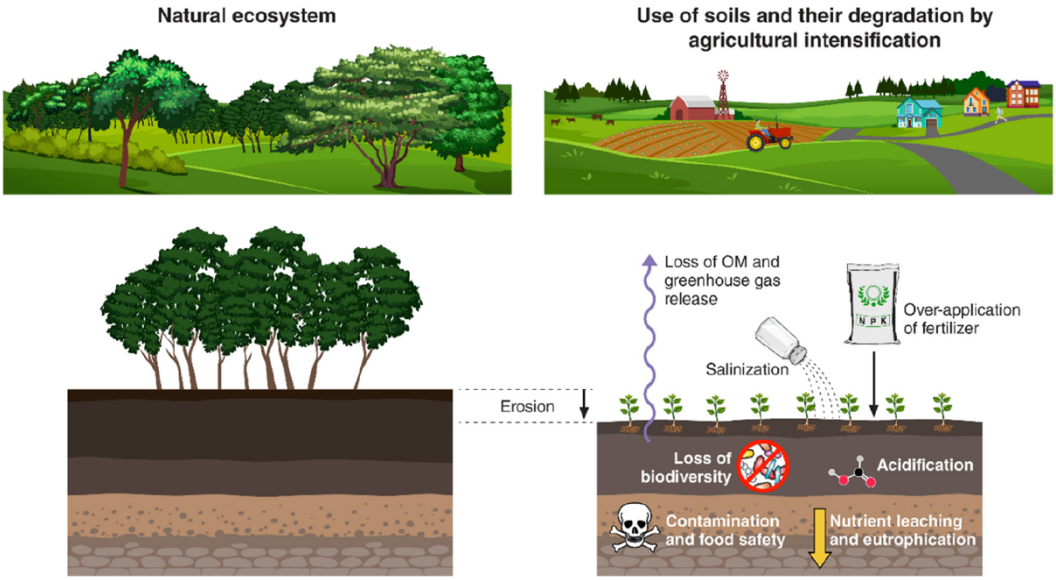

Figure 1.6. Impact of agriculture on natural soils. As a result of intensive agricultural applications such as tilling, fertilization and intense irrigation, there is erosion of fertile topsoil over time, leading to, and linked to acidification of soil and release of greenhouse gasses and leaching of nutrients respectively. All this affects overall fertility of the soil over time and leads to reduced soil biodiversity (taken from Kopittke *et al.*, 2019)

It is a fact that use of nitrogen fertilizers achieve significant crop yield increases around the globe. However, effectiveness of nitrogen fertilizers have diminished over time from 68% in 1961 to 47% in 2010 (Lassaletta et al., 2014). With such reduction, overfertilization as a result of intent to keep yields high became a major issue. This mal-practice created the main source of nitrous oxide release, a greenhouse gas with

significantly more potential contribution to global warming than CO_2 (Shcherbak et al., 2014). Consequently, nitrogen-fixing legume plants have become increasingly popular in recent years to enrich N-depleted fields since they can be grown without fertilizer dependency. This thus contributes towards development of sustainable agricultural practice and reduction of greenhouse gas emissions (Valentine et al., 2018). On top of this, it was reported that the presence of legume plants contributed to sustaining a healthy soil microbiome that improves agricultural yields (Zhou et al., 2017). For these reasons, legume-rhizobia symbiosis is becoming an increasingly popular topic in research for generating a complete understanding of the complex molecular mechanism of nodulation in development of next generation, sustainable agricultural practices. One crucial aspect of this mechanism is the effect of available soil nitrogen on nodulation and responses stemming from specific tissue types in legume roots at different soil nitrogen levels.

Biotic factors, including pests and pathogens, present an equally large challenge to agriculture (Bebber et al., 2014). Intervention of humans in the ecosystem over time has changed the way that biotic factors affect agriculture today. For thousands of years, agricultural practices adopted use of crops with high genetic diversity that were adapted to their local environments. Approximately fifty years ago, with green revolution these genetically diverse crop populations were slowly replaced by monoclonal crop populations with high yield. These crop varieties often possess reduced plasticity and thus reduced resistance to pathogen infections as a collective response. This has been seen to result in an increase in the chance that a widespread infection can emerge in agricultural practices (Crews et al., 2018). To address these problems, first response was to utilize chemicals such as pesticides in high-density agriculture. However, it was found that chemical-based pest and pathogen management had long-term detrimental effects on both environment and human health (Wilson and Tisdell, 2001). As a result, re-integration of biodiversity to agriculture received greater attention

Classical selective breeding programs were popular for transferring desired traits from related species in this endeavour however, they were very slow, with years required to make a stable product and with the unpredictability of biology they had trouble delivering the required agricultural robustness gains (Stamp and Visser, 2012). With the situation as it is, potentials of using molecular methods and biotechnological

approaches to meet the challenges for increasing both crop yield and resistance were recognized (Brookes and Barfoot, 2016). However, public concern about genetically modified organisms (GMOs) presented a great obstacle for these gains to be brought to market. Backlash against GMOs led to their prohibition in many countries, despite the great benefits they can offer.

With discovery and then application of the CRISPR/Cas9 gene editing system, biotechnological solutions have moved back into the spotlight. This approach promises fast and reliable targeted allele swapping of desired genes between varieties of the same species without losing agricultural robustness in market quality (Zaidi et al., 2018). However, still considered genetically modified by some, even transgene-free systems are not fully accepted by society as the Cartagena Protocol on Biosafety to regulate safe handling of biotechnologically modified living organisms (https://bch.cbd.int/protocol/) has not yet been ratified by countries such as Argentina, Australia, Canada and USA among others (Dalla Costa et al., 2017).

1.4. CELL TYPE SPECIFIC AND SINGLE-CELL RESEARCH IN PLANTS

Plants, like other multicellular organisms, consist of many different specialized cell types that are highly coordinated in their growth and development. Each cell type possesses a distinct pattern of chromatin structure that dictates gene expression. Because of this, the response of each cell type to a stimulus, be it abiotic or biotic, is highly specific. In context of agriculture, roots of plants consist of highly specialized cell types, each with its own distinct function, gene expression pattern as well as cellular processes. In legumes, particular cell types (cortex and pericycle) must be coordinated during regulation of nodulation. Thus, investigating cell type specific gene expression and understanding the interaction of biological processes between cell types can help pave the way for the biotechnological work in the future for improvement of nitrogen fixing plants and enhancement of sustainable agriculture.

However, cell type specific mechanisms cannot be investigated through classical approaches that typically involve profiling a whole organ or organism. Over the last 20 years, interest in uncovering tissue type specific responses spurred on development of new technologies, making use of different approaches (reviewed in Hu *et al.*, 2016). Today it is possible to measure mRNA levels in a single cell and this data can be analysed to uncover the functions of specific cell types.

One of these techniques is the isolation of nuclei tagged in specific cell types (INTACT) (Deal and Henikoff, 2011). In this method, transgenic lines are generated to express biotin in the nuclear envelope of their cell types of interest. These materials can then be subjected to necessary treatments and lysed. Subsequently, biotin tagged nuclei are isolated using streptavidin coated metal beads and magnets. Authors suggest the whole process of nuclear isolation, cDNA synthesis and chromatin immunoprecipitation (ChIP) can be completed within two days (Deal and Henikoff, 2011). While this method provides a fast and clean protocol for isolating cell nuclei, it is not a viable system for studying cytoplasmic transcriptome or cell specific responses.

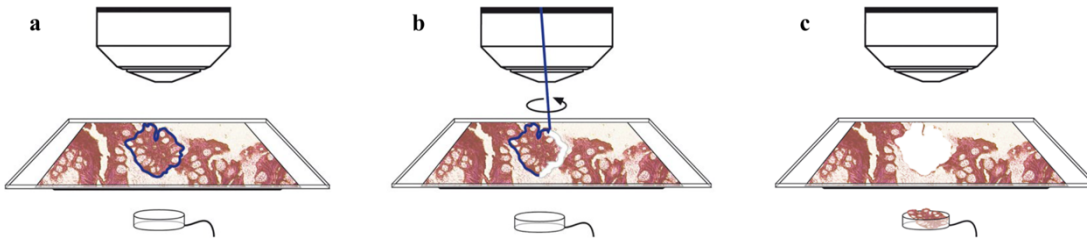

Figure 1.7. Laser microdissection of a sample. a) Tissue of interest is fixed to halt cellular activities, embedded in paraffin and thin sections are mounted on microdissection slide. Area of interest is selected using the equipment interface. **b)** A high-power UV laser traces the marked borderline to excise the tissue from the slide. **c)** Excised area is collected in a receptacle for downstream processes such as nucleic acid or protein extraction. (taken from https://www.leica-microsystems.com/solutions/life-science/laser-microdissection/)

Another technique to study tissue specific properties is laser microdissection. It is a method that allows precise excision of an area from an intact tissue sample with the use of a high-powered laser (Figure 1.7). In order to achieve this, the tissue is fixed with non-crosslinking chemicals to prevent interference with the downstream procedures (Emmert-Buck et al., 1996). However, the method tends to result in degradation of cellular contents, including mRNA transcripts due to invasive fixation and embedding procedures. While this method possesses incredible specificity, it is fairly limited to excision of cell clusters, rather than single cells or thousands of cells.

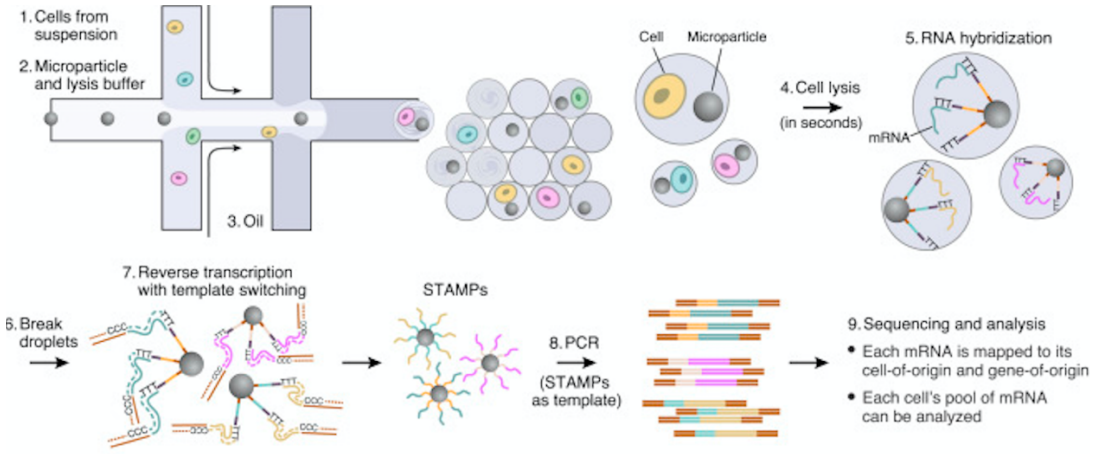

Figure 1.8. Workflow of a Drop-seq technique. 1) Cells are disaggregated and used to create a cellular suspension. **2)** Cells in suspension are fed into the microfluidic chamber to be mixed with a microparticle containing primers with unique sequence tags and lysis buffer. **3)** After mixing, a continuous flow of oil creates droplets containing a combination of either cells, microparticles, both or none. **4)** Following droplet formation, lysis buffer causes immediate cell lysis and **5)** RNA is hybridized to the primers on the microparticles. **6)** At this stage, droplets are broken and mRNA bound to drop-specific tagged primers on beads is used for **7)** reverse transcription, **8)** amplification of transcripts and **9)** sequencing (taken from Macosko *et al.*, 2015).

Drop-Seq (Single cell RNA-Seq) is another technique for studying single cell gene expression. It was made possible by recent advances in microfluidics technology for cell encapsulation and also development of cell-by-cell sequence barcoding (Macosko et al., 2015). In this method, a tissue of interest is disaggregated and loaded into a microfluidics system where each cell is encapsulated in a droplet of reaction mixture (Figure 1.8.1&2). Next, a bead conjugated with primers carrying a specific barcode is delivered to each droplet (Figure 1.8.3). Cells are then lysed within the droplets and release intracellular mRNAs that can now bind to the barcoded primers (Figure 1.8.4&5). This step is followed by reverse transcription, amplification and sequencing (Figure 1.8.6-9). The power of this protocol stems from its high-throughput nature. Thousands of cells can be sequenced in parallel, and the barcodes can be used to trace sequences to individual cells. While the technique itself is indiscriminate in sequencing of disaggregated cell populations, with specialized bioinformatic approaches applied to the sequencing data it is possible identify unique cell identities from gene expression data (Rodriguez-Villalon and Brady, 2019).

The last technique to be discussed in this subsection is fluorescence activated cell sorting (FACS). A well-established technique commonly used for cell type specific studies in both animals and plants (Figure 1.9). Its power comes from its ability to identify cell types through use of cellular morphology (Mammalian cells only) and fluorophore markers or cell type specific reporters. For fluorescence detection applications, fluorophores can be expressed in cells of interests in transgenic lines or cells can be labelled using fluorescent antibodies binding to known cell type specific marker proteins. Similar to the Drop-seq method, cells have to be disaggregated for the protocol. Once they are in a suspension, cells can be interrogated by lasers for their relative size, density and fluorescence. Cells with desired traits can be isolated and studied. Using this method, it is possible to obtain either single or thousands of cells within minutes with a high level of purity for a multitude of downstream processes (Bonner et al., 1972).

As one of the oldest techniques for enrichment of cell types from a heterogenous population of cells, FACS was initially used to study bacteria (Ito et al., 2009), yeast (Li et al., 2000) and mammalian cells (Hang and Fox, 2004) and was rapidly taken up by the plant biology field (Bargmann and Birnbaum, 2010; Herzenberg et al., 2002). Since then, FACS has been used to study tissue type specific transcriptomes (Birnbaum et al., 2003; Brady et al., 2007a; Gifford et al., 2008), metabolomes (Moussaieff et al., 2013), proteomes (Petricka et al., 2012) and chromatin structure (Frerichs et al., 2019) in model plant species such as *A. thaliana*. It was also used to study transcriptomic changes in *A. thaliana* root cell types to changing environmental salinity (Geng et al., 2013), pH, sulphur (Iyer-Pascuzzi et al., 2011) and nitrate (Gifford et al., 2008), as well as oomycete biotic stress responses (Coker et al., 2015). Thus FACS was the technique of choice in this work due to its versatility, ease of use and availability of established protocols.

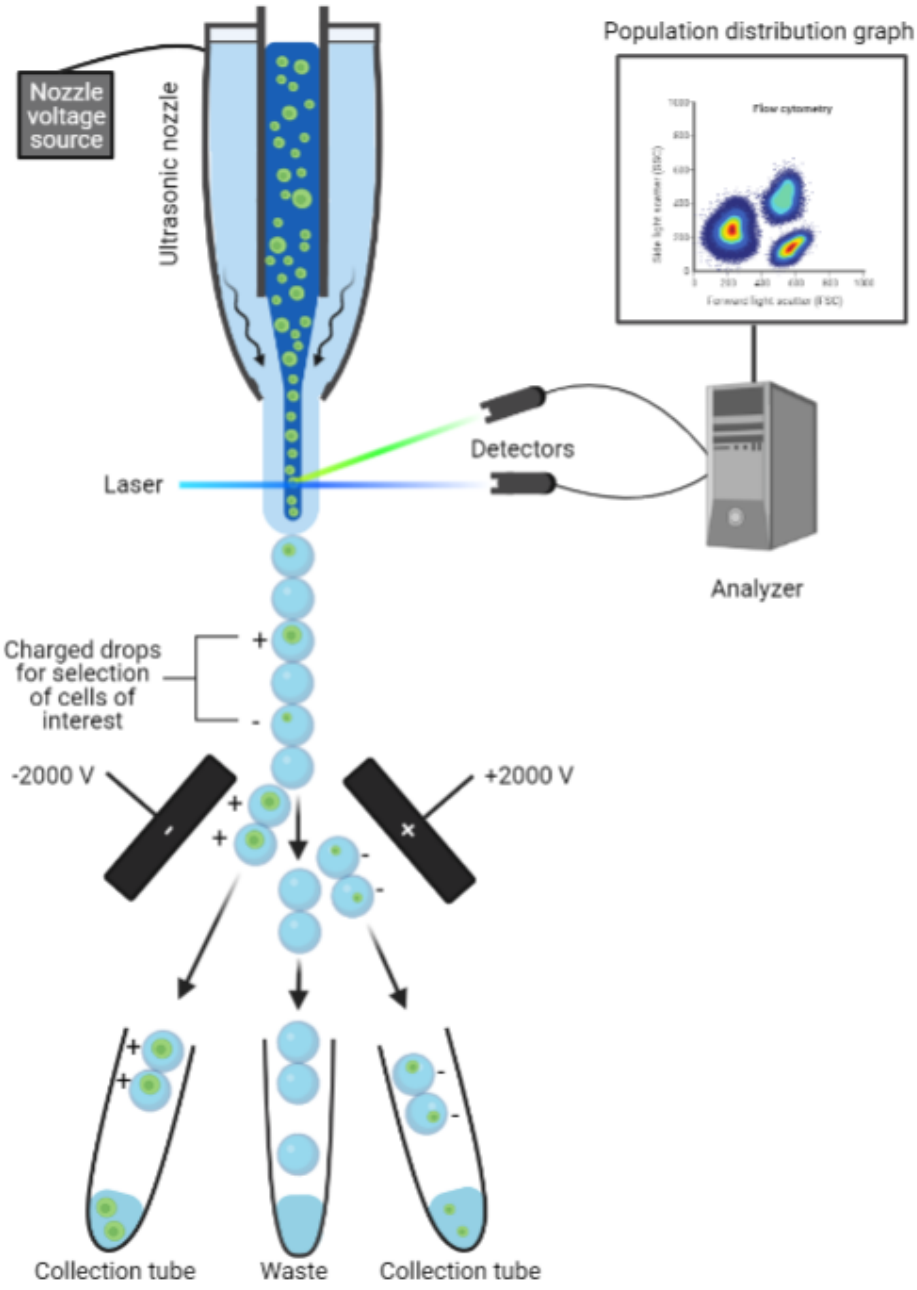

Figure 1.9. Schematic representation of FACS. Disaggregated cell suspension is fed into FACS system where cells are aligned to create single file hydrodynamic focusing. This allows a single cell to be interrogated by lasers and the reflected or refracted light to be detected as an event and plotted as a histogram in the linked software. The stream leaves the nozzle vibrating at a high frequency. These vibrations cause the continuous stream to break into droplets with ideally one cell being within each droplet. Events with preferred specifications are selected through gating on histograms in the linked software (following analysis of the data on a linked computer) and droplets containing these events are charged. Charged droplets enter an electric field and their trajectory is diverted to the collection tubes. (Adapted from: https://nanocellect.com/blog/how-does-flow-cytometry-work/)

1.5. PRINCIPLES OF FACS FOR INVESTIGATING CELLULAR PROPERTIES

FACS is a technique made possible through integration of hydrodynamics, acoustics, optics and electronics principles from physical sciences (Bonner et al., 1972). Thus, its components can be studied under these four areas.

In order to accurately profile cells, each cell has to be interrogated one by one by the lasers in the equipment. For this reason, cells have to align in a single file. In order to achieve this effect, hydrodynamic focusing principles are used. In hydrodynamics, when two fluids with different velocities are run alongside each other, they do not mix due to the difference in speed (Golden et al., 2012). The fluidics system includes three components: sample line, carrying sample fluid with cells; sheath line, carrying sheath fluid and the nozzle (Fulwyler, 1965). In the system, sample line runs within the sheath line and inject the sample fluid into a faster moving sheath fluid. This configuration results in encapsulation of sample fluid carrying the cells with sheath fluid before both shoot out of the nozzle (Figure 1.10.A). By changing the speed of each fluid, it is possible to adjust the thickness of the sample fluid encapsulated by the sheath fluid (Golden et al., 2012). For example, increasing the velocity of the sheath fluid will create a thinner sample stream in the core, forcing cells to retain a single file alignment (Figure 1.10.B). For this reason, in most studies the size of particles that can be sorted varies around one third of the nozzle size used (Golden et al., 2012).

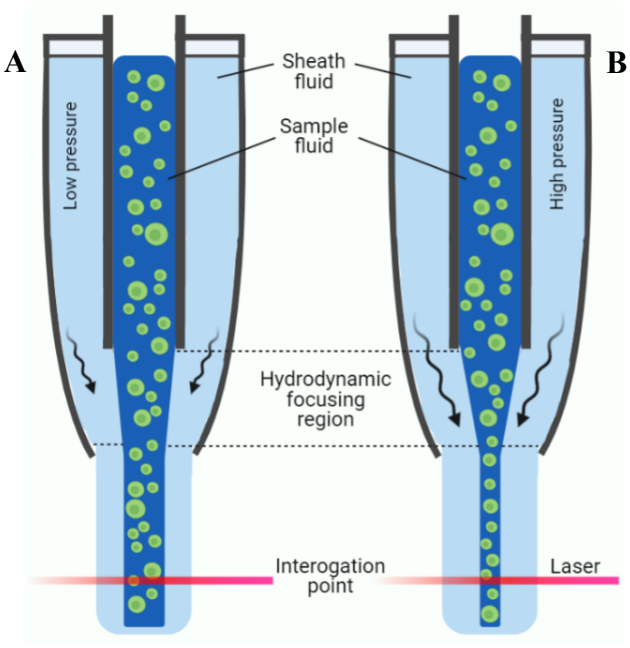

Figure 1.10. Hydrodynamic focusing at a FACS nozzle. Sheath fluid (light blue) encases the sample fluid (dark blue) to create a core stream. **A)** When sheath fluid pressure is low, the core stream is wide enough that the cells can move freely around and can block each other when interrogated by the laser. **B)** By increasing the sheath fluid pressure, thickness of the sample fluid can be adjusted to a point where the core stream is one cell thick, enabling cell-by-cell interrogation with lasers. (adapted from: https://static.bdbiosciences.com/training/itf/Module%203%20-%20Fluidics/presentation_html5.html)

Once the cells are aligned, they pass through a laser which interrogates the relative size, density and fluorescence of each one (Figure 1.11.A). Relative size of cells are interrogated by forward scatter, depending on the scattering of transmitted light (Figure 1.11.B) (Mourant et al., 2000). Relative internal complexity of a cell is interrogated by side scatter by measuring intensity of refracted light at 90° (Figure 1.11.C) (Marina et al., 2012). Fluorescence is measured by quantifying the emitted light from cells after excitation with different lasers (Bonner et al., 1972) (Figure 1.11.D). Depending on the specifications of the equipment, and availability of fluorophores up to 52 combinations can be detected with current FACS equipment (Herzenberg et al., 2002).With larger size, higher internal complexity or higher fluorophore level of an interrogated cell, detectors produce a higher voltage pulse (Marina et al., 2012). These voltage pulses are then converted into data points and can be visualised in population histograms and/or scatterplots (Figure 1.11.E, F). Using these graphs, it is possible to select a subset of the overall population by assigning 'gates' to events/cells with traits of interest (Figure 1.11.F).

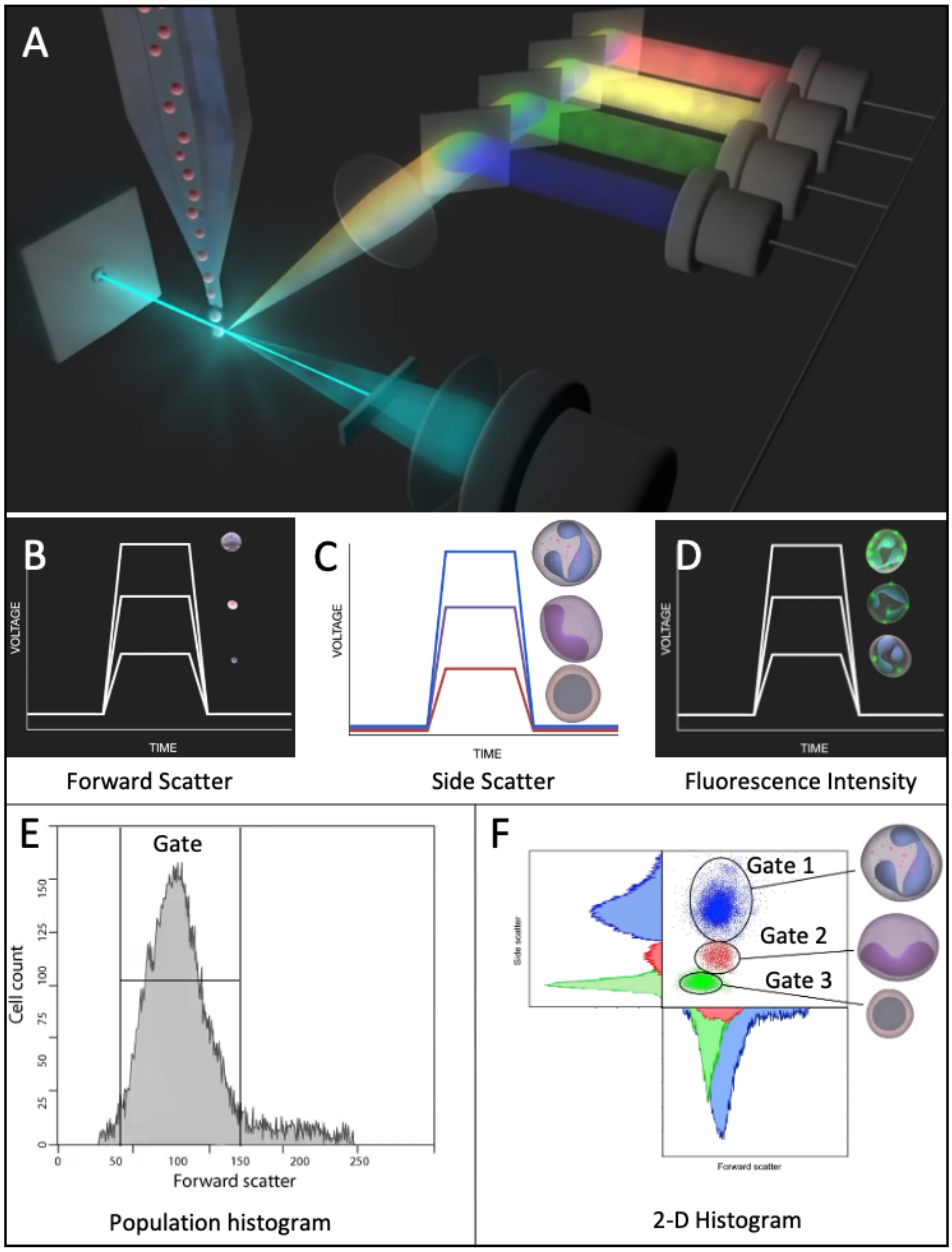

Figure 1.11. Optics and electronics of FACS. A) Schematic of optics system in a FACS. Each event/cell is interrogated by a laser with forward scatter detected by the forward detector while side scatter and fluorescence quantity are detected by the side detectors. **B-D)** Correlation between voltage production and cell size, internal complexity and fluorescence intensity. **E,F)** Conversion of voltage signals to data points and their representation as population histogram plots for visualization. These plots can be either one dimensional **E)** or multiple histograms can be combined to create a 2-D population distribution **F)** for visualization of multiple parameters at one point where the events can be gated for sorting. Gate 1 represents large cells with high internal complexity, Gate 2 represents large cells with lower internal complexity and Gate 3 represents small cells with lowest internal complexity (taken from:https://youtu.be/EQXPJ7eeesQ?list=PLZhxzzyMIQIHhQ2TOGm3HNLA04ZsTmOLW).

Following interrogation of cells, the stream is broken into droplets by high frequency vibrations ideally encapsulating 1 cell per droplet. (Figure 1.9). Since the flow speed of the fluid, and the distance to interrogation point is known, based on parameters recorded when the machine is set up, it is possible to calculate the amount of time required for a cell to reach the breaking point (Bonner et al., 1972). At the time of droplet break if a droplet contains a cell of interest selected for sorting, the stream is charged and thus after the breaking point, that droplet retains the charge. After breaking from the stream, the droplets enter a strong electric field. Trajectory of charged droplets are altered in the electric field and droplets are directed towards a collection tube (Figure 1.9) (Bonner et al., 1972). Depending on the type and quantity of charge applied to a droplet it is possible to perform 2- or 4-way sorting (2 or 4 gates) of events/cells and also sorting cell-by-cell into individual wells of a collection plate (Herzenberg et al., 2002).

1.6. Importance of investigating cell-type and single-cell responses in plants

Studying plant responses to environmental stress has been the topic of many studies over the years. However, many of these studies focused on responses at the whole plant level. With widespread adoption of cell-type isolation methodologies such as FACS in plant science, it can be seen that each cell-type possesses its own unique response to the same triggering environmental stimuli. For example, by isolating individual cell types in *A. thaliana* roots after increased nitrogen treatment, 4,931 genes out of 6,202 were found to be differentially expressed only at cell-type level (Gifford et al., 2008). Similar reports have been accumulating in the last decade (Coker et al., 2015; Frerichs et al., 2019; Geng et al., 2013; Moussaieff et al., 2013; Petricka et al., 2012) suggesting these differences to stem from epigenetic variations. Collectively, these subtle differences makeup the mechanism creating the stress response throughout the plant. Thus, study of cell-type and single-cell responses in this work contributes towards a holistic understanding of how plants respond to environmental stress and can enable exploration of if these subtle differences can be exploited for crop improvement.

In the first part of this thesis, this work focuses on studying cell-type specific responses in legume plant roots under high-soil-nitrogen stress. This system was chosen based on environmental aspects explained in Section 1.2. and because legumes belong to the Fabaceae family which is the second most important plant crop family accounting for 27% of the world crop yield (Smýkal et al., 2015). With increasing number of annotations on legume model species *M. truncatula* genome, it has become possible to perform high accuracy omics research from individual cell-types. Using these annotations, implications of such subtle changes in molecular mechanisms between cell types can be understood. This will lead to development of better agricultural practices during utilization of legumes in land regeneration and sustainable agriculture practices. To achieve his goal, in this work, transgenic *M. truncatula* lines harbouring tissue type specific promoters driving fluorescent marker proteins will be generated and tested for specificity with FACS technique.

Second part of this work focuses on investigating cell-specific responses within *A. thaliana* leaf spongy mesophyll tissue upon perception of pathogen stress. This topic was chosen as it was found that even though each cell in an organism is considered genetically identical it was observed that there are subtle differences among individuals of monoclonal populations or cells of same tissue type. While these were attributed to differences in epigenetic traits and spontaneous genetic mutations (Feinberg and Irizarry, 2010), role of cell-to-cell variation in responses to environmental cues are yet to be investigated in plants. To achieve this goal, spongy mesophyll tissue of transgenic *A. thaliana* pathogen responsive reporter lines will be interrogated with confocal microscopy for differences in reporter protein accumulation. Subsequently, cells exhibiting variation will be isolated using FACS for investigation of the differences at genetic, transcriptomic and molecular level.

Third and final part of this work focuses on investigating possible exploitation of cell-to-cell variations in plants for establishing a novel crop improvement method. This topic was pursued as it was found that variation among cells can play a role in providing better adaptation to changing environmental factors. For example, such function was demonstrated in mammalian cells in their response to *Salmonella typhimurium* infection where different subpopulations of genetically identical macrophages arose upon pathogen attack (Avraham et al., 2015). Thus, by detecting and selecting desirable variations with the help of cell sorting methods, we can

potentially select novel ‘natural’ mutations for use in crop biotechnological applications. To that end, high responsive spongy mesophyll cells towards pathogen stimulus will be isolated from transgenic *A. thaliana* pathogen responsive reporter lines using FACS. Subsequently, sorted cells will be cultivated in suspension cultures for regeneration into an adult plant.

2. MATERIALS AND METHODS

2.1. PLANT MATERIALS

All *Medicago truncatula* plants used in this study possess A17 Jemalong ecotype.

All *Arabidopsis thaliana* plants used in this work possess Col-0 ecotype background. *A. thaliana* pAtWRKY11::3xmVenus-NLS transgenic lines used for the stochasticity experiments were generated in the work of Poncini et al., 2017 (NASC: N2107974).

2.2. GROWTH CONDITIONS

Medicago truncatula

M. truncatula A17 seeds to be used for in vitro studies were scarified in 95 % sulphuric acid (5 ml/100 seeds) for 25-35 mins at room temperature with constant agitation until 2-3 dark spots appeared on the majority of them. After that, sulfuric acid was removed and seeds were washed three times with 10 ml cold dH_2O, discarding the washing liquid each time. Following scarification, seeds were surface-sterilized for 5 mins in 7 % sodium hypochlorite (NaOCl) solution (5 ml/100 seeds) and washed eight times using dH_2O. Seeds were then sown on 1.5 % dH_2O-phytoagar in 12x12 cm square plates with 2 cm spacing. For seeds to rehydrate, a drop of dH_2O was added on each seed and left for 30 mins with an open lid under a class 2 sterile laminar flow cabinet. This was repeated twice. Two growth pouches (CYGTM Germination Pouch, Mega International, Newport, MN, USA) cut to size were placed in the lids of the plates and dampened with dH_2O. Plates were then closed upside down, sealed with micropore tape and wrapped in aluminium foil to ensure darkness before stratification. Seeds were kept at 4 °C for 4 days if they had been collected more than 8 months ago or 7 days if collected < 8 months. Following stratification, seeds were moved to a 24 °C growth cabinet with 16 hr photoperiod at 100 $m^{-2}s$ light intensity. Still upside down, they were left covered with aluminium foil for 24 hrs to germinate. Germinated seeds exhibiting straight roots with over 2 cm length were used for hairy root transformation studies or transferred to sterile liquid Modified Fahräeus Media (MFM) (0.5 mM $MgSO_4*7H_2O$, 0.7 mM KH_2PO_4, 0.8 mM $Na_2HPO_4*2H_2O$, variable NH_4NO_3, 20 µM Ferric Citrate, 8 µM $MnSO_4*H_2O$, 4 µM $CuSO_4*5H_2O$, 7.34 µM $ZnSO_4*7H_2O$, 16 µM H_3BO_3, 4.13 µM Na_2MoO_4, 1mM $CaCl_2$, pH 6.50; for solid media 1.5% PhytoAgar was added before autoclaving) for downstream applications.

In order to grow *M. truncatula* A17 on soil, seeds were sown in 9x9 cm pots containing M peat mix (Sphagnum Moss peat and sand, pH 5.3-5.8, supplemented with 180 mg/L N, 90 mg/L P, 299 mg/L K), covered and stratified for 4-7 days. After stratification, seeds were transferred to a 24 °C growth room with 16 hr photoperiod at 100 m^{-2}s light intensity. One week after germination, individual seedlings were transferred to 13x13 cm plastic pots containing F2 soil (Supplier: ICL, UK; Sphagnum Moss peat and sand, pH 5.3-5.8, supplemented with 144 mg/L N, 73 mg/L P, 239 mg/L K) and grown to maturity in a growth chamber at 24 °C with a 16 hr photoperiod at 100 m^{-2}s light intensity. After the formation of first seed pods, plants were subjected to drought conditions to stimulate seed set. Dried aboveground tissue was harvested into paper bags and seed pods were separated from all debris manually. Seed pods were then stored in paper bags in a dry location.

Arabidopsis thaliana

For in vitro studies, *A. thaliana* seeds were surface sterilized by chlorine treatment. To achieve this, 300 seeds were first treated with 1 ml 0.02% Tween-20 solution for 10 seconds. Then the tween solution was discarded and replaced with 1 ml 70% Ethanol solution and incubated for 10 seconds. Finally, 70 %Ethanol solution was discarded and replaced with 1 ml 8% NaOCl solution and incubated for 5 mins with constant agitation. After incubation, the NaOCl solution was discarded and seeds were washed with 1 ml dH_2O eight times before sowing on solid half-Murashige and Skoog (MS) medium (Duchefa Biochemie), with 1% sucrose, pH 5.80 ± 0.02 and 0.5% Phytagel (Sigma). If required for selection, Glufosinate (BASTA) was added to the medium at a final concentration of 20 µg/mL after the media is autoclaved and cooled down before pouring plates.

To grow on soil, *A. thaliana* seeds were sown in 9x9 cm plastic pots containing Arabidopsis mix (~45% wt/wt F2 mixture, ~20% Silver sand, ~35% fine vermiculite, 56 g intercept) and stratified for 2 to 3 days at 4 °C in darkness. After stratification, seeds were germinated in a growth chamber with 10 h light, 22 °C, 60 % humidity for two weeks. After germination, each seedling was transferred to an individual pot with same soil composition and grown under same conditions for 4 additional weeks (to a total of 6 weeks) at which point they were used in experiments. For seed propagation, plants were transferred to a growth chamber with 22 °C and 16 hr light photoperiod. After primary shoot emergence, plants were placed in perforated plastic bags and

watered until late flowering stage. After formation of first siliques, plants were subjected to drought conditions to stimulate seed set. Dried aboveground tissue was harvested into paper bags and seeds were separated from all debris using a 425 μm gap mesh sieve.

2.3. PLANT TREATMENTS

Medicago truncatula ammonium nitrate treatment

Liquid MFM with deplete (1 mM), replete (5 mM) and excess (10 mM) ammonium nitrate (NH_4NO_3)were prepared as treatments. Each solution was used to fill a 12x12 cm square petri dish. 14-day old hairy root transformed *M. truncatula* seedlings were removed from the growth chamber immediately after dawn, so each biological repeat is at the same stage of circadian rhythm. Plates were uncovered under a class 2 sterile laminar flow cabinet and growth pouches were submerged in MFM solutions in the 12x12 petri dishes for 30 secs with gentle agitation. After 30 secs, growth pouches were transferred back onto their original solid media, covered with the plate lid and incubated at 25 °C, for 2 hrs. At the end of the incubation period, roots were harvested into Eppendorf tubes and immediately frozen in liquid nitrogen.

Infiltration of *Arabidopsis thaliana* leaves

A. thaliana plants were grown for 6 weeks as described in Section 2.2. For each experiment, two healthy plants were selected and removed from the growth cabinet immediately after dawn. The developmental age of leaves was determined by counting and leaf numbers 7-8-9 were marked (Figure 2.1). Two of the most similar stage leaves out of the three were selected. One side of the leaf was infiltrated with water (mock), while the other side was infiltrated with 100 nM flg22 peptide (treatment). Infiltrated leaves were immediately used for microscopy.

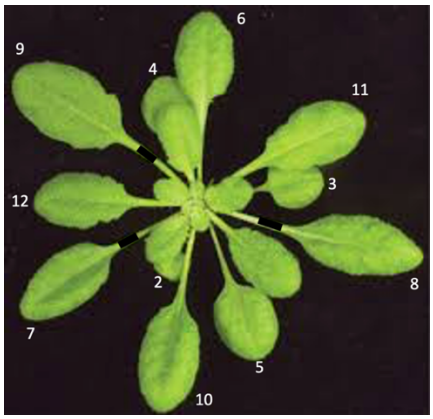

Figure 2.1. *A. thaliana* leaf numbering according to leaf developmental age. (adapted from Berens *et al.*, 2019).

2.4. MICROBIAL STRAINS

In this study, *Escherichia coli* TOP10 bacteria were used for amplification of plasmid constructs. *Agrobacterium rhizogenes* Arqua1 was used for transient transformation of fluorescence plasmid constructs in *M. truncatula* hairy roots. *Pseudomonas syringae* DC3000 and *P. syringae* DC3000-GFP-AvrRpm1 was used for pathogenesis and bacterial tracking studies.

Table 2.1. Microbiological material generated or used in this study.

Microbe Name	Plasmid	Insert	Antibiotic
E. coli TOP10	None	None	None
E. coli TOP10	pBGWFS7	pAtEXPA7 pSlyEXT1 pAtCO2 pAtPEP pMtrNRT2 pMtrN21	Spectinomycin (50 µg/ml) + Streptomycin (50 µg/ml)
A. rhizogenes Arqua1	None	None	None
A. rhizogenes Arqua1	pBGWFS7	pAtEXPA7 pSlyEXT1 pAtCO2 pAtPEP pMtrNRT2 pMtrN21	Spectinomycin (50 µg/ml) + Streptomycin (50 µg/ml)
P. syringae DC3000	None	None	Rifampicin (100 µg/ml)
P. syringae DC3000-YFP-AvrRpm1	pVSP61	AvrRpm1	Rifampicin (100 µg/ml) + Kanamycin (25 µg/ml)

2.5. MICROBIAL GROWTH CONDITIONS

All microbiological material was stored at -80°C in 20 % glycerol. To prepare these stocks, 600 µl of overnight grown bacterial culture was added to 200 µl autoclave-sterilized 80 % glycerol solution, mixed thoroughly and flash frozen in liquid nitrogen. For each bacterial study, glycerol stocks were initially streaked onto the appropriate solid media to make a master plate. These master plates were stored at 4°C and used as necessary for a week before being discarded. Both *E. coli* TOP10 and *A. rhizogenes* Arqua1 bacteria were grown in Luria-Bertani (LB) media (1 % tryptone, 0.5 % yeast extract, with 1 % NaCl for liquid, pH 5.5; and also, with 1.5 % agar for plates) (Bertani, 2004) containing the appropriate antibiotics at 37 °C and 28 °C respectively (Table

2.1). Liquid LB cultures of *E. coli* and *A. rhizogenes* were grown overnight at 37 °C and 28 °C respectively in a shaking incubator with constant agitation at 220 rpm.

P. syringae DC3000 and *P. syringae* DC3000-GFP-AvrRpm1 bacteria were grown in King's Broth (KB) media (20 g/L proteose peptone, 8.6 mM K_2HPO_4, 163 mM glycerol, pH adjusted to 7.0 with HCl before autoclaving, for liquid; with 1.5% agar, added for solid) (King et al., 1954) containing the appropriate antibiotics (Table 2.1) and incubated at 28 °C overnight in a shaking incubator with constant agitation at 220 rpm.

All work with *A. rhizogenes* Arqua1 was carried out under DEFRA plant health license. To that end, all *A. rhizogenes* Arqua1 biological material was transported with triple containment in air-tight containers. All media and inoculated biological material were labeled and autoclaved immediately. All equipment in contact with *A. rhizogenes* Arqua1 biological material along with the surfaces where the work has been performed were either autoclaved for sterilization or sterilized with 10% bleach followed by 70% ethanol.

2.6. Molecular Biology

2.6.1. DNA extraction

Genomic DNA was extracted from fresh plant material using Chelex (Bio-Rad, Cat no: 1421253) following the method of de Lamballerie *et al.*, 1992. Extracted samples were eluted in nuclease free dH2O. Quality of the extracted gDNA was assessed using a Nanodrop ND-1000 (Thermo Fisher Scientific) and stored at -20 °C.

Plasmids were extracted from *E. coli* liquid cultures using the QIAprep spin miniprep kit (Quigen, Cat no: 27014) following the manufacturer's specifications. For optimal plasmid extraction from *A. rhizogenes* the protocol was modified in accordance to the specifications defined in Weber et al., 1998. Bacteria were grown in 10 ml liquid LB instead of 5 ml. Harvested cells were lysed with 250 µl lysis buffer, inverted 10 times and 350 µl neutralization buffer was added right after. The mixture was immediately inverted until the solution turned colorless. Remaining steps of the protocol were unchanged. Finally, plasmids were eluted in nuclease free dH2O. Quality of the plasmid DNA was assessed using Nanodrop ND-1000 (Thermo Fisher Scientific) and stored at -20°C.

2.6.2. POLYMERASE CHAIN REACTION (PCR)

Amplification of promoter sequences was performed using Q5 high fidelity DNA polymerase (NEB, Cat no: M0491). Primer specifications and PCR conditions used for amplification of regions are given in Table 2.2 and Table 2.3 and Table 2.4 respectively. All primers were synthesised by Integrated DNA Technologies (IDT; Leuven, Belgium). Lyophilized primers were resuspended with dH_2O to 100 µM and stored at -20 °C as stocks. Fresh aliquots were taken from these stocks before experiments and diluted to10 µM to set up PCRs. These aliquots were kept at -20 °C up to a month.

Table 2.2. PCR primer specifications. Underlined sequences represent overhangs required for successful gateway transformation.

Primer Name	Sequence	Tm (°C)	GC %	Product Size
prAtEXPA7-F	**CACC**ACCCTGACATTCTCTCCCAA	65	50	630
prAtEXPA-R	AGAGGGGATTTTCAACGACAG	64	48	
prSlyEXT1-F	**CACC**GCAGAAGTTTTAAGCTCTAAG	58	38	1132
prSlyEXT1-R	AGAAGAATTGGATTCTAAGGC	59	38	
prAtPEP-F	**CACC**AACTGGTTGACAATGTGGGC	66	50	1261
prAtPEP-R	TCGAGTGTGATGTGGCCTTT	67	50	
prAtCO2-F	**CACC**GGGCCTAATCGCTCAAAACA	65	50	520
prAtCO2-R	ATGTGACCCGTGACTCTTGT	66	50	
prMtrNRT2-F	**CACC**GTTTTCCGATGGCACTATTTGT	63	41	902
prMtrNRT2-R	TGTTATGTGGCCCAAAATGC	64	45	
prMtrN21-F	**CACC**CCCCAATTACAACTCCGTAGA	64	48	1029
prMtrN21-R	TGCCACAAGAATGAAATAGCAC	63	41	

Table 2.3. Components used for 25 µl PCR with Q5 high fidelity DNA polymerase

Component	Stock Concentration	Volume used (µl)
Q5 Reaction Buffer	5X	5
dNTP	10 mM	0.5
Forward primer	10 µM	1.25
Reverse primer	10 µM	1.25
Template DNA		variable
Q5 High-Fidelity DNA Polymerase		0.25
Nuclease-free water		to 25

Table 2.4. PCR thermal cycle specifications

Step Name	Temperature	Duration	# of Cycles
Initial Denaturation	95 °C	1 min	1
Denaturation	95 °C	10 sec	
Annealing	See **Table 2.2**	20 sec	25
Extension	72 °C	1 min	
Final extension	72 °C	2 min	1

PCR products were run on 1 % agarose gel in TAE buffer (1 mM EDTA disodium salt, 40 mM tris, 20 mM acetic acid/glacial) using NEB 1 kb DNA ladder (NEB, Cat no: N3232L) as size marker. Amplified products with the correct length were extracted from the gel using Monarch Gel extraction kit (NEB, Cat no: T1020S) according to the manufacturer's specifications, eluted in nuclease free dH2O and stored at -20 °C.

2.6.3. RNA EXTRACTION

Plant tissue from *A. thaliana* leaves or *M. truncatula* roots was stored in an Eppendorf tube and frozen in liquid nitrogen upon harvest. The Monarch Total RNA Miniprep Kit (NEB, Cat no: T2010S) was used for obtaining total RNA from plant tissue following the manufacturer's specifications.

Protoplasts to be used for RNA extraction were frozen in liquid nitrogen immediately after sorting and kept at -80 °C until processing. The Monarch Total RNA Miniprep Kit (NEB, Cat no: T2010S) was used for obtaining total RNA from the protoplasts,

with minor modifications to manufacturer's specifications. In this procedure, steps required for sample disruption and homogenization were skipped since this was not required for protoplasts and the procedure was followed as instructed from RNA binding and elution section.

2.6.4. cDNA SYNTHESIS AND QUANTITATIVE PCR(qPCR)

cDNA synthesis was performed with 100 ng of RNA using the SuperScript™ II Reverse Transcriptase (Thermo Fisher Scientific, Cat no: 18064), following manufacturer's specifications, using a primer for polyA tails (TTTTTTTTTTTTTTTTTTTAGCN); an additional 10 µl nuclease free dH_2O was added to a final volume of 30 µl and cDNA was stored at -20 °C.

qPCR was performed with SYBR® Green JumpStart™ Taq ReadyMix™ (Sigma, S4438). Minor modifications were made to the protocol in master mix compositions (Table 2.4). For 96 well setup, 61 µl aliquots were made into tubes and 5 µl of sample cDNA was added before distributing 20µl in each well of the reaction plate. For 384-well setup, 36.9 µl aliquots were made into tubes and 3.1 µl sample cDNA was added before 9 µl was distributed in the reaction plate. Primer pairs, components, and conditions used for the reactions are given in Table 2.5, Table 2.6, Table 2.7 and Table 2.8 respectively. Each cDNA sample was run three times as technical replicates and experiments were performed for three biological replicate samples. A 384-well plate CFX384 Touch™ Real-Time PCR Detection System (Bio-Rad Laboratories), and a 96-well plate Mx3005P qPCR System (Agilent Technologies) were used for thermal cycling and fluorescence detection.

Table 2.5. Master mix compositions per triplicate in 96 and 384-well qPCR setup.

	V for 96-well setup (µl)	V for 384-well setup (µl)
Primer F	2.96	1.8
Primer R	2.96	1.8
dH2O	22.66	13.3
SYBR Green	33.0	20

For samples whose amplification level passed a threshold of fluorescence intensity (Ct), cycle crossing points were extracted from the software (Bio-Rad CFX manager software; Agilent MxPro qPCR) and imported to Microsoft Excel. Data was analysed using the ΔΔCT method defined by Livak and Schmittgen, 2001. *TIP41* and *β-Tubulin* genes were used as reference genes for *A. thaliana* and *M. truncatula* respectively due to their highly consistent expression levels at the studied conditions (Unpublished data, Gifford lab, University of Warwick).

Table 2.6. Primers used for *M. truncatula* qPCR.

Primer Name	Sequence	Tm (°C)	GC %	Product Size
q-NRT2.1-F	TTCGGAATGCGAGGAAGAATA	61.91	43	138
q-NRT2.1-R	TGCTTGTGCTCCAACTGAGAA	62.09	48	
q-NIA1-F	TGGAACCAAGGAGATTGCTGT	61.96	48	144
q-NIA1-R	ATTTCTCCTTTGTGGGGCCTA	62.01	48	
q-NIR-F	AGACATGTGGCTGTGAGCAAA	61.85	48	108
q-NIR-R	CCTAGCCATGCATCCCATAAA	62.03	48	
qβ-Tub-F	TTTGCTCCTCTTACATCCCGTG	60.35	50	101
qβ-Tub-R	GCAGCACACATCATGTTTTTGG	59.52	46	

Table 2.7. Primers used for *A. thaliana* qPCR.

Primer Name	Sequence	Tm (°C)	GC %	Product Size
q-WRKY11-F	GGCAGCGTCTCCAATGGAAAA	61.49	52	231
q-WRKY11-R	TGCACTTATCGCCGGTACTCT	61.29	52	
q-PHI1-F	TTGGTTTAGACGGGATGGTG	57.52	50	130
q-PHI1-R	ACTCCAGTACAAGCCGATCC	59.18	55	
q-FRK1-F	ATCTTCGCTTGGAGCTTCTC	57.00	50	108
q-FRK1-R	TGCAGCGCAAGGACTAGAG	60.00	58	
q-NHL10-F	TTCCTGTCCGTAACCCAAAC	59.75	55	72
q-NHL10-R	CCCTCGTAGTAGGCATGAGC	56.16	50	
q-TIP41-F	GAACTGGCTGACAATGGAGTGT	60.81	50	161
q-TIP41-R	GTTGGTGCCTCATCTTCGCC	61.65	60	

Table 2.8. Components used for qPCR with SYBR® green Jumpstart™ Polymerase.

Component	Volume per triplicate (µl)	
	66 µl (96-well)	**30 µl (384-well)**
2 x JumpStart Taq ReadyMix ™	33	15
10 µM Forward Primer	2.96	1.35
10 µM Reverse Primer	2.96	1.35
100µg/µl Template DNA	5	2.3
dH_2O	22.66	10

Table 2.9. Thermal cycling conditions used in qPCR with SYBR® green Jumpstart™ Polymerase.

Step	Temperature	Time	Cycles
Initial Denaturation	94 °C	2 min	1
Denaturation	94 °C	15 sec	40
Annealing, elongation & fluorescence reading	*60/62 °C	60 sec	
Dissociation curve	40 – 98 °C	10 sec / 0.5 °C	1

2.6.5. GATEWAY CLONING AND BACTERIAL TRANSFORMATION

pENTR/D-TOPO ligation

PCR-amplified and gel purified fragments extracted from agarose gel were cloned into the entry vector using pENTR™/D-TOPO™ Cloning Kit (Thermo Fisher Scientific, Cat No: K240020) using the manufacturer's specifications.

***E.coli* TOP10 electro-transformation**

E. coli TOP10 electro-competent cells were prepared with the following method. A single bacterial colony from a master plate was inoculated in 10 ml liquid LB media. A culture was grown overnight and sub-cultured the next day into 50 ml liquid LB media without antibiotics. In order to quantify bacterial concentration, optical density

measurements of the bacterial culture were taken with a spectrophotometer at the 600 nm wavelength light every hour. The culture was grown until OD_{600}=0.5 and immediately transferred onto ice. The bacterial suspension was centrifuged at 2000g, 4 °C for 5 mins and the supernatant discarded. The pellet was resuspended in 15 ml ice-cold TB1 buffer (30 mM CH_3COOK, 50 mM $MnCl_2.4H_2O$, 100 mM $RbCl_2$, 10 mM $CaCl_2.2H_2O$, 15 % Glycerol v/v, pH 5.8; filter sterilized and stored at -20 °C), and centrifuged again at 2000 g, 4 °C for 5 mins. The supernatant discarded again, and pellet was resuspended in 2 ml TB2 buffer (10 mM MOPS, 10 mM $RbCl_2$, 75 mM $CaCl_2.2H_2O$, 15 % Glycerol, pH 5.8; filter sterilized and stored at -20 °C). The final suspension was split into 50 µl aliquots, flash frozen in liquid nitrogen and stored at -80 °C.

For transformation, 10-50 ng (in a maximum of 2 µl) plasmid were added to 50 µl *E. coli* TOP10 electro-competent cells thawed on ice, incubated for 5 mins and transferred to a pre-chilled electroporation cuvette (Scientific Laboratory Supplies Ltd., Cat no: FBR-201) with 1 mm gap. Transformation was performed on the *Escherichia coli* (Ec1) setting (1.8 kV, 1 pulse) of Bio-Rad MicroPulser electroporator and 500 µl LB media with no antibiotics was added to cells immediately afterwards. The suspension was homogenized by gentle pipetting, transferred to an Eppendorf tube then incubated at 37 °C for 2 hrs, shaken at 220 rpm. The suspension was spread onto an LB plate with appropriate antibiotic selection (Table 2.1) and incubated at 37 °C overnight. Eight colonies were selected for colony PCR using primers in Table 2.2. Colonies containing an insert were inoculated in liquid LB media with antibiotics and grown overnight 37 °C, then used for plasmid extraction.

LR recombination reaction

Plasmid DNA extracted from positive colonies were used for LR recombination with Gateway™ LR Clonase™ II Enzyme Mix (11791, Invitrogen™, Thermo Fisher Scientific) into destination vector pBGWFS7 (Karimi et al., 2002) according to manufacturer's specifications. After recombination, products were immediately transformed into *E.coli* TOP10 bacteria as described above. Extracted plasmids were subjected to Sanger sequencing (LIGHTRUN, GATC Biotech) with primers designed to the flanking region of the insertion site on pBGWFS7 plasmid to obtain complete sequence of insert (seqPrimer pBGWFS7-F: TGCAAGCTCTCCCATATG, seqPrimer pBGWFS7-R: CTGAACTTGTGGCCGTTTA).

A. rhizogenes Arqua1 electro-transformation

Plasmids containing an insert with the correct orientation and no mutations were transformed into *A. rhizogenes* Arqua1. For this, *A. rhizogenes* Arqua1 electro-competent cells prepared with the following method. A single colony of bacteria from an LB-agar master plate was inoculated in 10 ml liquid TY media (1.6% wt/vol tryptone, 1% wt/vol yeast extract, 0.5% wt/vol NaCl) with antibiotics. The culture was grown overnight, and 2 ml were sub-cultured the next day into 200 ml liquid TY media without antibiotics. The culture was grown until OD_{600}=0.5 and immediately transferred onto ice. The bacterial suspension was split into 50 ml aliquots, centrifuged at 4000 g, 4 °C for 15 mins and supernatant discarded. The pellet was resuspended in 50 ml ice-cold dH_2O and centrifuged at 4000 g, 4 °C for 15 mins. The same resuspension and centrifugation steps were sequentially repeated using 25 ml, 1 ml and 0.5 ml ice-cold dH_2O. The final 0.5 ml bacterial suspension was split into 50 µl aliquots, flash frozen in liquid nitrogen and stored at -80 °C.

For electro-transformation, *A. rhizogenes* Arqua1 a vial of electro-competent cells was thawed on ice and 600 ng plasmid (in a maximum of 2 µl solution) was added. The suspension was incubated on ice for 5 mins and transferred into a pre-chilled electro-transformation cuvette with 1 mm gap (Scientific Laboratory Supplies Ltd., Cat no: FBR-201). Cells were electroshocked using the *Agrobacterium tumefaciens* (Agr) setting (2.2 kV, 1 pulse) on Bio-Rad MicroPulser electroporator and 1 ml cold TY media without antibiotics was immediately added into the cuvette. The suspension was incubated at 28 °C, for 3 hrs, at 220 rpm, then spread on an LB-agar plate with antibiotic selection and incubated overnight. Eight colonies were selected for colony PCR using primers in Table 2.2. Colonies containing the insert were used to make bacterial stocks as described in Section 2.4.

2.6.6. *A. RHIZOGENES* MEDIATED HAIRY ROOT TRANSFORMATION OF *M. TRUNCATULA*

M. truncatula A17 hairy root transformation was performed following the protocol described in (Chabaud et al., 2006) with following minor modifications. Seedlings inoculated with transformed *A. rhizogenes* Arqua1 were placed inside a growth pouch soaked with MFM containing 1mM NH_4NO_3. No selective chemicals were used in the growth media post transformation. Seedlings were grown for two days in at 22 °C growth cabinets with 12 hr light cycle before being transferred to 25 °C growth

cabinets with 12 hr light cycle. They were then grown for the appropriate time before being used in experiments.

2.6.7. PROTOPLAST GENERATION

Medicago truncatula

Protoplast isolation from *M. truncatula* roots was performed using the method described in Jia, Zhu and Xie, 2018 with the following minor modifications. Root tissue was harvested onto an acetate paper containing 1 ml of digestion solution made with 0.5 M Mannitol as osmoticum (10 mM MES pH 5.7, 1.5% (wt/vol) Cellulase R-10 (Duchefa), 2% (wt/vol) Maceroenzyme R-10 (Duchefa), 0.5 M D-Mannitol, 10 mM $CaCl_2$, 5% Viscozyme (Thermo-fischer), 1% Bovine serum albumin). Roots were chopped with a razor-blade until <1 mm and transferred into a 70 µm cell strainer (Fisher Scientific, Cat No: 11597522) which was then transformed into a small petri dish containing 2.5 ml digestion solution. The suspension was incubated at room temperature for 1 hr with 100 rpm agitation in darkness. After incubation, the cell strainer was washed with W5 (10 mM MES, 154 mM NaCl, 125 mM $CaCl_2$, 5 mM KCl and pH 5.7) solution and the cell suspension was transferred to a round bottom polypropylene tube. Cell suspension was centrifuged at 100 g and resuspended with W5 solution twice before finally resuspend in WI solution prepared with 0.5 M Mannitol (4 mM MES, 0.5 M D-Mannitol, 20 mM KCl, pH 5.7). Final protoplast concentration was determined using a hemacytometer and adjusted to $1x10^4$ protoplasts/ml with WI solution before proceeding with FACS.

Arabidopsis thaliana

For protoplast preparation of Arabidopsis leaves, the tape-sandwich method by Wu *et al.*, 2009 was employed. Plants were grown as described in Section 2.1 and leaf numbers 7-8-9 were marked for use. Plants were watered before dawn to open stomata and harvested right after dawn for synchronization of circadian rhythms between biological repeats. Leaves were cut from the base of the leaf blade and stuck on a 2 cm wide green tape (STARLABS, Mat No:E9055-1912) with adaxial side towards the tape. Then, the abaxial side of the leaf was covered with Magic Tape (M3, Cat no: 810) and tapes were ripped open to remove the abaxial epidermal layer. Distal and proximal sides of the leaf were then trimmed off along with excess green tape and the exposed leaf tissue was submerged into the enzyme solution (ES) (20 mM MES pH

5.7, 0.6 M mannitol, 20 mM KCl, 10 mM $CaCl_2$, 0.1 % BSA, 1.5 % cellulase R10, 0.4 % Maceroenzyme R10). A maximum of 8 leaves per 3 ml of ES were used per digestion reaction. The leaves were incubated at room temperature for 1 hr without agitation and in darkness. Following incubation, Tapes with leaf tissue were washed off using 1 ml micropipette tips with enlarged nozzles by cutting to gently release the protoplasts into the media. Protoplast suspension was then transferred to a round bottom polystyrene culture tube (STARLABS, Mat No: I1485-2810). An equal volume of W5 solution (2 mM MES pH 5.7, 154 mM NaCl, 125 mM $CaCl_2$, 5 mM KCl) was added. The protoplast suspension was centrifuged at 100 g for 3 mins and the supernatant removed. The wash step was repeated with an equal volume of W5 and supernatant removed. A half volume of MMG solution (4 mM MES pH 5.7, 0.6 M Mannitol, 15 mM $MgCl_2$) was added. Intact protoplasts were counted on a Fuchs-Rosenthal hemacytometer. Protoplasts were centrifuged at 100 g for 3 mins and Protoplast Induction Media (PIM) (Table 2.9.) was added to obtain a concentration of $2x10^5$ protoplasts/ml and used for FACS.

2.6.8. FLUORESCENCE ACTIVATED CELL SORTING (FACS)

Medicago truncatula

Protoplasts resuspended in WI solution were filtered through a 40 μm mesh (Fisher Scientific, Cat no: 11587522) and 1ml of protoplast suspension was added to a 5 ml polypropylene sorting tube (FALCON, Cat No: 352063). Protoplasts obtained from non-transformed *M. truncatula* Jemalong A17 leaves were used as a non-fluorescence reference to distinguish GFP positive population. Gates were set to capture protoplasts exhibiting high green (B488-530/30-A) and red (B488-695/40-A) fluorescence levels, with these populations absent in the non-transformed plant protoplast samples. Gated protoplasts were sorted directly into ice-cold RNA extraction buffer of Monarch Total RNA extraction kit (NEB, Cat no: T2010S) and immediately used for RNA extraction.

Arabidopsis thaliana

Protoplasts resuspended in PIM solution were filtered through a 40 μm mesh (Fisher Scientific, Cat no: 11587522) and 1ml of protoplast suspension was added to two 5 ml polypropylene sorting tubes (FALCON, Cat No: 352063). 100 nM of flg22 or an equal volume of dH_2O was added to the tubes as treatment or mock, respectively. A BD FACSAria Fusion cell sorter was used for sterile sorting of protoplasts using a

homemade sheath fluid (4 mM MES pH 5.8, 0.185 M KCl, 5 mM $CaCl_2$), 130 µm nozzle, 10 psi sheath pressure, 50 mV laser power and cooler unit set to 0 °C. Intact protoplasts were identified using scatter plots indicating forward scatter (FS), GFP filter (B488-530/30-A) and autofluorescence (B488-695/40-A) (Grønlund et al., 2012).

Protoplasts obtained from *A. thaliana* Col-0 leaves were used as a non-fluorescence reference for setting a threshold to distinguish protoplasts with low and high green (B488-530/30-A) and red (B488-695/40-A) fluorescence intensity levels in reporter line *A. thaliana* pAtWRKY11::3xmVenus-NLS. $2x10^4$ protoplasts were sorted of both high and low fluorescence intensity populations from mock and flg22 treated samples. These samples were flash frozen and used for RNA extraction.

For live cell sorting and culturing, the BD FACSAria Fusion cell sorter was used to sort sterile protoplasts. Previous settings were utilized; however, sheath fluid was modified to contain to contain a sugar osmoticum with the composition 0.3 M glucose, 4 mM MES pH 5.8, 20 mM KCl. Protoplasts were either sorted singly in each well of a 96-well plate containing 100 µl PIM solution, or in bulk ($1x10^4$) into wells of a 24-well plate containing 2 ml PIM solution.

2.6.9. PROTOPLAST REGENERATION

The protoplast regeneration method used in this project is based on the work by (Chupeau et al., 2013) with the following modifications. Concentration of protoplasts used in the study was decreased from proposed $8x10^4$ pp/ml to either single cells or $1x10^4$ pp/ml. Protoplasts were centrifuged at 100 g for 2 min at room temperature after sorting into 4 ml of PIM solution. 3 ml of supernatant solution was removed and the protoplasts at the bottom of the tube were resuspended, then transferred into wells of a 24-well plate (FALCON, Cat No: 351147).

Protoplast regeneration requires sequential replacement of growth media for promotion of cell division. Solutions used for this process were given in Table 2.9 and timeline of media replacement was described in Chupeau *et al.*, 2013. Samples were imaged using an epifluorescence microscope on dates of media replacement (ZEISS, AxioVert.A1).

Table 2.10. Macro and micronutrients table required for preparation of protoplast regeneration media.

	PIM (mg/L)	*CIM1 (mg/L)*	*CIM2 (mg/L)*	*SIM (mg/L)*
Macrosalts				
KNO_3	505	505	1010	1010
NH_4NO_3	160	400	800	0
$CaCl_2$, $2H_2O$	440	440	440	220
$MgSO_4$, $7H_2O$	370	370	370	185
KH_2PO_4	170	170	170	85
Microelements				
Fe Citrate NH_4	30	30	30	50
KI	0.01	0.01	0.01	0.8
H_3BO_3	1	1	1	3
$MnCl_2$, $4H_2O$	0	0	0	30
$MnSO_4$, $4H_2O$	0.1	0.1	0.1	0
$ZnSO_4$, $7H_2O$	1	1	1	12
Na_2MoO_4, $2H_2O$	0	0	0	0.9
$CuSO_4$, $5H_2O$	0.03	0.03	0.03	0.09
$CoCl_2$, $6H_2O$	0	0	0	0.09
$AlCl_3$	0.03	0.03	0.03	0
$NiCl_2$, $6H_2O$	0.03	0.03	0.03	0
Vitamins				
myo-Inositol	100	100	100	100
PanthotenateCa	1	1	1	1
Biotin	0.01	0.01	0.01	0.01
Nicotinic acid	1	1	1	1
Pyridoxin	1	1	1	1
Thiamin	1	1	1	1
Folic acid	0.2	0	0	0
Other constituents				
Glucose	40000	0	0	0
Sucrose	0	30000	20000	20000
Mannitol	60000	70000	60000	40000
2,4-D	1	0	0	0
Thidiazuron (TZ)	0.022	0.11	0.22	0
Indole-3-butyric acid (IBA)	0	0	0	0.1
Meta-topolin	0	0	0	0.2
MES	700	700	700	700
Bromocresol purple (BCP	8	8	8	8
pH of fresh medium	5.6	5.6	5.6	5.6

2.7. MICROSCOPY

2.7.1. MEDICAGO TRUNCATULA

Fluorescence microscopy

M. truncatula A17 seedlings subjected to hairy root transformation with tissue-specific reporter constructs were tested for the presence of green fluorescence in emerging roots using a fluorescence stereomicroscope (ZEISS, AxioVert.A1) with blue epifluorescence light at 488 nm. Fluorescent sections were then used as material for generating protoplasts as described in section 2.6.7.

Root tissue cross-sectioning and confocal microscopy

Excised GFP-expressing root tissue was used for cross-section sample preparation. Bacteriological agar (Sigma Aldrich, Cat no: 9002-18-0) was dissolved in water as 5% w/v, boiled and poured into a petri dish to the brim. It was cooled down slowly by mixing, with the temperature measured constantly. Upon reaching 55 °C, excised root tissue was embedded into the agar vertically and the dish was transferred to 4 °C. After solidification, blocks of agar containing the embedded roots were cut and a Vibratome 1000 Classic was used to take 100 μm slices creating the cross-sections. Sections were imaged first under a light microscope then those with a perpendicular cut to the root were stained with 1 % propidium iodide (PI) for 5 mins before imaged using Zeiss LSM 710 confocal microscope. Samples were interrogated using 488 nm excitation laser and emission was collected at both 493-541 nm for GFP fluorescence and 645-735 nm for PI signal.

2.7.2. ARABIDOPSIS THALIANA

Imaging of nuclear fluorescence and bacterial tracking in *A. thaliana* was performed using a Nikon Eclipse-Ti inverted microscope fitted with an ANDOR CSU-X Confocal Spinning Disc and ANDOR TuCam dual camera adapter units. Experiments were performed on 5-6 week-old *Arabidopsis thaliana* Col-0 and pWRKY11:NLS-YFP plants. Leaves were counted and leaf numbers 7-8-9 were marked (Figure 2.1). The healthiest leaf among the chosen three was selected for infiltration.

Pathogenesis induction with flg22 peptide

Half of the leaf was infiltrated from the abaxial side with dH_2O (mock) and the other half was infiltrated from abaxial side with 100 nM flg22 (elicitor) in dH_2O. Two

chambers of 5 mm diameter were punched out from a double-sided tape and stuck onto a microscope slide. Chambers were loaded with 5 µl of mock or elicitor liquid. 3 mm diameter leaf discs were cut from the middle of the infiltrated section of either side of the leaf and mounted on the slide with the adaxial side facing towards the slide in the chamber. The coverslide was closed onto the sample, ensuring no air bubbles on the leaf disc and the slide was loaded onto the microscope stage with immersion oil. Confocal microscopy was performed using a 40X objective lens, 488 nm laser with 30 % power, 300 gain, 100 ms exposure time and no binning. Images were taken 10 mins post infiltration (T0) and 1 hr post infiltration (T1), starting from stomata on abaxial epidermis with a 2 µm step size for 30 steps, ending in the mid spongy mesophyll layer.

Bacterial tracking

Half of the leaf was infiltrated from the abaxial side with dH_2O (mock) and the other half was infiltrated from abaxial side with OD 0.1 *P. syringae* DC3000 YFP-AvrRpm1 in dH_2O. Two chambers of 5 mm diameter were punched out from a double-sided tape and stuck onto a microscope slide. Chambers were loaded with 5 µl dH_2O and 3 mm diameter leaf discs were cut from the middle of the infiltrated section of either side of the leaf. Cut leaf discs were mounted on the slide with the adaxial side facing towards the slide in the chamber. The coverslide was closed onto the sample, ensuring no air bubbles on the leaf disc and the slide was loaded onto the microscope stage with immersion oil. Confocal microscopy was performed using a 20X objective lens, 488 nm laser with 30 % power, 300 gain, 100 ms exposure time and no binning. Continuous imaging property of the ANDOR CSU-X spinning disc confocal microscope was utilized to record live movements of bacteria within the spongy mesophyll leaf tissue for 5 min at 10 mins post infiltration (T0) and 5 hr post infiltration (T1).

2.8. COMPUTATIONAL METHODS

2.8.1. IMAGE GREY VALUE EXTRACTION

Image analysis from confocal microscopy was performed with Fiji free software (https://fiji.sc/). Z-projections were created by summation of pixel intensity of all z-stacks taken for each image. Background was subtracted using the rolling ball method with a 50 µm ball radius. The resulting image was subjected to an intensity threshold

adjusted manually to create a mask for fluorescent nuclei. The created mask was used to define regions of interest. Area, min&max grey value, centre of mass, shape descriptors, integrated density and mean grey value traits for all regions bigger than 40 μm^2 were extracted into excel for further analysis.

2.8.2. IMAGE DATA ANALYSIS

Image grey value extraction was performed for 15 biological replicates of Mock-T0, Mock-T1, flg22-T0 and flg22-T1 samples. Integrated density and mean values of each biological replicate were normalized by division using the batch mean of 0 hr timepoint of each treatment. Replicate data after batch normalization was pooled. Data was further normalized for photobleaching effect during confocal microscopy. Difference between mean values of Mock-T0 and Mock-T1 samples was added to all values of 1hr samples to compensate for photobleaching and final data were analyzed by the statistical tools in Prism v8.0 software (Tests outlined in results).

2.8.3. META-ANALYSIS OF GENE EXPRESSION DATA

A. thaliana tissue type specific gene expression data in response to excess (5 mM) N (KNO_3) treatment was obtained from the work of Gifford *et al.*, 2008. In this work, *A. thaliana* transgenic lines expressing GFP in their lateral root cap (E4722), epidermis and cortex (E1001), endodermis and pericycle (E470), pericycle (E3754) (obtained from http://enhancertraps.bio.upenn.edu) and stele tissues (pWOL::GFP) (Bonke et al., 2003) were used. Experiments were performed in triplicate and 6000 seeds per replicate were grown for 12 days at 16-h light (50 mmol photons $m^{-2}s^{-1}$light intensity)/8-h dark cycles at 22°C in 1x Murashige and Skoog basal medium supplemented with 3 mM sucrose and 0.5 mM ammonium succinate as N source to ensure healthy plant development. N treatments were performed at the start of the light period on day 12 with KNO_3 addition to the media to a final concentration of 5mM for 2 hours. Mock treated samples were supplemented with 5mM of KCl. Following treatment, roots were harvested and subjected to protoplast generation. Protoplasts exhibiting fluorescence were isolated from sample using FACS. Total RNA was extracted from isolated protoplasts using Qiagen RNAeasy RNA clean-up kit. Extracted RNA was then quantified in Affymetrix ATH1 GeneChip following standard procedures for amplifying, labelling, and hybridizing RNA samples. Transcriptome expression data was normalized using dChip software (http://www.dchip.org) while reproducibility of replicates was analysed using the

correlation coefficient and r2 value of replicate pairs in the S-PLUS 7.0 software package (Insightful Corp.). ANOVA was used to determine genes with significant differential gene expression specific cell types in comparison to all cell types. All genes exhibiting significant differential expression, either upregulation above 2-fold or downregulation below 0.5-fold after excess N treatment were selected to create a list of N-responsive gene IDs. Gene IDs in this list were used in a search against *M. truncatula* using Legume IP V3 online homology search tool (http://plantgrn.noble.org/LegumeIP/gdp/0/NA) (Dai et al., 2020) in order to identify putative orthologs.

*M truncatul*a var. Jemalong A17 whole root and root protoplast response to excess N treatment (5 mM KNO_3) was obtained from Gifford lab. (Unpublished work). In this work, experiments were performed in triplicate with 8 *M. truncatula* seedlings grown vertically on modified Fahräeus medium supplemented with 0.3mM NH_4NO_3 as the sole nitrogen source for 7 days with 16-h light (50 mmol photons $m^{-2}s^{-1}$light intensity)/8-h dark cycles at 24°C. At the start of the light period on 8th day, seedlings were treated with either 5 mM of KNO_3 in dH_2O for 2 hrs or with 5 mM KCl in dH_2O as mock. Following treatment, roots were harvested to either freeze in liquid nitrogen or subjected to protoplast generation. Total RNA was extracted using Qiagen RNeasy plant mini kit and 50ng of each sample was used for LIQA (Agilent)-kit one cycle amplification and hybridisation to 4x44k 60mer Medicago truncatula (A17) one-colour Agilent arrays. Microarray data (Agilent array 60mer probe, 43,803 sequences) obtained from this study was normalised and expression values for probes were extracted using the LIMMA Bioconductor package in R. Samples were first pooled by taking the median for each gene across all arrays, within array normalisation was carried out using a LOESS local regression, and between array normalisation carried out using a quantile method. The microarray was designed against an old *M. truncatula* genome version (*M. truncatula* (A17) Mt3.0), thus in order to determine which genes were represented on the microarray compared to a more recent annotation, nBLAST (NCBI) was used to search for similar sequences within *M. truncatula* (A17) Mt4.0 genes based on identifying best hits (E-value<20). Global expression levels between replicates, and between protoplast and whole root arrays were then compared using an R^2 test to analyse reproducibility of the experiment.

To characterise changes in expression patterns, a linear model was fit for each gene across the series of arrays by a least square's regression (lmFit function in LIMMA). To assess model fit, a t-statistic test was used, and *P*-values calculated by computing empirical Bayes statistics for differential expression (eBayes function in LIMMA). Genes with a statistically different (*P*-value<0.05) expression in N-treated vs. against mock-treated samples with regulation above 2-fold or downregulation below 0.5-fold were selected for further analysis. Genes exhibiting statistically different (*P*-value<0.05) expression in mock-treated whole root samples compared to expression in mock-treated root protoplast samples were excluded from differentially expressed list of genes since they might represent changes simply due to the protoplast generation protocol.

Expression patterns of putative ortholog pairs were investigated between the tissue specific N-response list from *A. thaliana* and the *M. truncatula* N-response list using MS Excel. Numbers of genes were visualized in Venn diagrams created using the online tool Venny 2.0 (Oliveros, 2007). GO terms for the genes identified to have similar expression patterns in both lists were extracted using PhytoMine tool (https://phytozome.jgi.doe.gov/phytomine/begin.do) in Phytozome 12 (Goodstein et al., 2012).

3. IDENTIFYING CELL-TYPE SPECIFIC TRANSCRIPTOMIC EFFECTS OF NITROGEN AVAILABILITY IN *M. TRUNCATULA*

3.1. INTRODUCTION

3.1.1. SOIL NITROGEN AVAILABILITY

Nitrogen (N) is a critical element for all living organisms, found in the chemical structure of nucleic acids and amino acids. For this reason, N is one of the biggest limiting factors for plant growth (Masclaux-Daubresse et al., 2010) . In soil, plants forage for nitrogen in either organic (amino acids and nucleic acids) or inorganic (ammonia (NH_4^+) and nitrate (NO_3^-)) form (Galloway, 2013). While organic nitrogen comes from decomposing remains or wastes of living organisms (Figure 3.1) (Galloway et al., 2004), inorganic nitrogen comes from the largest reservoir of N on earth, the atmosphere (Hans Wedepohl, 1995; Ward, 2013). However, atmospheric nitrogen (N_2) is inaccessible to organisms in its gaseous form. Yet, it can be made available for terrestrial and marine life through a process called nitrogen fixation.

Nitrogen fixation is the process of combining N_2 gas with hydrogen to create ammonium (NH_4^+). This reaction can occur either abiotically, during lightning strikes and fossil fuel combustion (Andreae, 2019; Jickells, 2006); or biotically by specialized nitrogen fixing organisms such as rhizobia (Capone, 2001; Galloway et al., 2004). In its simplest form, incorporation of nitrogen from atmosphere to terrestrial and marine environment by nitrogen fixation, utilization of terrestrial and marine-bound nitrogen by organisms and subsequent release of this nitrogen back to the atmosphere through various methods are the main stages of the nitrogen cycle (Figure 3.1).

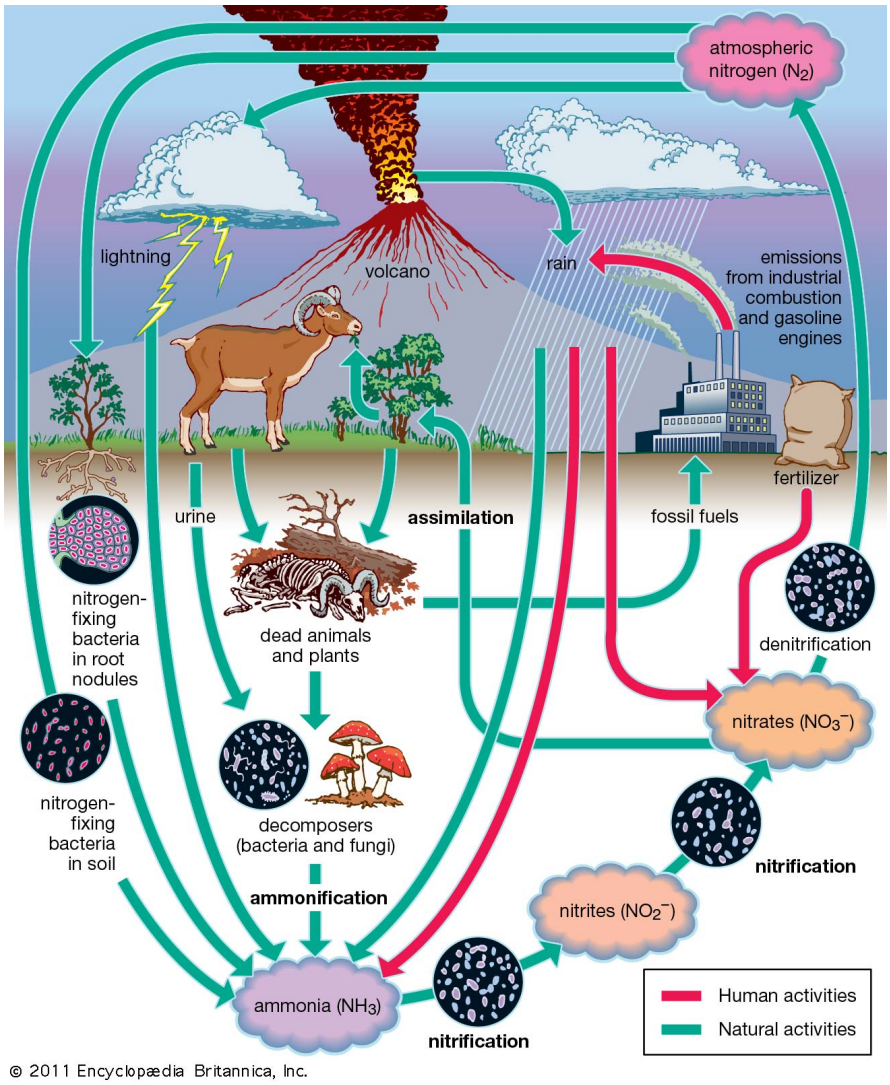

Figure 3.1. The nitrogen cycle. Starting from the top right, atmospheric nitrogen is converted into ammonia through nitrogen fixation process either abiotically through lightning or biotically through microbes. Although it is possible for plants to utilize N in NH_3 form, some of it is converted into nitrates through nitrification by nitrifying microbes. Nitrates can then either be assimilated by plants and integrated into their structure or return to the atmosphere as N_2 through denitrification process by denitrifying bacteria. Assimilated nitrogen in plants return to the soil as organic material after death or through death of animals which consumed them. Their remains are decomposed by microbes and the nitrogen released re-enter the cycle as ammonia. While all these processes occur naturally, human intervention through fertilization or burning of fossil fuels can also create an ammonia and nitrate input to the cycle. (Taken from: https://www.britannica.com/science/nitrogen-cycle)

Without human intervention, the nitrogen cycle would continuously move to balance itself. On the other hand, mankind has an ever-growing need for more efficient food production due to the exponentially increasing population. In the 1900s, discovery of the Haber-Bosch process to chemically mass-produce nitrogen fertilizers, allowed agricultural practices to utilize fertilizers to increase yields significantly in a movement

called the green revolution (Erisman et al., 2008). While this movement has increased food production significantly, it was later found that the human intervention to natural processes had a negative impact on the environment. Over the years, researchers studied the effects of this extensive fertilizer use on agricultural lands. It has been found that efficiency of fertilizer use has decreased from 80% in 1960s to 30% in 2014 for cereal crops (Lassaletta et al., 2014) and that approximately 80% of nitrogen fertilizers were leached from soil by irrigation runoff into water bodies, oceans or rivers (UNEP and WHRC, 2007). Leaching of such high concentrations of nitrogen into water bodies resulted in significant increases in eutrophication, overgrowth of algal and plant life in affected areas due to abundance of nutrients (Carpenter et al., 1998). These overgrowths lead to depletion of dissolved inorganic carbon sources and production of greenhouse gasses (NO_2) 300 times more dangerous than CO_2 (Billen et al., 2013). Upon realization of these drawbacks, tight regulations put in place in 1980s allowed partial recovery of damages done over the decades, however agricultural practices still continue to utilize excessive amounts of fertilizers (Storkey et al., 2015).

With growing concerns for food security and aims to create sustainable agricultural practice, incorporation of economically important natural nitrogen-fixing legumes such as pea, alfalfa, clover, common bean, or peanut (Smýkal et al., 2015) into the agricultural processes presents a promising way to reduce extensive fertilizer use (Stagnari et al., 2017). Thus, plant science study has turned to examine these plants in more detail. Some researchers have focused on increasing the effectiveness of economically important nitrogen-fixing legume plants in ways of disease resistance, increased yields and adaptability to different geographies (Venkateswarlu et al., 2007). Others have considered utilizing biotechnological approaches to integrate nitrogen fixing machineries into non-legume crops in hopes to reduce dependency on extensive fertilizer use (Huisman and Geurts, 2020). In either case, their ability to form symbiotic relationship with nitrogen fixing bacteria makes nitrogen-fixing legume plants an attractive organism to pursue for addressing current agricultural problems.

3.1.2. PLANT ROOT PHYSIOLOGY AND SPECIALIZED ROOT STRUCTURES

Legumes do not differ from other plants in their general physiology. They can be divided into two parts with systems above-ground (shoot), and below-ground (root). While shoot systems: leaves, stem etc., are specialized for photosynthetic activity, structural stability and transport; root structures: primary roots (PR), lateral roots (LR) and root hairs (RH) etc., provide structural support while growing in a solid media (soil) as well as provide access to water and essential molecules for growth. One characteristic in their root systems set legumes aside from the rest of the plants; these are nodules. These are specialized structures formed to house the symbiotic nitrogen fixing bacteria. To understand the function of the nodule, it is important to understand each component of the root system architecture (RSA) (Koevoets et al. 2016).

In seedlings and mature legumes RSA is set around a primary root (De Smet et al., 2010). As they develop, these roots can be divided into three distinct zones in the apical-basal axis of root growth (Figure 3.2) (Verbelen et al., 2006). Starting from the tip of the root, the first zone is the division zone which contains the root meristem and the quiescent centre formed of undifferentiated cells that divide continuously to give rise to all other cells in the root (Figure 3.2.I). Next, is the elongation zone where cells are no longer dividing but have started to increase in size (Figure 3.2.II). Finally, furthest from the root tip is the maturation zone where cells slow down their elongation and reach to their final size, completing their path of differentiation depending on their spatial location (Figure 3.2.III). This is the zone where formation of specialized structures such as root hairs and nodules can be first observed (Verbelen et al., 2006).

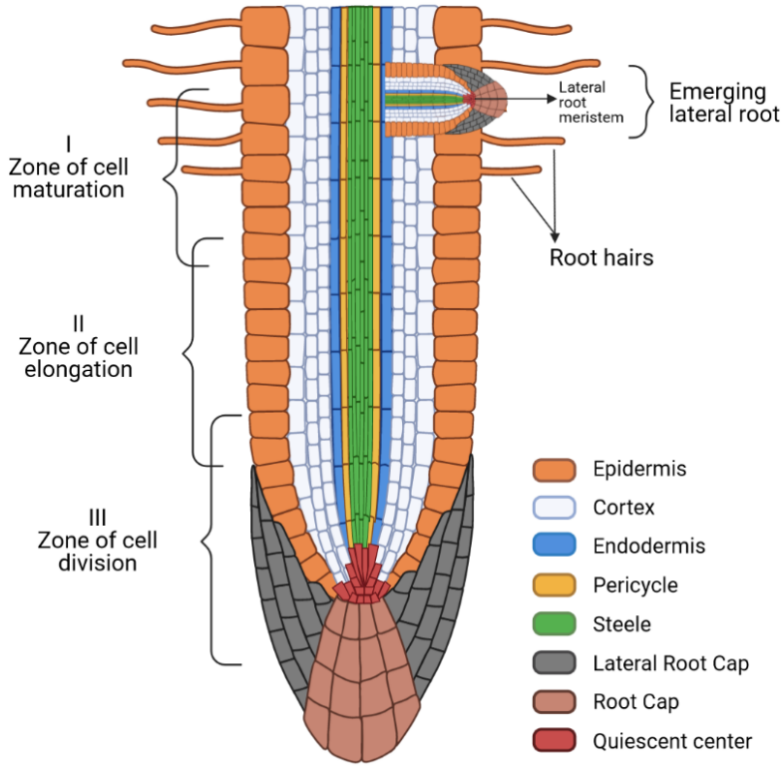

Figure 3.2. Plant root architecture. A longitudinal-section of a plant root tip showing the three distinct developmental zones during root growth. From root tip to the top, **I)** first is the zone of cell division where undifferentiated cells in quiescent centre divide to create new cells. **II)** As the root grows further these newly formed cells start increasing in size in the zone of elongation. **III)** Following sufficient enlargement, cells start differentiating into their pre-designated fates to form specialized structures or attain tissue specific properties. At the cross-section is the root shows concentric layers of cell types. From outer to inner layers, first is the epidermis, first point of contact for nutrient and water uptake from the environment. Next, is the cortex, mainly functioning in transportation of nutrients and water between epidermis and stele as well as carbohydrate storage shipped from the aboveground tissues. Then comes the endodermis which secretes suberin to create the Casparian strip for preventing water loss from the vascular bundle in stele. Finally, the innermost tissue is the formed of pericycle, origin of lateral root formation, and the vascular bundle formed of xylem and phloem. (adapted from Macmillan higher education)

Plant roots are not only formed of zones on the apical basal axis but also are composed of tightly packed concentric rings of tissue types with distinct cell identities and functions on the radial axis (Figure 3.2). From the outside, the first layer is the epidermis. It is the first point of contact for water and nutrient intake from the environment (Evert and Eichhorn, 2006). Cells in this layer can also form specialized structures called root hairs which play a very important role in water and nutrient uptake as well as plant-microbe interactions (Sprent, 2009) . The next layer is the

cortex, and amongst other roles, this layer is responsible for transportation of water and nutrients scavenged by the epidermis towards the vascular tissue and store carbohydrates transported from leaves in form of starches. Cortical tissue can be formed of a different number of cell layers. While cortex in *A thaliana* is a single layer of cells, there are 3-5 cell layers in *M. truncatula* roots. Further towards the centre of the root is the endodermis. At this layer, tightly packed cells with lignin deposits form the Casparian strip, a barrier for water transport between the vascular tissue and the cortex, preventing water loss from the vascular tissue (Naseer et al., 2012). Closest to the core is the pericycle tissue where a subset of cells undergo de-differentiation then cell division to form LR founder cells (LR-FC) (de Smet, 2012). Lastly, the bundle of vascular tissue composed of xylem and phloem in the centre of all these layers form the stele. This layer is responsible for the transportation of water between belowground and aboveground systems. Therefore, each cell layer in the root plays a vital role in uptake of nutrients from the environment and distribution of it throughout the plant.

In addition to PR, plants deploy LRs that are developed post-embryonically to improve nutrient and water foraging capacity. These structures originate from LR-FCs that reside in localized sections of root pericycle. Up to this day, there is no conclusive evidence showing how founder cells are selected to initiate the LR formation (Torres-Martínez et al., 2020). However, it was found that regulation of local auxin levels in pericycle cells was a morphogenetic trigger for LR-FC differentiation to LR and can be regulated by a nitrogen sensing protein NITRATE TRANSPORTER1.1 (NRT1.1, now known as NPF6.3) (Banda et al., 2019; Dubrovsky et al., 2008; Tian et al., 2014). Lateral root initiation occurs in sequence of cell divisions. In the first stage, pericycle cells undergo a series of anticlinal divisions (Figure 3.3.A-B). This is followed by a second stage with continuing anticlinal divisions in pericycle and endodermis accompanied with periclinal divisions of pericycle cells (Figure 3.3.C). At the third stage, endodermis and pericycle cells undergo periclinal division, along with anticlinal division of inner cortex cells and initiate early LR formation (Figure 3.3.D) (Herrbach et al., 2014).

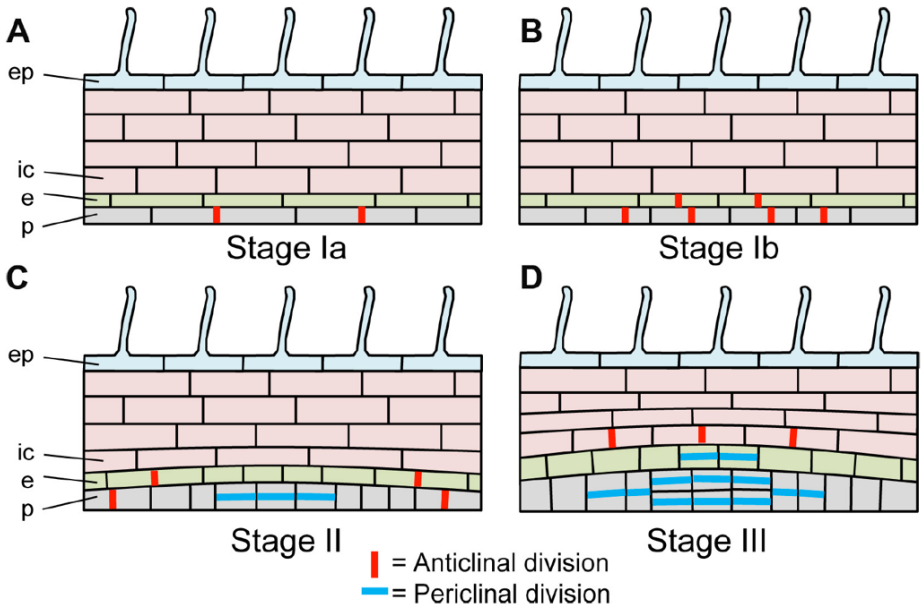

Figure 3.3. Lateral root initiation. In stage I, **A)** LR formation initiates from pericycle by anticlinal division of LR-FC. Later in this stage, these divisions expand further **B)** to neighbouring cells of LR-FC in pericycle and endodermis. In Stage II, **C)** Pericycle cells start dividing periclinally as anticlinal divisions continue rippling out in pericycle and endodermis. In Stage III, **D)** Periclinal divisions further expand to the neighbouring cells in pericycle and endodermis. Also, at this stage, inner cortex cells start dividing anticlinally. Following initiation, LR primordium occurs with repeated alternating asymmetric divisions of these cells and eventually adopts the root meristem organization to emerge from the overlaying tissue (Herrbach et al., 2014).

3.1.3. NODULATION: INTERACTION WITH NITROGEN-FIXING BACTERIA

LRs can only increase nutrient uptake if there are nutrients readily available in soil for uptake. In the case of N depletion, most plants would suffer developmental impairment since it is a key macro-nutrient. However, during legume-rhizobia symbiosis, legumes can form specialized structures called nodules to house N-fixing bacteria and gain access to an otherwise unusable N source. Nodulation is a complex process with tightly controlled parallel events occurring within and at the surface of the root (Madsen et al., 2010). In order to attract rhizobia, flavonoids are released from epidermal cells to the immediate vicinity of the root (rhizosphere) (Bauer and Caetano-Anollés, 1990). These flavonoids attract rhizobia towards the root and cause them to secrete molecules known as Nod-factors (Figure 3.4.A) (Bensmihen et al., 2011). Recognition of nod-factors by root hairs results in oscillations of Ca^{+2} levels inside epidermal cells, inducing the symbiosis signalling pathway. Upon activation of this pathway, the root hair tip starts curling around the rhizobia, trapping it (Esseling et al., 2003). An

infection thread is formed by invagination of the plant cell membrane to create a pathway for rhizobia towards cortical tissue (Figure 3.4.B) (Timmers et al., 1999). Simultaneously, cortical cells start dividing immediately below the bacterial infection site and create a nodule meristem (Figure 3.4.C (Patriarca et al., 2004). The infection thread continues growing and branches out into the early nodule meristem (Gage, 2004). Rhizobia is then released into the early nodule formations encapsulated in membrane-bound structures. The bacteria start dividing to form bacteroids (Figure 3.4.D) (Downie, 2014) and form N-fixing symbiosomes. Due to the anaerobic nature of nitrogen fixing bacteria, leghaemoglobin molecules are produced in nodules to regulate O_2 levels before nitrogen fixation can start (Wittenberg et al., 1974). Finally vascular structures extend towards the root stele, from the symbiosomes establishing pathways to exchange organic carbon from shoot system and nitrogen fixed in nodules (Figure 3.4.E) (Brewin, 1991).

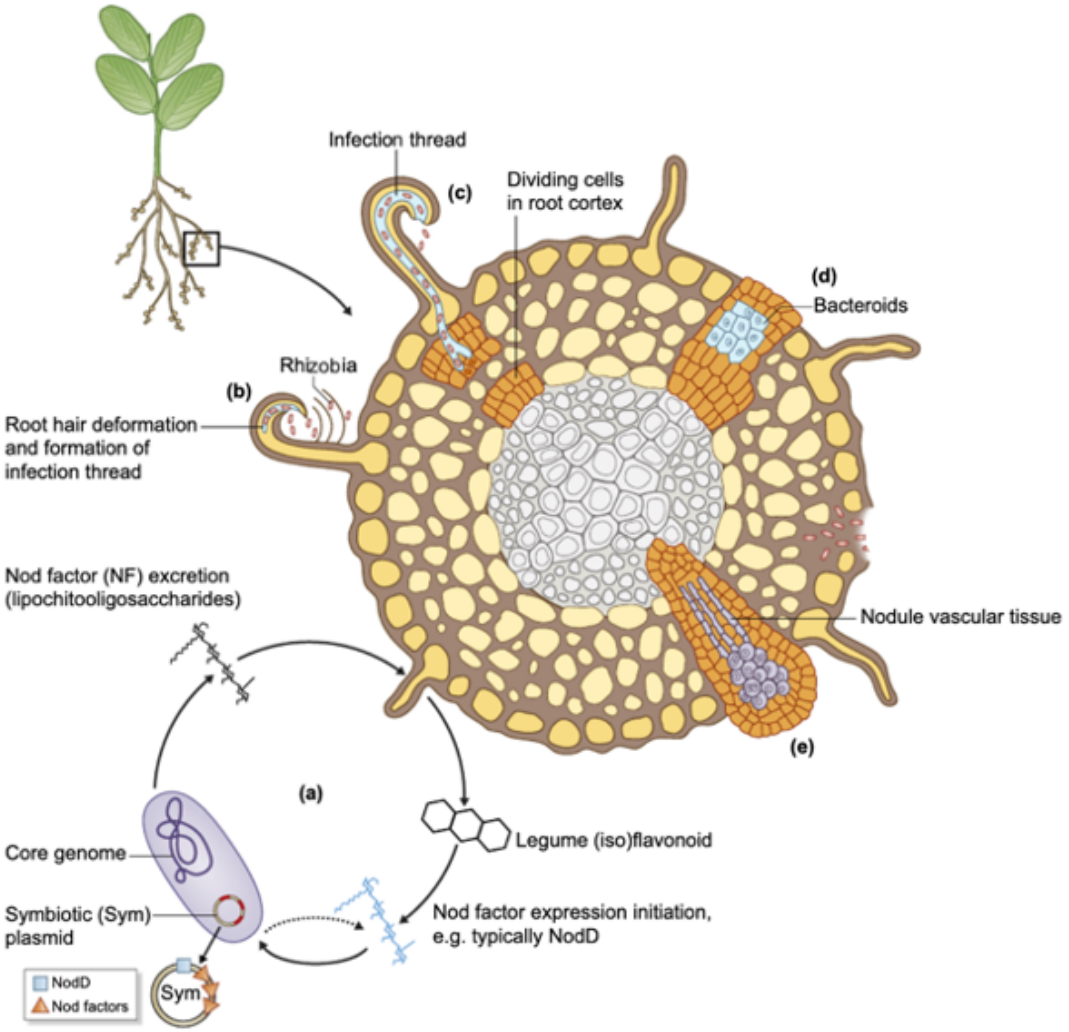

Figure 3.4. Nodule development. Legume plant roots exude flavonoids into root rhizosphere to attract symbiotic bacteria. These flavonoids attract nearby symbiotic bacteria into root hairs where the bacteria secrete Nod factors (NF) to initiate nodulation **(A)**. Upon detection of NF, root hair starts curling around the bacteria and an infection thread is formed in the middle of the root hair **(B)**. The infection thread elongates to create a path towards the cortical tissue where the cortex cells are simultaneously dividing to create an early nodule meristem **(C)**. Rhizobia growing through the infection thread is released into membrane bound structures the in early nodule meristem cells and divide to create bacteroids **(D)**. Finally, nodule reach maturation after synthesis of leghaemoglobin and formation of nodule vascular tissue with the stele for food-nutrient exchange (taken from Le Roux et al., 2017).

3.1.4. NITROGEN UPTAKE BY PLANTS

Plants can direct roots to areas rich in N, however it is the transporter proteins that perform the uptake of N from the environment. There are two main type of N transporter proteins in plant roots, one is trying to take N into the cells (influx) while the other tries to expel it (efflux) (Figure 3.5) (O'Brien et al. 2016). The exact function

of efflux proteins remains unclear however, it was hypothesized that they take part in transport of N into xylem for transport to shoot systems (Hanson, 1978; Wang et al., 2012). The delicate balance in the activity of both transporters keep the root internal nitrogen concentrations in check.

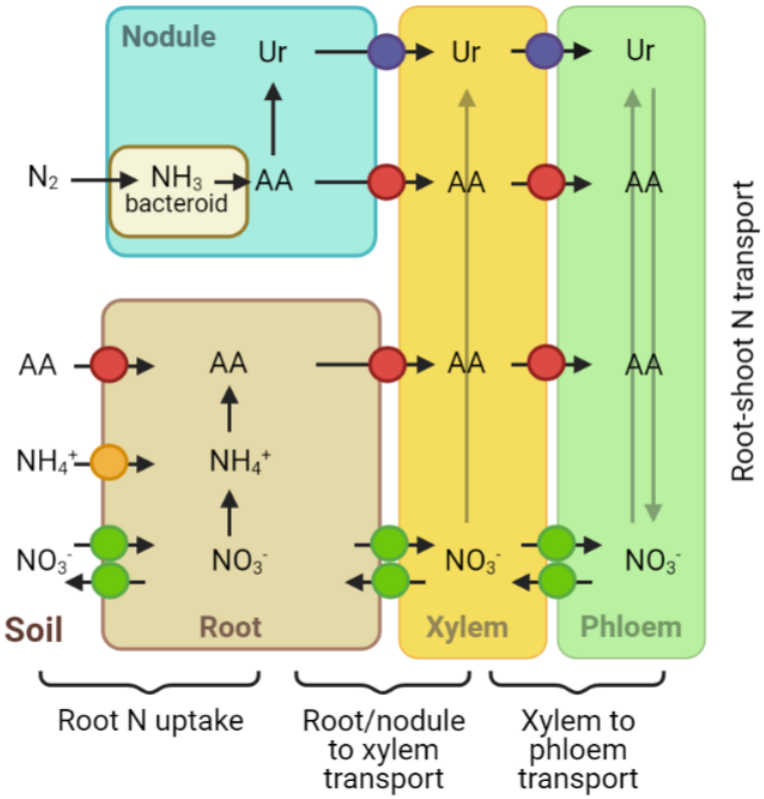

Figure 3.5. Schematic of nitrogen import and export in the root. Nitrate (green), ammonia (orange), amino acid (red) and ureide (purple) transporters performing in root N uptake, root/nodule to xylem transport and xylem/phloem transport. Once nitrogen reaches the xylem or phloem, it is transported to shoots in one direction from xylem or in both directions via phloem. (Abbreviations are: NO_3^-, nitrate; NH_4^+, ammonium; AA, Amino acid; Ur, ureides adapted from Tegeder and Masclaux-Daubresse, 2018).

NO_3^- was found to be the predominant form of N source in agricultural land (Von Wirén et al., 2000). Thus, its transporters have been extensively studied. Its transporters were classified into two distinct groups based on their affinity towards NO_3^-. Low-affinity transport systems (LATS) which facilitate N transport from high external N concentrations (N_{EXT}) (>1 mM) and high-affinity transport systems (HATS) which performed best in low N_{EXT} (~0.2 mM) (Crawford and Glass, 1998). Later it was shown that HATS could be further classified into two subclasses

depending on their type of expression. Transporters with expression levels changed by N_{EXT} were classified as inducible HATS (iHATS) while others with independent gene expression from N_{EXT} were classified as constitutive HATS (cHATS) (Aslam et al., 1992; Behl et al., 1988). Both of these systems were found to be present in the root at all times and expressed simultaneously, with their ratios changing depending on the N_{EXT} levels (Kronzucker et al., 1999).

So far, the identified NO_3^- transporters were categorized under four gene families (NPF, NRT2, CLC and SLAC/SLAH). Among these transporters, first one to be identified in *Arabidopsis thaliana* was NRT1.1 (AT1G12110), currently known as NPF6.3, belonging to the NPF gene family with specificity towards multiple substrates such as peptides and hormones along with NO_3^- (Figure 3.5.1-5) (Krouk et al., 2010b; Tsay et al., 1993). This transporter was found to have dual-affinity properties, meaning that it can perform both as a HATS and a LATS (Liu and Tsay, 2003). What was more, NPF6.3 was found to play a key role in sensing N_{EXT} like a receptor and activate downstream signalling pathways for regulating gene expression in response to changing N_{EXT} in both short and long term (Bouguyon et al., 2015; Ho et al., 2009).

Compared to the NPF gene family, NRT2 gene family possesses less members, however transporters of this family have a high substrate specificity for NO_3^- and mostly perform as HATSs (Von Wittgenstein et al., 2014; Wirth et al., 2007). Main characteristic of NRT2 transporters is that they require a partner protein belonging to the NAR2 (NRT3) gene family for their function (Kotur et al., 2012). Components of this mechanism are still under investigation however it was found that NRT2.1 (AT1G08090) gene in this family plays a key role in regulation of LR initiation under changing N_{EXT} (Little et al., 2005).

N can also be taken up from the environment as NH_4^+ whose transporters are mostly monovalent cation channels with high substrate specificity (Tyerman et al., 1995). NH_4^+ can easily become toxic to plants if its uptake is not regulated. For this reason, its transport is performed by HATS with saturable kinetic patterns and LATS with non-saturable kinetic patterns to prevent excess uptake even in high external NH_4^+ concentrations (Tegeder and Masclaux-Daubresse, 2018).

3.1.5. COMMUNICATION OF NITROGEN STATUS

Expression of N transporter proteins is regulated by a feedback mechanism where NO_3^- and its assimilation products, NH_4^+ and glutamine, were found to act as signalling molecules (Orsel et al., 2002).

One of the key receptors in this pathway was found to be the dual-transporter protein previously identified in *Arabidopsis,* NPF6.3. A working model of NO_3^- signal perception and transduction by NPF6.3 was reviewed in O'Brien et al. 2016 where it was shown that changing N_{EXT} causes NPF6.3 to activate phospholipase C (PLC) which in turn triggers the Ca^{+2} signalling pathway to result in activation of transcription factors responsible for regulation of NO_3^- response genes including but not limited to major NO_3^- transporter genes *NPF6.3*, *NRT2.1*, *NRT2.2* (Bouguyon et al., 2015; Riveras et al., 2015).

Regulation of N responses can also be controlled by hormone signalling. Hormones such as; auxin (Ma et al., 2014), cytokinin (CK) (Sakakibara et al., 2006), ET (Tian et al., 2009), ABA (Ondzighi-Assoume et al., 2016) and JA (Sun et al., 2006) were found to play role in these regulations and N availability also effects hormone biosynthesis, and transport (O'Brien et al., 2016). Consequently, hormones regulate transcriptional networks related to N responses. For example, CK production was found to be altered by transcriptional regulation of CK biosynthesis genes through NPF6.3 signalling activity (Medici and Krouk, 2014). Moreover, NPF6.3 transporter activity was required for upregulation of an auxin receptor gene AUXIN SIGNALING F-BOX 3 (AFB3) (AT1G12820) to trigger auxin signalling pathway and activate a NAC family TF gene NAC4 (AT5G07680) to control LR initiation (Vidal et al., 2010). On the other hand, it was also shown that NPF6.3 can also directly take part in transport of auxin in low NO_3^- concentrations, regulating its distribution in the root tissue (Krouk et al., 2010b).

3.1.6. INFLUENCE OF N_{EXT} ON ROOT SYSTEM ARCHITECTURE

Plants, forage necessary nutrients in the most energy efficient way possible. Foraging capacity can be maximized by the size, angle, and number of PR, LRs, RH and nodules in RSA. Composition of this architecture is plastic and can be altered over the lifespan of the plant in response to changing environmental conditions (Robinson, 1994). One of the conditions effecting RSA is the soil N content and at the core of the molecular

mechanisms regulating N-dependent RSA lie the nitrogen transporter proteins. These proteins not only take part in the uptake and distribution of N, but some also act as signal receptors, transducers and hormone transporters to regulate LR formation as well as nodulation.

It was observed that when *A. thaliana* encounters high N_{EXT} at a location, it produces more LRs into that location to increase foraging capacity while inhibiting LR meristem activation if it encounters low N_{EXT} (Figure 3.6 A) (Gruber et al., 2013; Zhang and Forde, 1998). Many genes responsible for regulation of LR activation in response to N_{EXT} were identified over the years and were reviewed in O' Brien et al. 2016. Among these genes, two NO_3^- transporter proteins NPF6.3 and NRT2.1 were found to play a key role in repression of LR emergence under N deprivation and C/N availability, respectively (Krouk et al., 2010a; Little et al., 2005).

While N signal is perceived locally by plants, the responses were observed to be both local as well as systemic. A MADS-box TF, ANR1 was identified to be involved in production of some of the local responses along with NPF6.3. It was proposed that at high N_{EXT}, NPF6.3 sensing of NO_3^- induce ANR1 expression which in turn trigger local LR proliferation (Gan et al., 2012; Krouk et al., 2010b). At low N_{EXT}, NPF6.3 would act as an auxin transporter, removing auxin from LR primordia and preventing initiation (Krouk et al., 2010b; Mounier et al., 2014).

To understand systemic responses, experiments were performed in vertical and split root systems with heterogenous supply of N to the plant root (Figure 3.6.A&B) (Linkohr et al., 2002; Ruffel et al., 2011). These experiments lead to the understanding of systemic N-supply which represses LR formation in root areas in contact with low N concentrations and systemic N-demand which activates LR formation in areas in contact with high N concentrations (Figure 3.6.B). While the exact mechanism of these systemic responses is still under investigation it was hypothesized that cytokinin plays an important part in systemic N-demand signalling but not in systemic N-supply signalling (Ruffel et al., 2011).

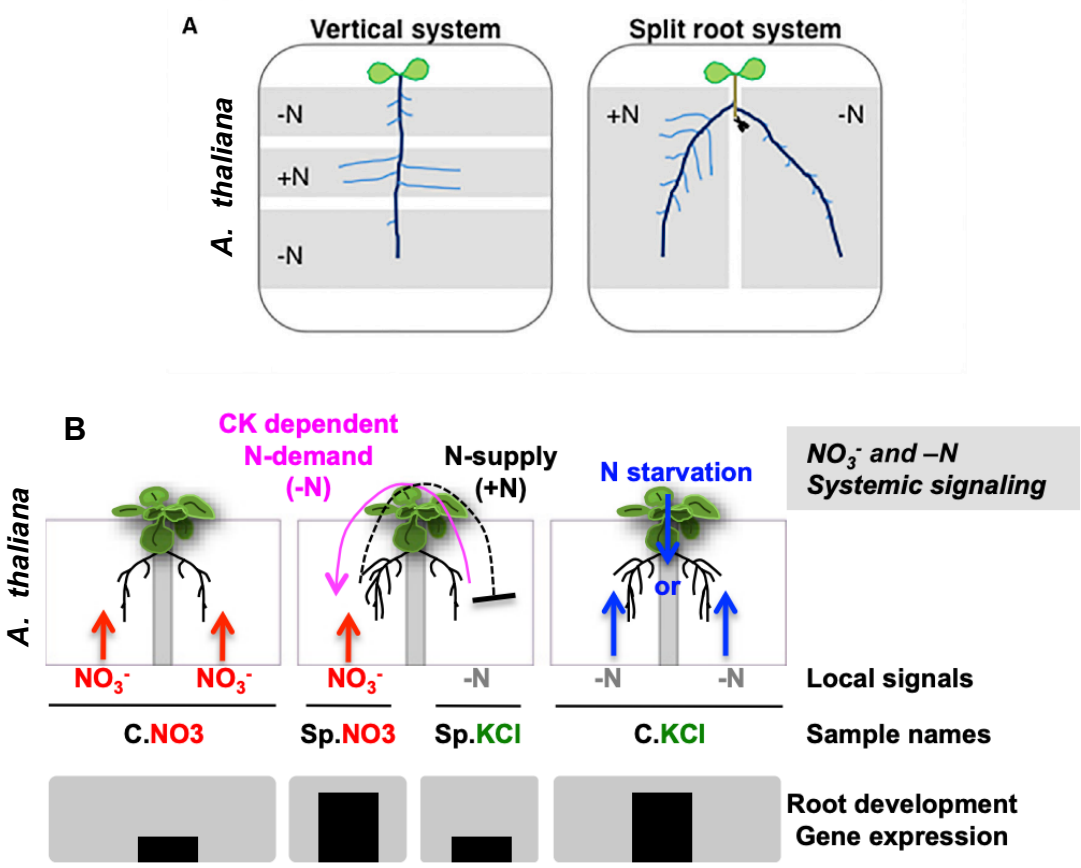

Figure 3.6. Systemic LR responses to heterogenous nitrogen concentrations. A) Vertical and split root experimental systems in *A. thaliana* which apply heterogenous N concentrations to the same PR or different PR of the same plant to uncover local and systemic regulation of N signalling and RSA. **B)** Split root systems were constructed with *A. thaliana* in three set-ups to study systemic N responses. Either both roots of a plant were supplied with either high NO_3^- (red) and low NO_3^- (grey) or each root was supplied with either high or low NO_3^- concentrations. In the end, a CK-dependent N demand signal (pink) was found to systemically induce root development, while a N-supply signal (black) was found to systemically repress root development (Figure A: Zhang and Forde, 1998; Figure B: Mounier et al., 2014; Ruffel et al., 2011; Walch-Liu et al., 2006;).

Nodules, as another specialized component of RSA, can also be influenced by the changes in N_{EXT}. Significant reduction in total nodule number, size and nitrogen fixation ability was observed when a legume plant was supplied with high NO_3^- (Figure 3.7) (Hodge, 2004; Walch-Liu et al., 2006; Wong, 1988). It was found that this decrease was more pronounced with higher N_{EXT} and could persist for days even after removal of excess N from the environment (Jeudy et al., 2010). Thus, it was hypothesized that this response was because foraging a readily available N source is much more energy efficient for a plant than maintaining a symbiotic relationship with bacteria when the N source is present (Wong, 1988).

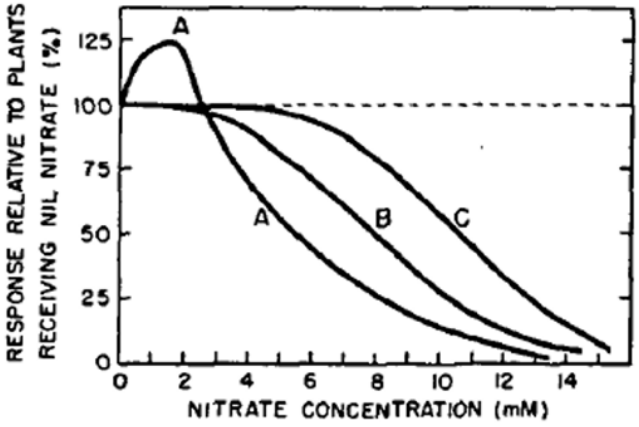

Figure 3.7. Effects of changing nitrogen concentrations on nodules. A) Nodule mass/plant, **B)** N_2 fixed/unit nodule mass and **C)** number of nodules/plant was observed to decrease significantly with increasing N_{EXT} (Wong, 1988).

Similar to systemic responses in LR regulation, in split root experiments performed with legume plant *M. truncatula*, it was shown that the overall nitrogen fixation capacity of the plant was significantly reduced when a portion of the root was supplied with sufficient N although the remaining root tissue was still in starvation (Ruffe et al., 2008). These findings suggested a systemic signal in plants for the regulation of N fixation in response to nitrogen availability (Ruffe et al., 2008). In systemic regulation of nodulation, NO_3^- itself was found to act as a signalling molecule to inhibit various stages of nodulation from as early as flavonoid signalling stage to nodule maturation stage (reviewed in Nishida and Suzaki, 2018). However, this was not the only mechanism identified for regulation of nodulation. Legume plants also utilize a feedback inhibition pathway called autoregulation of nodulation (AON). In *M. truncatula*, this pathway utilizes CLAVATA3/embryo-surrounding region (CLE) peptides to prevent colonization of the root by rhizobia upon recognition of high N_{EXT} (Reid et al., 2011). In the absence of CLE receptor super numerary nodules (SUNN) plants present hyper-nodulation as they cannot regulate their nodule number (Schnabel et al., 2005). On top of these pathways, plants can also present altered hormone concentrations when conditions are not favourable for nodulation. Increased ET, JA and SA were all found to inhibit nodulation in legume plants potentially through a defence/growth trade-off mechanism (Sun et al., 2006; Van Spronsen et al., 2003). Mechanisms for regulation of nodulation at high N_{EXT} remains unclear despite the implications of this having large agricultural value, making it all the more worthwhile for investigation.

3.1.7. OBJECTIVE OF THIS WORK

Nodulation responses to changing N concentrations has been well studied at whole root level on legume model plant *M. truncatula*. However, given the unique cell identity of each cell type found in roots, we hypothesize that each tissue could have a unique set of gene expression changes in response to N changes. In order to investigate the transcriptomic changes of each tissue type, epidermis, cortex and pericycle cells should be isolated from the whole root using a FACS approach.

This chapter aims to generate the plant material required for isolation of epidermis, cortex or pericycle cells using FACS. To that end, new tissue specific reporter constructs were created and *M. truncatula* plants were transformed using hairy-root transformation method. This would allow generation of mosaic plants expressing fluorescence marker proteins. Following transformation, localization of fluorescence protein expression was investigated by confocal microscopy. Constructs with correct expression patterns were subjected to protoplast generation and used for FACS to isolate tissue specific cells to lay the groundwork for future studies.

High N_{EXT} was reported to result in reduced nodule formation and N-fixation efficiency in *M. truncatula*. To investigate the changes toxic N_{EXT} induces in the tissue type-specific transcriptomic landscape, microarray data obtained from high N_{EXT}-treated *M. truncatula* whole roots were compared with microarray data obtained from high N_{EXT} treated *A. thaliana* root cell types.

3.2. RESULTS

3.2.1. NEW REPORTER CONSTRUCTS FOR TISSUE-SPECIFIC FLUORESCENCE EXPRESSION IN *M. TRUNCATULA* ROOTS

Isolation of tissue specific cells using FACS requires plant material expressing reporter molecules (e.g., fluorescent proteins, β-glucuronidase (GUS) etc.) in tissues of interest. Stably transformed plant material expressing tissue specific reporter proteins is widely available for model plant species *A. thaliana* (Brady et al., 2007a). However, such transformants are not so common for legume model plants *M. truncatula* or *L. japonicus* due to a longer labour-intensive transformation process. So, in this chapter we focused on designing and generating the necessary vectors for transformation of *M. truncatula,* and subsequently evaluating the feasibility of using hairy root transformation system for investigating any changes in tissue-type specific gene expression of nitrogen responsive elements upon external N treatments.

Plant root cells are highly differentiated and genes with specific or unique expression are associated with the development or function of individual tissue types. The first aim of this study was to identify putative promoter regions with potential root tissue specific expression. Previously, upstream regulatory elements of tissue type specific genes identified in *Arabidopsis* were used to express GUS in pericycle, endodermis, cortex and epidermis of *Lotus japonicus* in physiological studies to understand contribution of tissue types in the developmental stages of nodulation (Gavrilovic et al., 2016). In another work, tissue specific promoters of *Arabidopsis* were used to drive expression of GUS gene in model legume species *M. truncatula* (Sevin-Pujol et al., 2017), suggesting that promoter sequences retain some cell type specificity across species.

Many such genes have been investigated through transcriptome-wide studies performed on *Arabidopsis* (Birnbaum et al., 2003; Brady et al., 2007a). Some of these genes have been well characterised and widely used as markers in tissue type specific studies for the expression of reporter proteins (Table 3.1). Epidermis marker genes used in previous studies include: EXTENSIN (EXT1), a rodlike flexuous glycoprotein component of cell wall structure (Lamport, 1966); EXPANSIN A7 (EXPA7), a protein that plays a key role in root hair initiation and root growth (Cho and Cosgrove, 2002); WEREWOLF (WER), encoding a MYB transcription factor protein for regulation of

position dependent fate determination of epidermal cells into hair and non-hair cells (Lee and Schiefelbein, 1999) and COBRA-LIKE9 (COBL9), which is a glycosylphosphatidylinositol (GPI) anchored cell membrane protein responsible for correct orientation of microfibrils and cellulose crystallization (Roudier et al., 2002). Cortex marker genes include: ENDOPEPTIDASE (PEP), and a bifunctional inhibitor/lipid-transfer protein (CO2) identified in *Arabidopsis* (Ron et al., 2014); and C2H2 zinc-finger domain transcription factor proteins E49 and LRC1 (Lee et al., 2006). Marker genes of pericycle include: NITRATE TRANSPORTER1.3 (NRT1.3), a nitrate influx transporter (Unpublished data, Gifford Lab, University of Warwick); N21, an EamA-like transporter family protein (Young et al., 2011); E29, a basic helix-loop-helix TF and E47, RING/FYVE/PHD zinc finger TF (Lee et al., 2006).

Table 3.1. Genes commonly used as markers to study epidermis, cortex and pericycle.

Gene Name	Expressed Tissue	Sequence origin	Locus/Accession	Gene product	References
EXT1	Epidermis	*S. lycopersicum*	NM_001247899	Extensin like protein	(Bucher et al., 2002)
EXPA7	Epidermis	*A. thaliana*	AT1g12560	Alpha expansin protein	(Cho and Cosgrove, 2002)
WER	Epidermis	*A. thaliana*	AT5g14750.1	MyB-related protein	(Ryu et al., 2005)
COBL9	Epidermis (Trichoblast)	*A. thaliana*	AT5g49270	COBRA-like protein	(Brady et al., 2007b)
PEP	Cortex	*A. thaliana*	AT1g09750	Endopeptidase	(Lee et al., 2006; Sevin-Pujol et al., 2017)
CO2	Cortex	*A. thaliana*	AT1g62500	Bifunctional inhibitor/ lipid-transfer protein	(Heidstra et al., 2004)
E49	Cortex	*A. thaliana*	AT3g05150	C2H2 TF	(Lee et al., 2006)
LRC1	Cortex / Atrichoblast	*A. thaliana*	AT1g08930	C2H2 TF	(Lee et al., 2006)
NRT1.3	Pericycle	*M. truncatula*	MEDTR5g085850	Nitrate transporter	Unpublished data, Gifford lab, University of Warwick
N21	Pericycle	*M. truncatula*	MEDTR7g100050	EamA-like transporter family protein	(Young et al., 2011)
E29	Endodermis / Pericycle	*M. truncatula*	AT4g05170	basic helix-loop-helix TF	(Lee et al., 2006)
E47	Endodermis / Pericycle	*M. truncatula*	AT2g37950	RING/FYVE/PHD zinc finger TF	(Lee et al., 2006)

With that in mind, AtEXPA7, SlyEXT1, AtCO2, AtPEP, MtrNRT1.3 and MtrN21 genes were selected as primary candidates for creating transgenic plants based on the fact they had been partially tested in the past. The promoter region of SlyEXT1 (epidermis) and promoter regions of AtPEP, AtCO2 (cortex) were previously used in *M. truncatula* to drive tissue-type expression of GUS (Sevin-Pujol et al., 2017). However, none of these promoters had been used to create a reporter construct expressing a fluorescent reporter protein in *M. truncatula*. The promoter regions of MtrNRT1.3 (pericycle) (Unpublished data, Gifford Lab, University of Warwick) and AtEXPA7 (epidermis) (Lagunas et al., 2018) had been previously studied in *M. truncatula* to drive tissue type fluorescence reporter expression, however, results from different studies showed that the expression of the genes' promoters varied depending on the developmental age of plants (Lagunas et al., 2018; Unpublished data, Gifford Lab, University of Warwick), posing a problem for carrying out studies with extended time frames. Within this study we aimed to use these promoters but optimise them for use with fluorescent reporter protein procedures.

Upstream region of each gene was identified between the start codon of the gene of interest and stop codon of its preceding gene. This sequence was considered as the maximum usable upstream region and primers were designed within these boundaries with maximum possible coverage (Table 3.2). After designing the primers, a "CACC" overhang was added to the 5' end of forward primers (Table 3.2) to provide directionality for insertion into amplification vector pENTR-D/TOPO used in this study (Figure 3.8).

Table3.2. Primer sequences for amplifying cloned promoter regions of interest.

Primer name	Sequence origin	Product size (bp)	Sequence
pAtEXPA7 Forward	*A. thaliana*	630	CACCACCCTGACATTCTCTCCCAA
pAtEXPA7 Reverse	*A. thaliana*		AGAGGGGATTTTCAACGACAG
pSlyEXT1 Forward	*S. lycopersicum*	1132	CACCGCAGAAGTTTTAAGCTCTAAG
pSlyEXT1 Reverse	*S. lycopersicum*		AGAAGAATTGGATTCTAAGGC
pAtPEP Forward	*A. thaliana*	1261	CACCAACTGGTTGACAATGTGGGC
pAtPEP Reverse	*A. thaliana*		TCGAGTGTGATGTGGCCTTT
pAtCO2 Forward	*A. thaliana*	520	CACCGGGCCTAATCGCTCAAAACA
pAtCO2 Reverse	*A. thaliana*		ATGTGACCCGTGACTCTTGT
pMtrNRT1.3 Forward	*M. truncatula*	902	CACCGTTTTCCGATGGCACTATTTGT
pMtrNRT1.3 Reverse	*M. truncatula*		TGTTATGTGGCCCAAAATGC
pMtrN21 Forward	*M. truncatula*	1029	CACCCCCCAATTACAACTCCGTAGA
pMtrN21 Reverse	*M. truncatula*		TGCCACAAGAATGAAATAGCAC

Promoters were amplified from the genomic DNA of the origin of the gene sequence given in Table 3.2. pAtEXPA7, pAtCO2 and pAtPEP were amplified from *A. thaliana* Col0 ecotype, pMtrNRT1.3 and pMtrN21 were amplified from *M. truncatula* A7 ecotype and lastly pSlyEXT1 was amplified from *S. lycopersicum* Money-maker ecotype. Amplified sequences were then cloned into the gateway compatible amplification vector pENTR/D-TOPO and transformed into *E.coli* TOP10 bacteria. After antibiotic selection, colony PCR was performed to confirm the presence of the insert then eight positive colonies were grown overnight in liquid media for plasmid DNA extraction.

Next an appropriate plasmid expressing a fluorescent protein reporter in which to insert the tissue-specific promoter was determined. In studies involving tissue specific work, a major challenge is the mobility of proteins between cells (Crawford and Zambryski, 2000; Lagunas et al., 2018). Due to the highly compact nature of roots that have a high surface contact area between cells, this was of particular concern. It was possible to address this problem in two different ways. One of the major factors for protein mobility was identified as diffusion through plasmodesmata (Han and Kim, 2016), In a previous approach implemented by researchers, they increased protein product size beyond the maximum exclusion limit of plasmodesmata. A way to achieve this is by conjugating other proteins to the reporter protein. Previously, expression of a double conjugated reporter molecule (2xGFP) with 54 kDa size was

enough to significantly restrict its movement into neighbouring cells (Araújo et al., 2017; Crawford and Zambryski, 2000). Another common solution to restrict mobility was to direct reporter proteins into sub-cellular compartments using localization signals (Balkunde et al., 2017). This approach also significantly decreases mobility of proteins and increases targeting specificity.

Since constructs for tissue-specific *M. truncatula* expression were being created with future work in mind, it was decided to conjugate a second reporter protein that also allows detection with a different approach. GUS staining is a widely used technique to visualize protein localizations in root tissues (Quaedvlieg et al., 1998). Stable lines expressing GUS as well as GFP would be an extremely valuable asset in the future for researchers studying legume root and nodule development (Lagunas et al., 2018). To that end, two vectors; pKGWFS7 and pBGWFS7 (Karimi et al., 2002), were found to satisfy the conditions set above. Since these gateway compatible vectors were designed to express a GFP-GUS conjugated protein, the final size of the reporter would be 106 kDa. Knowledge from previous work on reporter protein mobility in plant tissues suggest a reporter protein with such size will have its movement to neighbouring cells significantly reduced (Crawford and Zambryski, 2000).

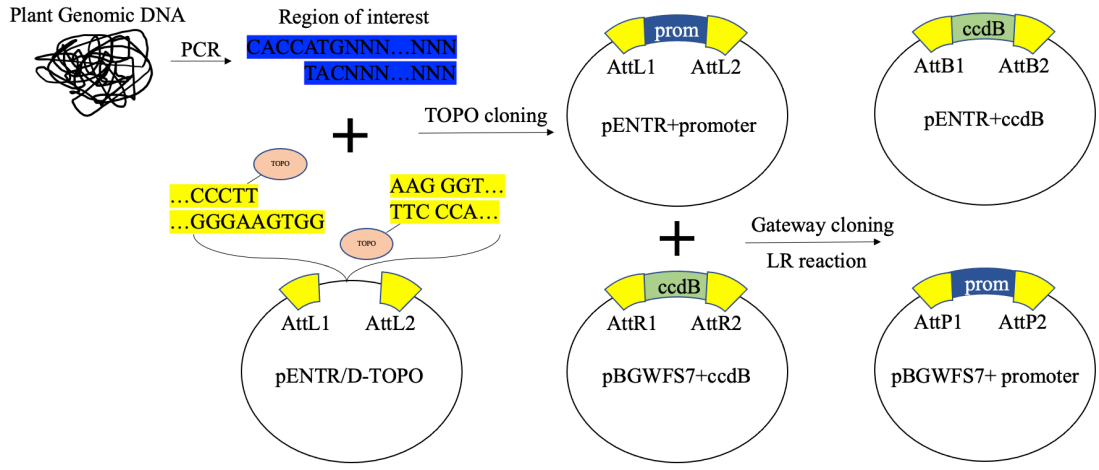

Figure 3.8. Gateway cloning strategy of promoters of interest. Upstream regulatory regions of genes of interest will be amplified by PCR using gateway compatible primers containing a CACC sequence at the 5' end of the forward primer. Amplified fragments will be inserted into gateway compatible amplification vector pENTR using D-TOPO insertion. After amplification of the plasmid, LR reaction will be carried out with pBGWFS7 vector to obtain the final product.

Gateway cloning reactions were carried out from the pENTR entry plasmid to the pBGWFS7 destination vector for each promoter sequence. Inserts were sequenced to determine the orientation of ligation as well as to confirm that there were no mutations (School of Life Sciences Genomics facility, University of Warwick. All plasmids possessed inserts with the correct orientation and no point mutations. pSlyEXT1, pAtEXPA7, pAtCO2, pAtPEP, pMtrNRT2 and pMtrN21 were successfully cloned into the pBGWFS7 destination vector. Destination vectors were then transformed into *A. rhizogenes* Arqua1 and *A. tumefaciens* GV3101 bacteria for transient and stable transformation studies respectively.

3.2.2. HAIRY ROOT TRANSFORMED PLANTS EXHIBIT RANDOM LOCALIZATIONS OF REPORTER PROTEIN

The second step in creating plant material with tissue type specific reporter expression was testing the accuracy of reporter protein localization. Since stable transformation of plants is a long and laborious process, localization of reporter proteins was investigated using hairy root transient transformation system (Chabaud et al., 2006).

First, effects of transformation on plant development and time for emergence of fluorescent roots was investigated (Figure 3.9). Although transformed plants showed slower root formation 7 days post transformation (dpt) (Figure 3.9.A), this difference was not observable after 10 dpt (Figure 3.9.A, J, D, M). No fluorescence was observed in emerging roots until 10 dpt (Figure 3.9.B, C, K, L). 75% (~23) of 30 plant roots showed florescence signal in approximately 10% (~0.5 cm) of the newly emerged root tissue at both 10 dpt and 14 dpt (Figure 3.9.O,R). Intensity and the area of fluorescence signal was increased after 14 dpt (Figure 3.9.R). In light of these results, it was decided to investigate localization of reporter proteins at 14 dpt for each vector.

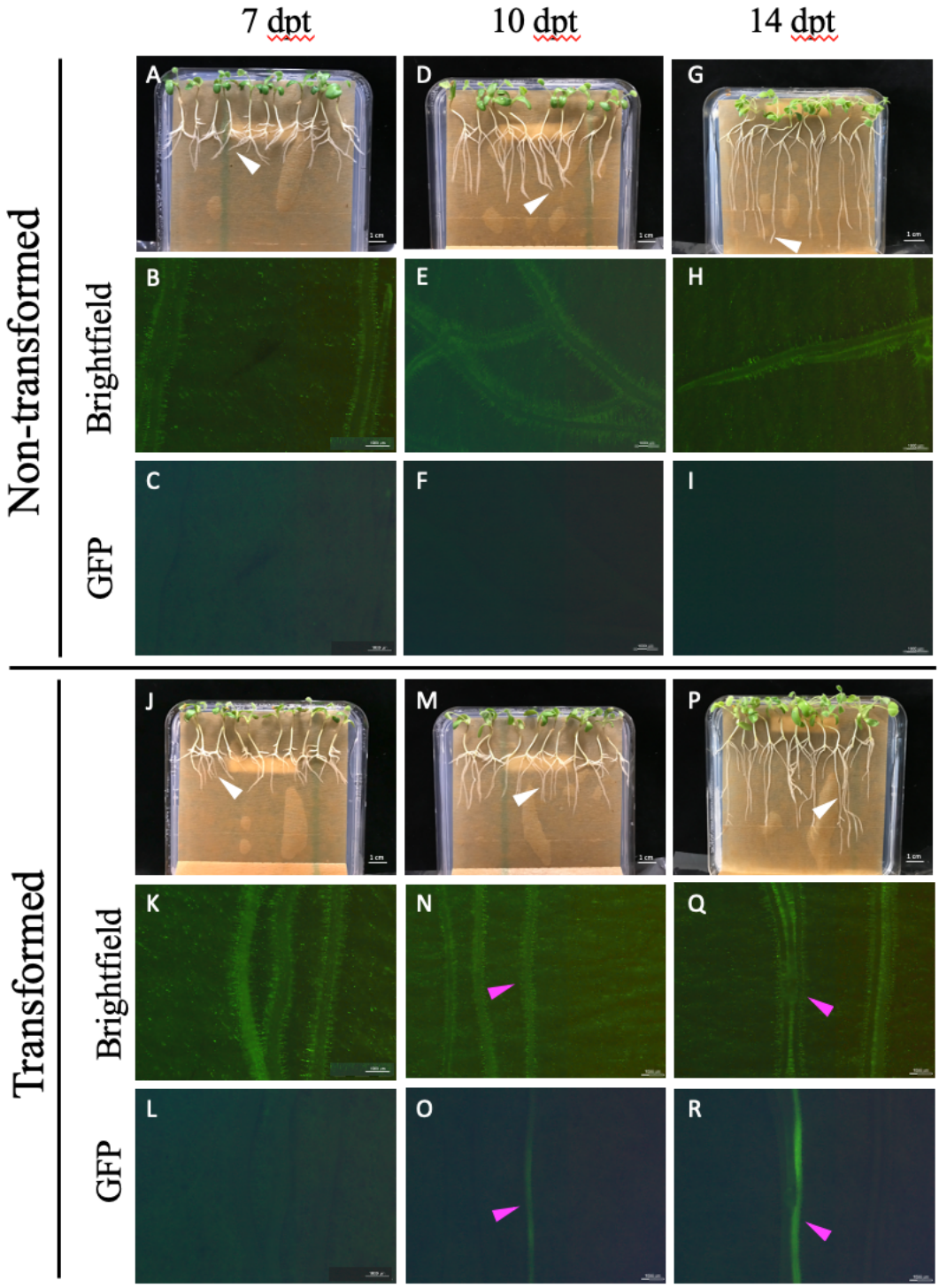

Figure 3.9. Stages of plant growth for non-transformed and hairy root transformed *M. truncatula.* Plants were transformed with pBGWFS7 plasmid containing prAtCO2::GFP-GUS at 7 (A-C, J-K), 10 (D-F, M-O) and 14 (G-I, P-R) days after transformation. White arrows indicate location of imaging from the whole root. Magenta arrows indicate presence of fluorescence. Scale bars for images A, D, G, J, M, P represent 1 cm. Scale bars for images B, C, E, F, H, I, K, L, N, O, Q, R represent 1 mm.

M. truncatula A17 ecotype seedling roots were transformed using *A. rhizogenes* Arqua1 containing the vectors created in Section 3.2.1. At 14 dpt, root sections exhibiting fluorescence were excised from four transformed seedlings (Figure 3.10) and used to prepare cross sections for confocal microscopy embedded in 5% bactoagar (Figure 3.11; 3.12; 3.13). Among the samples transformed with epidermal construct pSlyEXT1::GFP-GUS, only one of the transformed plants showed epidermal localisation, while the other three showed localisation in cortex tissue (Figure 3.11.G-I). All of the four samples for the second presumed epidermis specific construct, pAtEXPA7::GFP-GUS, showed localization in cortex tissue (Figure 3.11.D-F). All four samples prepared for presumed cortex-specific constructs pAtCO2::GFP-GUS and pAtPEP::GFP-GUS expressed GFP in the cortex (Figure 3.12.A,B). No signal was detected for plants transformed with the pericycle specific, pMtrNRT2::GFP-GUS and pMtrN21::GFP-GUS constructs (Figure 3.13.D-I).

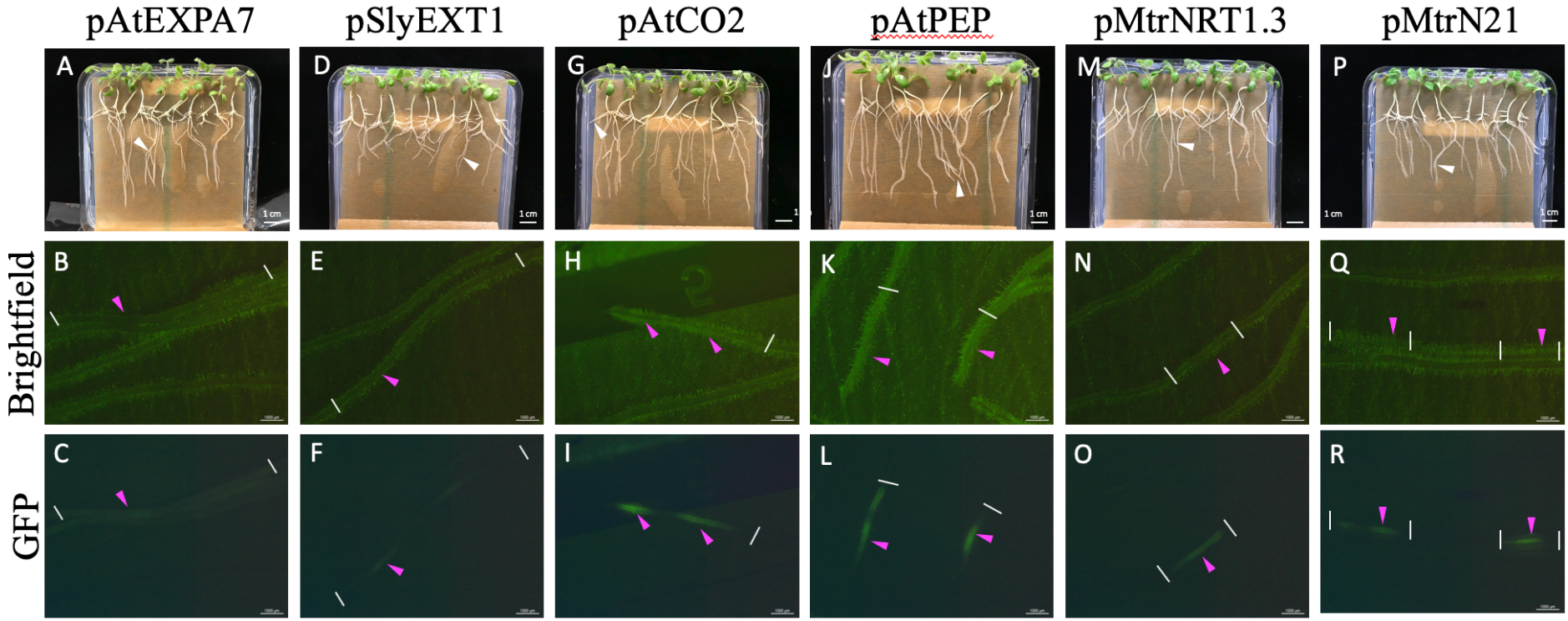

Figure 3.10. Stereomicroscope and epifluorescence images of hairy root transformed *M. truncatula* 14 days after transformation. Plants were transformed with *A. rhizogenes* containing pBGWFS7 plasmid with tissue-specific promoter. For epidermal expression, prAtEXPA7 (**A-C**), prSlyEXT1(**D-F**); cortex expression prAtCO2 (**G-I**), prAtPEP (**J-L**); pericycle expression; prMtrNRT1.3 (**M-O**), prMtrN21 (**P-R**) White arrows indicate location of imaging from the whole root. Magenta arrows indicate presence of fluorescence in the root. White lines indicate the incision points for excision of fluorescent regions to be used in preparing cross-sections. Scale bars in images **A,D, G, J, M, P** represent 1 cm. Scale bars in images **B, C, E, F, H, I, K, L, N, O, Q, R** represent 1 mm.

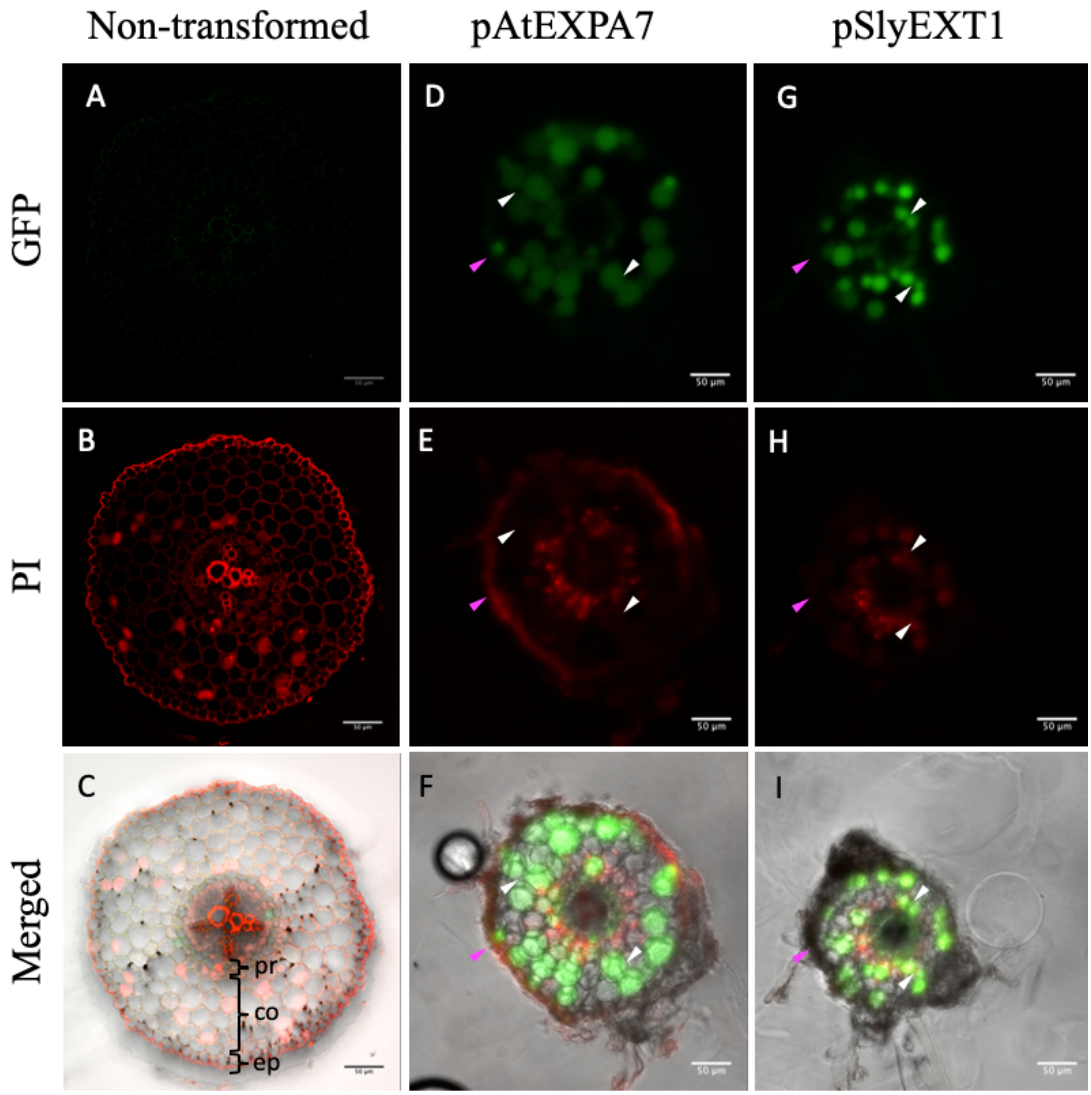

Figure 3.11. Confocal microscopy images of fluorescence positive *M. truncatula* roots transformed with epidermis specific constructs. A-C) Root cross sections of untransformed *M. truncatula* Jemalong A17 embedded in 5% bactoagar. Fluorescence positive root cross sections embedded in 5% bactoagar were obtained from hairy root transformed *M. truncatula* plants with epidermis specific promoter regions prAtEXPA7 (**D-F**) and prSlyEXT1 (**G-I**). Fluorescence signal was localized in epidermis for only one out of the four samples prepared for the prSlyEXT1 transformant (Data not shown). Fluorescence signal was localized in cortex for all four samples prepared for the prAtEXPA7. Images are representative of four cross section sample prepared from individual transformation events. White arrows represent presence of fluorescence, magenta arrows represent expected location of fluorescence presence. Scale bars represent 50 µm. (**GFP**: green fluorescence protein, **PI**: propidium iodide, **pr**: pericycle, **co**: cortex, **ep**: epidermis.)

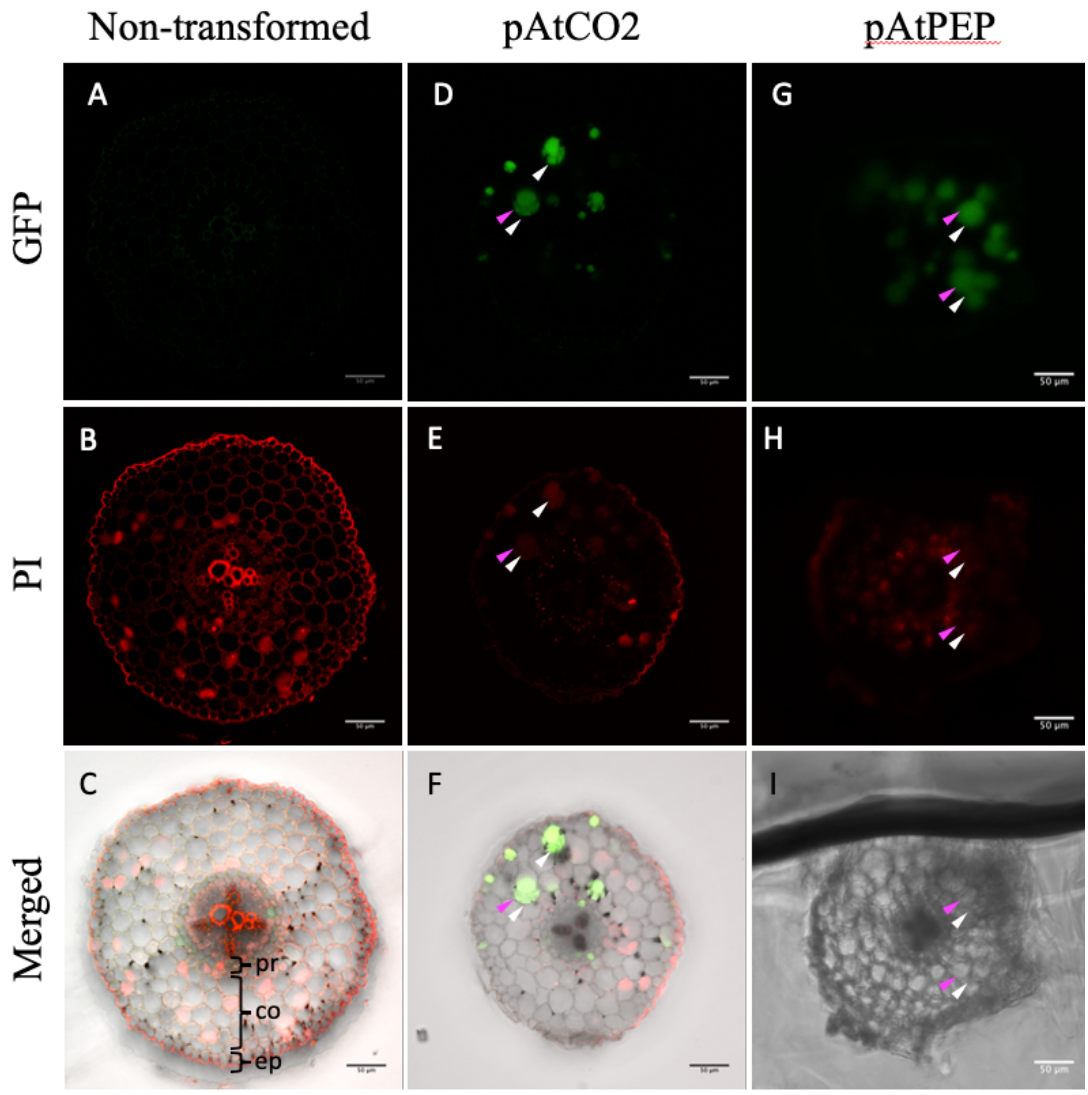

Figure 3.12. Confocal microscopy images of fluorescence positive *M. truncatula* roots transformed with cortex specific constructs. A-C) Root cross sections of untransformed *M. truncatula* Jemalong A17 embedded in 5% bactoagar. Fluorescence positive root cross sections embedded in 5% bactoagar were obtained from hairy root transformed *M. truncatula* plants with cortex specific promoter regions prAtCO2 (**D-F**) and prAtPEP (**G-I**). Fluorescence signal was localized in cortex in all four samples for plants transformed with prAtCO2 (**D**) and prAtPEP (**H**). Images are representative of four cross section sample prepared from individual transformation events. White arrows represent presence of fluorescence, magenta arrows represent expected location of fluorescence presence. Scale bars represent 50 µm. (**GFP**: green fluorescence protein, **PI**: propidium iodide, **pr**: pericycle, **co**: cortex, **ep**: epidermis.)

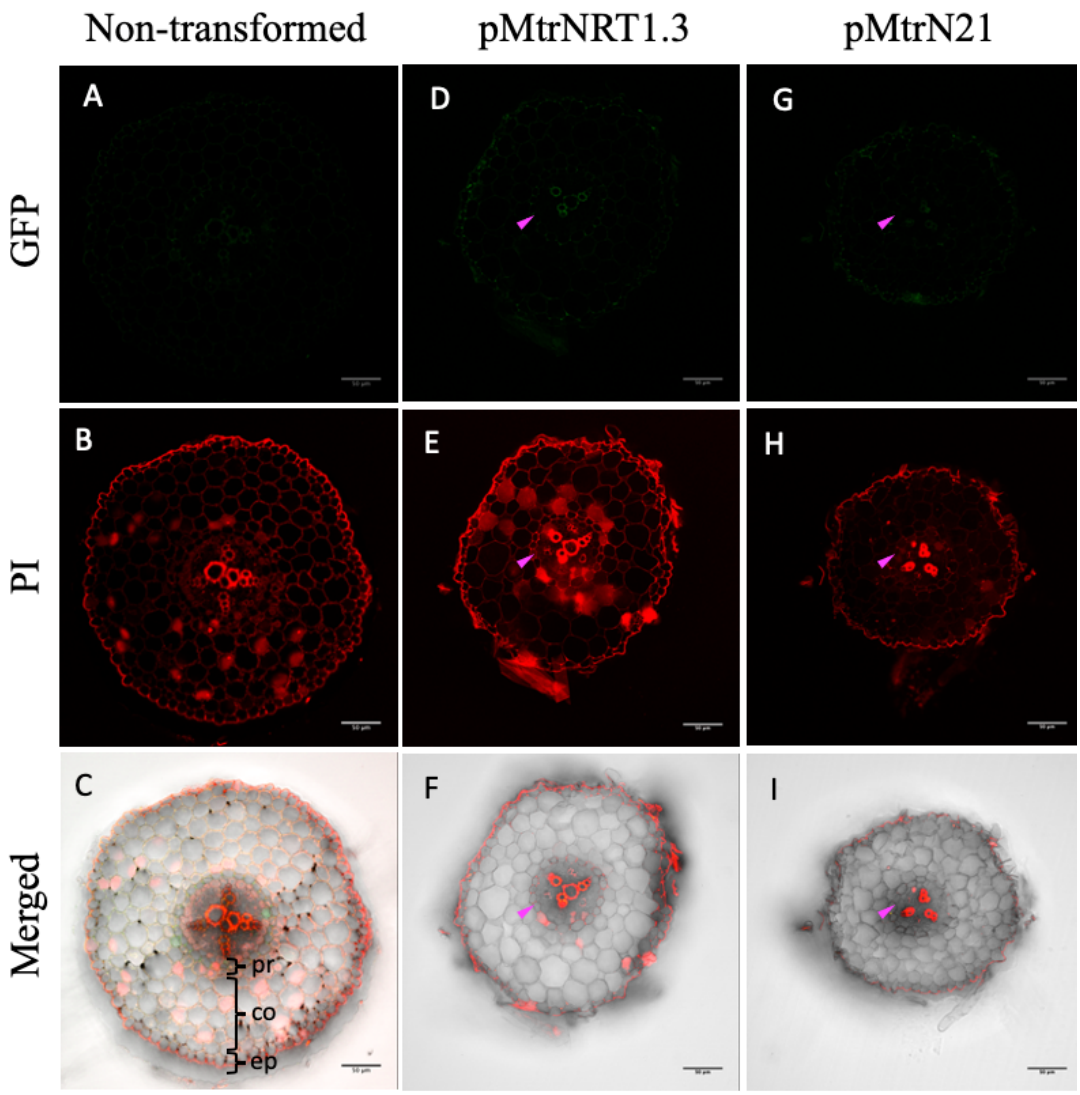

Figure 3.13. Confocal microscopy images of fluorescence positive *M. truncatula* roots transformed with pericycle specific constructs. A-C) Root cross sections of untransformed *M. truncatula* Jemalong A17 embedded in 5% bactoagar. Fluorescence positive root cross sections embedded in 5% bactoagar were obtained from hairy root transformed *M. truncatula* plants with pericycle specific promoter regions prMtrNRT1.3 (**D-F**) and prMtrN21 (**G-I**). No fluorescence signal was detected in any of the four samples for plants transformed with prMtrNRT1.3 (**D**) and prMtrN21 (**H**) when compared to images obtained from non-transformed samples (**A**). Images are representative of four cross section sample prepared from individual transformation events. White arrows represent presence of fluorescence, magenta arrows represent expected location of fluorescence presence. Scale bars represent 50 µm. (**GFP**: green fluorescence protein, **PI**: propidium iodide, **pr**: pericycle, **co**: cortex, **ep**: epidermis.)

At the end of the second stage of this study, two of the six vectors originally created for tissue type specific expression in *M. truncatula* A17 roots showed correct localization to their respective tissue types while one showed mixed but promising results. So, in light of these findings, it was possible to expand the library of material available for tissue type specific studies in *M. truncatula*. Materials showing positive results can be used in future studies for stable transformation of legume model plants, providing visualization with both fluorescent and GUS staining methods.

3.2.3. HAIRY ROOT TRANSFORMATION TRIALS FOR STUDYING TISSUE SPECIFIC RESPONSES USING FACS

As previously mentioned, stable transformation of *M. truncatula* is a long and laborious process. In the previous stages of this study, two reporter constructs; pAtPEP::eGFP-GUS and pAtCO2::eGFP-GUS, were successfully created for marking the cortex using hairy root transformation method. At this stage of the study, feasibility of working with transiently transformed plants to study tissue-type specific responses upon changing nitrogen concentrations was investigated.

In this workflow, 40 *M. truncatula* plants were subjected to hairy root transformation and grown on N-deficient (0.5 mM) media for two weeks. However, it was observed that the efficiency of transformation was reduced when plants were grown in N-deficient concentrations (0.5 mM) following hairy root transformation, as compared to the efficiency when they were grown on N-sufficient media (1 mM). In order to understand the effects of N availability on transformation efficiency, 80 *M. truncatula* plants were subjected to hairy root transformation with pAtCO2::GFP-GUS construct and split into two groups. While one group was grown on N-deficient (0.5 mM) media the other was grown on N-sufficient (1 mM) media. This experiment was replicated twice and transformed number of roots and length of fluorescence signal was observed at 7, 10 and 14 dpt in each experiment (Figure 3.14). It was found that number of transformed plants per experiment was increased from ~8 (20%) to ~30 (~75%) when they were supplied with sufficient nitrogen concentrations following transformation (Figure 3.14.B). It was also observed that the average length of transformed root sections were longer in samples supplied with sufficient nitrogen, with an increase from 5±2 mm, to 7±3 mm (Figure 3.14. F, O; I, R).

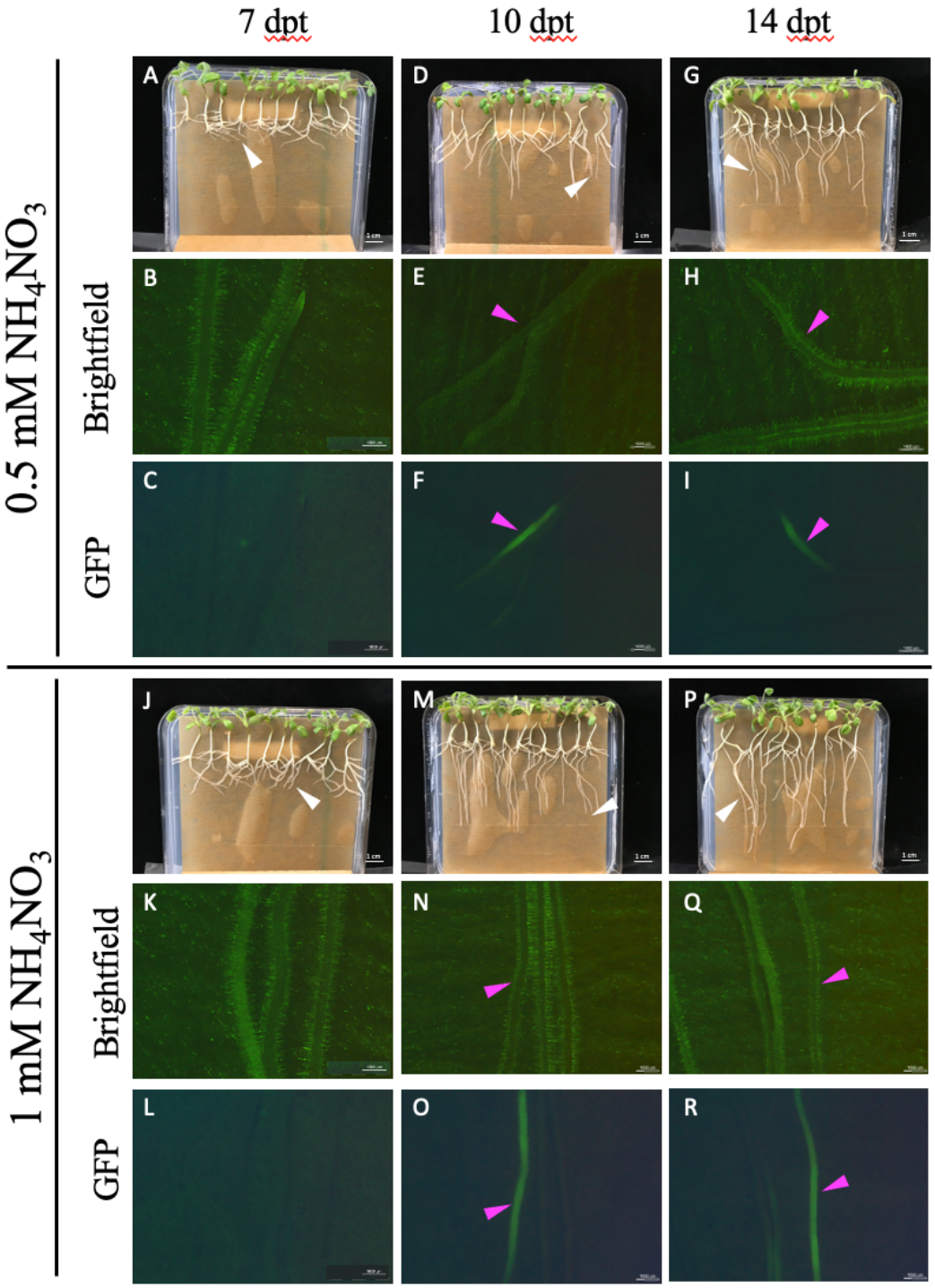

Figure 3.14. Stages of hairy root transformed *M. truncatula* growth on MFM with deficient (0.5 mM) and sufficient (1 mM) N concentrations. Plants were transformed with pBGWFS7 plasmid containing prAtCO2::GFP-GUS. Fluorescence presence in roots were investigated 7 (**A-C, J-K**), 10 (**D-F, M-O**) and 14 (**G-I, P-R**) days after transformation using epifluorescence microscopy. White arrows indicate location of imaging from the whole root. Magenta arrows indicate presence of fluorescence. Scale bars for images **A, D, G, J, M, P** represent 1 cm. Scale bars for images **B, C, E, F, H, I, K, L, N, O, Q, R** represent 1 mm.

This reduction in sample availability has direct effect on the number of material available for protoplast generation as it reduces the number of protoplasts available to run through FACS for isolation. In order to obtain a high number of transformants, samples might need to be grown on media with sufficient N post transformation. However, this raised the question; could plants still produce a distinguishable response towards excess N treatments (>5 mM) if they were grown on N sufficient (1 mM) concentrations? To test this, 40 *M. truncatula* A17 seedlings were transiently transformed with pAtCO2::GFP-GUS, split into three groups and were grown on MFM media supplied with sufficient (1mM) NH_4NO_3; with three replicates. After 14 days, roots of each group were treated with either 1 mM NH_4NO_3, 5 mM NH_4NO_3 or 10 mM NH_4NO_3 for 2 hours. Roots were subjected to protoplast generation and total mRNA was extracted from protoplasts. qPCR analysis was performed to quantify expression levels of known nitrogen responsive genes; NRT2.1, a HATS nitrate transporter; NITRATE REDUCTASE 1 (NIA1), the first enzyme in the nitrate assimilation pathway of higher plants (Yu et al., 1998) and NIR (Figure 3.15). It was found that despite being grown on a media with sufficient nitrogen source, plants retain their ability to respond to excess nitrogen concentrations. Gene expression was increased 3-fold for NRT2.1, 7-fold for NIA1 and 4-fold for NIR gene when plants were treated with 5 mM NH_4NO_3 in comparison to the mock treatment with 1 mM NH_4NO_3. This response was found to be dose dependent for NIA1 and NIR genes which exhibited a 24-fold and 8-fold change in gene expression when treated with 10 mM NH_4NO_3 in comparison to the mock treatment with 1 mM NH_4NO_3. Whereas NRT2.1 gene expression did not change after treatment with 10 mM NH_4NO_3. Collectively, these results indicate it was possible to induce gene expression by excess N applications even if the plants were grown on media supplied with sufficient N.

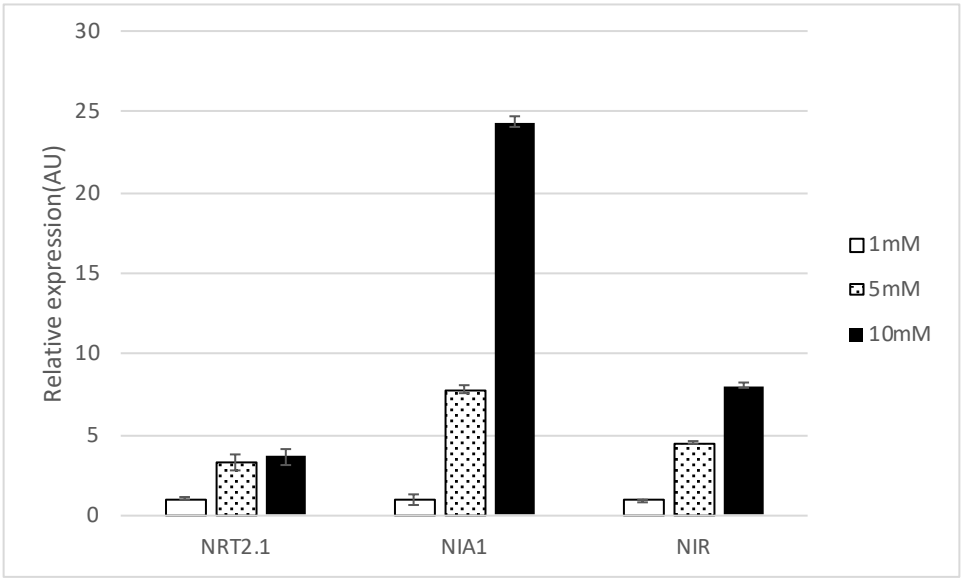

Figure 3.15. Expression levels of N responsive genes after treatment with mock (1 mM) and excess (5 mM, 10 mM) N concentrations. *M. truncatula* were subjected to hairy root transformation with pBGWFS7 vector containing pAtCO2::GFP-GUS and grown on 1 mM MFM plates for 14 days before treating with mock (1 mM NH_4NO_3), 5 mM (**Dotted columns**) or 10 mM (**Black columns**) NH_4NO_3. NRT2.1 gene expression increased 3-fold after 5 mM NH_4NO_3 treatment (**Dotted columns**) compared to mock treated plants. Same fold change was observed in plants treated with 10 mM NH_4NO_3 (**Black columns**). NIA1 gene expression increased 7-fold and 24-fold after while NIR gene expression increased 4 and 8-fold after 5 mM (**Dotted columns**) and 10 mM (**Black columns**) NH_4NO_3 treatment respectively. Graph depicts results obtained from one biological replicate and error bars represent technical replicates.

3.2.4. Testing protoplast generation efficiency in M. truncatula roots after hairy root transformation and N treatment

In order to determine the efficiency of protoplast generation from transformed roots, transformed plants were grown on MFM media containing sufficient (1 mM) NH_4NO_3 for 14 days and then treated with MFM media supplied with excess (10 mM) NH_4NO_3 concentrations. With sufficient NH_4NO_3 supply, transformation efficiency was observed to be ~75% (22) out of 30 transformed plants. Root sections exhibiting fluorescence were harvested to generate protoplasts. Protoplast suspension mixture was then profiled using FACS with gates created in 2-D scatter plots containing forward scatter (FS) or autofluorescence (B488-695/40-A) at x- axis, and GFP filter (B488-530/30-A) on y-axis (Figure 3.16) (Section 2.6.8) (Grønlund et al., 2012). Data obtained from this profiling was then used to quantify ratio of fluorescent protoplasts obtained per transformed plant.

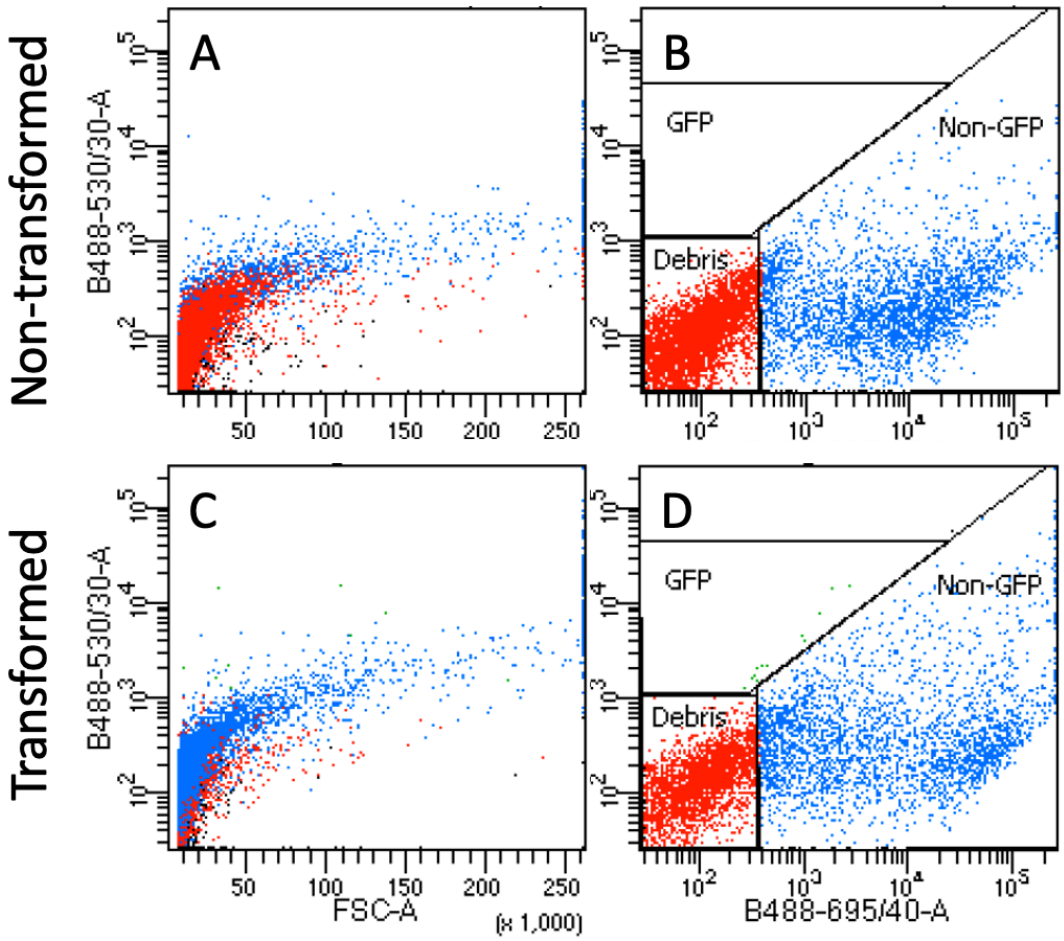

Figure 3.16. Protoplast profiles of fluorescence positive hairy root transformed and non-transformed *M. truncatula* roots. A&C) 2-D scatterplot of events showing green fluorescence intensity levels (Excitation: 488nm, Emission: 530±15 nm) and forward scatter values. Each dot represents an interrogated event by FACS. Colours of the dots indicate which gate they belong to in panel B&D. **B&D)** 2-D scatterplot of events showing green fluorescence intensity levels (Excitation: 488 nm, Emission: 530±15 nm) and red fluorescence intensity levels (Excitation: 488 nm, Emission: 695±20 nm). Gates are drawn around events exhibiting GFP presence (Green), no/low GFP presence (Blue) and cell debris (Red). No GFP events were identified in non-transformed plants while GFP events cells totalled ~1% of the total events interrogated from transformed plants.

This experimental design was run with two biological replicates and for each experiment a maximum of 500 fluorescent positive protoplasts were identified out of all protoplasts ($5x10^4$) generated.

To obtain high enough mRNA concentrations for standard RNAseq, a minimum of $1x10^3$ protoplasts were required. From flow cytometry profiles, it can be seen that the fluorescent population is approximately 1% of the total number of events. This means that a total of $1x10^5$ protoplasts would be required to achieve the necessary number of fluorescent protoplasts. From protoplast generation experiments during the study, it

was found that approximately 37 protoplasts could be generated per mm root tissue used following the protocol in Section 2.3.7. Also, from previous transformation studies in this work, it was found that approximately 7 mm section of each transformed root exhibited fluorescence. Using these numbers, it was calculated that the average number of total protoplasts obtained from one transformed plant was approximately 259. Taking into account that only 75% of plants exhibit fluorescence after hairy root transformation, 515 seedlings would have to be transformed per biological replicate. Due to the dynamic nature of plant nitrogen responses, handling >515 plants for transformation and harvesting fluorescence positive fluorescence tissue might lead to missing expression frames for detection. Thus, hairy root transformation method utilized in this study for transformation of *M. truncatula* roots was concluded to be an inefficient system to study tissue type specific expression changes to environmental stimuli compared to the reliable expression and abundant material provided by plant material with stable transformations. In light of these findings, reporter plasmid constructs were used to start stable transformation of *M. truncatula*.

3.2.5. META-ANALYSIS OF NITROGEN RESPONSES IN M. TRUNCATULA COMPARED TO A. THALIANA AT THE TISSUE TYPE LEVEL

With the decrease of inorganic N fertilizer efficiency, overfertilization of land has had to increase to retain total yields (Lassaletta et al., 2014). This in turn leads to run-off of excess nitrogen to water bodies which causes significant environmental damage due to eutrophication (FAO and ITPS, 2015). Recent agricultural practices have started to make more use of biological fertilization methods through application of nodulating legume plants (Valentine et al., 2018). However, elevated N levels remaining in soil can inhibit nodule formation in legumes (Streeter, 1985). Thus, in order to gain a better understanding into the nodulation mechanism of legumes, potential overlap between nitrogen responses between species was investigated. In order to achieve this, differential expression of N-responsive orthologs genes were identified in *A. thaliana* root epidermis, endodermis, pericycle and stele tissues and compared with the N-responsiveness of these genes in *M. truncatula* whole roots in response to excess N treatment (5mM KNO_3).

In this approach, the microarray dataset obtained from Gifford et al. 2008 that was analysed consisted of *A. thaliana* transgenic lines expressing GFP in either epidermis, endodermis, pericycle or stele tissue. Plants were grown for 12 days and treated with

either 5 mM KNO_3 (excess N treatment) or 5 mM KCl (mock). Protoplasts were generated from N-treated roots and those exhibiting fluorescence (indication of a tissue type) were isolated using FACS for each transgenic line. Total RNA was extracted from sorted protoplasts and used in microarray gene expression analysis (Gifford et al., 2008). The microarray data from this work was re-analysed and genes exhibiting significant (*P*-value<0.05) upregulation (UR) above 2-fold or downregulation (DR) below 0.5-fold in response to excess N were determined for each tissue type out of a total of 22810 genes represented on the *A. thaliana* microarray used (Table 3.3).

Table.3.3. Number of tissue-specific DE genes in *A. thaliana* and number of their corresponding homologs in *M. truncatula*. (UR = N-upregulated, DR = N-downregulated.)

Tissue types	# *A. th* genes
Epidermis-UR	41
Epidermis-DR	113
Endodermis-UR	20
Endodermis-DR	35
Pericycle-UR	4321
Pericycle-DR	40
Stele-UR	14
Stele-DR	1529

Next, corresponding putative orthologs of these DE genes in *A. thaliana* were identified in *M. truncatula*, as described in Section 2.8.3. In doing so, lists of genes were obtained with potential tissue specific expression in *M . truncatula* root tissues. Since no tissue specific transcriptomic work is available in *M. truncatula* roots, expression of these ortholog gene lists were interrogated in transcriptomic analysis of *M. truncatula* whole roots with excess N treatment (Gifford lab, Unpublished data, University of Warwick) to at least determine if they were N-responsive in whole roots, and the direction of regulation (N-upregulated or N-downregulated). In the N-response experiment used to generate this dataset, 8 *M. truncatula* seedlings had been grown for 8 days and roots were subjected to either 5 mM KNO3 (excess N treatment) or 5 mM KCl (mock) for 2 hrs. Treated roots had either been used directly for total RNA

extraction or subjected to protoplast generation followed by total RNA extraction, or order to ask which genes were affected by the protoplast generation procedure. Extracted RNA had been amplified and hybridized to microarrays.

The dataset was obtained and first, in order to utilise more up to date bioinformatic analysis, *M. truncatula* v3.0 gene IDs used at the time of the experiment for constructing microarray probes were converted into their JCVI *M. truncatula* v4.0 equivalents (see Section 2.8.3) (Tang et al., 2014). Likely because the v3.0 genome annotation of *M. truncatula* consisted of genes identified by bioinformatic approaches, there is a low overlap between genes annotated in v3.0 and v4.0. Therefore, during conversion of gene IDs into v4.0, only approximately 40% of the microarray probes were found to map to v4.0 possessed equivalents.

In order to remove genes whose expression was affected by protoplast mock treated samples of whole root and root protoplast were compared. 1463 genes were found to exhibit significant differential expression between them, indicating expression changes due to protoplast generation. No significant GO enrichment was found for these protoplast generation stress responsive genes and they were excluded from any further analysis

Table.3.4. Number of overlapping or opposing N responsive genes after comparison of tissue specific ortholog genes identified in *A. thaliana* with genes identified in *M. truncatula* whole roots.

	Overlapping (*A.th*/*M.tr*)		Opposite (*A.th*/*M.tr*)	
	UR/UR	DR/DR	UR/DR	DR/UR
Epidermis	0	0	0	0
Endodermis	0	0	0	0
Pericycle	13	1	3	0
Stele	0	2	0	5

From this N responsive genes, ones exhibiting significant UR (*P*-value<0.05) above 2-fold or DR below 0.5-fold in response to excess N treatment were identified. After this comparison, a total of 88 genes were found to have significant (*P*-value<0.05) DE with 53 UR and 35 DR genes in *M. truncatula* whole roots in response to 5 mM KNO_3 treatment. When the N-responsive ortholog list from the *A. thaliana* study and N responsive gene list from the *M. truncatula* study were compared, there were a total of

16 overlapping DE genes. Of these 16 genes, 14 (13 UR, 1 DR) were identified in pericycle and 2 (0 UR, 2DR) were identified in stele tissue types (Table 3.4). There were no overlap of orthologous genes found to be N-regulated in *M. truncatula* whole roots and in *A. thaliana* epidermis or endodermis.

Next, the identity and annotation of each gene was investigated in order to ask whether their common regulation by nitrogen in *M. truncatula* and *A. thaliana* might make sense. In pericycle, 5 of the UR genes were hypothetical, thus were not followed up on. Although analysis of their *A thaliana* orthologs could be useful in future. The remaining 8 non-hypothetical UR genes in pericycle were found to localize to a wide range of cellular components including nucleus, cytoplasm, mitochondria and plasma membrane. Two of these UR genes, SEVEN IN ABSENTIA (SINA) (Medtr5g076540) and Ubiquinol oxidase 1a (Medtr5g026620) were found to have activity in ubiquitin dependent protein degradation. Two other UR genes, Triacylglycerol lipase SDP1 (Medtr1g087300) and P21-Rho-binding domain protein (Medtr1g041515) had functions in lipid catabolic processes and transfer. The remaining three UR and one DR genes exhibited a variety of functions including metal ion binding, DNA binding and kinase activity.

In stele tissue two genes were identified to be N-down-regulated in both species. These were: Pentameric polyubiquitin (Medtr6g061930), involved in ubiquitin dependent protein degradation pathway and chorismate mutase (Medtr1g013900), involved in shikimate pathway.

Table. 3.5. List of overlapping genes differentially expressed in both *A. thaliana* tissue types and *M. truncatula* whole roots after N treatment. (DE gene selection performed as described in Section 2.8.3. GO terms are descriptive of identified genes)

A. thaliana Tissue	v.4.0 ID	Expressed protein	GO Terms		
			Cellular Component	Molecular Function	Biological Process
Upregulated					
Peri	Medtr1g087300	Triacylglycerol lipase SDP1		GO:0004806	GO:0016042
Peri	Medtr5g076540	Seven in absentia family protein	GO:0005634	GO:0004839 GO:0008270 GO:0016746	GO:0007275 GO:0006511
Peri	Medtr5g083820	DUF1639 family protein		GO:0016301	
Peri	Medtr7g070715	PIF1-like helicase		GO:0005524 GO:0003678	GO:0000723 GO:0006281 GO:0006310
Peri	Medtr5g026620	Ubiquinol oxidase 1a	GO:0005739 GO:0016021 GO:0070469	GO:0009916 GO:0046872 GO:0102721	GO:0010230
Peri	Medtr1g041515	P21-Rho-binding domain protein	GO:0005737	GO:0120013	GO:0120009
Peri	Medtr1g019680	Agenet domain protein		GO:0046872	GO:0030001
Peri	Medtr4g006330	Hypothetical		GO:0003676 GO:0004523	
Peri	Medtr3g057920	Hypothetical	GO:0016592		GO:0006355
Peri	Medtr5g034180	Hypothetical	GO:0000793	GO:0030674	GO:0007131 GO:0042138
Peri	Medtr6g465290	Hypothetical	GO:0009507		
Peri	Medtr2g047120	Hypothetical	GO:0016021		
Downregulated					
Peri	Medtr1g105840	Cysteine-rich receptor-kinase-like protein	GO:0005886 GO:0016021	GO:0004674 GO:0005524	GO:0006468
Stele	Medtr6g061930	Pentameric polyubiquitin	GO:0005634 GO:0005737	GO:0031386 GO:0031625	GO:0016567 GO:0019941
Stele	Medtr1g013900	Chorismate mutase		GO:0004106	GO:0009073 GO:0046417

GO Terms legend

Cellular Component		Molecular Function		Biological Process	
GO Term	Description	GO Term	Description	GO Term	Description
GO:0000793	Condensed Chromosome	GO:0003676	Nucleic acid binding	GO:0046417	Chorismate metabolic process
GO:0005634	Nucleus	GO:0003678	DNA helicase activity	GO:0000723	Telomere maintenance
GO:0005737	Cytoplasm	GO:0004106	Chorismate mutase activity	GO:0006281	DNA repair
GO:0005739	Mitochondrion	GO:0004523	RNA-DNA hybrid ribonuclease activity	GO:0006310	DNA recombination
GO:0009507	Chloroplast	GO:0004674	Protein serine/threonine kinase activity	GO:0006355	Regulation of transcription, (DNA-templated)

GO:0016021	Integral component of membrane	GO:0004806	Triglyceride lipase activity	GO:0006468	Protein phosphorylation
GO:0016592	Mediator complex	GO:0004839	Ubiquitin activating enzyme activity	GO:0006511	Ubiquitin dependent protein catabolic process
GO:0070469	Respirasome	GO:0005524	ATP binding	GO:0007131	Reciprocal meiotic recombination
GO:0005886	Plasma membrane	GO:0008270	Zinc ion binding	GO:0007275	Multicellular organism development
		GO:0009916	Alternative oxidase activity	GO:0009073	Aromatic amino acid family biosynthetic process
		GO:0016301	Kinase activity	GO:0010230	Alternative respiration
		GO:0016746	Transferase activity (Acyl groups)	GO:0016042	Lipid catabolic process
		GO:0030674	Protein-macromolecule adaptor activity	GO:0016567	Protein ubiquitination
		GO:0031386	Protein tag	GO:0019941	Modification-dependent protein catabolic process
		GO:0031625	Ubiquitin protein ligase binding	GO:0030001	Metal ion transport
		GO:0046872	Metal ion binding	GO:0042138	Meiotic DNA double-strand break formation
		GO:0102721	Ubiquinol: Oxygen reductase activity	GO:0120009	Intermembrane lipid transfer
		GO:0120013	Lipid transfer activity		

As well as the commonly regulated genes (i.e., N-regulated in the same direction in both species, which were the majority of common responses), we also found a total of 8 oppositely DE genes when two studies were compared (Table 3.4). Of these, 3 were identified in pericycle and all were UR in *A. thaliana* while being DR in *M. truncatula* roots. One of the two genes was ANAC079/ANAC080/ATNAC4 (Medtr7g011120) which is found in nucleus and involved in regulation of gene expression while the other was Pentameric polyubiquitin (Medtr6g061930), which is also found in nucleus with a function in ubiquitin dependent protein degradation process. The remaining 5 genes in this list were DR in the *A. thaliana* stele and UR in *M. truncatula* roots. Two genes out of 5 were hypothetical thus were not investigated further. The remaining three genes were: SINA family protein (Medtr5g076540) which is associated with nucleus and functions in ubiquitin dependent protein degradation processes (the same gene that is UR in *A. thaliana* pericycle) while others were DUF1639 family protein (Medtr5g083820) and a G-type lectin S-receptor-like Serine/Threonine-kinase (Medtr2g011240) with no defined activity in a particular nitrogen-related process (Table 3.6).

Table.3.6. List of genes oppositely differentially expressed in *A. thaliana* tissue types and *M. truncatula* whole roots after N treatment. (DE gene selection performed as described in Section 2.8.3. GO terms are descriptive of identified genes)

A. thaliana Tissue	v.4.0 ID	Expressed protein	GO Terms		
			Cellular Component	Molecular Function	Biological Process
UR/DR (A.th/M.tr)					
Peri	Medtr7g011120	ANAC079/ANAC080/ATNAC4 protein	GO:0005634	GO:0003677	GO:0006355
Peri	Medtr6g061930	Pentameric polyubiquitin	GO:0005737 GO:0005634	GO:0031386 GO:0031625	GO:0016567 GO:0019941
Peri	Medtr2g010840	Putative Transmembrane protein	GO:0016021		
DR/UR (A.th/M.tr)					
Stele	Medtr5g076540	Seven in absentia family protein	GO:0005634	GO:0004839 GO:0008270 GO:0016746	GO:0007275 GO:0006511
Stele	Medtr2g047120	Hypothetical	GO:0016021		
Stele	Medtr5g083820	DUF1639 family protein		GO:0016301	
Stele	Medtr2g011240	G-type lectin S-receptor-like kinase	GO:0005886 GO:0016021	GO:0004674 GO:0005524 GO:0030246	GO:0006468 GO:0048544
Stele	Medtr4g006330	Hypothetical		GO:0003676 GO:0004523	

GO Terms legend

Cellular Component		Cellular Component		Cellular Component	
GO Term	GO Term	GO Term	GO Term	GO Term	GO Term
GO:0005634	Nucleus	GO:0003676	Nucleic acid binding	GO:0006355	Regulation of transcription, (DNA-templated)
GO:0005737	Cytoplasm	GO:0003677	DNA binding	GO:0006468	Protein phosphorylation
GO:0005886	Plasma membrane	GO:0004523	RNA-DNA hybrid ribonuclease activity	GO:0006511	Ubiquitin dependent protein catabolic process
GO:0016021	Integral component of membrane	GO:0004674	Protein serine/threonine kinase activity	GO:0007275	Multicellular organism development
		GO:0004839	Ubiquitin activating enzyme activity	GO:0016567	Protein ubiquitination
		GO:0005524	ATP Binding	GO:0019941	Modification-dependent protein catabolic process
		GO:0008270	Zinc ion binding	GO:0048544	Recognition of pollen
		GO:0016301	Kinase activity		
		GO:0016746	Transferase activity (Acyl groups)		
		GO:0030246	Carbohydrate binding		
		GO:0031386	Protein tag		
		GO:0031625	Ubiquitin protein ligase binding		

In this study some genes were found to have different expression patterns depending on the tissue type that they were expressed in. While SINA family protein (Medtr5g076540), DUF1639 family protein (Medtr5g083820) and two hypothetical proteins (Medtr4g006330, Medtr2g047120) were all UR in pericycle, in stele tissue they were found to be DR in *A. thaliana* and UR in *M. truncatula*. Similarly, Pentameric polyubiquitin (Medtr6g061930) was found to be DR in both *A. thaliana* stele and *M. truncatula* roots. However, it was found to be UR in *A. thaliana* pericycle, but DR in *M. truncatula*. This shows the importance of tissue specific work in accurately quantifying gene expression in a multicellular organism.

3.3. DISCUSSION

Tissue specific reporter expression in hairy root transformed *M. truncatula* roots

In this work it was possible to express a fluorescent reporter protein in *M. truncatula* root cells without any diffusion to neighbouring cells using cell type specific promoter expression via the transient transformation 'hairy root' protocol. Compared to previous work conducted with hairy root transformation for GUS reporter protein expression, the length of transformed root area/plant seemed to be significantly lower in this study (Díaz et al., 2005; Mysore and Senthil-Kumar, 2015). Previously it was indicated that use of selection molecules such as kanamycin improved selection efficiency (Boisson-Dernier et al., 2001), however research conducted in Gifford lab (Unpublished data, University of Warwick) suggests use of selection using antibiotics did not bring any increase in the number of root segments found to be transformed. Thus, it might be worthwhile to adopt a different method of culture for hairy root transformed *M. truncatula* seedlings more suitable for use of selective molecules such as kanamycin or BASTA. These molecules are contact selective molecules meaning that in order for them to function, plant tissue has to be in contact with the media containing these molecules. Thus, it is possible the use of growth pouches could be preventing the molecules from working. So, here it is proposed that post-transformation culture conditions without use of growth pouches should be optimized if hairy root transformed plants are to be used in future studies.

Of the six constructs designed for the purpose of tissue-specific expression of GFP-GUS reporter protein, only two, pAtCO2::YFP-GUS and pAtPEP::YFP-GUS were truly cell-type specific. Tissue-specific expression of the other four promoters had been found in previous studies (Hayashi et al., 2014; Lee et al., 2006; Sevin-Pujol et al., 2017); thus, it is possible that the issue lies with the protocol used in this work, rather than the constructs. A previous study also reported mis-localization in hairy root transformations and hypothesized that they were caused by random integration of inserts into the genome of the organism (Boisson-Dernier et al., 2001). Activity of promoter regions is highly dependent on chromatin topology of the cell at a given time. Tissue-specific genes of differentiated cells are often found in genomic regions with euchromatin conformation (Marstrand and Storey, 2014). If the transformed sequence is integrated into the heterochromatin region of the genome, reporter proteins cannot be transcribed, leading to silencing. Alternatively, it is also possible for the insert to

integrate itself to a genomic region also active in different tissue types. In such an event, the promoter driving expression of the reporter could express the reporter protein in a different location. In this study, it was found that the majority of vectors led to reporter expression in cortex tissue. It is possible that the transformation events observed in the study resulted in integration of the insert into locations that are accessible for the cortical tissue of the root, and it would be interesting to investigate this further.

Despite being a fast method for testing constructs, the inability to produce consistent material with reliable expression has been acknowledged as the main drawback of hairy root transformation protocol should the researcher want to isolate transformed cells for further analysis (such as via FACS) (Bortesi and Fischer, 2015). Besides, although it is possible to perform single cell RNA sequencing with current technology from a small number of (transformed) cells, information obtained from low quantity RNA-seq experiments could be skewed due to gene 'dropouts' where gene expression can be observed in one sample but not in another as a result of mRNA starting quantity, quality and amplification efficiency during sequencing (Kharchenko et al., 2014). Thus, generation of good sequencing data requires a minimum of $1x10^3$ cells for high accuracy results and it was calculated that this would require an immensely large amount of plant material to start with (Section 3.2.4). For these reasons, it is suggested that the future experiments involving isolation of *M. truncatula* root tissue-type transcriptome data utilizes stable transformants expressing tissue-specific reporters.

Exploring tissue specific genes in *M. truncatula* using bioinformatic approaches

In the Section 3.2.5, a number of genes with similar N-response patterns were identified in pericycle or stele tissues in *A. thaliana* compared to in *M. truncatula* roots using bioinformatic investigation. The fact that these genes were DE in both whole root of *M. truncatula* as well as pericycle or stele of *A. thaliana* suggests that they might indeed have a functional role in root N responses, and it is possible to predict that they might be N-responsive in these inner cell types in *M. truncatula*. This could be explored in future work using cell type specific reporter lines from the promoters of the genes that were identified. Similar to described in Gifford *et al.*, 2008, different expression patterns for the same genes were observed depending on the tissue they were expressed in *A. thaliana*, compared to their whole root expression directions in *M. truncatula*, strengthening the importance of carrying out tissue specific studies.

One such protein that has different N-responses depending on cell type was SEVEN IN ABSENTIA (SINA), an E3 ligase that is involved in determining ubiquitination specificity by 'selecting' the target proteins (Herder et al., 2008). It was UR upon N treatment in *A. thaliana* pericycle tissue as well as *M. truncatula* roots, but DR in *A. thaliana* stele tissue and UR in *M. truncatula* roots after N treatment. This protein contains an N-terminally located RING finger domain and a conserved SINA domain (Hu and Fearon, 1999). Functionally, SINAs were found to regulate auxin-induced lateral root (LR) formation in *A. thaliana.* This effect was linked to SINA5 targeting of NAC1 transcription factor for ubiquitin dependent proteolysis (Xie et al., 2002). NAC1 is a member of the *NO APICAL MERISTEM/CUP-SHAPED COTYLEDON* (NAM/CUC) family (Xie et al., 2000) that functions as an auxin signal transducer downstream of *TRANSPORT INHIBITOR RESPONSE 1* (TIR1) for auxin dependent LR formation (Ruegger et al., 1998). SINA proteins function in dimers, and expression of a non-functional counterpart (a dominant negative mutant) was shown to inhibit SINA5 activity in *A. thaliana* (Xie et al. 2002). This feature was used to investigate SINA function in *A. thaliana*. By expressing a dominant-negative SINA5 protein mutant (SINA5DN) in *A. thaliana* more LR production was observed (Xie et al., 2002). This would explain its N-upregulation in pericycle tissue in *A. thaliana* as recognition of increased N concentrations would induce LR formation (O'Brien et al., 2016), and it suggests that it might also be N-upregulated in the pericycle in *M truncatula*.

In other experimental work, it was shown that expression of the dominant negative SINA5DN in *M. truncatula* roots had an adverse effect on nodule development. The authors reported delayed nodule primordia formation as well as interference to infection thread formation or symbiosome development when SINA5DN was expressed (Herder et al., 2008). It already reported that high external N concentrations inhibited nodule formation and efficiency (Wong, 1988). With this information here it is hypothesized that SINA may be a key regulatory node in RSA pathways across species and could act to co-regulate lateral root and nodulation numbers. In this hypothesis, transcription of SINA would be significantly downregulated in a nodulating plant, with the consequence of reducing the auxin influx into pericycle. This would then affect development of new LR or nodule primordia formation in response to increased environmental N concentrations (Mathesius, 2008). For this

reason, SINA proteins could present a valuable target for investigating RSA responses to external N concentrations in future *M. truncatula* tissue specific studies.

Pentameric polyubiquitin (Medtr6g061930) is another protein involved in the ubiquitin molecular process and is differentially expressed across tissue types of *A. thaliana*. It was DR in both *A. thaliana* stele and *M. truncatula* whole roots, however in pericycle, it was UR in *A. thaliana* and DR in *M. truncatula* whole roots. It has been found that ubiquitin mediated protein activation could regulate amino acid (glutamine) export from *A. thaliana* root tissue through ubiquitination of GLUTAMINE DUMPER 1 (GDU1), a xylem/phloem localized protein, by a RING-type E3 ubiquitin ligase LOSSOFGUD2 (LOG2) (Pratelli et al., 2012). Ubiquitination was also found to function in responses to changing C/N through activity of RING -type E3 Ub ligase activity of NITROGEN LIMITATION ADAPTATION (NLA) found in xylem (Peng et al., 2007). This function was further supported by the discovery of ubiquitin function in C/N response by ligases ATL31 and ATL6 (Sato et al., 2009). While ubiquitin mediated gene regulation and protein activation was found to be an important player in modulating N responses in root pericycle and stele, the reason for expression of pentameric polyubiquitin having different N-regulation in different tissues in *A. thaliana* and possibly in *M. truncatula* is not yet clear and could be investigated further.

With the knowledge obtained from experiments performed in this work, this chapter is concluded with the recommendation to use stable transformants expressing tissue specific reporter protein for studying tissue specific gene expression responses to environmental conditions. Importance of carrying out tissue specific gene expression studies and identifying genes with potential tissue-specific activity was also shown for the pursuit of holistic understanding regarding plant root nitrogen responses. Further work on this topic will generate invaluable information for assessing relationships between tissue types of *M. truncatula* under N toxicity responses at the transcriptomic level as well as understanding molecular regulation mechanisms of root systems architecture under various changing environmental conditions.

4. INVESTIGATING CELL SPECIFIC IMMUNE RESPONSES IN ARABIDOPSIS THALIANA

4.1. INTRODUCTION

4.1.1. *A. THALIANA – PSEUDOMONAS SYRINGAE* PATHOSYSTEM

A. thaliana, also known as thale cress, is a small, flowering annual plant. It is a member of Brassicaceae family along with other flowering crop plants such as broccoli, cauliflower, brussel sprouts etc. Its close relationship to crop plants, relatively small genome, rapid growth rate and ease to cultivate means this model plant system has long enabled molecular and genetic study of plant growth and development (Liu et al., 2014). Its genome has been extensively sequenced and is highly annotated (Koornneef and Meinke, 2010). Its transcriptomic (reviewed in Zhu and Wang, 2000) and proteomic profile (reviewed in Wienkoop, Baginsky and Weckwerth, 2010) has been studied under various abiotic and biotic conditions, which led to identification of mechanisms underlying metabolic and cellular processes that enable responses to these factors. In the endeavour towards identification of gene function, numerous gene mutants and transgenic lines of *A. thaliana* have been created and gathered in extensive collections e.g. the Arabidopsis Biological Resource Centre (ABRC), the Nottingham Arabidopsis Stock Centre (NASC), and the Sendai Arabidopsis Seed Stock Centre (SASSC) (Scholl et al., 2000).

A. thaliana has a wide range of pathogens such as: bacteria (Meyer et al., 2005), fungi (Van Baarlen et al., 2007) and oomycetes (Roetschi et al., 2001), making it a great candidate for studying biotic stress responses. Among its bacterial pathogens, *P. syringae* is an important one with hemibiotrophic properties which can infect almost all economically important crop species to cause bacterial spec disease (Bull et al., 2010). *P. syringae* pathogenesis follows two stages. First is the epiphytic stage where the bacteria live on the surface of above ground tissues (leaves stems, flowers etc.) and replicate (Figure 4.1.A&B) (Hirano and Upper, 2000). Over time they start entering the plant structure that they are occupying, through stomata or open-wounds (Figure 4.1.C) (Melotto et al., 2008); this is the start of the endophytic phase. Upon entry, the bacteria replicate exponentially and colonize the apoplastic space. During the final stages of pathogenesis, bacterial infection leads to localized necrosis of the tissue, creating the signature black specs (Figure 4.1. D&E).

With a wide range of hosts, different strains of *P. syringae* are identified by pathovar (pv.) names derived from their hosts (Xin and He, 2013). It was found that despite having tomato as its host species, *P. syringae* pv. Tomato (*Pst*) was also able to infect *A. thaliana* and induce pathogenesis (Whalen et al., 1991). Following this discovery, extensive biological and experimental resources available in *A. thaliana* increased popularity of this pathosystem for investigating mechanisms underlying bacterial pathogenesis and plant immunity (reviewed in Xin and He, 2013).

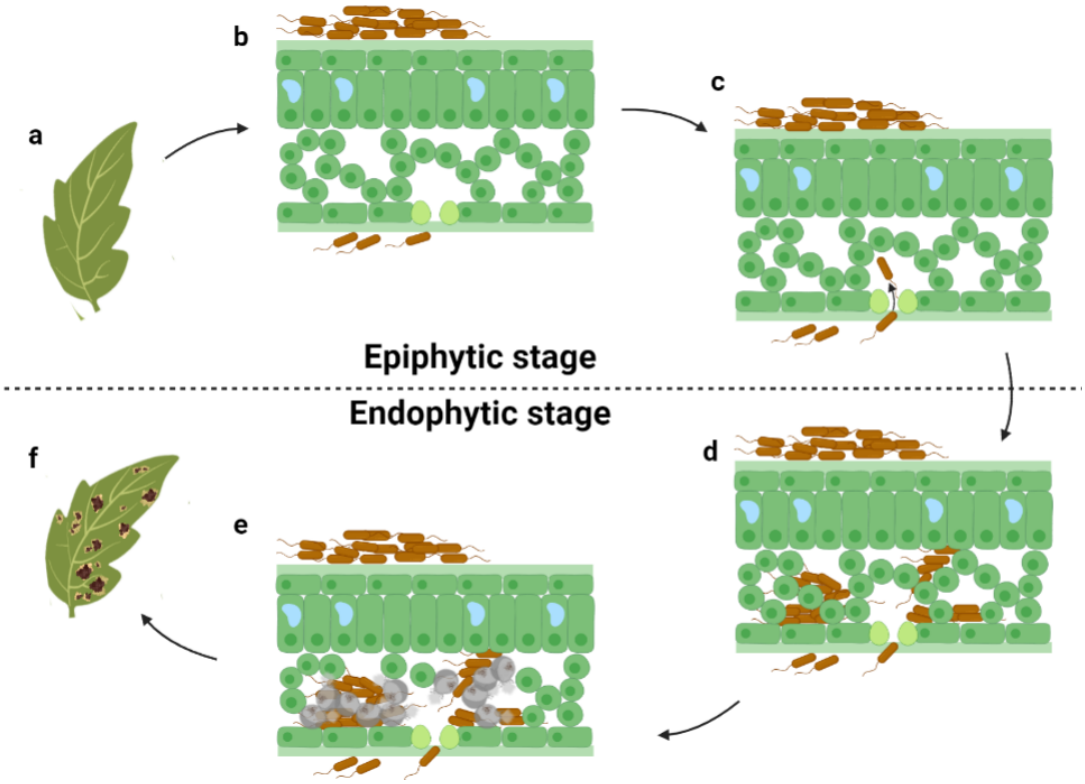

Figure 4.1. Infection stages of *P. syringae* DC3000 pv. Tomato. **A-C)** Epiphytic stage, **D-F)** Endophytic stage. **A)** Uninfected leaves but with the pathogen on the outside of the leaf, **B)** *P. syringae* replicating to form a biofilm on the leaf surface, **C)** *P. syringae* breaching physical barriers and entering the plant apoplastic space through stomata, **D)** *P. syringae* replicating exponentially within the apoplastic space, **E)** cell death leading to localized necrosis of plant tissue, **F)** Disease specific symptom emergence as necrotic specs on leaves. (adapted from Xin and He, 2013).

4.1.2. IMMUNE SYSTEMS OF *A. THALIANA*

Unlike animals, plants lack the benefits of a dynamic, somatic adaptive immune system. This means animals can acquire pathogen-specific receptors after an encounter with a pathogen, preparing the organism for future pathogenic challenges ("Molecular Biology of the Cell (4th Ed)," 2002). However, plants cannot acquire such pathogen-

specific receptors throughout their lifetime. Instead, they possess innate immune systems with components already present in the germline that have to provide resistance to a broad range of pathogens presenting as physical barriers or molecular mechanisms (Jones and Dangl, 2006).

Physical barriers in plant innate immunity include a cuticle made of waxes to prevent penetration of pathogens into the tissues (Martin et al., 1976) along with rapid stomata closure upon recognition of pathogen signal (Gudesblat et al., 2009). These barriers delay or prevent entry of pathogens into the plant tissue. Some pathogens evolved to circumvent these defences. For example fungal spores can secrete cutinases for digestion of cuticle layer and penetrate into the plant tissue to establish themselves (reviewed in Serrano *et al.*, 2014). In another mechanism, pathogens secrete coronatine (a similar molecule to methyl-jasmonate) to revert pathogen induced closure of stomata to gain entry into plant tissue (Gudesblat et al., 2009) When that happens, plants rely on their molecular defence mechanisms.

First line of molecular defence is called Pathogen Associated Molecular Pattern (PAMP)-Triggered Immunity (PTI). This mechanism is able to recognize molecules with conserved structures that are unique to pathogens called PAMPs. For example, highly conserved 22 amino acid motif (flg22) present on the flagellin protein of a bacteria (Felix et al., 1999) or an 18 amino acid motif (elf18) present in bacterial elongation factor EF-Tu protein are considered bacterial PAMPs (Kunze et al., 2004). Recognition of these motifs occurs via specific Pattern Recognition Receptors (PRRs) such as FLAGELLIN SENSING 2 (FLS2) for flg22 and ELONGATION FACTOR-TU RECEPTOR (EFR) for elf18 which are localised on the plant cell membrane (Newman et al., 2013; Postel and Kemmerling, 2009) PAMP recognition triggers a burst in ROS production and calcium influx. Following this, activation of MAPKs or Calcium Dependent Protein Kinase (CDPK) pathways lead to activation of transcription factors such as WRKY transcription factor gene family to regulate defence response genes (Boudsocq et al., 2010; Jixin Dong, Chunhong Chen, 2003). Members of this family are transcription factors, possessing a conserved WRKYGQK amino acid sequence followed by a Cys2His2 or Cys2HisCys zinc-binding motif (Eulgem and Somssich, 2007). WRKY gene superfamily members have diverse functions. Some members of this family are positive regulators of stress responses, e.g. WRKY53 and WRKY70 (Hu et al., 2012), while others, have a negative

regulatory effect on regulation of stress responses, e.g. WRKY11 and WRKY17 (Journot-Catalino et al., 2006). Remodelling of chromatin with such TFs lead to activation of defence response genes. Some such defence response genes include, FLG22-INDUCED RECEPTOR-LIKE KINASE 1 (FRK1) which is preferentially activated through MAPK signalling cascade, PHOSPHATE INDUCED 1 (PHI1), preferentially activated by the CDPK signalling pathway and NDR/HIN1-LIKE 10 (NHL10) activated through the synergistic effect of both signalling pathways (Zheng et al., 2005).

In *A. thaliana*, PTI responses can halt progression of infection for *Pst* strains unable to circumvent these responses (Figure 4.2). However, some *Pst* strains possess molecules evolved through natural selection of traits which promote successful infection (Chisholm et al., 2006). These molecules are virulence factors called effectors which are delivered into plant cells by the bacteria using a Type III secretion system (Xin and He, 2013). When inside the host cell, these effectors can recognize and interfere with the functions of key plant proteins involved in PTI responses. In the absence of protection against such interference, pathogens are able suppress plant defences, leading to Effector Triggered Susceptibility (ETS) (Figure 4.2). An example of ETS is seen in reduced PMR4-dependent callose deposition following the degradation of RIN4 protein, a plasma membrane associated negative regulator of PTI, by the *Pst* effector AvrRpt2 (Kim et al., 2005).

To overcome this, plants have also evolved to possess resistance (R) genes producing nucleotide binding-leucine rich repeat (NB-LRR) proteins that uses such effectors as cues to inform a more specialized immune system called Effector Triggered Immunity (ETI) (Figure 4.2). ETI responses are significantly stronger than PTI and generally results in hypersensitive response (HR), which is in essence localized programmed cell death of infected cells to stop progression of the infection (Dodds and Rathjen, 2010). NB-LRR proteins recognize effectors within the cytoplasm through direct or indirect protein-protein interactions (Dodds and Rathjen, 2010). Direct recognition occurs when effectors interact with NB-LRRs directly to trigger ETI gene activation. First example of this model was discovered in rice-*Magnaporthe grisea* pathosystem where the NB-LRR protein produced by the Pi-ta R gene in rice showed direct affinity to the AvrPi-ta effector protein produced by *M. grisea* in a yeast two-hybrid system (Jia et al., 2000). This model was further supported when a similar direct recognition was

observed in *A. thaliana*-bacterial wilt pathosystem where RRS1 NB-LRR protein exhibited positive interaction with bacterial effector protein PopP2 in a yeast two-hybrid system (Deslandes et al., 2003). In indirect recognition, effector target proteins are guarded by NB-LRRs through different models. One is the guard model where the effector target protein is the guardee and the NB-LRR protein recognizes the modification of effector protein on the guardee (Dangl and Jones, 2001). For example, in *A. thaliana-P. syringae* pathosystem, AvrRpm1 effector phosphorylates RIN4 which is then recognized by RPM1 NB-LRR to trigger ETI (Li et al., 2014). Another is the decoy model, where a modified version of effector target protein with little to no role in PTI or ETI signalling acts as the target of the effector. NB-LRRs recognize the modification on the decoy protein to induce ETI response (van der Hoorn and Kamoun, 2008). An example of this model was first found in Tomato-*Pst* pathosystem where the effectors AvrPto and AvrPtoB phosphorylates a serine/threonine protein kinase. Pto, oligomerized with its NB-LRR, Prf. Upon phosphorylation of Pto, Prf induces ETI responses (reviewed in Ntoukakis *et al.*, 2014).

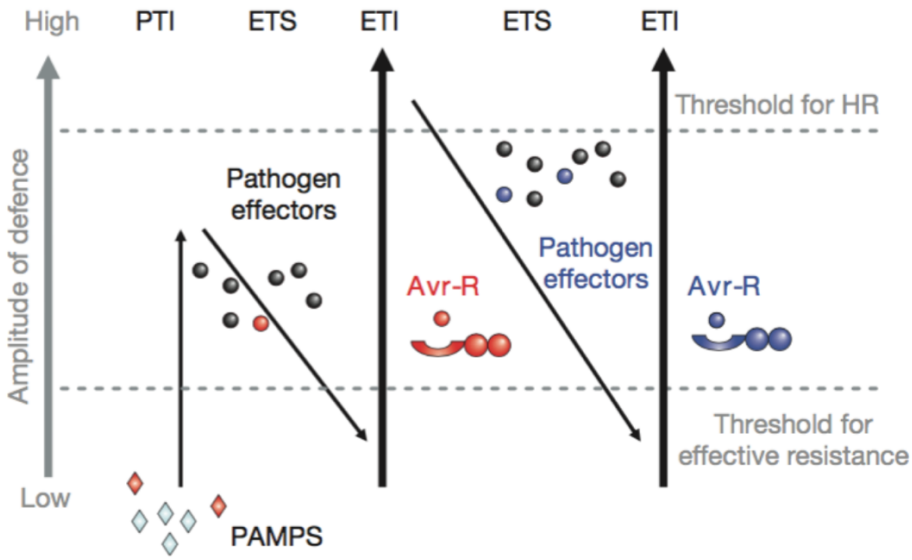

Figure 4.2. Zig-zag model of plant pathogen interactions. This model involves three stages. First, proximity of pathogens and presence of PAMPs in their conserved structures trigger a PTI response which include increase in ROS production, calcium influx and extracellular callose deposition. These responses can prevent further colonization of host plant by the pathogen. However, at times, pathogens can obtain gain-of -function mutations to express proteins called effectors which can suppress key regulators of PTI responses to cause ETS. This allows these pathogens to have an evolutionary advantage over the rest and increase rate of colonization. In turn, plants can also obtain gain-of-function mutations in proteins called NB-LRRs produced by R genes which to recognize the novel effectors and activate ETI to induce cell death to prevent further spread of the disease. Plants with such mutations gain an evolutionary advantage over the corresponding pathogens. This alternation between ETS and ETI underpins the constant evolutionary 'arms race' between pathogens and plants (taken fromJones and Dangl, 2006).

In order for defence mechanisms to ensure survival of a plant, each cell should be able to produce a similar response to the pathogen stress. However, it is known that molecular capabilities of each cell can differ despite identical genetic content. In order to gain a better understanding on how this affects immune responses we should first look at the concepts of stochastic gene expression and cellular noise.

4.1.3. Stochasticity of Gene Expression

Rates of reactions are defined by the number of molecules spatially present for the reaction. When interacting molecules are found in abundance for a reaction, removal of a single molecule does not affect the overall reaction rate. However, components of reactions in living systems are present in low copy numbers (Swain, Elowitz and Siggia, 2002). For this reason, even minute changes in one of the components in biological reactions can have a significant affect. And, because of the interconnected

nature of biological pathways, this affect can be transferred through the entire system. With this in mind, stochastic effects were proposed to have a major function in the cell-to-cell gene expression variation observed in clonal populations (Swain, Elowitz and Siggia, 2002).

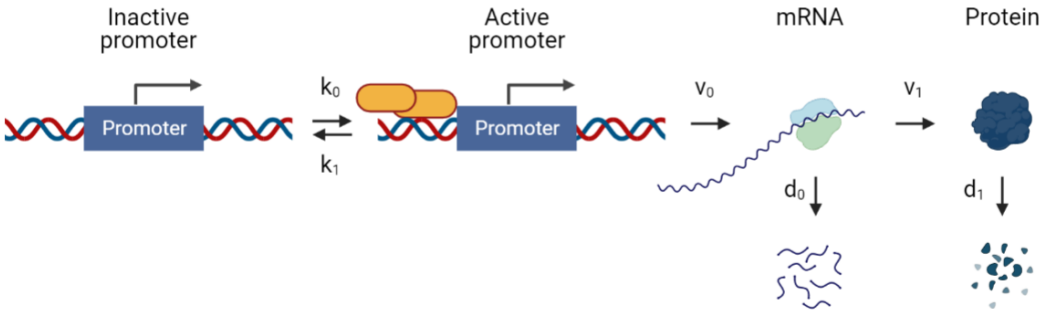

Figure 4.3. Central dogma model and where variability can be introduced. k_0 and k_1 are the rates of change between active and passive promoter states. V_0: rate of transcription, d_0: rate of mRNA degradation, v1: rate of translation, d1: rate of protein degradation. (adapted from Shahrezaei and Swain, 2008).

At gene expression level, these stochastic effects were found to originate from intrinsic or extrinsic sources to create intrinsic or extrinsic cellular gene expression noise (Raj and van Oudenaarden, 2008). Intrinsic sources are locally defined through the stochastic nature of biochemical reaction rates in biological metabolic processes due to heterogenous spatial distribution of molecules required for transcription, translation machineries. This positioning of euchromatin domains in relation to transcription machinery localization as well as spatial positioning of mRNAs in relation to translation machinery localization (Figure 4.3) (Singh and Soltani, 2013). Intrinsic cellular noise can be observed through comparison of gene expression levels of two genes regulated by the same promoter within the same cell (Figure 4.4). On the other hand, extrinsic sources are related to the temporal fluctuations in number of molecules that take part in the biological processes such as RNA polymerases (RNAPs), ribosomes and mRNA degradation machinery within a cell, over the course of its lifetime (Figure 4.3) (Swain et al. 2002). These sources result in extrinsic cellular noise which can be observed through comparison of gene expression levels of one gene between cells in a clonal cell population (Figure 4.4).

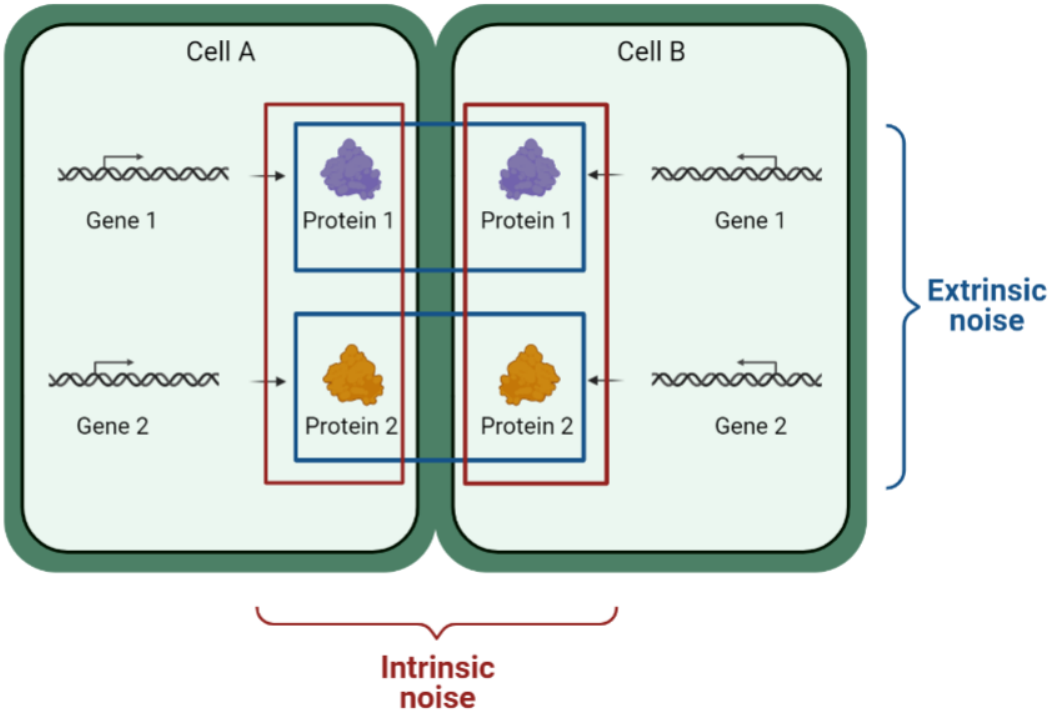

Figure 4.4. Graphical representation of intrinsic and extrinsic noise. Intrinsic noise is the difference in expression of two different genes within a cell due to chromosome position, promoter structure etc. Extrinsic noise is the difference in expression of a gene between two different cells in a genetically identical population (adapted from Araújo et al., 2017).

So far, three major functions have been proposed for cellular stochasticity. One of the proposed functions was to enhance cellular physiological regulation of gene expression. This enabled thorough coordination of a large set of genes with varying activity states, that respond to the same stimuli (Cai et al., 2008).

Another function was proposed in driving adaptive evolution of organisms through creation of a wide range of phenotypes without a mutation. This function was investigated in *E. coli*, where cellular noise resulted in state-switching of some bacteria into a 'persistent' state to create a heterogenous population which enabled the 'persistent' individuals within the clonal population to survive an antibiotic treatment (Balaban et al., 2004) (Figure 4.5.A). In another study performed on *E. coli*, researchers observed an increased range of fluorescence phenotype (Broad mutants) in a clonal *E. coli* population (Narrow mutants) expressing GFP under selective pressure. This increased range of phenotype was caused by cellular noise and researchers were able to exploit this heterogeneity to select for cells with increased GFP fluorescence to create a population with higher average GFP intensity than the original clonal population utilizing FACS (Ito et al., 2009) (Figure 4.5.B).

Cellular noise was also proposed to have an influence on cellular differentiation in multicellular organisms (Eldar and Elowitz, 2010). In studies performed on rat neural crest stem cells, it was found that only a fraction of the clonal population adopted neural fates. Size of this fraction was found to be affected by the abundance of Bone morphogenic protein 2 (BMP2) and Transforming Growth Factor-β (TGF- β) protein in cells which was stochastically determined (Shah et al., 1996). It was also reported that transcription factor Nanog influencing pluripotency and self-renewal capabilities of embryonic stem cells along with TF Oct4, also shows stochastic expression within a clonal population (Eldar and Elowitz, 2010; Loh et al., 2006) (Figure 4.5.C). Another example of developmental regulation of cellular noise was found in plants where, fluctuations in protein levels of transcription factor ATML1 in giant cells in plant sepals initiate pattern formation (Meyer et al., 2017).

While function of stochastic gene expression has been a research topic in many organisms, its function in plants have not been extensively studied beyond its role in aspects of development. As stochastic gene expression has been observed to be involved in adaptive evolution for may organisms, it can be hypothesized that it might also have a role in stress perception and response of plants to environmental stress factors.

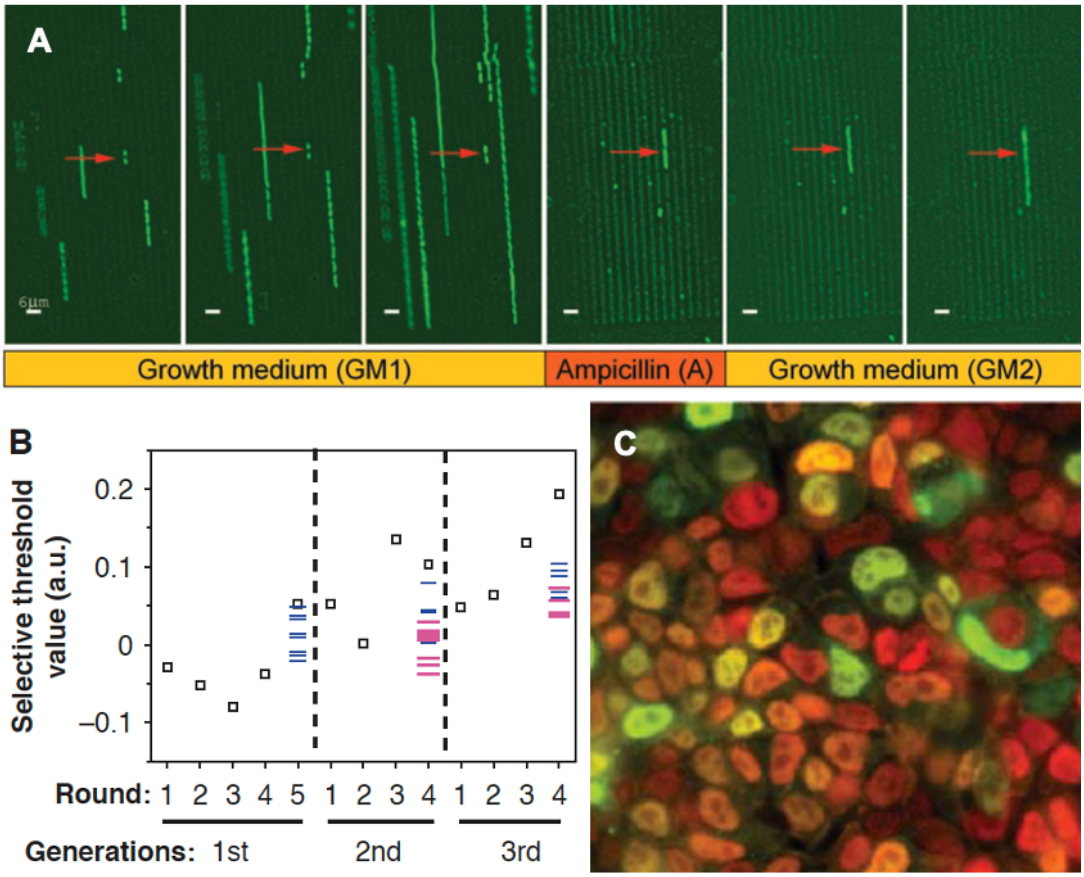

Figure 4.5. Examples of stochastic gene expression functionality in various organisms. A) *E. coli* grown in a microfluidic chamber supplemented with enough growth medium. Upon application of Ampicillin, most bacteria die while a colony which underwent a state-switching to become a persistent cell survives the treatment and can continue growth. Merged image of a clonal *E. coli* population expressing a red and green fluorescent protein regulated by identical, constitutive promoter regions. Green to red intensity differs for each cell due to intrinsic noise. **B)** A clonal population of *E. coli* cells were subjected to 5 rounds of selection in 1st generation and 4 rounds of selection in 2nd and 3rd generations to obtain higher average GFP intensity levels per forward scatter (FI/FS) (**Black boxes**) values representing cell size at the end of selection process. During this selection process, mutants arose with showing large (broad mutants, **magenta lines**) or small (narrow mutants, **blue lines**) fluctuation in their FI/FS levels narrow. **C)** Merged image of clonal mouse embryonic stem cell population expressing fluorescent proteins under regulation of Oct4 promoter (**Red**) or pluripotency regulator Nanog gene promoter (**Green**). Red florescence protein seems to be expressed more homogenously than the green fluorescent protein (Eldar and Elowitz, 2010).

4.1.4. OBJECTIVE OF THIS WORK

Stochasticity is known to play a role in adaptive evolution of unicellular organisms. Here, one hypothesis is that that the extrinsic noise among the cells of a plant tissue type could result in a fraction of cells presenting with more active defence states at a given time which could play a role in plant immunity to a pathogen.

This chapter aims to investigate role of cellular noise in plant immune responses against pathogen recognition using *A. thaliana* Col0 - *P. syringae pv.* tomato DC3000 pathosystem. To that end, an *A. thaliana* recombinant line expressing a fluorescent reporter protein regulated by an immune response gene promoter was sought among previously identified immune response genes. After obtaining reporter lines, cell-to-cell variation in reporter gene expression upon pathogen elicitor recognition were measured using a confocal microscopy and image analysis. Transcriptomic source of variability was investigated using qPCR after isolating cells showing highest and lowest variation utilizing FACS.

4.2. RESULTS

4.2.1. SELECTION OF BIOTIC STRESS SPECIFIC MARKER GENES

To study cellular stochasticity in plants, previous research utilized promoter regions of genes to drive expression of nuclear localized reporter proteins (Araújo et al., 2017; Shahrezaei and Swain, 2008). Accumulation of these reporter proteins were then quantified by confocal microscopy and used as a proxy to extrapolate gene expression levels in each cell (Araújo et al., 2017). This work follows a similar rationale to investigate the role of stochastic gene expression in spongy mesophyll cells on PTI responses, using characterisation of expression levels with confocal microscopy and in cells isolated using FACS. Towards this goal in studying cellular responses to biotic stress, the first step was to identify promoter regions of genes exhibiting expression changes upon perception of biotic stress.

Identifying genes with a very specific response to a particular biotic stress is crucial but can be hard to do. This is because reporter protein quantification techniques (confocal microscopy, FACS) can introduce unintended abiotic stresses (wounding, cold, salt, osmotic etc.). It is known that biotic and abiotic stress pathways can influence each other through crosstalk (Saijo and Loo, 2020). For this reason, a gene of interest should show a high expression change in response to biotic stress, and a minimal change in expression in response to any abiotic stress. Over 8,200 PTI genes were found to have altered gene expression within 60 mins of bacterial perception in *A. thaliana* seedlings (Zipfel et al., 2004). A way to minimize cross-talk between defence related genes is to minimize time of elicitor treatment, which can be achieved by utilizing genes with rapid responses. Thus, 252 flagellin rapidly elicited (FLARE) genes induced within 30 mins of flg22 treatment were used from a microarray study to narrow down the list (Navarro et al., 2004). To aim to select genes with the highest expression levels, candidates were chosen from this list. In the end, 16 genes with more than 10-fold expression change were selected to create a primary candidate gene list (Table 4.1).

Next, the effect of wounding, cold, salt and osmotic stresses on expression of these primary candidate genes were investigated using the abiotic stress database under tissue and experiment viewers of eFP Browser (Kilian et al., 2007; Toufighi et al., 2005; Winter et al., 2007). Three genes out of 16 were found to have a very low gene expression change under abiotic stresses defined previously.

Table 4.1. List of highly upregulated FLARE genes in leaves of 12-day old *A. thaliana* Col-0 seedlings 30 minutes after flg22 treatment (Kilian et al., 2007; Navarro et al., 2004).

AGI Number	Gene description	Fold-change after treatment relative to control				
		flg22	**wounding**	**cold**	**salt**	**osmotic**
FLARE genes with known or putative roles in signal perception*						
AT2g40000	Putative nematode-resistance protein	22.70	2.12	1.25	1.01	1.75
AT4g26090[1]	**RPS2**	**18.00**	**1.75**	**0.70**	**0.88**	**1.12**
AT2g39200	Putative Mlo protein	13.90	1.13	0.65	0.70	2.70
AT1g61560	Similar to Mlo protein	10.90	1.66	1.24	1.01	2.22
AT2g31880	RLK-LRR5	13.40	3.24	0.45	0.96	1.47
AT5g25930	RLK-LRR22	11.30	2.80	0.40	0.74	1.40
AT2g33580	RLK-Lys	17.70	2.44	0.40	0.85	1.09
AT2g19130[1]	**RLK-SD**	**17.60**	**1.12**	**0.71**	**0.81**	**1.19**
AT4g23220	RLK-DUF26	33.20	12.28	0.47	1.51	1.40
FLARE genes with known or putative roles in signal transduction**						
AT4g23810	AtWRKY53	34.6	1.51	0.48	1.22	4.63
AT4g18170	AtWRKY28	32.2	0.88	0.79	1.27	2.56
AT4g01250	AtWRKY22	24.1	1.68	0.91	1.34	1.74
AT2g38470	AtWRKY33	28.6	2.46	0.62	1.07	2.51
AT4g31550[1]	**AtWRKY11**	**13**	**1.39**	**0.49**	**0.81**	**1.31**
AT4g35480	RING-H2 finger protein, RHA3b	28	6.14	0.96	1.34	1.74
AT2g42360	Putative RING finger protein	10.3	7.57	2.01	0.98	4.04

***** Genes involved in signal perception produce receptors with extracellular domains that function in recognition of extracellular pathogen presence and triggering of intracellular signalling cascades
****** Genes involved in signal transduction produce intracellular proteins which receive signals from signalling cascades initiated by the receptor proteins.
1) Genes exhibiting high induction levels within 30 mins after flg22 treatment while also having low induction levels upon abiotic stress treatment.

One candidate was RPS2 (AT4G26090), a plasma membrane NB-LRR protein which has been found to provide resistance to *P. syringae* containing the avirulence effector gene *avrRpt2* (Bent et al., 1994). A second candidate was an S-domain lectin protein kinase (RLK-SD) (AT2G19130) with an unknown function in *A. thaliana*. Last candidate, a member of WRKY transcription factor family, WRKY11 (AT4G31550) was found to have a strong response to flg22 but only a weak response to abiotic stress changes. This gene has been found to be involved in negative regulation of plant basal pathogen resistance in *A. thaliana* (Journot-Catalino et al., 2006).

As mentioned in Section 2.2.1, in order to limit mobility of reporter proteins between the cells and for the ease of fluorescence quantification, reporter proteins should include a nuclear localization signal. According to these specifications, the NASC and TAIR databases as well as previous studies were investigated for the presence of a stable transformant of *A. thaliana* nuclear localized fluorescent reporter line regulated by the promoter of RPS2, RLK-SD or WRKY11 gene. While no existing reporter plant material was found for RPS2 or RLK-SD promoters, one was found in NASC database for WRKY11 promoter (NASC no: N2107974) (Poncini et al., 2017). This reporter plant line is a stable transformant of the *A. thaliana* Col-0 ecotype and was previously used to visualize expression of reporter proteins in *A. thaliana* root structures after various PAMP treatments (Poncini et al., 2017). The transformant contained a 1.7kb long WRKY11 promoter region regulating expression of three conjugated mVENUS (YFP) fluorescent proteins and a nuclear localization signal. This line was chosen as the primary plant material to work with throughout this study and is referred to as pWRKY11::YFP-NLS.

4.2.2. *Subpopulations with high and low fluorescence exist among A. thaliana* pWRKY11::YFP-NLS spongy mesophyll cells

100 pWRKY11::YFP-NLS seeds were grown on BASTA selective media to select confirmed homozygous insertion plants; selection was repeated in triplicate. Over 90% of the 100 pWRKY11::YFP-NLS seeds germinated in each replicate. Following mendelian genetics, since the number of germinating seeds exceeded 75%, it was concluded that the lines were indeed homozygous. Failed germination of 10% of the seeds was attributed to variable seed germination efficiency.

In order to determine if the pWRKY11::YFP-NLS reporter line expressed the reporter protein in the leaves, germinated seeds were grown to adulthood (6 weeks old) and fluorescence activity in leaf mesophyll cells investigated using confocal microscopy without flg22 or *P. syringae* induction. It was found that pWRKY11::YFP-NLS plants exhibited high levels of fluorescence in their leaf tissues including epidermis, palisade parenchyma and spongy mesophyll tissue even without biotic stress induction (Figure 4.6). So far, WRKY11 promoter was not reported to have tissue type specific activity so reporter protein expression in all tissue types was expected. Such a high level of fluorescence observed in uninduced plants however suggests that the *WRKY11* promoter is predominantly found in a highly active state.

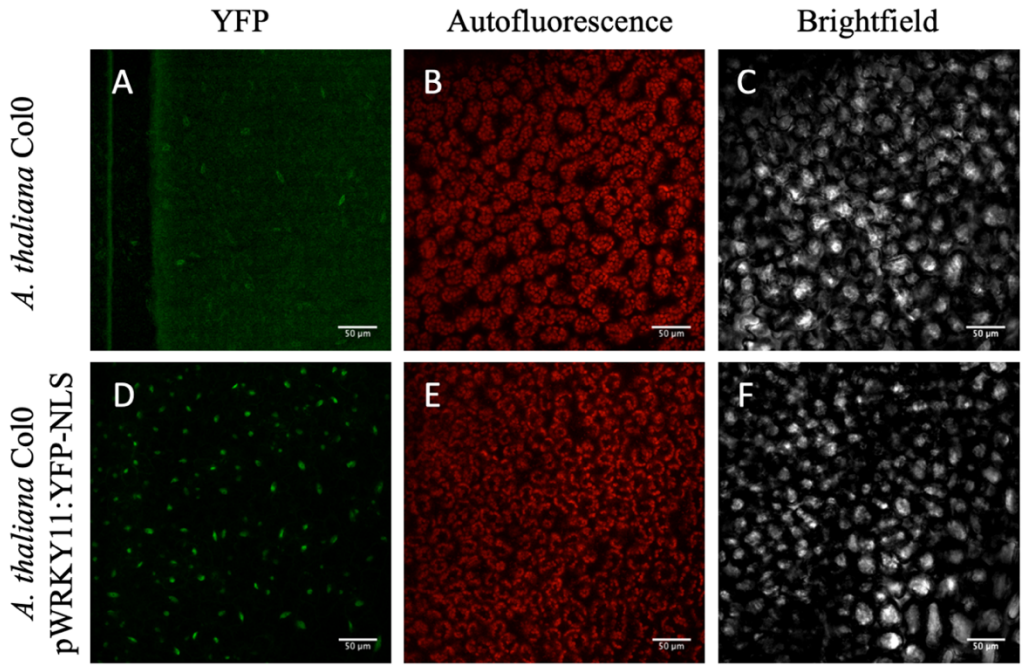

Figure 4.6. Confocal microscopy images of *A. thaliana* Col-0 and *A. thaliana* Col0 prWRKY11:NLS-YFP stable transformant mesophyll cells. **A)** No YFP fluorescence was observed in mesophyll tissue *A. thaliana* Col-0. **D)** Nuclear localization of YFP in mesophyll cells of prWRKY11:NLS-YFP stable transformants without flg22 induction. **B, E)** Chlorophyll autofluorescence was used to show viability of cells. **E, F)** Leaf tissue integrity can be seen in brightfield images. (Scale bar = 50µm).

In a previous study, it was stated that GFP and its derived proteins (such as YFP) fold into a compact protein structure that is highly resistant to protein degradation in a number of cells from *Saccharomyces cerevisiae*, to *Caenorhabditis elegans*, to *Nicotiana benthamiana* (Ward and Bokman, 1982). This feature was favourable for

marking cell lineages or locations within a cell; however, it was stated that the same feature could result in accumulation of GFP or its derived proteins inside a cell and cause reduced sensitivity in confocal imaging for detection of dynamic processes (Corish and Tyler-Smith, 1999; Cubitt et al., 1995). With this in mind, a high WRKY11 promoter activity in uninduced plants, could result in over-accumulation of YFP which is already insensitive to observe dynamic processes and interfere with measurement of changes in YFP expression under WRKY11 promoter control. For this reason, it was asked if it would still be possible to identify changes in pWRKY11::YFP-NLS fluorescence intensities in cells upon biotic stress treatments. To accomplish this, leaves of 6-week old plants were treated with flg22 and imaged immediately using confocal microscopy. In order to quantify changes in individual nuclei over time, a fixed location on a sample was imaged at 10 mins (T0) and 1hr (T1) after flg22 treatment (Figure 4.7.A,B). Fluorescence intensities of cells with nuclear sizes between 25 μm^2 and 100 μm^2 (n=28) were quantified (Figure 4.7.C, D). This way, epidermal cell nuclei were excluded while focusing on mesophyll tissue since pathogens colonize the air spaces within mesophyll tissue upon entry into the leaf (Xin and He, 2013). Next, values were normalized to reduce the impact of batch effects, photobleaching over time and use of different leaves to obtain relative fluorescence (RF) (Section 2.6.1 & Section 2.6.2)(Figure 4.7.E).

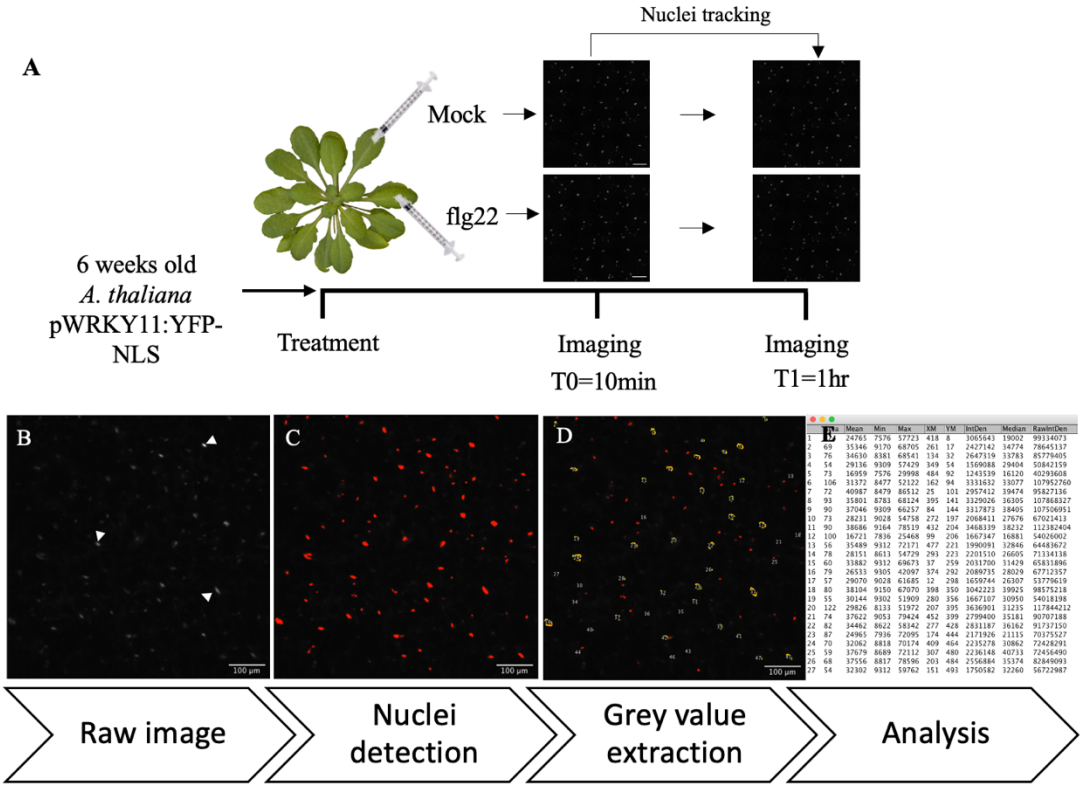

Figure 4.7. Workflow for single-cell fluorescence imaging and quantification under biotic stress. A) *A. thaliana* plants were grown for 6 weeks and leaf number 7 and 8 were infiltrated with either mock or flg22. 3 mm diameter leaf discs were cut out of infiltrated leaves and imaged with confocal microscope immediately (T0) and 1 hr after infiltration (T1). **B, C, D, E)** Fluorescence intensity in raw images **(B)** were quantified using ImageJ software. Since reporter protein is nuclear localized, an intensity threshold allowed defining nuclear outlines **(C).** Total fluorescence intensity of each nucleus was extracted using ImageJ software pixel analysis **(D)** into worksheets for further analysis **(E)**.

It was found that flg22-treated cells had a significant increase in RF of YFP at T1 in comparison to T0 (Mann-Whitney u-test, $p<0.001$) (Figure 4.8). This result showed the accumulation of YFP reporter protein was not interfering with the detection of change in RF upon induction of biotic stress. However, no difference was observed between RF of mock and flg22 treated samples at T1. Since samples were normalized for the use of different leaves, the starting fluorescence intensity values showed no difference, so, no change in RF was expected for mock treated samples. The fact that there was no significant difference between mock T1-RF and flg22 T1-RF was an indication that unintended abiotic stress factors introduced during the confocal microscopy procedure could be causing induction of reporter protein expression in mock-treated samples as much as flg22 treated samples.

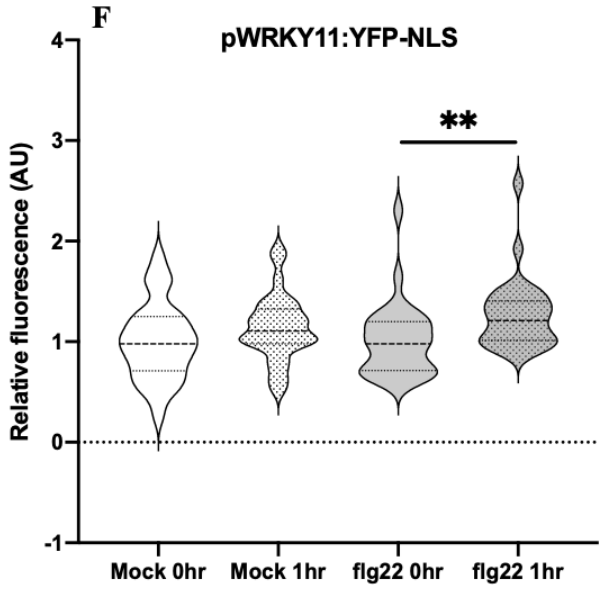

Figure 4.8. pWRKY11::YFP-NLS stable transformants exhibit increased average RF values upon induction with flg22. RF distribution of pWRKY11::YFP-NLS spongy mesophyll cells 1 hour after mock (water) or flg22 (100nm flg22) treatment. RF values of flg22-treated cells showed an increase over time (Mann-Whitney u-test, $p<0.001$). However, RF values of mock and flg22 treated samples increased at a similar rate and no significant difference was found at T1. Mock n= 28 nuclei, flg22 n=32 nuclei.

4.2.3. Investigating effect of wounding stress on WRKY11 gene expression upon biotic stress recognition

The effect of wounding stress and biotic stress on *WRKY11* expression was investigated in adult *A. thaliana* leaves using qRT-PCR. Leaves were either: left untreated, mock (dH_2O) treated, wounded, treated with flg22 or both wounded and flg22-treated. Tissue samples were collected 1hr post-treatment and gene expression was compared to a non-treated sample collected at 0 hr (Figure 4.9.A). It was found that after wounding stress, WRKY11 gene expression was increased when compared to a mock treated sample (Figure 4.9.B). It was seen that WRKY11 expression was found to increase to a higher level when leaves were treated with flg22, and even higher when applied in combination with wounding (Figure 4.9.B**)**. In comparison to the untreated sample, *WRKY11* gene expression showed a 2-fold increase after wounding stress, 5-fold increase after flg22 treatment and 8-fold increase after the combination of both treatments (Figure 4.9.B). This data shows that although wounding stresses can influence expression of *WRKY11* gene, its influence is significantly lower than flg22. Since the two are additive it is possible that the

influence of wounding and biotic stress might be via at least partially non-overlapping pathways.

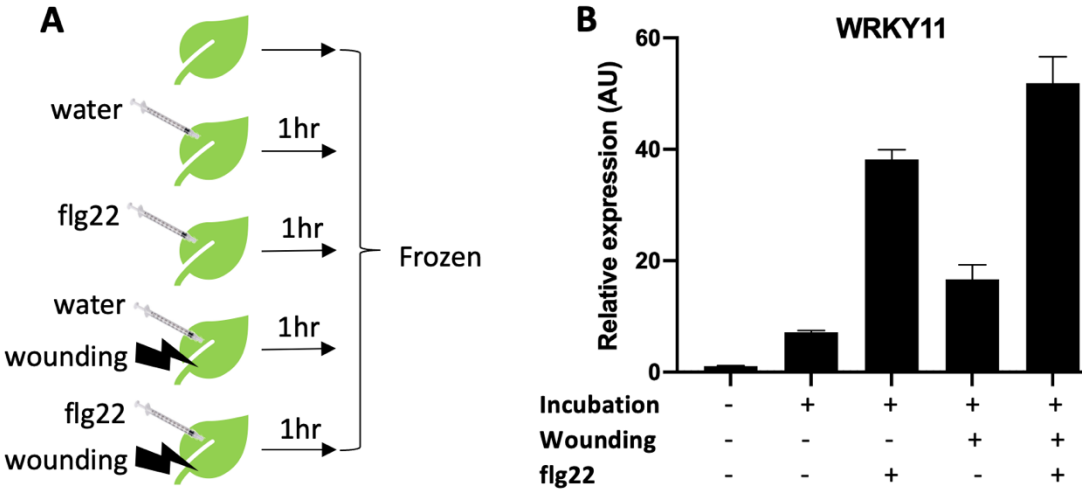

Incubation	Wounding	flg22	Relative gene expression fold difference		
			Rep 1	**Rep 2**	**Rep 3**
-	-	-	1.00±0.15	1.00±0.12	1.00±0.14
+	-	-	7.19±0.06	6.73±0.04	8.06±004
+	-	+	38.14±0.07	37.01±0.05	41.93±0.06
+	+	-	16.56±0.22	15.24±0.17	17.55±0.20
+	+	+	51.74±0.14	48.17±0.08	52.22±0.12

Figure 4.9. WRKY11 gene expression measured under a combination of biotic and abiotic stresses. A) Experimental design for wounding and biotic stress treatment of 6 weeks old pWRKY11::YFP-NLS leaves. **B)** *WRKY11* gene expression was found to be affected by both wounding and flg22 treatment, compared to untreated control. However, flg22 induction resulted in a significantly higher *WRKY11* mRNA production when compared to wounding-treated samples. This increase could also be observed in samples already wounded. Graph in Figure B depicts Rep 1; the trend is representative of three biological replicates. Error bars represent technical replicates. No fitting statistical test was found as distribution of data cannot be determined.

4.2.4. Increased sample size can overcome WRKY11 induction effect by unintended abiotic stress

Previous work to investigate the influence of cellular stochasticity utilizing confocal microscopy took advantage of a high number of data points for measurement and analysis (n≥500) (Araújo et al., 2017). Thus, it was hypothesized that in order to characterise immune responses across cells in a leaf, a large number of data points

would be required. For this reason, the same experiment, measuring changes in fluorescence intensity over time (Figure 4.7.A) was replicated thirteen more times with plants grown in exactly the same conditions, harvested at exactly the same time of the day and imaged with same microscopy settings; in total, 268 nuclei were imaged (Section 2.4 & Section 2.5.2). Data was normalized to attempt to eliminate batch effects and technical biases (Section 2.6.1 & Section 2.6.2) and to determine relative fluorescence (RF) values for measurements at 10 mins (T0) and 1hr (T1) post flg22 treatment (Figure 4.10.A).

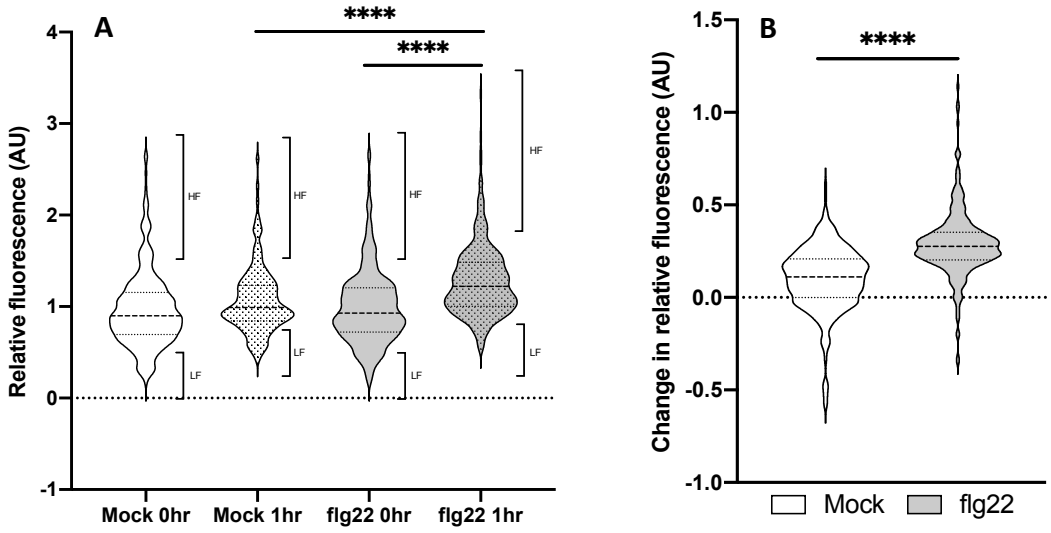

Figure 4.10. Nuclear fluorescence intensity of pWRKY11::YFP-NLS in spongy mesophyll tissue cells. A) Relative nuclear fluorescence intensities for population of spongy mesophyll cells followed a non-normal distribution for each sample and time point (Kolmogorov-Smirnov normality test, $p<0.0005$). The flg22-treated sample showed higher pWRKY11::YFP-NLS value after 1 hr, compared to all other samples and time points (Mann-Whitney t-test, $p<0.0005$). (**HF**: Top 10% cells with highest nuclear RF, **LF**: Bottom 10% cells with lowest nuclear RF; Table 4.2) **B)** Relative fluorescence change of cells 1 hr after treatment. flg22-treated cells have a higher expression change over time compared to mock-treated cells. Mock and flg22 n= 268 nuclei obtained from 14 biological replicates, normalized for batch effects and analysed together. Mann-Whitney u-test, $p<0.0001$.

Table 4.2. Legend for acronyms used in this Subsection.

Acronym	Meaning
pWRKY11::YFP-NLS	*A. thaliana* Col-0 transformant expressing nuclear localized YFP under WRKY11 promoter
RF	Relative fluorescence
T0-RF	Relative fluorescence at T0
T1-RF	Relative fluorescence at T1
RF-CoT	Relative fluorescence change over time
HF	Top 10% cells with highest relative fluorescence
LF	Bottom 10% cells with lowest relative fluorescence

Using a larger sample size (268 cells compared to 28 cells analysed previously), the significant increase in mean population RF was more evident 1 hr after flg22 treatment when compared to all other samples and time points (Figure 4.10). This showed that it was possible to overcome the potential variation introduced during the procedure (i.e. wounding effects as a result of sample harvesting) on pWRKY11::YFP-NLS activity during confocal microscopy technique with higher number of data points.

Cellular RF data of each sample was non-normally distributed and possessed a positive skew (Figure 4.10.A). This type of distribution suggested the majority of the cells tend to have a relatively low RF with some cells having a significantly higher expression of the reporter protein. In each sample there was a subpopulation of cells forming the top 10% of the total population exhibiting significantly higher RF compared to the population mean (Figure4.10.A). In this work, RF was used as an idicator of WRKY11 promoter activity, thus it was concluded that some cells had higher WRKY11 expression at a given point in time than others. This phenomenom was attributed to extrinsic noise that can result from temporal fluctuations in the number of molecules that take part in biological processes, such as RNA polymerases (RNAPs), ribosomes and mRNA degradation machinery within a cell. While abundance of these molecules fluctuates over the lifetime of a cell regulated by the cell cycle stage, ploidy number of a cell has been found to determine the potential range and level of fluctuations within a cell (Jovtchev et al., 2006; Katagiri et al., 2016).

4.2.5. DNA CONTENT OF SPONGY MESOPHYLL SUBPOPULATIONS ARE POSITIVELY CORRELATED WITH GENE EXPRESSION LEVELS

Given that plant somatic cells can obtain autopolyploidy spontaneously and stochastically, it was hypothesized that HF cells observed in single cell fluorescence imaging studies could possess higher ploidy numbers. To investigate this hypothesis, ploidy numbers within the population were to be inferred and analysed to ask if there was any correlatation to the RF values. It was previously found that nuclear size could be an indicator of ploidy number among epidermal cells of plant leaf population (Araújo et al., 2017; Katagiri et al., 2016) . By comparing the RF values of cells with the lowest nuclear size and the highest nuclear size, it was planned to compare cells with high and low ploidy numbers without needing to quantify the precise ploidy level.

Following the rationale set out above, T0-RF and nuclear size for the top 10% cells based on the largest nuclear area and the bottom 10% cells with the smallest nuclear area were determined and then compared. It was found that T0-RF of top 10% cells were much higher than that of bottom 10% cells ($p<0.001$) (Figure 4.11.A,B). To further investigate the relationship between these variables, nuclear area and RF values were analysed and it was found that nuclear area and RF were significantly positively correlated for both mock ($r= 0.7672$, $p<0.0001$) and flg22-treated samples ($r= 0.6782$, $p<0.0001$); one-tailed non-parametric Spearman correlation analysis (Figure 4.11.C,D). This positive correlation between T0-RF and nuclear size suggested that ploidy level could indeed be an indicator of or influence on levels of gene expression. In light of this information, it could be that the top 10% cells T0-RF (HF) cells in the population might have this higher level of RF because they are able to produce more reporter protein due to their high ploidy number. If this is true, it should be possible to observe a larger RF change over time (RF-CoT) in the HF cells, due to increased capacity to produce new protein.

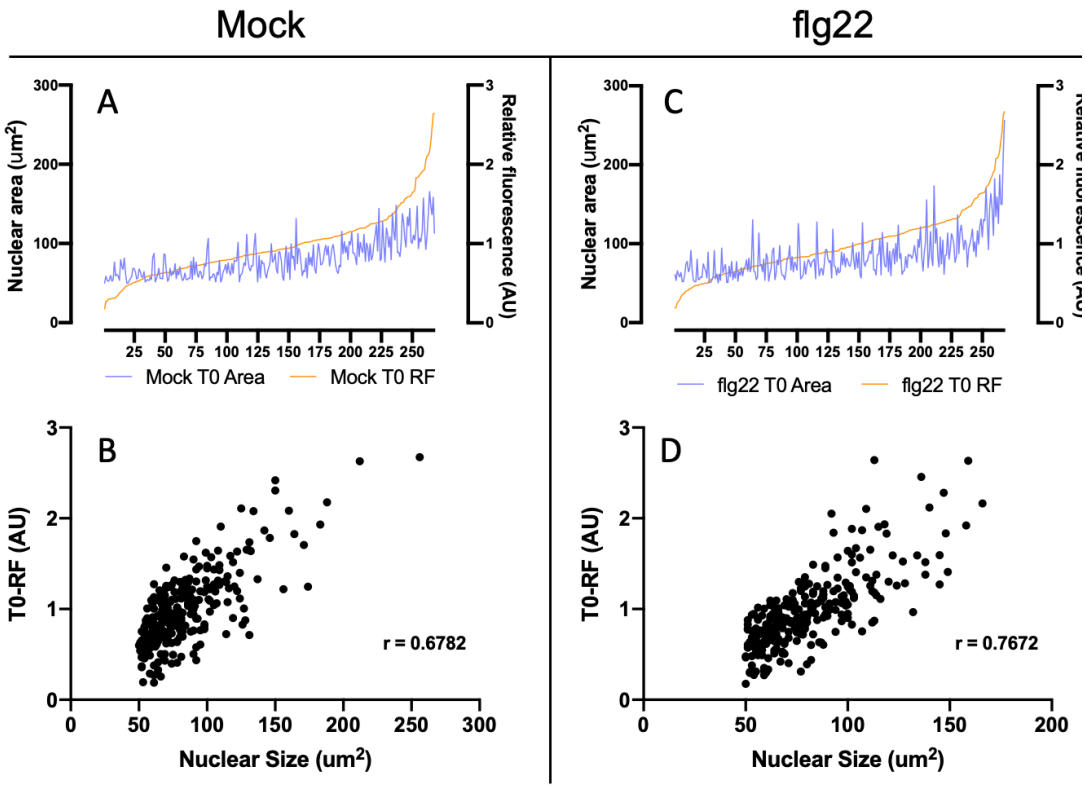

Figure 4.11. Nuclear area of corresponding RF values and their correlation at T0. A, C) Nuclear area values are increasing with increased RF values for both mock and flg22 treated samples at T0. **B, D)** A high, significant positive correlation between relative fluorescence and nuclear size in pWRKY11::YFP-NLS spongy mesophyll cells was observed after a non-parametric spearman test for both mock and flg22 treated samples at T0 ($p<0.001$).. For XY distribution plots, each value on the x-axis represents a cell. Right y-axis represents the corresponding T0hr RF value (orange) and left y-axis represents the corresponding nuclear area (blue).

To ask if HF cells have a larger RF response, RF-CoT was calculated for each cell by subtracting T0-RF values from T1-RF values (Figure 4.10.B). In line with the prediction, the RF-CoT population mean for flg22-induced samples was higher than that of mock-treated samples ($p<0.0001$) (Figure 4.12). However, there was a negative correlation between T0-RF and RF-CoT values for both mock ($p<0.0001$, $r= -0.5419$) and flg22-treated samples $p<0.0001$, $r= -0.3864$); one-tailed non-parametric Spearman correlation analysis. This indicates that although cells with higher ploidy possess high expression of reporter protein at steady state, their inducibility is significantly lower than the rest of the population.

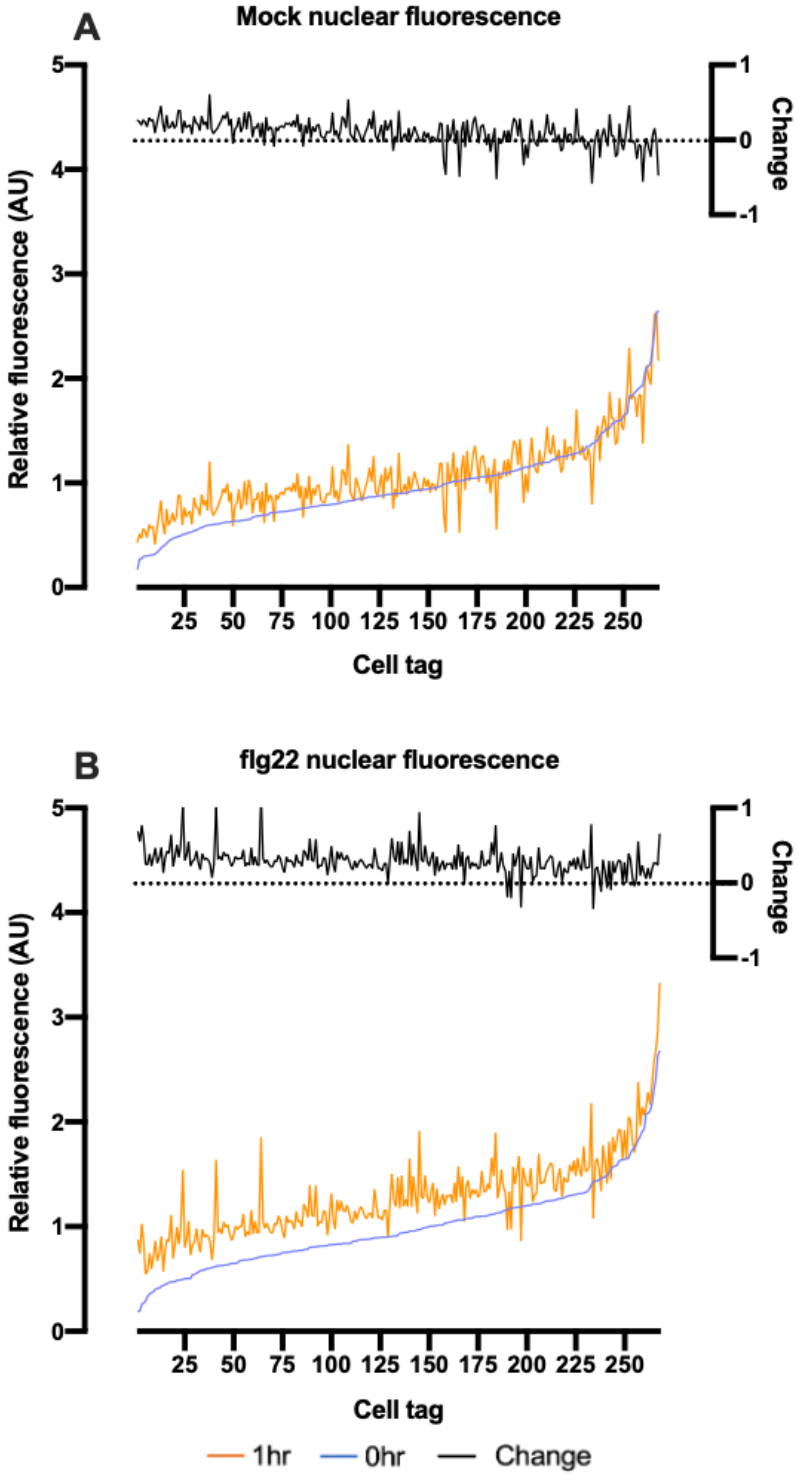

Figure 4.12. Temporal changes in single-cell pWRKY11::NLS-GFP spongy mesophyll nuclear fluorescence intensity in mock and flg22 treated samples. flg22 treated cells **(B)** exhibit a higher change in RF values **(black line)** compared to the RF change in mock treated cells **(A-black line)**. Each value on the x-axis represents a cell and each value on the left y-axis represents the corresponding T0hr RF value (blue), T1hr RF value (orange) and each value of the right y- axis represents the corresponding RF change over time (black) after 1 hr.

As previously explained, low turnover rate of GFP derived reporter proteins can lead to accumulation within the cell and limit the ability to detect dynamic changes, including gene expression levels (Corish and Tyler-Smith, 1999). However, this obstacle can be overcome by investigating these dynamic changes at gene expression level. In order to test this hypothesis, HF cells and bottom 10% cells with lowest fluorescence after flg22 treatment (LF) (Figure 4.11) were isolated among a population of protoplasts generated following the procedure described in Section 2.6.7 and subjected to qPCR analysis to quantify relative *WRKY11* gene expression. The protoplast generation procedure in preparation for FACS can induce stress-responsive gene expression, although the effected genes have been largely defined (Gifford et al., 2008), to ask if *WRKY11* was affected by protoplast generation, an experimental workflow was set up, with protoplast samples frozen at each step. *WRKY11* gene expression for mock and flg22-treated leaf samples that subsequently were processed through this workflow was then measured using qPCR (Figure 4.13.A). It was found that *WRKY11* expression was increased during protoplast generation, but to a much lower level than it was induced by flg22 treatment (Figure 4.13.B).

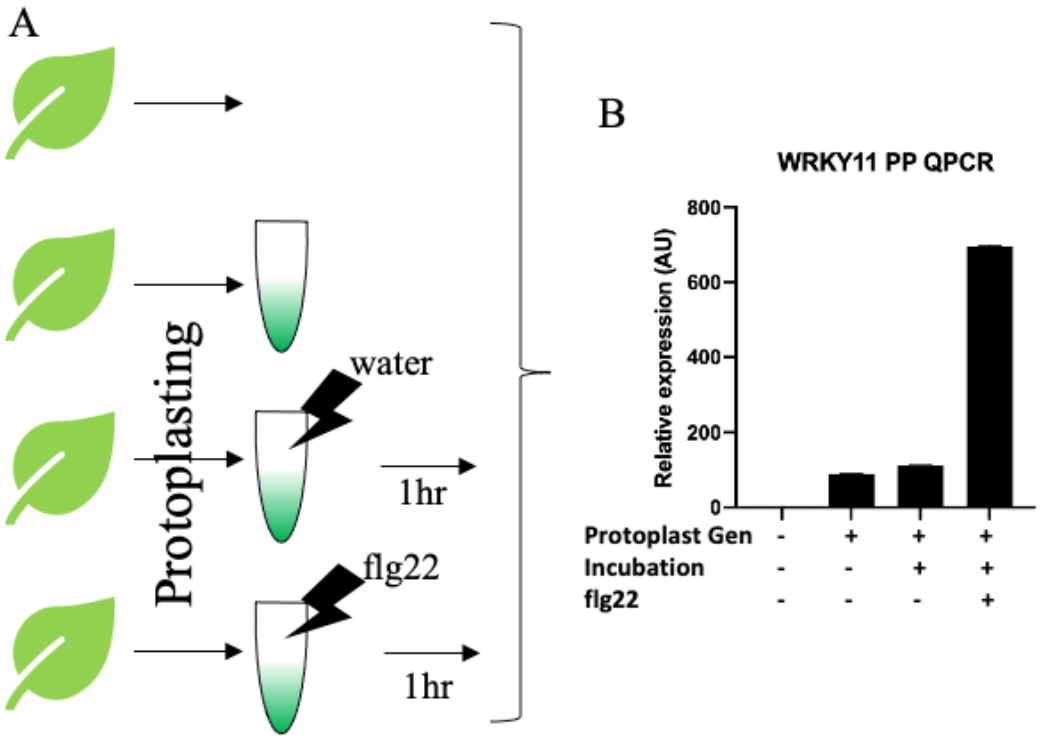

Protoplast Generation	Incubation (1hr)	flg22	Relative gene expression fold difference		
			Rep 1	**Rep2**	**Rep3**
-	-	-	1.00±1.4	1.00±0.92	1.00±0.93
+	-	-	89.26±0.94	91.14±0.86	122.22±0.97
+	+	-	110.66±1.82	114.83±1.72	189.58±1.17
+	+	+	696.19±0.31	691.38±0.28	905.98±0.23

Figure 4.13. Effect of protoplast generation on spongy mesophyll cell *WRKY11* gene expression with and without flg22 treatment. A) Experimental design of protoplast generation. Samples were frozen either without treatment, right after protoplast generation, 1 hr after mock (water) treatment or 1hr after flg22 treatment. **B)** Protoplasts showed increased *WRKY11* gene expression immediately after protoplast generation. However, no further increase in *WRKY11* gene expression was found in mock (water) treated samples after 1hr incubation while a significant increase was observed in *WRKY11* expression 1 hr after flg22 (100 nM) treatment. Graph in Figure B depicts Rep 1; the trend is representative of three biological replicates. Error bars represent technical replicates. No fitting statistical test was found as distribution of data cannot be determined.

Since flg22 treatment was found to significantly induce *WRKY11* gene expression even after protoplast generation, it was possible to proceed with isolation of HF and LF cells from a population of protoplasts using FACS. Plant leaf protoplasts possess chlorophyll which has a wide autofluorescence range (550-700 nm) and can influence

detection in the YFP channel. For this reason, protoplasts obtained from *A. thaliana* Col-0 ecotype were used to set a threshold in each FACS experiment (Figure 4.14.A). After the threshold was set, protoplasts obtained from pWRKY11:YFP-NLS plants were run through FACS. All events above the threshold were considered to have high fluorescence and thus were considered to correspond to HF cells, while all events falling below the threshold possessed low fluorescence and thus were considered belong to the LF group. However, it was observed that majority of the pWRKY11:YFP-NLS protoplast fluorescence values fell below the non-fluorescence threshold, suggesting that although pWRKY11:YFP was expressed in all cells, it was so low that the fluorescence was hard to detect during FACS. To identify the exact nature of these subpopulations, the peak below the fluorescence threshold was divided into two gates (P3 gate and P4 gate) and the fluorescence zone above the threshold was gated as initially designed (P5 gate). Events were sorted from P3, P4, P5 gates and isolated protoplasts were observed under epifluorescence microscope.

Based on microscopy, events sorted from the P3 gate consisted mostly of cell debris or broken cells (Figure 4.14.C&D). Events sorted from gates P4 and P5 (Figure 4.14.E-H) consisted mostly of intact cells. When their fluorescence intensities were compared qualitatively, it was seen that protoplasts isolated from P5 gate exhibited much brighter fluorescence emission compared to the protoplasts isolated from P4 gate (Figure 4.14.F&H) when excited with the same intensity of epifluorescence light. For this reason, the P4 gate was set to isolate LF cells whilst the P5 gate was set to isolate HF cells (Figure 4.15).

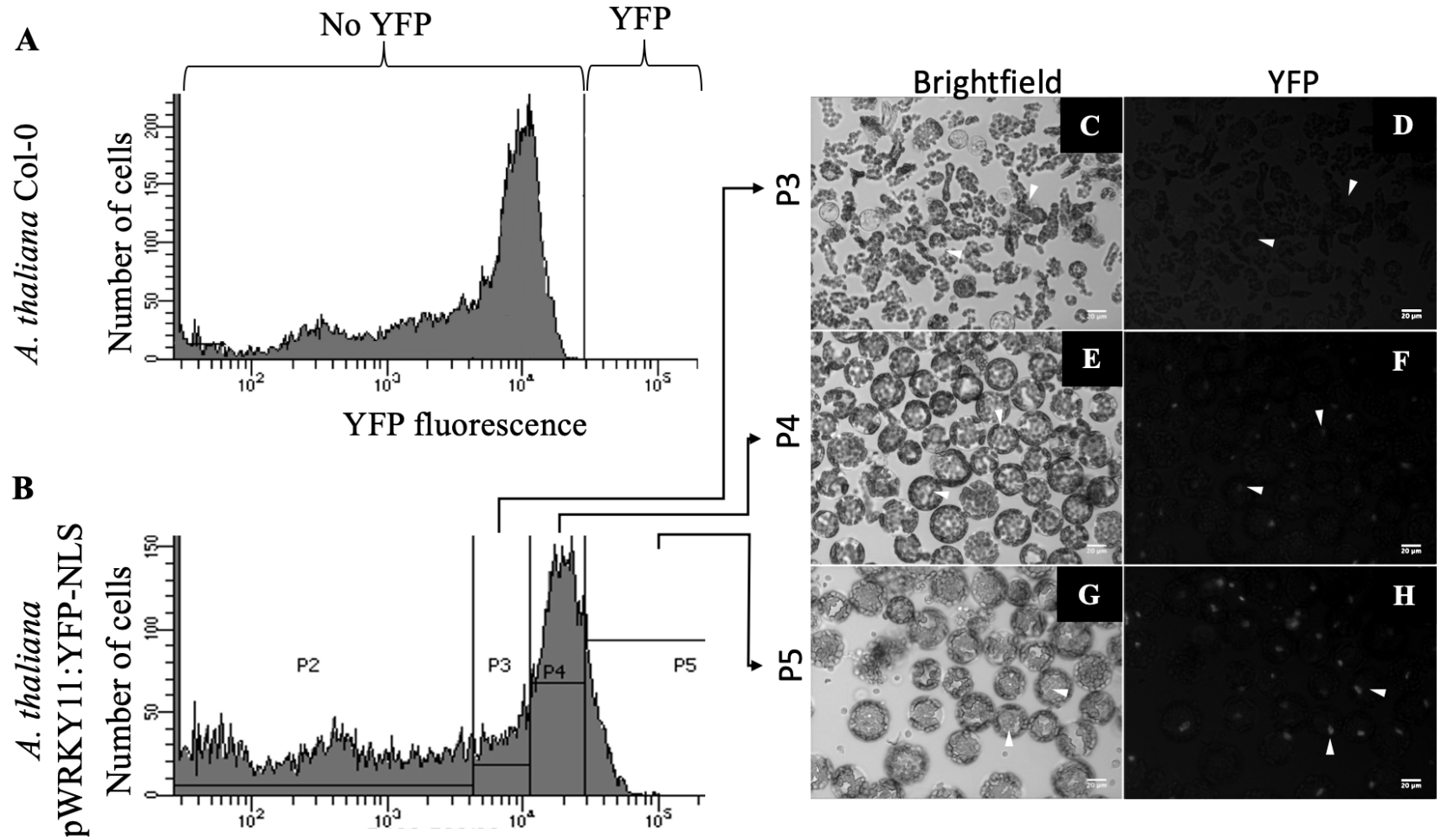

Figure 4.14. Protoplasts with distinct properties can be isolated from a genetically identical population using FACS. A&B) Population fluorescence histograms of *A. thaliana* Col-0 **(B)** and pWRKY11::YFP-NLS **(B)**. **C-H)** Sorted protoplast microscopy showing cell debris from P3 gate **(C&D)**, live protoplasts with low fluorescence from P4 gate **(E&F)** and live protoplasts with high fluorescence from P5 gate **(G&H)**.

With gates selected for isolating LF and HF protoplasts, experiments in triplicate were designed to obtain LF and HF protoplasts after flg22 treatment and sort into RNA extraction buffer for qPCR analysis of *WRKY11* expression (Figure 4.15.A) In this setup, after protoplasts were obtained from leaf tissue after they were treated with mock (water) or 100nM flg22 for one hour then sub-populations isolated using FACS (Figure 4.15.B&C). It was found that there was a ~1% increase in number of induced cells between mock and flg22 treated populations (Figure 4.15.B&C). This difference was lower than the 100% increase that was seen when cells were viewed with confocal microscopy (Figure 4.10). There might be two possible explanations for such a change. Firstly, stress caused by protoplast generation and FACS procedure could alter cellular responses and limit the extent of activation of the *WRKY11* promoter. Secondly, it might be that the data normalization to reduce batch and technical biases after confocal microscopy might have affected quantification of changes. Despite the fact that it was not possible to observe an apparent response to induction in the form of increased reporter fluorescence of the total population, HF and LF populations could still be observed within the protoplast population and could be isolated.

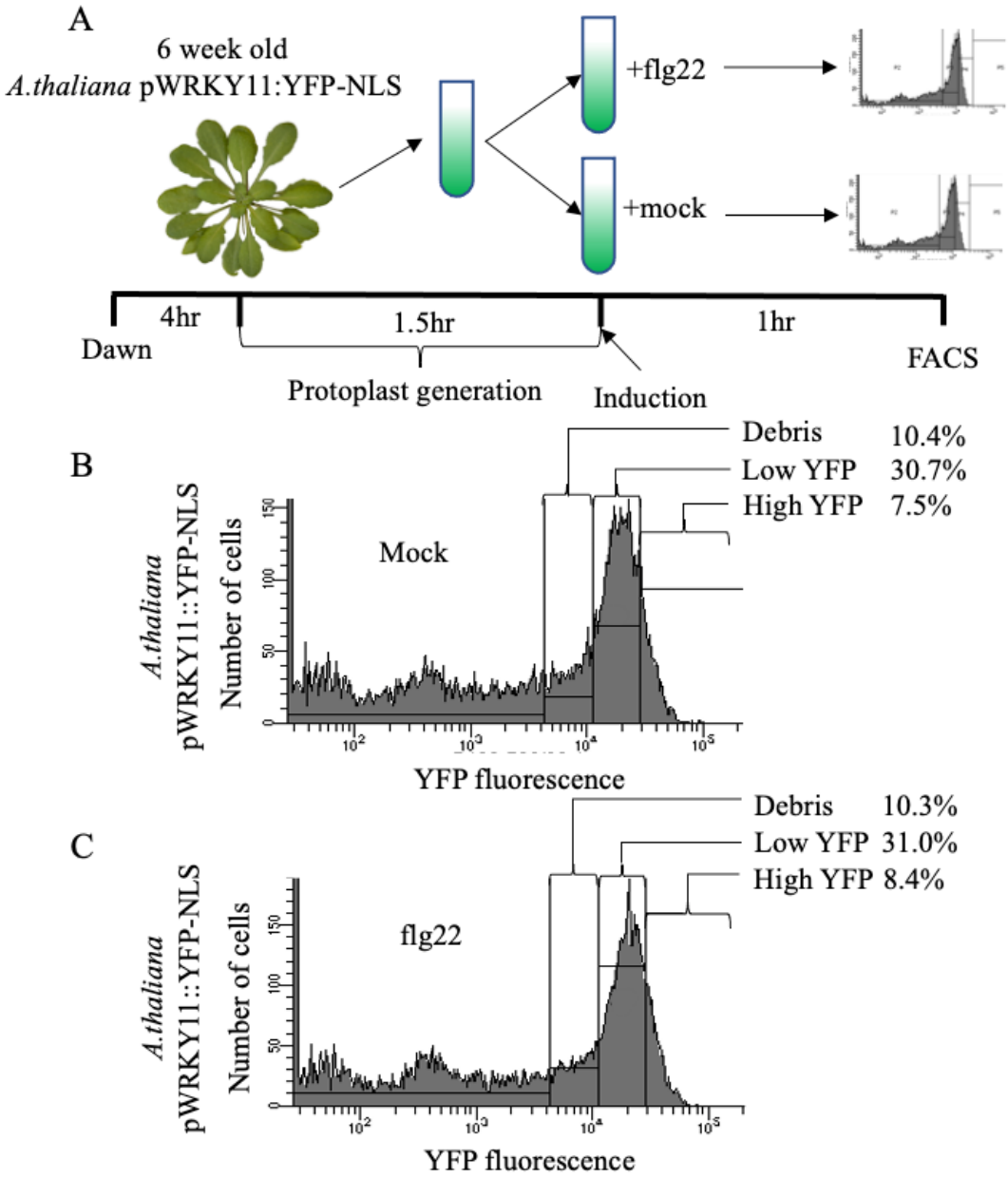

Figure 4.15. YFP signal intensity distribution histograms of protoplasts treated with mock and flg22, generated using FACS. A) Experimental design for protoplast generation, induction and FACS analysis of protoplasts. **A, B)** YFP intensity distribution profile of protoplast populations generated from 6 week old *A. thaliana* pWRKY11::YFP-NLS plants using FACS 1hr after mock **(A)** or flg22 **(B)** treatment. Gates for high YFP fluorescence (HF), low YFP fluorescence (LF) and cell debris were previously defined in **Figure 4.14**. ~1% increase in number of HF cells was observed after flg22 treatment compared to mock treated samples.

qPCR analysis was performed using the Livak-Schmittgen Method (Livak and Schmittgen, 2001) based on normalization against the *TIP41* housekeeping gene. With this analysis, no significant difference was observed in *WRKY11* expression between LF and HF populations in mock or flg22 samples (Figure 4.16.A). However, it was seen that *TIP41* expression levels were consistently higher in HF cells in comparison

to LF cells among the replicates (Figure 4.16.C). It was hypothesized that this difference could be due to the greater DNA content found in HF cells (as found earlier) and thus Livak-Schmittgen method might not be suitable to normalise *WRKY11* expression levels.

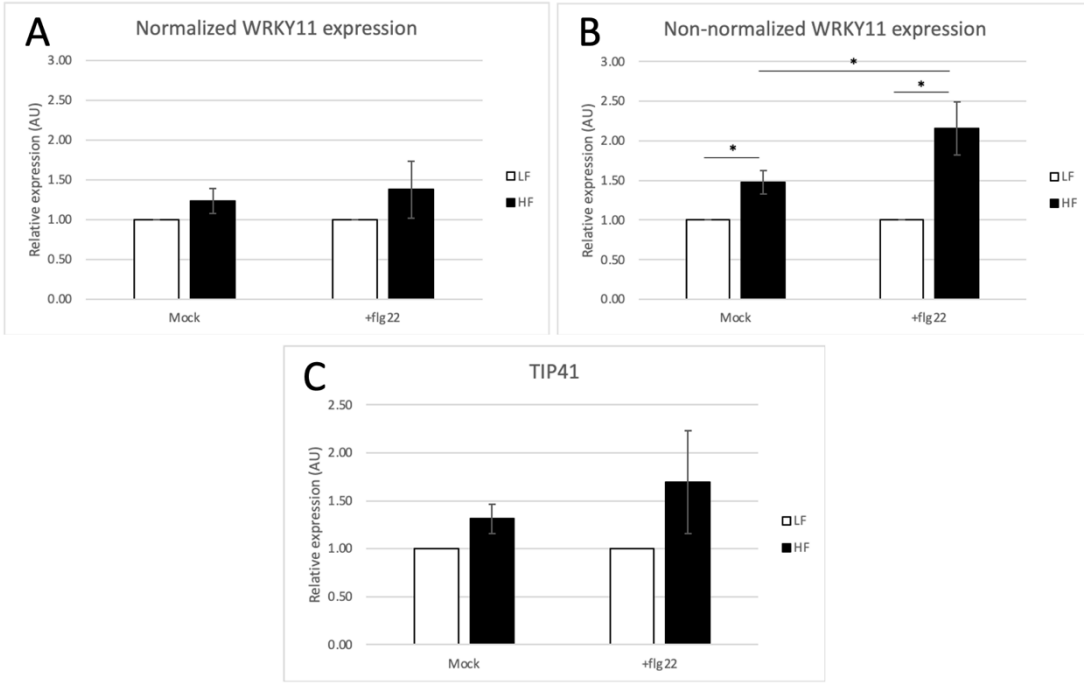

Figure 4.16. Average *WRKY11* gene expression of HF and LF cells 1 hr after mock or flg22 treatment from three biological replicates. A) Relative mRNA abundances calculated using the Livak normalization method; no significant differences were observed between samples. **B)** When relative mRNA abundances calculated without housekeeping gene normalization. There is a significant difference between HF and LF subpopulations in both mock and flg22 treated populations. **C)** Relative expression levels of housekeeping genes for HF and LF cells. all plots are representative of three biological replicates, error bars represent standard deviation from technical replicates. Error bars represent three biological replicates. No fitting statistical test was found as distribution of data cannot be determined.

For this reason, we performed gene expression calculations without normalization to *TIP41*. It was observed that *WRKY11* gene expression in flg22-treated HF cells was much higher than in mock-treated HF cells, and also higher than in LF cells in both mock and flg22 samples (Figure 4.16.B). The greatest increase in *WRKY11* expression was observed in HR flg22-treated cells compared to LF flg22-treated cells. This suggests a change in *WRKY11* transcription upon flg22 treatment linked to the transcriptional ability of the cell , even if the change is not evident at the level of YFP reporter fluorescence intensity (Figure 4.15).

4.2.6. INFLUENCE OF CELLULAR HETEROGENEITY ON BACTERIAL HOST SELECTION

Based on the findings of the previous experiments, it was hypothesized that the difference between gene expression levels of HF and LF cells could have a physiological impact on the selection of host cells by the pathogen *P. syringae* DC3000. For example, infection might be seen preferentially on cells with a lower *WRKY11* expression level, with a lower defence response. Bacterial establishment and ETI was expected in tissues between 3hrs-5hrs after inoculation. This was based on previous studies where ETI presence and severity was measured in *P. syringae* infected *A. thaliana* Col-0 plant leaves (Mackey et al., 2002). In order to test this hypothesis, a suspension of *P. syringae* DC3000 GFP AvrRpm1 (OD=0.1) was injected from the abaxial side of *A. thaliana* pWRKY11:3xYFP-NLS leaf to fill the air gaps. Leaf discs were cut immediately after injection and leaves were imaged at 1.5 hrs and 5.5 hrs post injection. Due to their rapid and 3-D movements, it was not possible to track movements of an individual bacteria over the time period using the microscope setup in this experiment, but some observations about their location was inferred. At 30 mins, bacteria exhibited rapid and random movements within the spongy mesophyll air gaps filled with liquid (Figure 4.17, white arrows). At 5.5 hrs, bacteria exhibited three different movement types: either (a) a twitching motion at a fixed location; this was observed close to a cell adjacent, suggesting that there might be establishment followed by bacterial cell division (Figure 4.17, magenta arrows). (b) a slow, random motion within the liquid filled air pockets of the spongy mesophyll (Figure 4.17, golden arrow). (c) a fast, random motion (Figure 4.17, white arrows) similar to the bacterial behaviour at 30 mins. However, it was not possible to observe an HR response in potentially infected cells (Figure 4.17, white asterisk) at the point of imaging. For this reason, it was not possible to determine whether variation in *WRKY11* expression plays a role in host selection in the *P. syringae* - *A. thaliana* interaction.

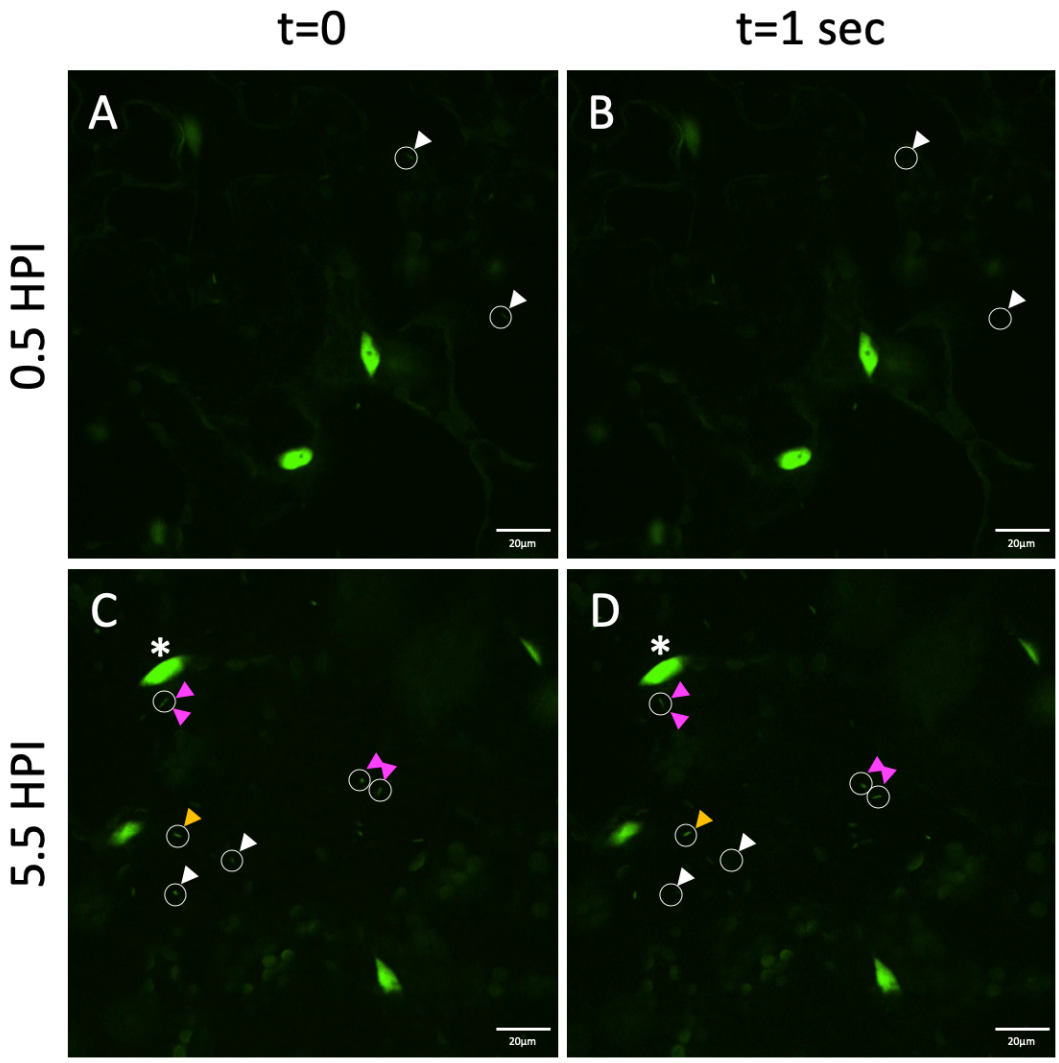

Figure 4.17. *P. syringae* DC3000 GFP AvrRpm1 bacteria tracking in *A. thaliana* Col0 pWRKY11:YFP-NLS spongy mesophyll tissue. Bacteria was syringe infiltrated from the abaxial side of the leaf with OD 0.1 concentration. Confocal imaging of the mesophyll tissue was performed from abaxial side of the leaf to create a live video in order to observe bacterial movement. Here, two images with 1 second apart were captured from the video sequence taken at the exact same location at 30 mins **(A, B)** and 5.5 hrs **(C, D)** after infiltration to observe cellular states and movement speed of bacteria. White arrows represent rapid movement of bacteria in and out of the focal plane. Golden arrows represent slow moving of bacteria. Magenta arrows represent bacteria with twitching motion accompanied by possible daughter cells. White asterisk indicates potentially infected plant spongy mesophyll cell nucleus (Scale bars = 20 µm)

4.3. DISCUSSION

In this study, it was able to observe stochastic, inducible activity of *WRKY11* promoter in genetically identical spongy mesophyll cells with confocal microscopy based on assessing variation in reporter protein expression upon pathogen elicitor treatments. During this process, it was found that a large sample size (many cells) was imperative to observe differences stemming from biotic stress while reducing effects of technical procedure on the results. The change in YFP fluorescence intensity (proxy to *WRKY11* expression) in cells with already high *WRKY11/YFP* expression was found to be significantly reduced upon flg22 treatment. Since this trend was observed in both mock and flg22 treated samples, it was hypothesized to be due to the saturation of YFP reporter protein inside a cell rather than a response directly linked to biotic stress perception. It was hypothesized that this YFP accumulation was caused by higher basal activity levels of *WRKY11* promoter than expected, in conjunction with the long half-life of the mVenus YFP reporter protein. In order to overcome these issues in future studies, it is proposed that new reporter lines should be generated with a promoter region with lower to no activity under un-infected conditions and exhibit better inducibility upon biotic stress perception. *RPS2* (AT4G26090), a plasma membrane NB-LRR protein which has been found to provide resistance to *P. syringae* containing the avirulence effector gene *avrRpt2* (Bent et al., 1994) and *RLK-SD* (AT2G19130) an S-domain lectin protein kinase with an unknown function in *A. thaliana*, were two other genes identified in this work. Both possess lower expression levels compared to *WRKY11* in un-infected conditions, hence they are good candidates for generation of new promoter lines. To further increase detection sensitivity, reporter proteins should also consist of a single fluorescent molecule with two nuclear localization tags along with a degron tag. A single copy of the reporter protein will not only reduce the saturation of the signal but also allow quantification of its transcript by qPCR analysis. This is because conjugation multiple reporter proteins of same type causing random fragment amplification in qPCR. While this might cause increased leaking to neighboring cells, inclusion of double nuclear localization tags has been shown to overcome this effect (Balkunde et al., 2017). Addition of a degron tag will direct the reporter protein to the degradation complex for rapid turnover, reducing its half-life and prevent its overaccumulation in the cell (Wilmington and Matouschek, 2016) allowing more sensitive detection of changes in cells with already high fluorescence

upon flg22 perception, and use towards the biological aims of this work. On the other hand, bioluminescence microscopy, a novel technique for imaging luminescence in live cells could also be utilized by expressing luciferase-like reporter proteins under promoters of interest (Horibe et al., 2016).

Among the variation of the reporter protein expression in mesophyll tissue, fluorescence intensity levels were found to be significantly positively correlated to the size of the cell nucleus. It has previously been shown that cell size was indicative of cellular ploidy level (Jovtchev et al., 2006) and, in previous crop plant research, higher cell ploidy numbers were found to be closely related to higher increased gene expression (Osbon *et al.*, 2003). With this knowledge, two subpopulations, called HF and LF, were selected from cells consisting of the top 10% and bottom 10% fluorescence intensities respectively. Then, the level of *WRKY11* expression in both HF and LF populations were investigated where it was observed that *WRKY11* expression in HF cells was significantly higher than that of LF cells in both mock and flg22 treated samples. This was supportive of the hypothesis of higher genetic material in HF cells as more starting material would produce larger quantities of transcripts. And a way of obtaining larger genetic content in genetically identical cells is through spontaneous autopolyploidy events. This was in support of the findings in section 4.2.5 where a positive correlation was identified between cell size and fluorescence intensity levels of spongy mesophyll cells through confocal microscopy. However, it is also possible that this difference is caused by a difference in abundance or activity of transcriptional machinery between HF and LF cells. Thus, further investigation is required at the genomic and proteomic levels to accurately determine the source of this difference. A wider view of the transcriptomic landscape for both LF and HF populations is also necessary in order to understand differences for non-biotic stress responsive genes as well as biotic stress responsive genes in response to flg22 treatment. For this reason it is proposed next step of this work to be an RNA-Seq, ATAC-Seq, INTACT or protein-seq experiment in isolated HF and LF populations.

Based on knowledge that relative gene expression quantification methods can mask physiological differences stemming from sources of extrinsic noise, it is proposed that any future transcriptomic or proteomic work investigating single-cell stochastic gene expression should adopt a method for absolute quantification of transcripts which accurately quantifies number target transcripts in a solution rather than comparing it

to an internal reference gene (Dhanasekaran et al., 2010). With this approach, an accurate prediction of molecule abundance could be performed for each individual cell or subpopulation. In this approach, use of housekeeping genes should still be mandatory to enable detection of differences due to technical or biological variation.

Investigating if the variation in *WRKY11* promoter activity is truly correlated with ploidy levels is highly relevant for investigating mechanisms underlying plant adaptaion to stress. Increased ploidy levels were found to be associated with a better ability to adapt to the stresses caused by a dynamic environment due to allele dosage effect which causes non-additive increase in production of transcripts due to more available genetic material (reviewed in Udall and Wendel, 2006). This could affect the extent of response by a cell if it possesses different genetic content from the rest of the cells within the same cell/tissue type or cellular region. Thus an experiment was designed in order to ask if cells with different nuclear sizes (and theoretically a higher ploidy number) affected bacterial host selection mechanisms or exhibited any differences in their response upon pathogen perception. However, it was not possible to test this hypothesis due to technical limitations regarding capturing of bacteria via microscopy or the ability to generate a large enough sample population, due to restricted objective scope area. One method to test this hypothesis would be; rather than observing mobility of bacteria, assessing if reporter protein expression levels are correlated with the number of immobile bacteria carrying a reporter protein could be used. In this approach, a 20x objective should be used in conjunction with sample scanning and image-stitching method to maximize observed area. However, bias from image stitching should be taken into account during analysis. Samples should be imaged at 0 mins, 30 mins, 3 hrs, 6 hrs and 9 hrs to observe responses of plant cells over time with immobile bacteria adjacent to them. It is also imperative to include a control sample from the same plant, imaged in the same conditions as the bacteria-treated sample and adjusting for the photobleaching effect on reporter proteins caused due to long term confocal scanning.

It can be postulated that stochastic gene expression has a role in adaptability of plants to dynamic environments by maintaining a wide range of phenotypes to utilize a bet hedging strategy (Balaban et al., 2004). Understanding the sources of this stochasticity might help discover novel mechanisms between plant-stress relationships which can be applied to improving agricultural practices.

5. APPROACHES TOWARDS EXPLOITING STOCHASTICITY OF GENE EXPRESSION

5.1. INTRODUCTION

5.1.1. EPIGENETIC TRAIT INHERITANCE

Epigenetics refers to all non-genomic contributors within a cell that are involved in the regulation of gene activity states (Deans and Maggert, 2015). These contributors can be inherited mitotically or meiotically in somatic or germline cells respectively (Bohacek and Mansuy, 2017). So far, three major contributors in epigenetic regulation have been identified (Cooper and Hausman, 2007). One, covalent modification of DNA where a methyl group (CH_3) is covalently bound to the fifth position of a cytosine residue. Following this modification, DNA undergoes a structural change that can result in altered gene expression. In promoter regions, this modification can cause gene silencing, whereas in transcribed regions, it can cause increased transcriptional activity (Jones, 2012). Two, covalent modification of histone tails with molecules including (but not limited to) methyl, acetyl and phosphate groups. These modifications can cause conformation changes chromosome regions between euchromatin and heterochromatin states, ultimately regulating transcription of genes. Three, regulation of gene expression through activity of non-coding RNAs (ncRNA). These are RNA molecules smaller than 200 nucleotides that are not translated into proteins. These molecules can also be regulated by other epigenetic mechanisms and they are thought to play a role in mRNA regulation similar to transcription factors (Peschansky and Wahlestedt, 2014). All epigenetic mechanisms are dynamic and are known to be significantly modified by environmental factors (Bräutigam et al., 2013). Because of this, their role in affecting transmission of acquired traits to following generations has been a topic for investigation (Bohacek and Mansuy, 2017; Wibowo et al., 2018).

Along with their ability to be induced by environmental factors, it has been proposed that epigenetic factors might function as an adaptation mechanism to give an edge to the offspring (reviewed in (Sahu et al., 2013). An example of this is “priming” in plants, whereby recognition of stress triggers changes in the physiological, transcriptional, proteomic and epigenetic landscapes, resulting in the plant having an activated immune system, called a primed state (reviewed in Mauch-Mani *et al.*,

2017). In this state, if the plant is challenged again with the same triggering stress, it generates a faster, stronger response. This hypothesis was supported by experiments conducted on *A. thaliana-P. syringae* pathosystem (Slaughter et al., 2012). These epigenetic changes can occur in both somatic and germline cells, for that reason, it is also referred to as plant immunological memory (Molinier et al., 2006; Reimer-Michalski and Conrath, 2016).

Polyploidy is another factor that induces major epigenetic changes in the cell (Ding and Chen, 2018) and is an important mechanism for emergence of novel functional traits during evolution. Emergence of polyploid populations follows a two-stage path (Parisod et al., 2010). In the first stage, the emerging polyploid has to have some form of immediate benefit in order to be successfully establishment in its environment. These benefits, referred to as 'revolutionary changes', have been found to be influenced by a number of epigenetic factors including methylation of coding and non-coding DNA leading to gene silencing, and activation of retroelements (Levy and Feldman, 2004). These epigenetic changes in turn could induce epialleles that can be inherited in the next generation(s) to improve chances of establishment (Song et al., 2017). In the second stage, the polyploid has to have a high level of plasticity in order to be able to adapt to emerging challenges in the environment. These are referred to as 'evolutionary changes' and they occur over a longer span of time via mutation and remodelling of the genome (Flagel and Wendel, 2009).

5.1.2. PROTOPLAST REGENERATION

Protoplasts derived from plant cells have been found to possess the ability to reprogram their genetic material, allowing them to dedifferentiate into a totipotent state given the right culture conditions (Avivi et al., 2004). For this to happen, cells are generally induced with auxin and cytokinin phytohormones that are perceived as growth regulators, driving the de-differentiated cells to divide and produce microcalli. Following this stage, each consecutive media used in this procedure is produced with a varying ratio of auxin and cytokinin phytohormones to promote cell division, induce shoot or root formation to obtain a fully regenerated plant (Takebe et al., 1971). When protoplast regeneration was performed with different plant species, it was found that each species exhibited different rates of regeneration. While *Nicotiana benthamiana* exhibited regeneration rate of 100% (Bourgin, Chupeau and Onier, 1979), *A. thaliana* exhibited ~50% (Chupeau et al., 2013), *Brassica oleracea* ssp *botrytis* (cauliflower)

89% (Kirti et al., 2001), *Brassica oleracea* ssp *italica* (broccoli) 32% (Kirti et al. 2001) and *Brassica oleracea* ssp *capitata* (cabbage) 37% (Kirti et al. 2001).

Some researchers have utilized protoplast regeneration as a means to an end in studying early developmental events in plant cells or understanding transcriptomic mechanisms underlying plant de-differentiation (Chupeau *et al*., 2013, Avivi *et al*., 2004). An additional application was realised when used in conjunction with the methodology for somatic fusion of protoplasts to create hybrid plants that would otherwise be impossible through classical breeding methods (Evans, 1983). Using this approach many new hybrids of existing plants were introduced into agricultural collections (Waara and Glimelius, 1995).

5.1.3. Objective of this work

In Chapter 4, it was found that a genetically identical population of cells can exhibit stochastic gene expression and response to biotic stress stimuli. This heterogenous distribution was found to be in part correlated with the ploidy number of a cell which allowed higher levels of gene expression. Here, we hypothesize that by utilizing the power of FACS, it could be possible to select the previously identified high expressive subpopulation (HF) from pWRKY11::YFP-NLS protoplasts and culture them to regenerate a new plant. If this change was fixed via an epigenetic mechanism, the offspring could potentially inherit the high expression levels of its ancestor.

5.2. Results

5.2.1. Osmoticum in sheath fluid is an important component for high efficiency, live protoplast sorting

Protoplast regeneration is a sensitive and laborious procedure spanning months with many critical control points (Figure 5.1). For a successful workflow, there a number of considerations to be taken into account.

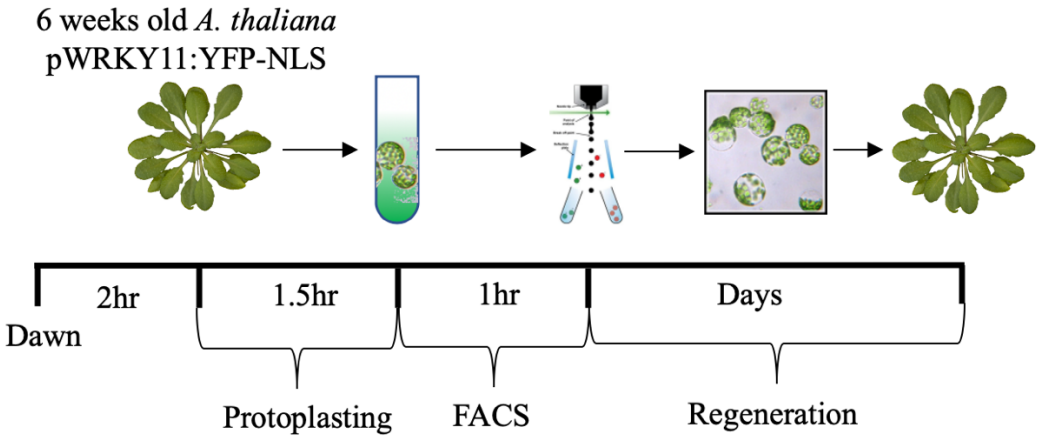

Figure 5.1. Protoplast regeneration workflow. Leaf number 9-10-11 from 6 weeks old healthy pWRKY11::YFP-NLS plants were used for protoplast generation. Cells exhibiting high fluorescence were selected by FACS and put into protoplast induction media. Media is changed as directed in section 2.6.9 for induction of dedifferentiation and microcalli formation.

First, regeneration efficiency of the protoplasts is dependent on the age and prior stress condition of the plant (Bourgin, Chupeau and Onier, 1979). For this reason, leaves at a younger developmental stage (leaf number 9-10-11) from plants with optimal health (no light stress effect, no wounding etc.) were chosen for protoplast generation.

In this work, second important point to consider is the number of live protoplasts that can be obtained from FACS procedure. Settings for FACS are given in Table 5.1, with three components to particularly consider. One specification was for the sheath fluid. During sorting, this fluid encapsulates protoplasts in drops, forming approximately ¾ of the drop volume. If the composition of this fluid does not sustain homeostasis of protoplasts, they will die before even reaching the collection tube. A crucial factor is maintaining the osmotic pressure of protoplasts. For this reason, an osmoticum was added in the design of the new sheath fluid composition. Glucose was chosen among four other candidates; fructose, galactose, mannose and mannitol since it does not form crystals upon evaporation of solvent, in this case water. Otherwise, the growing crystals would shear the delicate cell membrane or block the microtubing in a FACS machine. The pH of the sheath fluid was reduced to 5.8 as the optimal range for protoplast culturing, to sustain protoplast viability after sorting procedure. KCl salts were also added to allow charging of stream and correct functioning of the sorting system. Finally, NaN_3, a toxic chemical used to prevent contaminant growth in commercial sheath fluids was not included in the homemade sheath fluid composition.

The second component of FACS to be optimized was the physical equipment specifications. These include nozzle size, sheath and sample pressures. The diameter of sample fluid encapsulated by sheath fluid in FACS should usually be 1/3rd of the nozzle size used. Given the plant cells ranges from 10-100 µm, a 130 µm nozzle size (largest available) was used. This way, protoplasts up to ~45 µm in diameter could easily be sorted. In line with these specifications, all generated protoplasts were filtered using a 40 µm mesh to reduce creation of cell debris within FACS. Next, in order to reduce the mechanical stress on the sensitive membrane structures of protoplasts, sheath pressure was lowered from a commonly used 20 psi to 10 psi, and sample pressure was reduced from 10 psi to 2 psi.

The third component that was optimised was the sorting specification. To further increase membrane stability, samples were chilled to +4˚C before running through FACS to rigidify the cell membrane. Cells were then sorted into a collection tube filled to ¾ with protoplast induction media solution which provided cushioning for sorted cells.

Table 5.1. Specifications of not-optimized and optimized FACS procedures for high efficiency, live plant protoplast sorting.

	Variable	Not-optimized	Optimized
Sheath Fluid Specifications	pH	pH 7.4 PBS buffer	pH 5.8 MES buffer
	Osmotic Pressure	No osmoticum	0.4M Glucose
	Salts	NaCl, KCl, NaN_3	KCl
Equipment Specifications	Nozzle size	100µm	130µm
	Sheath pressure	20psi	10psi
	Sample pressure	10psi	2psi
Sorting Specifications	Temperature	Room temp	4˚C
	Sorting receptacle	Empty tube	Tube filled ¾ with PIM media
Sorting efficiency	Live cells/sorted events	~0.01%	~30%

To test the optimized FACS procedure, protoplasts were generated from leaf number 9-10-11 of six-weeks old *A. thaliana* plants and stained with the fluorescent viability dye fluorescein diacetate (FDA), and subjected to both non-optimized and optimized protocols. $2x10^3$ events with high fluorescence were sorted with each method. Protoplasts exhibiting fluorescence were counted under epifluorescence microscope (Figure 5.2) and the percent efficiency was calculated as the number of cells that survived per 100 events sorted (Table 5.1). Without optimization, efficiency of live cell sorting was calculated to be approximately 0.01%, after optimisation it was increased to approximately 30%, a number sufficient for further studies.

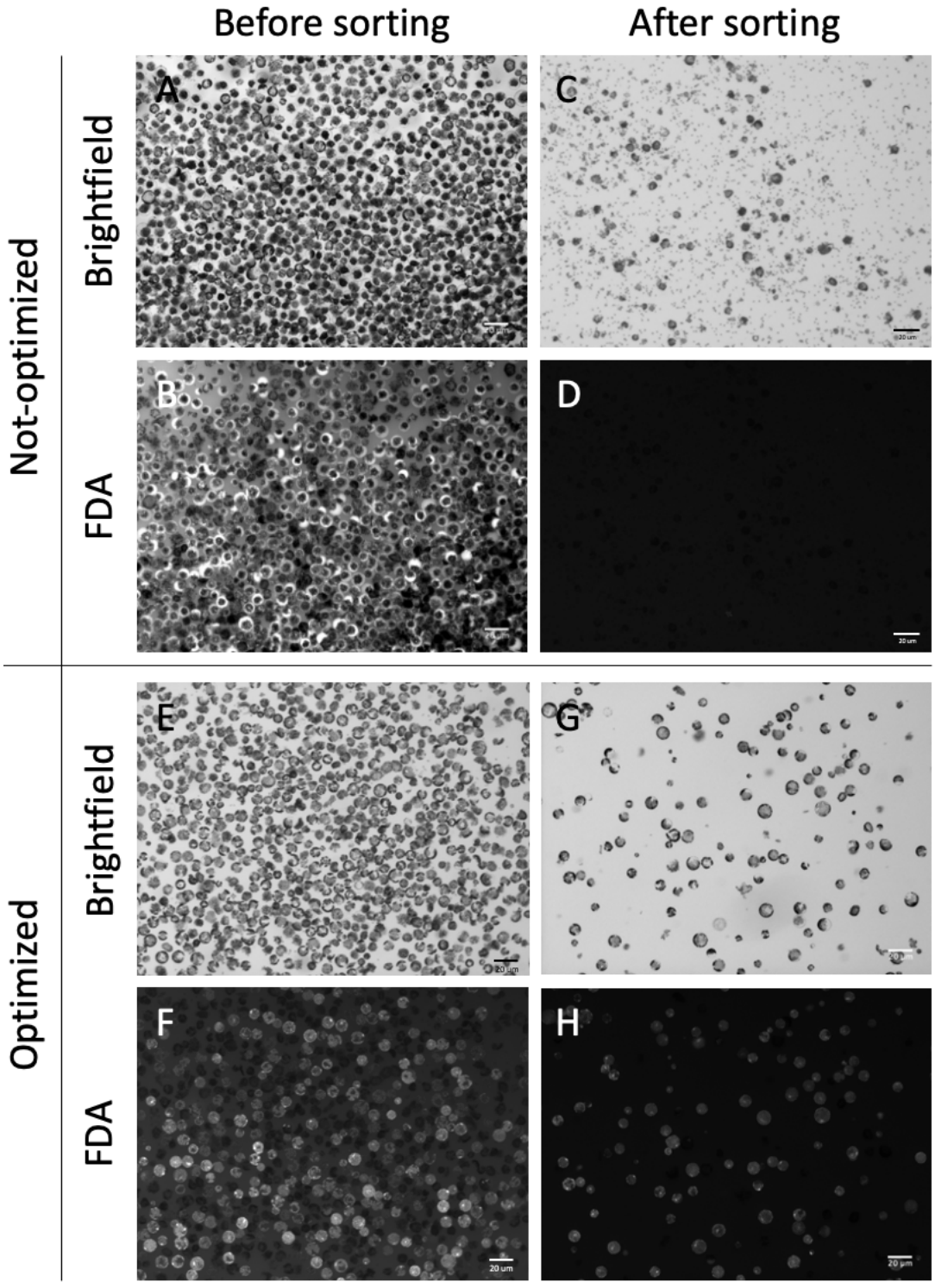

Figure 5.2. Optimization of live protoplast sorting efficiency. A,B,E,F) Images of protoplasts at $3x10^5$ PP/ml concentration as suspension in WI media before FACS. C,D) Images of sorted, FDA-stained protoplasts using non-optimized protocol. G,H) Images of sorted, FDA-stained protoplasts using optimized FACS protocol. Scale bars represent 20 μm for A,B,E,F; 50μm for C,D,G,H.

5.2.2. Regeneration studies of single-sorted protoplast cells in suspension cultures

Using the optimized protocol, pWRKY11::YFP-NLS single-protoplasts exhibiting high fluorescence were sorted from the P5 gate set in Section 4.2.3 (Figure 4.14) into 96 well tissue culture plates containing 100 µl of PIM solution with one cell sorted into each well. The media was changed as directed in Chupeau *et al*., 2013 to induce microcalli formation. Single-cell sorting experiments were performed three times and 576 single cells (6, 96-well plates) were sorted for each experiment with an average of a 25% viability rate, in line with optimization tests. It was reported that cells should exhibit division 2 days after sorting (Chupeau et al., 2013). No division was observed in any of the surviving cells after two days in PIM media. After 5 days, approximately 50% of the cells (~270) showed loss of chloroplasts, which was indicative of de-differentiation. However, no signs of nuclear-division was observed at this stage (Figure 5.3.A,B). At day 12, approximately 10% of the de-differentiated cells exhibited expanding cell wall structures. However, still no nuclear division was observed in the expanded cell, indicating an abortive fate and the other 90% of cells were no longer viable (Figure 5.3.C,D). Cells showing cell-wall expansion were imaged again at day 22 after culture media was refreshed. No further cell-wall expansions or nuclear divisions were observed at this time. After a month in culture, all cells exhibited significantly reduced nuclear fluorescence indicating they were no longer viable (Figure 5.3.E,F).

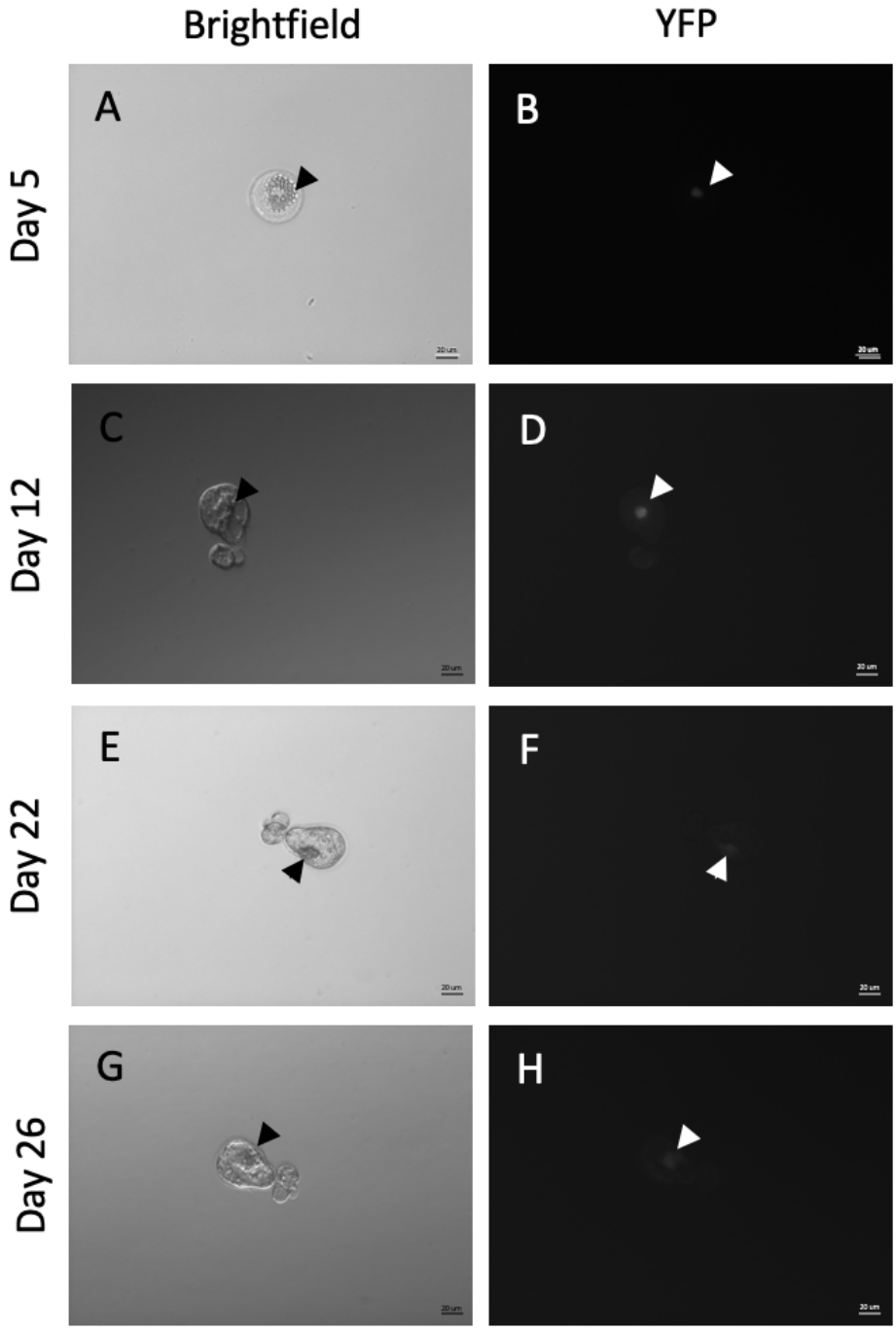

Figure 5.3. Single-cell sorting and regeneration of protoplasts in suspension culture. A,B) De-differentiating protoplast losing its chloroplasts after 5 days of culture in PIM. C,D) Expansion of cell wall without nuclear division signifying potential abortion of future cell division. E-F) No further expansion of cell-wall and gradual loss of nuclear fluorescence indicating cell death. G-H) No visible nuclear fluorescence indicating dead cells. (Scale bars = 20 µm)

5.2.3. Regeneration studies of sorted protoplast in low density suspension cultures

In the study of Chupeau *et al*., 2013, a minimum culture density of $8x10^4$ PP/ml was used, which was the only difference between the methods used in their study compared to the one PP/ml density used in this study. For this reason, it was hypothesized that the number of cultured protoplasts might be the reason for reduced regeneration rates. To test this hypothesis, $1x10^4$ PP exhibiting high fluorescence were sorted into 24 well tissue culture plates containing 1ml of PIM using P5 gate set in Section 4.2.3 PP as opposed to 1 PP/ml in a well. Due to technical limitations in this study, $1x10^4$ protoplasts was the maximum amount that could be sorted with each experiment. Compared to the single cell sorting protocol (Figure 5.3), protoplasts sorted in bulk had significantly greater division rates 2 days after sorting into PIM (Figure 5.4.A). At day 2, approximately 60% of the surviving PP retained their nuclear structure and did not de-differentiate, while the remaining 40% lost their chloroplasts, underwent chromosomal rearrangement and exhibited signs of cell division (Figure 5.4.A,B). After a week of incubation, at day 9, approximately 2% of the cells which lost their chloroplasts, underwent repeated divisions to result in microcalli formations. At this stage, approximately 10 microcalli could be seen in the protoplast suspension culture, all of which possessing multiple fluorescent nuclei. Remaining cells with arrested divisions were observed to have lost their cellular integrity with no nuclei in them (Figure 5.4.C,D). At this stage, the overall efficiency of regenerating PP/total number of PP sorted, was approximately 0.1%. 15 days after sorting, the remaining microcalli still possessed multiple nuclei but halted further growth, despite replacement of media. It was also observed that the nuclear fluorescence of the reporter protein was significantly reduced. This was an indication that the microcalli had aborted regeneration. After 30 days, it was found that all microcalli but one had lost their nuclear fluorescence. Eventually, this microcallus also lost fluorescence despite all efforts.

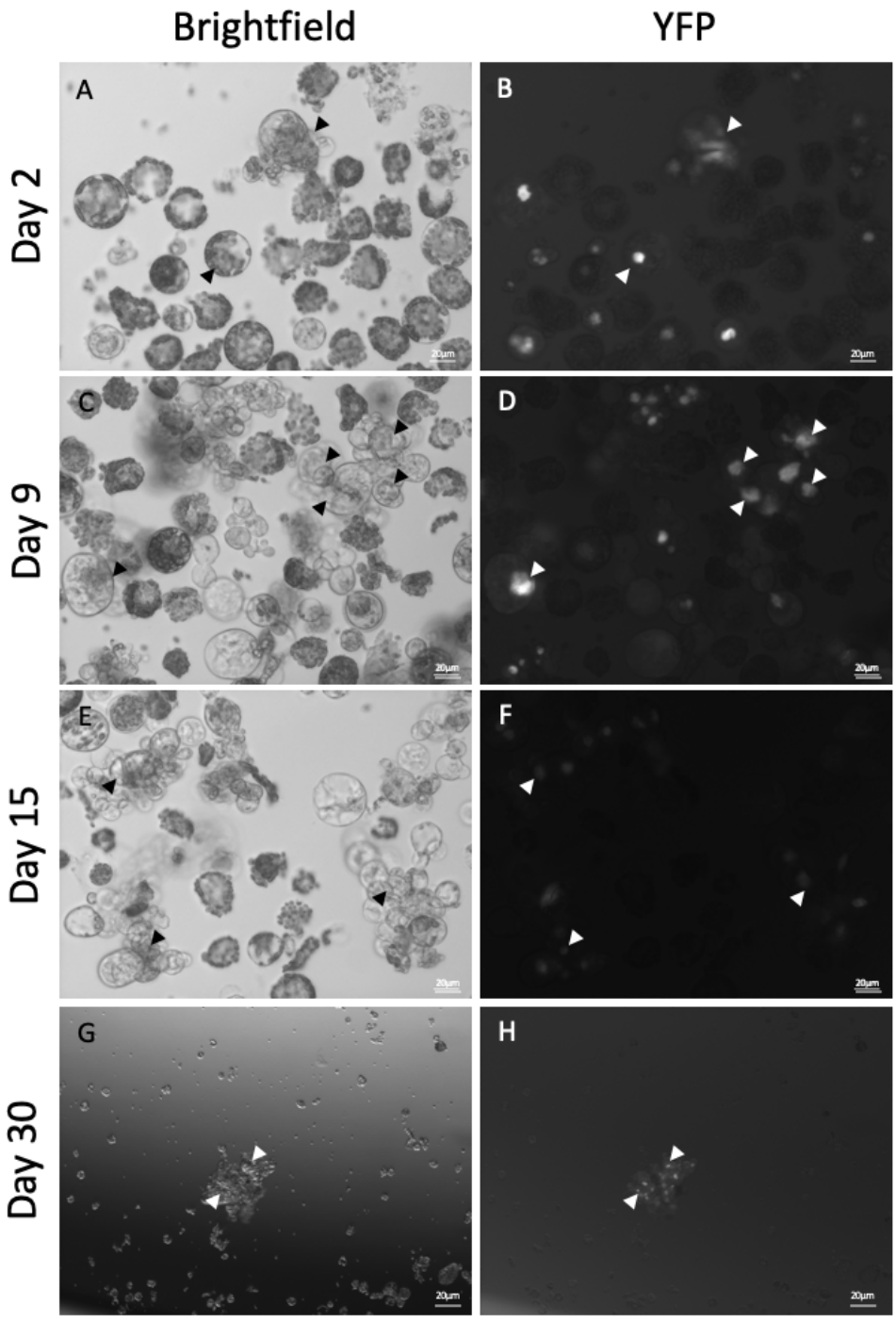

Figure 5.4. Low density sorting and regeneration of protoplasts in suspension culture. A,B) De-differentiating protoplast losing its chloroplast and nucleus for cell division 2 days after sorting in PIM. C,D) De-differentiated protoplasts divide to create multinuclear microcalli while most protoplasts lose their cell membrane and die 9 days after sorting into PIM. E,F) No further expansion of cell-wall and gradual loss of nuclear fluorescence. G,H) Last live microcalli remaining from $2x10^3$ sorted protoplasts. (Scale bars = 20 µm)

5.3. DISCUSSION

While the optimization of FACS and protoplasts was successful, regeneration of protoplasts using the suspension culture method presented challenges in testing hypotheses about the inheritance of defence responses state. However, the second round of testing showed that that using increased number of sorted protoplasts had a positive effect on stimulation of microcalli formation. Upon further research, it was found that protoplasts release signalling molecules to the environment to stimulate growth of other cells. This is known as media conditioning and was found to be possible only in high protoplast culture densities (Schäffler and Koop, 1990). To increase regeneration rate in low-density protoplast cultures, the best techniques were found to be ones utilized in single cell engineering and plant somatic embryogenesis studies. These studies suggest employment of either external media conditioning or protoplast nursing techniques (Schäffler and Koop, 1990). In the conditioning method, protoplast induction media is pre-incubated with a high density of protoplasts before use in single-cell regeneration studies. This method supplies the necessary signalling molecules for regeneration without having a need for incubating cells in high concentration. In the nursing method, the cells of interest are incubated in conjunction with other protoplasts separated by porous barriers, allowing exchange of signalling molecules. These barriers can either be made from low melting point agar in a designated area of growth or by micro-fluidic cell encapsulation (Grasso and Lintilhac, 2016; Schäffler and Koop, 1990). Employing these strategies in conjunction with the optimized protoplast generation and FACS techniques developed in this study should provide a chance to test the inheritance hypothesis in future.

6. GENERAL DISCUSSION

Transgenic legume model plants with tissue type reporter expression is important for development of agricultural practices

Global food demand is increasing with each passing year (Fischer et al., 2014), and at the same time current agricultural practices result in degradation of land, contamination of water and release of greenhouse gasses (Shcherbak et al., 2014; FAO and ITPS, 2015). This brings challenges to human health but also soil and environmental health. In order to address these pressing challenges, sustainable agricultural practices have to be adopted as soon as possible. These approaches need to be built on holistic land management principles, creating systems that support each other and minimize outside intervention. Due to their unique relationship with nitrogen-fixing bacteria, legumes are a key player in this process since they can enable nitrogen-enrichment of soils without using chemical fertilizers (Valentine et al., 2018). For this reason, it is crucial to understand molecular processes happening during nitrogen fixation in legume roots and nodules. While studies are ongoing on this topic, approaches have mostly focussed at looking at the whole root system (Mounier et al., 2014; Ruffel et al., 2011; Streeter, 1985; Zhang et al., 1999), despite the fact that since each tissue type in a root possesses different chromatin landscape and their molecular processes will vary. This means that valuable information about the regulation of nodulation will be missed or overlooked. Previous tissue-specific work in the model Brassicaceae species *A. thaliana* showed that thousands of genes are regulated at the cell-type level (Gifford et al., 2008). While such detailed work has been performed for *A. thaliana*, members of the Fabaceae (legume) family such as *M. truncatula* still require significant amount of research at the cell type level. One of the reasons for this is the fact that *M. truncatula* stable transformation is long and laborious, thus, research requires a significantly longer time (Song et al., 2013).

In this thesis, two tissue specific vectors for expression of a fluorescent and GUS reporter protein in cortex tissue were generated and tested via transient transformation. These are valuable resources for stable transformation practices in future tissue specific studies on legume plants as current tissue specific research in *M. truncatula* is dependent on laser-microdissection methodology which only allows isolation of a limited amount of cells at a time (Hogekamp et al., 2011; Sevin-Pujol et al., 2017). By creating these stable transgenic lines, it will be possible to study cell-type specific gene

expression in legumes with greater accuracy due to better sequence coverage. This will help understand the role of each tissue type in a variety of cellular processes such as nodulation and lateral root formation as well as for identifying specific responses produced by each tissue type under various environmental conditions such as variation in soil nutrient content, pH, pathogen stress etc. Understanding these responses will create a foundation for driving future work on wider use of N-fixing rhizobia and ultimately, improvement of agricultural practices.

One such improvement would be advances in research on engineering the nitrogen fixation ability of legumes into economically important crop species such as cereals (Bailey-Serres et al., 2019). In order to achieve this, it is imperative to understand the nitrogen fixation process as a whole with all its components in all parts of a root from initiation of nodule formation, to nodule maturation, nitrogen fixation machinery and distribution of fixed N to the necessary parts of the plant (Burén and Rubio, 2018; Yang et al., 2018). Besides, as root system architecture is managed by a combination of signals stemming from multiple tissue types (Herrbach et al., 2014; Le Roux et al., 2017), a holistic understanding of the root with all its components is required to understand how to influence the RSA by adjusting soil components for guiding the plants to have better adaptability to their environment. An example of this was published by Uroz, Courty and Oger, in 2019 where they explained legume-rhizobia symbiosis creating a symbiosis cascade, altering the microbial composition of the soil significantly. Such alterations could in turn create beneficial relationships between subsequent crops sown in such soil to improve crop quality and yield.

Stochastic gene expression could have a role in adaptation of plants against pathogen attack

On top of the complexity of variable cell-type specific expression, we know that genetically identical cells also have variation in gene expression such as in their extent of responses to changing environmental conditions. These responses were previously identified in prokaryotes (Balaban et al., 2004), single celled eukaryotes (Freddolino *et al.*, 2018; Liu *et al*., 2015) and multicellular organisms (Dragotakes et al., 2020)). In prokaryotes stochastic switching of genetically identical bacteria to growing or persistent states resulted in survival of persistent cells upon antibiotic treatment and death of cells at growth state allowing survival of the population as a whole (Balaban et al., 2004). In *S. cerevisiae*, increased CUP1 gene promoter noise was found to confer

better resistance to copper toxicity in industrial fermentation processes (Liu *et al*., 2015). And in mammals, macrophage phagolysosome pH was found to be stochastically determined within and between cells to allow preservation of energy while maintaining a wide range of defence against pathogens (Dragotakes et al., 2020).

In this work, it was possible observe the phenomenon of phenotypic variation in *A. thaliana* leaf spongy mesophyll cells challenged with pathogen stress (flg22 bacterial elicitor treatment) using fluorescent confocal microscopy. Results presented in this work indicate that the variation might be linked to the innate transcriptional ability of the cell that can be a result of increased genetic content through spontaneous autopolyploidy events. Indeed it was previously found that increased genetic material would result in higher, non-additive, gene expression through allele dosage effects (Osborn et al., 2003). It was found that differential expression of stress related genes were more pronounced in autotetraploid *A. thaliana* plants in comparison to diploid plants (Ng et al., 2012). However, it is also known that increased expression of stress responsive genes might have a negative impact on the development of a plant (Heil and Baldwin, 2002). Thus, it is possible that through spontaneous stochastic autopolyploidy, somatic plant cells enable a compromise for creating stronger responses upon stress, while still allowing healthy development of a plant. Spongy mesophyll cells identified with high initial responses in this work (Figure 4.10.A-HF cells), were proposed to be sentinel cells for rapid recognition of environmental stresses and generation of immediate responses. This is a novel concept for plant stress response. Its phenotypic implications as well as transcriptomic and proteomic sources should be investigated in future studies. To that end, it should be possible to utilize selective power of FACS in identification of these sentinel cells and measure RNA and protein levels at the same time using methods such as the RNA expression and protein sequencing assay (REAP-seq) (Peterson et al., 2017) or citing of transcriptomes and epitopes by sequencing (CITE-seq) (Stoeckius et al., 2017). Information gained from these studies will allow us to understand the adaptation function of heterogeneity present in seemingly identical cells in plants.

Transcriptional states can be inherited over generations, via the mechanism of transgenerational epigenetic inheritance in plants (Hauser et al., 2011). There is an intriguing possibility that stronger or more variable flg22 responses in one cell could be passed to the next generation. In this frame, each somatic cell can become a

potential precursor for improvement of the next plant generation, if cells with desired properties can be selected then they can be used as the basis for plant regeneration.

In this study, two methods were used for regeneration of sorted protoplasts with improvements in the protocol. First, a gentler sorting approach was studied to obtain high number of live protoplasts. However it is possible to achieve higher live sorting rates utilizing the recent advancements in microfluidic cell detection and sorting technologies (Yu et al., 2018). Moreover, in order to increase regeneration efficiency, sorted protoplasts require cultures with a specific topology that supports their growth (Schäffler and Koop, 1990). It was found that regeneration of low density or single protoplasts requires specialized approaches such as microdroplet encapsulation (Grasso and Lintilhac, 2016; Koop and Schweiger, 1985) or nursing culture (Eigel and Koop, 1989). Microdroplet encapsulation approach provides structural support to single cells while limiting the space in which the growth promoting hormones released from the protoplast can accumulate and increase regeneration efficiency. Nursing culture approach utilizes a microchamber allowing diffusion of growth promoting hormones from a high-density protoplast culture to a low density one without them mixing. With such tools, it might be possible to expand on the pool of material available for crop improvement, making each cell a potential new plant, without genetically modified methods, thus bringing new options for sustainable agriculture but addressing the lack of legislation enabling use of genetic modification.

Broader impact of findings

Future of food security is under threat by unsustainable agricultural practices and use of slow classical breeding methods. Thus, the scientific community carries the responsibility to investigate better possibilities to alleviate these threats by coming up with alternative methods. With developing technology and better understanding of molecular biology, each research project pushes mankind one step closer to this goal.

In order to make this goal into reality, this study presented the importance of understanding molecular mechanisms underlying phenotypes emerging from nitrogen effect on nodulation and pathogen stress response. In this study, multiple novel ideas with potential to grow were presented. One is the prospect of ‘sentinel cells’ in plant mesophyll tissue towards creating responses against pathogen stress. Along with recent research in transgenerational trait inheritance, these cells (once identified) could prove an invaluable source for next generation breeding technologies for cultivating

plants with better stress resistance. In another example, orthologs of *M. truncatula* nodulation genes in *A. thaliana* were found to have differential expression patterns in response to nitrogen treatment suggesting encouraging research on more information for legume cell-type specific gene expression profiles. To that end, novel transgenic legume plants with cell-type specific reporter expression has already been started. By utilizing these lines it could be possible to identify key players in nodulation and thus contributing to the efforts for utilizing bioengineering approaches to create crop species that are self-sufficient in their nitrogen requirement. In conclusion, findings of this study can be treated as valuable primers for creating sustainable agricultural practices and next generation plant breeding techniques.

BIBLIOGRAPHY

Abuqamar, S., Luo, H., Laluk, K., Mickelbart, M. V., Mengiste, T., 2009. Crosstalk between biotic and abiotic stress responses in tomato is mediated by the AIM1 transcription factor. Plant J. 58, 347–360.

Andreae, M.O., 2019. Emission of trace gases and aerosols from biomass burning – An updated assessment. Atmos. Chem. Phys. 19(13), 8523-8546

Andreasson, E., Ellis, B., 2010. Convergence and specificity in the Arabidopsis MAPK nexus. Trends Plant Sci. 15, 106–113.

Apel, K., Hirt, H., 2004. Reactive oxygen species: Metabolism, oxidative stress, and signal transduction. Annu. Rev. Plant Biol. 55, 373–399.

Apostol, I., Heinstein, P.F., Low, P.S., 1989. Rapid Stimulation of an Oxidative Burst during Elicitation of Cultured Plant Cells. Plant Physiol. 90, 109–116.

Araújo, I.S., Pietsch, J.M., Keizer, E.M., Greese, B., Balkunde, R., Fleck, C., Hülskamp, M., 2017. Stochastic gene expression in Arabidopsis thaliana. Nat. Commun. 8(1), 1-9 .

Asai, T., Tena, G., Plotnikova, J., Willmann, M.R., Chiu, W.L., Gomez-Gomez, L., Boller, T., Ausubel, F.M., Sheen, J., 2002. Map kinase signalling cascade in Arabidopsis innate immunity. Nature 415, 977–983.

Aslam, M., Travis, R.L., Huffaker, R.C., 1992. Comparative kinetics and reciprocal inhibition of nitrate and nitrite uptake in roots of uninduced and induced barley (Hordeum vulgare L) seedlings. Plant Physiol. 99, 1124–1133.

Atkinson, N.J., Lilley, C.J., Urwin, P.E., 2013. Identification of genes involved in the response of arabidopsis to simultaneous biotic and abiotic stresses. Plant Physiol. 162, 2028–2041.

Atkinson, N.J., Urwin, P.E., 2012. The interaction of plant biotic and abiotic stresses: From genes to the field. J. Exp. Bot. 63(10), 3523-3543

Avivi, Y., Morad, V., Ben-Meir, H., Zhao, J., Kashkush, K., Tzfira, T., Citovsky, V., Grafi, G., 2004. Reorganization of Specific Chromosomal Domains and Activation of Silent Genes in Plant Cells Acquiring Pluripotentiality. Dev. Dyn. 230, 12–22.

Avraham, R., Haseley, N., Brown, D., Penaranda, C., Jijon, H.B., Trombetta, J.J., Satija, R., Shalek, A.K., Xavier, R.J., Regev, A., Hung, D.T., 2015. Pathogen Cell-to-Cell Variability Drives Heterogeneity in Host Immune Responses. Cell. 162(6), 1309-1321.

Bailey-Serres, J., Parker, J.E., Ainsworth, E.A., Oldroyd, G.E.D., Schroeder, J.I., 2019. Genetic strategies for improving crop yields. Nature. 575(7781), 109-118.

Balaban, N.Q., Merrin, J., Chait, R., Kowalik, L., Leibler, S., 2004. Bacterial persistence as a phenotypic switch. Science (80-.). 305, 1622–1625.

Balkunde, R., Kitagawa, M., Xu, X.M., Wang, J., Jackson, D., 2017. SHOOT MERISTEMLESS trafficking controls axillary meristem formation, meristem size and organ boundaries in Arabidopsis. Plant J. 90, 435–446.

Banda, J., Bellande, K., von Wangenheim, D., Goh, T., Guyomarc'h, S., Laplaze, L., Bennett, M.J., 2019. Lateral Root Formation in Arabidopsis: A Well-Ordered LRexit. Trends Plant Sci. 24, 826–839.

Bargmann, B.O.R., Birnbaum, K.D., 2010. Fluorescence activated cell sorting of plant protoplasts. J. Vis. Exp. 36.

Bari, R., Jones, J.D.G., 2009. Role of plant hormones in plant defence responses. Plant Mol. Biol. 69, 473–488.

Bauer, W.D., Caetano-Anollés, G., 1990. Chemotaxis, induced gene expression and competitiveness in the rhizosphere. Plant Soil 129, 45–52.

Bebber, D.P., Holmes, T., Gurr, S.J., 2014. The global spread of crop pests and pathogens. Glob. Ecol. Biogeogr. 23(12), 1398-1407.

Behl, R., Tischner, R., Raschke, K., 1988. Induction of a high-capacity nitrate-uptake mechanism in barley roots prompted by nitrate uptake through a constitutive low-capacity mechanism. Planta. 176(2), 235-240.

Bensmihen, S., de Billy, F., Gough, C., 2011. Contribution of NFP LysM domains to the recognition of Nod factors during the Medicago truncatula/Sinorhizobium meliloti symbiosis. PLoS One. 6(11), e26114

Bent, A.F., Kunkel, B.N., Dahlbeck, D., Brown, K.L., Schmidt, R., Giraudat, J., Leung, J., Staskawicz, B.J., 1994. RPS2 of Arabidopsis thaliana: A leucine-rich repeat class of plant disease resistance genes. Science 265(5180), 1856-1860.

Berens, M.L., Wolinska, K.W., Spaepen, S., Ziegler, J., Nobori, T., Nair, A., Krüler, V., Winkelmüller, T.M., Wang, Y., Mine, A., Becker, D., Garrido-Oter, R., Schulze-Lefert, P., Tsuda, K., 2019. Balancing trade-offs between biotic and abiotic stress responses through leaf age-dependent variation in stress hormone cross-talk. Proc. Natl. Acad. Sci. U. S. A. 116, 2364–2373.

Bertani, G., 2004. Lysogeny at Mid-Twentieth Century: P1, P2, and Other Experimental Systems. J. Bacteriol. 186(3), 595-600.

Bilgin, D.D., Zavala, J.A., Zhu, J., Clough, S.J., Ort, D.R., Delucia, E.H., 2010. Biotic stress globally downregulates photosynthesis genes. Plant, Cell Environ. 33, 1597–1613.

Billen, G., Garnier, J., Lassaletta, L., 2013. The nitrogen cascade from agricultural soils to the sea: Modelling nitrogen transfers at regional watershed and global scales. Philos. Trans. R. Soc. B Biol. Sci. 368(1621), 20130123

Binder, B.M., 2020. Ethylene signaling in plants. J. Biol. Chem. 295, 7710–7725.

Birnbaum, K., Shasha, D.E., Wang, J.Y., Jung, J.W., Lambert, G.M., Galbraith, D.W., Benfey, P.N., 2003. A Gene Expression Map of the Arabidopsis Root. Science (80-.). 302, 1956–1960.

Bohacek, J., Mansuy, I.M., 2017. A guide to designing germline-dependent epigenetic inheritance experiments in mammals. Nat. Methods 14, 243–249.

Boisson-Dernier, A., Chabaud, M., Garcia, F., Bécard, G., Rosenberg, C., Barker, D.G., 2001. Agrobacterium rhizogenes-transformed roots of Medicago truncatula for the study of nitrogen-fixing and endomycorrhizal symbiotic associations. Mol. Plant-Microbe Interact. 14, 695–700.

Bonke, M., Thitamadee, S., Mähönen, A.P., Hauser, M.T., Helariutta, Y., 2003. APL regulates vascular tissue identity in Arabidopsis. Nature. 426(6963), 181-186.

Bonner, W.A., Hulett, H.R., Sweet, R.G., Herzenberg, L.A., 1972. Fluorescence activated cell sorting. Rev. Sci. Instrum. 234(3), 108-118.

Bortesi, L., Fischer, R., 2015. The CRISPR/Cas9 system for plant genome editing and beyond. Biotechnol. Adv. 33(1), 41-52.

Boudsocq, M., Willmann, M.R., McCormack, M., Lee, H., Shan, L., He, P., Bush, J., Cheng, S.-H., Sheen, J., 2010. Differential innate immune signalling via Ca2+

sensor protein kinases. Nature 464, 418–422.

Bouguyon, E., Brun, F., Meynard, D., Kubeš, M., Pervent, M., Leran, S., Lacombe, B., Krouk, G., Guiderdoni, E., Zazímalová, E., Hoyerová, K., Nacry, P., Gojon, A., 2015. Multiple mechanisms of nitrate sensing by Arabidopsis nitrate transceptor NRT1.1. Nat. Plants. 1(3), 1-8.

Bourgin, J. -P, Chupeau, Y., Onier, C., 1979. Plant Regeneration from Mesophyll Protoplasts of Several Nicotiana Species. Physiol. Plant. 45, 288–292.

Brady, S.M., Orlando, D.A., Lee, J.Y., Wang, J.Y., Koch, J., Dinneny, J.R., Mace, D., Ohler, U., Benfey, P.N., 2007a. A high-resolution root spatiotemporal map reveals dominant expression patterns. Science (80-.). 318, 801–806.

Brady, S.M., Song, S., Dhugga, K.S., Rafalski, J.A., Benfey, P.N., 2007b. Combining expression and comparative evolutionary analysis. The COBRA gene family. Plant Physiol. 143, 172–187.

Bräutigam, K., Vining, K.J., Lafon-Placette, C., Fossdal, C.G., Mirouze, M., Marcos, J.G., Fluch, S., Fraga, M.F., Guevara, M.Á., Abarca, D., Johnsen, Ø., Maury, S., Strauss, S.H., Campbell, M.M., Rohde, A., Díaz-Sala, C., Cervera, M.T., 2013. Epigenetic regulation of adaptive responses of forest tree species to the environment. Ecol. Evol. 3, 399–415.

Brewin, N.J., 1991. Development of the legume root nodule. Annu. Rev. Cell Biol. 7(1), 191-226.

Brookes, G., Barfoot, P., 2016. GM crops: global socio-economic and environmental impacts 1996-2012. PG Econ. Ltd, UK. 1-189

Bucher, M., Brunner, S., Zimmermann, P., Zardi, G.I., Amrhein, N., Willmitzer, L., Riesmeier, J.W., 2002. Erratum: The expression of an extensin-like protein correlates with cellular tip growth in tomato. Plant Physiol. 129, 911-923.

Bull, C.T., de Boer, S.H., Denny, T.P., Firrao, G., Fischer-Le Saux, M., Saddler, G.S., Scortichini, M., Stead, D.E., Takikawa, Y., 2010. Comprehensive list of names of plant pathogenic bacteria, 1980-2007. J. Plant Pathol. 92, 551–592.

Burén, S., Rubio, L.M., 2018. State of the art in eukaryotic nitrogenase engineering. FEMS Microbiol. Lett. 365(2), fnx274.

Cai, L., Dalal, C.K., Elowitz, M.B., 2008. Frequency-modulated nuclear localization

bursts coordinate gene regulation. Nature 455, 485–490.

Capone, D.G., 2001. Marine nitrogen fixation: what's the fuss? Commentary Douglas G Capone. Curr. Opin. Microbiol. 4, 341–348.

Carpenter, S.R., Caraco, N.F., Correll, D.L., Howarth, R.W., Sharpley, A.N., Smith, V.H., 1998. Nonpoint pollution of surface waters with phosphorus and nitrogen. Ecol. Appl. 8(3), 559-568

Chabaud, M., Boisson-dernier, A., Zhang, J., Taylor, C.G., Yu, O., Barker, D.G., 2006. Agrobacterium rhizogenes -mediated root transformation. Medicago truncatula Handb.

Cheng, Z., Li, J.F., Niu, Y., Zhang, X.C., Woody, O.Z., Xiong, Y., Djonović, S., Millet, Y., Bush, J., McConkey, B.J., Sheen, J., Ausubel, F.M., 2015. Pathogen-secreted proteases activate a novel plant immune pathway. Nature. 521(7551), 213-216.

Chinchilla, D., Zipfel, C., Robatzek, S., Kemmerling, B., Nürnberger, T., Jones, J.D.G., Felix, G., Boller, T., 2007. A flagellin-induced complex of the receptor FLS2 and BAK1 initiates plant defence. Nature 448, 497–500.

Chini, A., Fonseca, S., Fernández, G., Adie, B., Chico, J.M., Lorenzo, O., García-Casado, G., López-Vidriero, I., Lozano, F.M., Ponce, M.R., Micol, J.L., Solano, R., 2007. The JAZ family of repressors is the missing link in jasmonate signalling. Nature 448, 666–671.

Chinnusamy, V., Schumaker, K., Zhu, J.K., 2004. Molecular genetic perspectives on cross-talk and specificity in abiotic stress signalling in plants. J. Exp. Bot. 55, 225–236.

Chisholm, S.T., Coaker, G., Day, B., Staskawicz, B.J., 2006. Host-microbe interactions: Shaping the evolution of the plant immune response. Cell 124, 803–814.

Cho, H.T., Cosgrove, D.J., 2002. Regulation of root hair initiation and expansin gene expression in Arabidopsis. Plant Cell 14, 3237–3253.

Chupeau, M.-C., Granier, F., Pichon, O., Renou, J.-P., Gaudin, V., Chupeau, Y., 2013. Characterization of the Early Events Leading to Totipotency in an Arabidopsis Protoplast Liquid Culture by Temporal Transcript Profiling. Plant Cell 25, 2444–2463.

Coker, Timothy L.R., Cevik, V., Beynon, J.L., Gifford, M.L., 2015. Spatial dissection of the Arabidopsis thaliana transcriptional response to downy mildew using Fluorescence Activated Cell Sorting. Front. Plant Sci. 6, 527.

Cooper, G.M., Hausman, R.E., 2007. The Cell: A Molecular Approach 2nd Edition, Sinauer Associates.

Corish, P., Tyler-Smith, C., 1999. Attenuation of green fluorescent protein half-life in mammalian cells. Protein Eng. 12(12), 1035-1040.

Crawford, K.M., Zambryski, P.C., 2000. Subcellular localization determines the availability of non-targeted proteins to plasmodesmatal transport. Curr. Biol. 10, 1032–1040.

Crawford, N.M., Glass, A.D.M., 1998. Molecular and physiological aspects of nitrate uptake in plants. Trends Plant Sci. 3(10), 389-395.

Crews, T.E., Carton, W., Olsson, L., 2018. Is the future of agriculture perennial? Imperatives and opportunities to reinvent agriculture by shifting from annual monocultures to perennial polycultures. Glob. Sustain. 1.

Cristina, M., Petersen, M., Mundy, J., 2010. Mitogen-activated protein kinase signaling in plants. Annu. Rev. Plant Biol. 61, 621–649.

Cubitt, A.B., Heim, R., Adams, S.R., Boyd, A.E., Gross, L.A., Tsien, R.Y., 1995. Understanding, improving and using green fluorescent proteins. Trends Biochem. Sci. 20, 448–455.

Dai, X., Zhuang, Z., Boschiero, C., Dong, Y., Zhao, P.X., Parkway, S.N., 2020. OUP accepted manuscript. Nucleic Acids Res. 1–8.

Dalla Costa, L., Malnoy, M., Gribaudo, I., 2017. Breeding next generation tree fruits: Technical and legal challenges. Hortic. Res. 4, 1–11.

Dangl, J.L., Jones, J.D., 2001. Plant pathogens and integrated defence responses to infection. Nature 411, 826–833.

De Clercq, I., Vermeirssen, V., Van Aken, O., Vandepoele, K., Murcha, M.W., Law, S.R., Inzé, A., Ng, S., Ivanova, A., Rombaut, D., van de Cotte, B., Jaspers, P., Van de Peer, Y., Kangasjärvi, J., Whelan, J., Van Breusegem, F., 2013. The membrane-bound NAC transcription factor ANAC013 functions in mitochondrial retrograde regulation of the oxidative stress response in

Arabidopsis. Plant Cell 25, 3472–3490.

De Lamballerie, X., Zandotti, C., Vignoli, C., Bollet, C., de Micco, P., 1992. A one-step microbial DNA extraction method using “Chelex 100” suitable for gene amplification. Res. Microbiol. 143, 785–790.

De Lucas, M., Davière, J.M., Rodríguez-Falcón, M., Pontin, M., Iglesias-Pedraz, J.M., Lorrain, S., Fankhauser, C., Blázquez, M.A., Titarenko, E., Prat, S., 2008. A molecular framework for light and gibberellin control of cell elongation. Nature 451, 480–484.

De Smet, I., 2012. Lateral root initiation: One step at a time. New Phytol. 193, 867–873.

De Smet, I., Lau, S., Mayer, U., Jürgens, G., 2010. Embryogenesis - The humble beginnings of plant life. Plant J. 61, 959–970.

Deal, R.B., Henikoff, S., 2011. The INTACT method for cell typeg-specific gene expression and chromatin profiling in Arabidopsis thaliana. Nat. Protoc. 6(1), 56-68.

Deans, C., Maggert, K.A., 2015. What do you mean, “Epigenetic”? Genetics 199, 887–896.

Deslandes, L., Olivier, J., Peeters, N., Feng, D.X., Khounlotham, M., Boucher, C., Somssich, I., Genin, S., Marco, Y., 2003. Physical interaction between RRS1-R, a protein conferring resistance to bacterial wilt, and PopP2, a type III effector targeted to the plant nucleus. Proc. Natl. Acad. Sci. U. S. A. 100, 8024–8029.

Després, C., Chubak, C., Rochon, A., Clark, R., Bethune, T., Desveaux, D., Fobert, P.R., 2003. The Arabidopsis NPR1 disease resistance protein is a novel cofactor that confers redox regulation of DNA binding activity to the basic domain/Leucine Zipper transcription factor TGA1. Plant Cell 15, 2181–2191.

Dhanasekaran, S., Doherty, T.M., Kenneth, J., 2010. Comparison of different standards for real-time PCR-based absolute quantification. J. Immunol. Methods. 354(1-2), 34-39.

Díaz, C.L., Grønlund, M., Schlaman, H.R.M., Herman, P., 2005. Chapter 6.2 I 261–277.

Ding, M., Chen, Z.J., 2018. Epigenetic perspectives on the evolution and

domestication of polyploid plant and crops. Curr. Opin. Plant Biol. 42, 37-48.

Dodds, P.N., Rathjen, J.P., 2010. Plant immunity: towards an integrated view of plant–pathogen interactions. Nat. Rev. Genet. 11, 539–548.

Dong, X., 2004. NPR1, all things considered. Curr. Opin. Plant Biol. 7, 547–552.

Downie, J.A., 2014. Legume nodulation. Curr. Biol. 24, R184–R190.

Dragotakes, Q., Stouffer, K.M., Fu, M.S., Sella, Y., Youn, C., Yoon, O.I., de Leon-Rodriguez, C.M., Freij, J.B., Bergman, A., Casadevall, A., 2020. Macrophages use a bet-hedging strategy for antimicrobial activity in phagolysosomal acidification. J. Clin. Invest. 130, 7.

Driessche, R. v. d., 1998. Plant Analysis, an Interpretation Manual. Tree Physiol.

Dubrovsky, J.G., Sauer, M., Napsucialy-Mendivil, S., Ivanchenko, M.G., Friml, J., Shishkova, S., Celenza, J., Benková, E., 2008. Auxin acts as a local morphogenetic trigger to specify lateral root founder cells. Proc. Natl. Acad. Sci. U. S. A. 105, 8790–8794.

Eigel, L., Koop, H.U., 1989. Nurse Culture of Individual Cells: Regeneration of Colonies from Single Protoplasts of Nicotiana tabacum, Brassica napus and Hordeum vulgare. J. Plant Physiol.

Eldar, A., Elowitz, M.B., 2010. Functional roles for noise in genetic circuits. Nature 467, 167–173.

Emmert-Buck, M.R., Bonner, R.F., Smith, P.D., Chuaqui, R.F., Zhuang, Z., Goldstein, S.R., Weiss, R.A., Liotta, L.A., 1996. Laser capture microdissection. Science 274(5289), 998-1001.

Engelsdorf, T., Horst, R.J., Pröls, R., Pröschel, M., Dietz, F., Hückelhoven, R., Voll, L.M., 2013. Reduced carbohydrate availability enhances the susceptibility of arabidopsis toward Colletotrichum higginsianum. Plant Physiol. 162, 225–238.

Erisman, J.W., Sutton, M.A., Galloway, J., Klimont, Z., Winiwarter, W., 2008. How a century of ammonia synthesis changed the world. Nat. Geosci. 1, 636–639.

Esseling, J.J., Lhuissier, F.G.P., Emons, A.M.C., 2003. Nod factor-induced root hair curling: Continuous polar growth towards the point of nod factor application.

Plant Physiol. 132, 1982–1988.

Eulgem, T., Somssich, I.E., 2007. Networks of WRKY transcription factors in defense signaling. Curr. Opin. Plant Biol. 10, 366–371.

Evans, D.A., 1983. Agricultural applications of plant protoplast fusion. Bio/Technology. 1(3), 253-261

Evert, R.F., Eichhorn, S.E., 2006. Esau's Plant Anatomy: Meristems, Cells, and Tissues of the Plant Body: Their Structure, Function, and Development: Third Edition, Esau's Plant Anatomy: Meristems, Cells, and Tissues of the Plant Body: Their Structure, Function, and Development: Third Edition.

Feinberg, A.P., Irizarry, R.A., 2010. Stochastic epigenetic variation as a driving force of development, evolutionary adaptation, and disease. Proc. Natl. Acad. Sci. U. S. A. 107, 1757–1764.

Felix, G., Duran, J.D., Volko, S., Boller, T., 1999. Plants have a sensitive perception system for the most conserved domain of bacterial flagellin. Plant J. 18(3), 265-276.

Fischer, T., Byerlee, D., Edmeades, G., 2014. Crop yields and global food security: will copyright Act 1968 yield increase continue to feed the world? Aust. Cent. Int. Agric. Res. 634.

Flagel, L.E., Wendel, J.F., 2009. Gene duplication and evolutionary novelty in plants. New Phytol. 183(3), 557-564.

Fonseca, S., Chini, A., Hamberg, M., Adie, B., Porzel, A., Kramell, R., Miersch, O., Wasternack, C., Solano, R., 2009. (+)-7-iso-Jasmonoyl-L-isoleucine is the endogenous bioactive jasmonate. Nat. Chem. Biol. 5, 344–350.

Freddolino, P.L., Yang, J., Momen-Roknabadi, A., Tavazoie, S., 2018. Stochastic tuning of gene expression enables cellular adaptation in the absence of pre-existing regulatory circuitry. Elife. 7, e31867.

Frerichs, A., Engelhorn, J., Altmüller, J., Gutierrez-Marcos, J., Werr, W., 2019. Specific chromatin changes mark lateral organ founder cells in the Arabidopsis inflorescence meristem. J. Exp. Bot. 70, 3867–3879.

Fuglie, K., Heisey, P., King, J., Schimmelpfennig, D., 2012. Rising Concentration in Agricultural Input Industries Influences New Technologies. United States Dep.

Agric. Econ. Res. Serv. 10.

Fulwyler, M.J., 1965. Electronic separation of biological cells by volume. Science. 150(3698), 910-911.

Gage, D.J., 2004. Infection and Invasion of Roots by Symbiotic, Nitrogen-Fixing Rhizobia during Nodulation of Temperate Legumes. Microbiol. Mol. Biol. Rev. 68(2), 280-300.

Galloway, J.N., 2013. The Global Nitrogen Cycle. In: Treatise on Geochemistry: Second Edition.

Galloway, J.N., Dentener, F.J., Capone, D.G., Boyer, E.W., Howarth, R.W., Seitzinger, S.P., Asner, G.P., Cleveland, C.C., Green, P.A., Holland, E.A., Karl, D.M., Michaels, A.F., Porter, J.H., Townsend, A.R., Vörösmarty, C.J., 2004. Nitrogen cycles: Past, present, and future. Biogeochemistry. 70(2), 153-226.

Gan, Y., Bernreiter, A., Filleur, S., Abram, B., Forde, B.G., 2012. Overexpressing the ANR1 MADS-box gene in transgenic plants provides new insights into its role in the nitrate regulation of root development. Plant Cell Physiol. 53(6), 1003-1016.

Gao, Q.M., Zhu, S., Kachroo, P., Kachroo, A., 2015. Signal regulators of systemic acquired resistance. Front. Plant Sci. 6, 1–12.

Gavrilovic, S., Yan, Z., Jurkiewicz, A.M., Stougaard, J., Markmann, K., 2016. Inoculation insensitive promoters for cell type enriched gene expression in legume roots and nodules. Plant Methods 12, 1–14.

Gechev, T.S., Van Breusegem, F., Stone, J.M., Denev, I., Laloi, C., 2006. Reactive oxygen species as signals that modulate plant stress responses and programmed cell death. BioEssays 28, 1091–1101.

Geng, Y., Wu, R., Wee, C.W., Xie, F., Wei, X., Chan, P.M.Y., Tham, C., Duan, L., Dinneny, J.R., 2013. A spatio-temporal understanding of growth regulation during the salt stress response in Arabidopsis. Plant Cell 25, 2132–2154.

Ghanta, S., Chattopadhyay, S., 2011. Glutathione as a signaling molecule another challenge to pathogens. Plant Signal. Behav. 6(6), 783-788.

Gifford, M.L., Dean, A., Gutierrez, R.A., Coruzzi, G.M., Birnbaum, K.D., 2008. Cell-specific nitrogen responses mediate developmental plasticity. Proc. Natl. Acad. Sci. 105, 803–808.

Gill, S.S., Tuteja, N., 2010. Reactive oxygen species and antioxidant machinery in abiotic stress tolerance in crop plants. Plant Physiol. Biochem. 48, 909–930.

Glazebrook, J., 2005. Contrasting mechanisms of defense against biotrophic and necrotrophic pathogens. Annu. Rev. Phytopathol. 43, 205–227.

Golden, J.P., Justin, G.A., Nasir, M., Ligler, F.S., 2012. Hydrodynamic focusing-a versatile tool. Anal. Bioanal. Chem. 402(1), 325-335.

Goodstein, D.M., Shu, S., Howson, R., Neupane, R., Hayes, R.D., Fazo, J., Mitros, T., Dirks, W., Hellsten, U., Putnam, N., Rokhsar, D.S., 2012. Phytozome: A comparative platform for green plant genomics. Nucleic Acids Res. 40, 1178–1186.

Grant, J.J., Loake, G.J., 2000. Role of reactive oxygen intermediates and cognate redox signaling in disease resistance, Plant physiology, 124(1), 21-30.

Grasso, M.S., Lintilhac, P.M., 2016. Microbead Encapsulation of Living Plant Protoplasts: A New Tool for the Handling of Single Plant Cells. Appl. Plant Sci. 4, 1500140.

Grønlund, J.T., Eyres, A., Kumar, S., Buchanan-Wollaston, V., Gifford, M.L., 2012. Cell specific analysis of Arabidopsis leaves using fluorescence activated cell sorting. J. Vis. Exp. (68), e4214.

Gruber, B.D., Giehl, R.F.H., Friedel, S., von Wirén, N., 2013. Plasticity of the Arabidopsis root system under nutrient deficiencies. Plant Physiol. 163(1), 161-179.

Gudesblat, G.E., Torres, P.S., Vojnov, A.A., 2009. Stomata and pathogens: Warfare at the gates. Plant Signal. Behav. 4, 1114–1116.

Han, X., Kim, J.Y., 2016. Integrating Hormone- and Micromolecule-Mediated Signaling with Plasmodesmal Communication. Mol. Plant 9, 46–56.

Hang, H., Fox, M.H., 2004. Analysis of the mammalian cell cycle by flow cytometry. Methods Mol. Biol. (pp. 23-35). Humana Press.

Hans Wedepohl, K., 1995. The composition of the continental crust. Geochim. Cosmochim. Acta 59, 1217–1232.

Hanson, J.B., 1978. Application of the Chemiosmotic Hypothesis to Ion Transport Across the Root. Plant Physiol. 62, 402–405.

Hauser, M.T., Aufsatz, W., Jonak, C., Luschnig, C., 2011. Transgenerational epigenetic inheritance in plants. Biochim. Biophys. Acta - Gene Regul. Mech. 1809, 459–468.

Hayashi, T., Shimoda, Y., Sato, S., Tabata, S., Imaizumi-Anraku, H., Hayashi, M., 2014. Rhizobial infection does not require cortical expression of upstream common symbiosis genes responsible for the induction of Ca2+ spiking. Plant J. 77, 146–159.

He, H., Van Breusegem, F., Mhamdi, A., 2018. Redox-dependent control of nuclear transcription in plants. J. Exp. Bot. 69, 3359–3372.

Heidstra, R., Welch, D., Scheres, B., 2004. Mosaic analyses using marked activation and deletion clones dissect Arabidopsis SCARECROW action in asymmetric cell division. Genes Dev. 18, 1964–1969.

Heil, M., Baldwin, I.T., 2002. Fitness costs of induced resistance: Emerging experimental support for a slippery concept. Trends Plant Sci. 7(2), 61-67.

Herder, G. Den, De Keyser, A., De Rycke, R., Rombauts, S., Van De Velde, W., Clemente, M.R., Verplancke, C., Mergaert, P., Kondorosi, E., Holster, M., Goormachtig, S., 2008. Seven in absentia proteins affect plant growth and nodulation in Medicago truncatula. Plant Physiol. 148(1), 369-382.

Herrbach, V., Remblière, C., Gough, C., Bensmihen, S., 2014. Lateral root formation and patterning in Medicago truncatula. J. Plant Physiol. 171, 301–310.

Herzenberg, Leonard A., Parks, D., Sahaf, B., Perez, O., Roederer, M., Herzenberg, Leonore A., 2002. The history and future of the Fluorescence Activated Cell Sorter and flow cytometry: A view from Stanford. Clin. Chem. 48, 1819–1827.

Hirano, S.S., Upper, C.D., 2000. Bacteria in the Leaf Ecosystem with Emphasis onPseudomonas syringae—a Pathogen, Ice Nucleus, and Epiphyte. Microbiol. Mol. Biol. Rev. 64, 624–653.

Ho, C.H., Lin, S.H., Hu, H.C., Tsay, Y.F., 2009. CHL1 Functions as a Nitrate Sensor in Plants. Cell. 138(6), 1184-1194.

Hodge, A., 2004. The plastic plant: Root responses to heterogeneous supplies of

nutrients. New Phytol. 162, 9–24.

Hogekamp, C., Arndt, D., Pereira, P.A., Becker, J.D., Hohnjec, N., Küster, H., 2011. Laser microdissection unravels cell-type-specific transcription in arbuscular mycorrhizal roots, including CAAT-Box transcription factor gene expression correlating with fungal contact and spread. Plant Physiol. 157, 2023–2043.

Horibe, T., Torisawa, A., Kurihara, R., Akiyoshi, R., Hatta-Ohashi, Y., Suzuki, H., Kawakami, K., 2016. Monitoring Bip promoter activation during cancer cell growth by bioluminescence imaging at the single-cell level. Integr. Cancer Sci. Ther. 2(6), 291-299.

Hossain, M.A., Munné-Bosch, S., Burritt, D.J., Diaz-Vivancos, P., Fujita, M., Lorence, A., 2018. Ascorbic Acid in Plant Growth, Development and Stress Tolerance, Ascorbic Acid in Plant Growth, Development and Stress Tolerance.

Hou, X., Lee, L.Y.C., Xia, K., Yan, Y., Yu, H., 2010. DELLAs Modulate Jasmonate Signaling via Competitive Binding to JAZs. Dev. Cell 19, 884–894.

Hu, G., Fearon, E.R., 1999. Siah-1 N-Terminal RING Domain Is Required for Proteolysis Function, and C-Terminal Sequences Regulate Oligomerization and Binding to Target Proteins. Mol. Cell. Biol. 19(1), 724-732.

Hu, P., Zhang, W., Xin, H., Deng, G., 2016. Single cell isolation and analysis. Front. Cell Dev. Biol. 4, 1–12.

Hu, Y., Dong, Q., Yu, D., 2012. Arabidopsis WRKY46 coordinates with WRKY70 and WRKY53 in basal resistance against pathogen Pseudomonas syringae. Plant Sci. 185–186, 288–297.

Huisman, R., Geurts, R., 2020. A Roadmap toward Engineered Nitrogen-Fixing Nodule Symbiosis. Plant Commun. 1, 100019.

Huot, B., Yao, J., Montgomery, B.L., He, S.Y., 2014. Growth-defense tradeoffs in plants: A balancing act to optimize fitness. Mol. Plant. 7(8), 1267-1287.

Ichimura, K., Mizoguchi, T., Yoshida, R., Yuasa, T., Shinozaki, K., 2000. Various abiotic stresses rapidly activate Arabidopsis MAP kinases ATMPK4 and ATMPK6. Plant J. 24, 655–665.

Ichimura, K., Shinozaki, K., Tena, G., Sheen, J., Henry, Y., Champion, A., Kreis, M., Zhang, S., Hirt, H., Wilson, C., Heberle-Bors, E., Ellis, B.E., Morris, P.C., Innes,

R.W., Ecker, J.R., Scheel, D., Klessig, D.F., Machida, Y., Mundy, J., Ohashi, Y., Walker, J.C., 2002. Mitogen-activated protein kinase cascades in plants: A new nomenclature. Trends Plant Sci. 7, 301–308.

Ito, Y., Toyota, H., Kaneko, K., Yomo, T., 2009. How selection affects phenotypic fluctuation. Mol. Syst. Biol. 5, 1–7.

Iyer-Pascuzzi, A.S., Jackson, T., Cui, H., Petricka, J.J., Busch, W., Tsukagoshi, H., Benfey, P.N., 2011. Cell Identity Regulators Link Development and Stress Responses in the Arabidopsis Root. Dev. Cell 21, 770–782.

Jeudy, C., Ruffel, S., Freixes, S., Tillard, P., Santoni, A.L., Morel, S., Journet, E.P., Duc, G., Gojon, A., Lepetit, M., Salon, C., 2010. Adaptation of Medicago truncatula to nitrogen limitation is modulated via local and systemic nodule developmental responses. New Phytol. 185, 817–828.

Jia, N., Zhu, Y., Xie, F., 2018. An efficient protocol for model legume root protoplast isolation and transformation. Front. Plant Sci. 9, 1–7.

Jia, Y., Mcadams, S.A., Bryan, G.T., Hershey, H.P., Valent, B., 2000. Direct interaction of resistance gene and avirulence gene products confers rice blast resistance. The EMBO journal. 19(15), 4004-4014.

Jickells, T., 2006. The role of air-sea exchange in the marine nitrogen cycle. Biogeosciences Discuss. 3, 183–210.

Jixin Dong, Chunhong Chen, Z.C., 2003. Expression profiles of Arabidopsis WRKY superfamily during plant defense response.pdf. Plant Mol. Biol. 51, 21–37.

Jones, J.D.G., Dangl, J.L., 2006. The plant immune system. Nature 444, 323–329.

Jones, P.A., 2012. Functions of DNA methylation: Islands, start sites, gene bodies and beyond. Nat. Rev. Genet. 13, 484–492.

Journot-Catalino, H., Somssich, I.E., Roby, D., Kroj, T., 2006. The transcription factors WRKY11 and WRKY17 act as negative regulators of basal resistance in Arabidopsis thaliana. Plant Cell 18, 3289–3302.

Jovtchev, G., Schubert, V., Meister, A., Barow, M., Schubert, I., 2006. Nuclear DNA content and nuclear and cell volume are positively correlated in angiosperms. Cytogenet. Genome Res. 114(1), 77-82.

Ju, C., Yoon, G.M., Shemansky, J.M., Lin, D.Y., Ying, Z.I., Chang, J., Garrett, W.M., Kessenbrock, M., Groth, G., Tucker, M.L., Cooper, B., Kieber, J.J., Chang, C., 2012. CTR1 phosphorylates the central regulator EIN2 to control ethylene hormone signaling from the ER membrane to the nucleus in Arabidopsis. Proc. Natl. Acad. Sci. U. S. A. 109, 19486–19491.

Jung, C., Lyou, S.H., Yeu, S., Kim, M.A., Rhee, S., Kim, M., Lee, J.S., Choi, Y. Do, Cheong, J.J., 2007. Microarray-based screening of jasmonate-responsive genes in Arabidopsis thaliana. Plant Cell Rep. 26, 1053–1063.

Karimi, M., Inzé, D., Depicker, A., 2002. GATEWAY vectors for Agrobacterium-mediated plant.pdf. Trends Plant Sci. 7, 193–195.

Katagiri, Y., Hasegawa, J., Fujikura, U., Hoshino, R., Matsunaga, S., Tsukaya, H., 2016. The coordination of ploidy and cell size differs between cell layers in leaves. Dev. 143(7), 1120-1125.

Kazan, K., Manners, J.M., 2009. Linking development to defense: auxin in plant-pathogen interactions. Trends Plant Sci. 14, 373–382.

Kharchenko, P. V., Silberstein, L., Scadden, D.T., 2014. Bayesian approach to single-cell differential expression analysis. Nat. Methods 11, 740–742.

Kilian, J., Whitehead, D., Horak, J., Wanke, D., Weinl, S., Batistic, O., D'Angelo, C., Bornberg-Bauer, E., Kudla, J., Harter, K., 2007. The AtGenExpress global stress expression data set: Protocols, evaluation and model data analysis of UV-B light, drought and cold stress responses. Plant J. 50(2), 347-363.

Kim, M.G., Da Cunha, L., McFall, A.J., Belkhadir, Y., DebRoy, S., Dangl, J.L., Mackey, D., 2005. Two Pseudomonas syringae type III effectors inhibit RIN4-regulated basal defense in Arabidopsis. Cell 121, 749–759.

King, E.O., Ward, M.K., Raney, D.E., 1954. Two simple media for the demonstration of pyocyanin and fluorescin. J. Lab. Clin. Med. 44(2), 301-307.

Kirti, P.B., Bhat, S.R., Dinesh Kumar, V., Prakash, S., Chopra, V.L., 2001. A simple protocol for regenerating mesophyll protoplasts of vegetable Brassicas. J. Plant Biochem. Biotechnol. 10, 49–51.

Koop, H.U., Schweiger, H.G., 1985. Regeneration of Plants from Individually Cultivated Protoplasts using an Improved Microculture System. J. Plant Physiol.

Koornneef, M., Meinke, D., 2010. The development of Arabidopsis as a model plant. Plant J. 61, 909–921.

Kopittke, P.M., Menzies, N.W., Wang, P., McKenna, B.A., Lombi, E., 2019. Soil and the intensification of agriculture for global food security. Environ. Int. 132, 105078.

Kotur, Z., Mackenzie, N., Ramesh, S., Tyerman, S.D., Kaiser, B.N., Glass, A.D.M., 2012. Nitrate transport capacity of the Arabidopsis thaliana NRT2 family members and their interactions with AtNAR2.1. New Phytol. 194(3), 724-731.

Kronzucker, H.J., Glass, A.D.M., Siddiqi, M.Y., 1999. Inhibition of nitrate uptake by ammonium in barley. Analysis of component fluxes. Plant Physiol. 120, 283–291.

Krouk, G., Crawford, N.M., Coruzzi, G.M., Tsay, Y.F., 2010a. Nitrate signaling: Adaptation to fluctuating environments. Curr. Opin. Plant Biol. 13(3), 265-272.

Krouk, G., Lacombe, B., Bielach, A., Perrine-Walker, F., Malinska, K., Mounier, E., Hoyerova, K., Tillard, P., Leon, S., Ljung, K., Zazimalova, E., Benkova, E., Nacry, P., Gojon, A., 2010b. Nitrate-regulated auxin transport by NRT1.1 defines a mechanism for nutrient sensing in plants. Dev. Cell. 18(6), 927-937.

Kunze, G., Zipfel, C., Robatzek, S., Niehaus, K., Boller, T., Felix, G., 2004. The N terminus of bacterial elongation factor Tu elicits innate immunity in Arabidopsis plants. Plant Cell. 16(12), 3496-3507.

Lagunas, B., Walker, L., Hussain, R.M.F., Hands-Portman, I., Woolley-Allen, K., Gifford, M.L., 2018. Histological profiling over time to optimize root cell type-specific reporter lines for cell sorting. Methods Mol. Biol. 1761, 165–175.

Laloi, C., Apel, K., Danon, A., 2004. Reactive oxygen signalling: The latest news. Curr. Opin. Plant Biol. 7, 323–328.

Lamport, D.T.A., 1966. The Protein Component of Primary Cell Walls. Adv. Bot. Res. 2, 151–218.

Lassaletta, L., Billen, G., Grizzetti, B., Anglade, J., Garnier, J., 2014. 50 year trends in nitrogen use efficiency of world cropping systems: The relationship between yield and nitrogen input to cropland. Environ. Res. Lett. 9(10), 105011.

Latrasse, D., Jégu, T., Li, H., de Zelicourt, A., Raynaud, C., Legras, S., Gust, A.,

Samajova, O., Veluchamy, A., Rayapuram, N., Ramirez-Prado, J.S., Kulikova, O., Colcombet, J., Bigeard, J., Genot, B., Bisseling, T., Benhamed, M., Hirt, H., 2017. MAPK-triggered chromatin reprogramming by histone deacetylase in plant innate immunity. Genome Biol. 18, 1–19.

Le Roux, J.J., Hui, C., Keet, J.H., Ellis, A.G., 2017. Co-introduction vs ecological fitting as pathways to the establishment of effective mutualisms during biological invasions. New Phytol. 215, 1354–1360.

Ledgard, S.F., Steele, K.W., 1992. Biological nitrogen fixation in mixed legume/grass pastures. Plant Soil 141, 137–153.

Lee, J.Y., Colinas, J., Wang, J.Y., Mace, D., Ohler, U., Benfey, P.N., 2006. Transcriptional and posttranscriptional regulation of transcription factor expression in Arabidopsis roots. Proc. Natl. Acad. Sci. U. S. A. 103, 6055–6060.

Lee, M.M., Schiefelbein, J., 1999. WEREWOLF, a MYB-related protein in Arabidopsis, is a position-dependent regulator of epidermal cell patterning. Cell 99, 473–483.

Lee, S.C., Luan, S., 2012. ABA signal transduction at the crossroad of biotic and abiotic stress responses. Plant, Cell Environ. 35, 53–60.

Levy, A.A., Feldman, M., 2004. Genetic and epigenetic reprogramming of the wheat genome upon allopolyploidization. Biol. J. Linn. Soc. 82, 607–613.

Li, F., Flanary, P.L., Altieri, D.C., Dohlman, H.G., 2000. Cell division regulation by BIR1, a member of the inhibitor of apoptosis family in yeast. J. Biol. Chem. 275(10), 6707-6711.

Li, M., Ma, X., Chiang, Y.H., Yadeta, K.A., Ding, P., Dong, L., Zhao, Y., Li, X., Yu, Y., Zhang, L., Shen, Q.H., Xia, B., Coaker, G., Liu, D., Zhou, J.M., 2014. Proline isomerization of the immune receptor-interacting protein RIN4 by a cyclophilin inhibits effector-triggered immunity in arabidopsis. Cell Host Microbe 16, 473–483.

Linkohr, B.I., Williamson, L.C., Fitter, A.H., Leyser, H.M.O., 2002. Nitrate and phosphate availability and distribution have different effects on root system architecture of Arabidopsis. Plant J. 29(6), 751-760.

Little, D.Y., Rao, H., Oliva, S., Daniel-Vedele, F., Krapp, A., Malamy, J.E., 2005. The putative high-affinity nitrate transporter NRT2.1 represses lateral root initiation in response to nutritional cues. Proc. Natl. Acad. Sci. U. S. A. 102, 13693–13698.

Liu, K.H., Tsay, Y.F., 2003. Switching between the two action modes of the dual-affinity nitrate transporter CHL1 by phosphorylation. EMBO J. 22(5), 1005-1013.

Liu, S., Liu, Y., Yang, X., Tong, C., Edwards, D., Parkin, I.A.P., Zhao, M., Ma, J., Yu, J., Huang, S., Wang, Xiyin, Wang, Junyi, Lu, K., Fang, Z., Bancroft, I., Yang, T.J., Hu, Q., Wang, Xinfa, Yue, Z., Li, H., Yang, Linfeng, Wu, J., Zhou, Q., Wang, W., King, G.J., Pires, J.C., Lu, C., Wu, Z., Sampath, P., Wang, Z., Guo, H., Pan, S., Yang, Limei, Min, J., Zhang, D., Jin, D., Li, W., Belcram, H., Tu, J., Guan, M., Qi, C., Du, D., Li, Jiana, Jiang, L., Batley, J., Sharpe, A.G., Park, B.S., Ruperao, P., Cheng, F., Waminal, N.E., Huang, Yin, Dong, C., Wang, L., Li, Jingping, Hu, Z., Zhuang, M., Huang, Yi, Huang, J., Shi, J., Mei, D., Liu, J., Lee, T.H., Wang, Jinpeng, Jin, H., Li, Z., Li, X., Zhang, J., Xiao, L., Zhou, Y., Liu, Z., Liu, X., Qin, R., Tang, X., Liu, W., Wang, Y., Zhang, Y., Lee, J., Kim, H.H., Denoeud, F., Xu, X., Liang, X., Hua, W., Wang, Xiaowu, Wang, Jun, Chalhoub, B., Paterson, A.H., 2014. The brassica oleracea genome reveals the asymmetrical evolution of polyploid genomes. Nat. Commun. 5(1), 1-11.

Liu, Y., Zhang, C., Chen, J., Guo, L., Li, X., Li, W., Yu, Z., Deng, J., Zhang, P., Zhang, K., Zhang, L., 2013. Arabidopsis heat shock factor HsfA1a directly senses heat stress, pH changes, and hydrogen peroxide via the engagement of redox state. Plant Physiol. Biochem. 64, 92–98.

Livak, K.J., Schmittgen, T.D., 2001. Analysis of relative gene expression data using real-time quantitative PCR and the 2-ΔΔCT method. Methods 25, 402–408.

Livi-Bacci, M., 2017. A Concise History of World Population, John Wiley & Sons.

Loake, G., Grant, M., 2007. Salicylic acid in plant defence-the players and protagonists. Curr. Opin. Plant Biol. 10, 466–472.

Loh, Y.H., Wu, Q., Chew, J.L., Vega, V.B., Zhang, W., Chen, X., Bourque, G., George, J., Leong, B., Liu, J., Wong, K.Y., Sung, K.W., Lee, C.W.H., Zhao, X.D., Chiu, K.P., Lipovich, L., Kuznetsov, V.A., Robson, P., Stanton, L.W., Wei, C.L., Ruan, Y., Lim, B., Ng, H.H., 2006. The Oct4 and Nanog transcription network regulates pluripotency in mouse embryonic stem cells. Nat. Genet. 38, 431–440.

Ma, W., Li, J., Qu, B., He, X., Zhao, X., Li, B., Fu, X., Tong, Y., 2014. Auxin biosynthetic gene TAR2 is involved in low nitrogen-mediated reprogramming of root architecture in Arabidopsis. Plant J. 78, 70–79.

Mackey, D., Holt, B.F., Wiig, A., Dangl, J.L., 2002. RIN4 interacts with Pseudomonas syringae type III effector molecules and is required for RPM1-mediated resistance in Arabidopsis. Cell 108, 743–754.

Macosko, E.Z., Basu, A., Satija, R., Nemesh, J., Shekhar, K., Goldman, M., Tirosh, I., Bialas, A.R., Kamitaki, N., Martersteck, E.M., Trombetta, J.J., Weitz, D.A., Sanes, J.R., Shalek, A.K., Regev, A., McCarroll, S.A., 2015. Highly parallel genome-wide expression profiling of individual cells using nanoliter droplets. Cell 161, 1202–1214.

Madsen, L.H., Tirichine, L., Jurkiewicz, A., Sullivan, J.T., Heckmann, A.B., Bek, A.S., Ronson, C.W., James, E.K., Stougaard, J., 2010. The molecular network governing nodule organogenesis and infection in the model legume Lotus japonicus. Nat. Commun. 1(1), 1-12.

Marina, O.C., Sanders, C.K., Mourant, J.R., 2012. Correlating light scattering with internal cellular structures. Biomed. Opt. Express. 3(2), 296-312.

Marstrand, T.T., Storey, J.D., 2014. Identifying and mapping cell-type-specific chromatin programming of gene expression. Proc. Natl. Acad. Sci. U. S. A. 111.

Martin, C.E., Hiramitsu, K., Kitajima, Y., Nozawa, Y., Skriver, L., Thompson, G. a, 1976. Molecular control of membrane properties during temperature acclimation. Fatty acid desaturase regulation of membrane fluidity in acclimating Tetrahymena cells. Biochemistry 15, 5218–27.

Masclaux-Daubresse, C., Daniel-Vedele, F., Dechorgnat, J., Chardon, F., Gaufichon, L., Suzuki, A., 2010. Nitrogen uptake, assimilation and remobilization in plants: Challenges for sustainable and productive agriculture. Ann. Bot. 105, 1141–1157.

Mathesius, U., 2008. Goldacre paper: Auxin: At the root of nodule development? Funct. Plant Biol. 35(8), 651-668.

Mauch-Mani, B., Baccelli, I., Luna, E., Flors, V., 2017. Defense Priming: An Adaptive Part of Induced Resistance. Annu. Rev. Plant Biol. 68, 485–512.

Medici, A., Krouk, G., 2014. The Primary Nitrate Response: A multifaceted signalling pathway. J. Exp. Bot. 65, 5567–5576.

Melotto, M., Underwood, W., Sheng, Y.H., 2008. Role of stomata in plant innate immunity and foliar bacterial diseases. Annu. Rev. Phytopathol. 46, 101–122.

Meyer, D., Lauber, E., Roby, D., Arlat, M., Kroj, T., 2005. Optimization of pathogenicity assays to study the Arabidopsis thaliana-Xanthomonas campestris pv. campestris pathosystem. Mol. Plant Pathol. 6, 327–333.

Meyer, H.M., Teles, J., Formosa-Jordan, P., Refahi, Y., San-Bento, R., Ingram, G., Jönsson, H., Locke, J.C.W., Roeder, A.H.K., 2017. Fluctuations of the transcription factor atml1 generate the pattern of giant cells in the arabidopsis sepal. Elife. 6, e19131.

Miller, A.J., 2014. Plant Mineral Nutrition. eLS.

Mittler, R., Vanderauwera, S., Gollery, M., Van Breusegem, F., 2004. Reactive oxygen gene network of plants. Trends Plant Sci. 9, 490–498.

Molecular Biology of the Cell (4th Ed), 2002. . J. Biol. Educ.

Molinier, J., Ries, G., Zipfel, C., Hohn, B., 2006. Transgeneration memory of stress in plants. Nature 442, 1046–1049.

Morrison, D.K., Davis, R.J., 2003. Regulation of MAP Kinase Signaling Modules by Scaffold Proteins in Mammals. Annu. Rev. Cell Dev. Biol. 19, 91–118.

Mounier, E., Pervent, M., Ljung, K., Gojon, A., Nacry, P., 2014. Auxin-mediated nitrate signalling by NRT1.1 participates in the adaptive response of Arabidopsis root architecture to the spatial heterogeneity of nitrate availability. Plant, Cell Environ. 37, 162–174.

Mourant, J.R., Canpolat, M., Brocker, C., Esponda-Ramos, O., Johnson, T.M., Matanock, A., Stetter, K., Freyer, J.P., 2000. Light scattering from cells: the contribution of the nucleus and the effects of proliferative status. J. Biomed. Opt. 5(2), 131-137.

Moussaieff, A., Rogachev, I., Brodsky, L., Malitsky, S., Toal, T.W., Belcher, H., Yativ, M., Brady, S.M., Benfey, P.N., Aharoni, A., 2013. High-resolution metabolic mapping of cell types in plant roots. Proc. Natl. Acad. Sci. U. S. A. 110.

Mysore, K.S., Senthil-Kumar, M., 2015. Plant gene silencing: Methods and protocols. Plant Gene Silenc. Methods Protoc. 1–304.

Nakagami, H., Pitzschke, A., Hirt, H., 2005. Emerging MAP kinase pathways in plant stress signalling. Trends Plant Sci. 10, 339–346.

Naseer, S., Lee, Y., Lapierre, C., Franke, R., Nawrath, C., Geldner, N., 2012. Casparian strip diffusion barrier in Arabidopsis is made of a lignin polymer without suberin. Proc. Natl. Acad. Sci. U. S. A. 109(25), 10101-10106.

Navarro, L., Navarro, L., Zipfel, C., Zipfel, C., Rowland, O., Rowland, O., Keller, I., Keller, I., Robatzek, S., Robatzek, S., Boller, T., Boller, T., Jones, J.D.G., Jones, J.D.G., 2004. The Transcriptional Innate Immune Response to g22. Interplay and Overlap with Avr Gene-Dependent Defense Responses and Bacterial Pathogenesis. Plant Physiol. 135, 1113–1128.

Newman, M.A., Sundelin, T., Nielsen, J.T., Erbs, G., 2013. MAMP (microbe-associated molecular pattern) triggered immunity in plants. Front. Plant Sci. 4, 139.

Ng, D.W.K., Zhang, C., Miller, M., Shen, Z., Briggs, S.P., Chen, Z.J., 2012. Proteomic divergence in Arabidopsis autopolyploids and allopolyploids and their progenitors. Heredity (Edinb). 108(4), 419-430.

Nishida, H., Suzaki, T., 2018. Nitrate-mediated control of root nodule symbiosis. Curr. Opin. Plant Biol. 44, 129–136.

Ntoukakis, V., Saur, I.M.L., Conlan, B., Rathjen, J.P., 2014. The changing of the guard: The Pto/Prf receptor complex of tomato and pathogen recognition. Curr. Opin. Plant Biol. 20, 69–74.

O'Brien, J.A.A., Vega, A., Bouguyon, E., Krouk, G., Gojon, A., Coruzzi, G., Gutiérrez, R.A.A., 2016. Nitrate Transport, Sensing, and Responses in Plants. Mol. Plant 9, 837–856.

Oliveros, J.C., 2007. VENNY. An interactive tool for comparing lists with Venn Diagrams. http://bioinfogp.cnb.csic.es/tools/venny/index.html [WWW Document]. bioinfogp.cnb.csic.es/tools/venny/index.html.

Ondzighi-Assoume, C.A., Chakraborty, S., Harris, J.M., 2016. Environmental nitrate stimulates abscisic acid accumulation in arabidopsis root tips by releasing it from inactive stores. Plant Cell 28, 729–745.

Orsel, M., Filleur, S., Fraisier, V., Daniel-Vedele, F., 2002. Nitrate transport in plants: Which gene and which control? J. Exp. Bot. 53, 825–833.

Osborn, T.C., Chris Pires, J., Birchler, J.A., Auger, D.L., Chen, Z.J., Lee, H.S., Comai, L., Madlung, A., Doerge, R.W., Colot, V., Martienssen, R.A., 2003. Understanding mechanisms of novel gene expression in polyploids. Trends Genet. 19, 141–147.

Parisod, C., Holderegger, R., Brochmann, C., 2010. Evolutionary consequences of autopolyploidy. New Phytol. 186, 5–17.

Patriarca, E.J., Tatè, R., Ferraioli, S., Iaccarino, M., 2004. Organogenesis of Legume Root Nodules. Int. Rev. Cytol. 234, 201–262.

Peer, W.A., Murphy, A.S., 2006. Flavonoids as signal molecules: Targets of flavonoid action. In: The Science of Flavonoids. 239-268

Peng, M., Hannam, C., Gu, H., Bi, Y.M., Rothstein, S.J., 2007. A mutation in NLA, which encodes a RING-type ubiquitin ligase, disrupts the adaptability of Arabidopsis to nitrogen limitation. Plant J. 50, 320–337.

Peschansky, V.J., Wahlestedt, C., 2014. Non-coding RNAs as direct and indirect modulators of epigenetic regulation. Epigenetics 9, 3–12.

Peterson, V.M., Zhang, K.X., Kumar, N., Wong, J., Li, L., Wilson, D.C., Moore, R., Mcclanahan, T.K., Sadekova, S., Klappenbach, J.A., 2017. Multiplexed quantification of proteins and transcripts in single cells. Nat. Biotechnol. 35(10), 936-939.

Petricka, J.J., Schauer, M.A., Megraw, M., Breakfield, N.W., Thompson, J.W., Georgiev, S., Soderblom, E.J., Ohler, U., Moseley, M.A., Grossniklaus, U., Benfey, P.N., 2012. The protein expression landscape of the Arabidopsis root. Proc. Natl. Acad. Sci. U. S. A. 109, 6811–6818.

Poncini, L., Wyrsch, I., Tendon, V.D., Vorley, T., Boller, T., Geldner, N., Métraux, J.P., Lehmann, S., 2017. In roots of Arabidopsis thaliana, the damage-associated molecular pattern AtPep1 is a stronger elicitor of immune signalling than flg22 or the chitin heptamer. PLoS One 12, 1–21.

Postel, S., Kemmerling, B., 2009. Plant systems for recognition of pathogen-associated molecular patterns. Semin. Cell Dev. Biol. 20(9), 1025-1031.

Pratelli, R., Guerra, D.D., Yu, S., Wogulis, M., Kraft, E., Frommer, W.B., Callis, J., Pilot, G., 2012. The ubiquitin E3 ligase LOSS OF GDU2 Is required for GLUTAMINE DUMPER1-induced amino acid secretion in Arabidopsis. Plant Physiol. 158, 1628–1642.

Quaedvlieg, N.E.M., Schlaman, H.R.M., Admiraal, P.C., Wijting, S.E., Stougaard, J., Spaink, H.P., 1998. Erratum: Fusions between green fluorescent protein and β-glucuronidase as sensitive and vital bifunctional reporters in plants (Plant Molecular Biology (1998) 37 (715-727)). Plant Mol. Biol. 38, 917.

Raj, A., van Oudenaarden, A., 2008. Nature, Nurture, or Chance: Stochastic Gene Expression and Its Consequences. Cell 135, 216–226.

Reid, D.E., Ferguson, B.J., Gresshoff, P.M., 2011. Inoculation- and nitrate-induced CLE peptides of soybean control NARK-dependent nodule formation. Mol. Plant-Microbe Interact. 24, 606–618.

Reimer-Michalski, E.M., Conrath, U., 2016. Innate immune memory in plants. Semin. Immunol. 28, 319–327.

Riveras, E., Alvarez, J.M., Vidal, E.A., Oses, C., Vega, A., Gutiérrez, R.A., 2015. The calcium ion is a second messenger in the nitrate signaling pathway of Arabidopsis. Plant Physiol. 169(2), 1397-1404.

Robinson, D., 1994. The responses of plants to non-uniform supplies of nutrients. New Phytol. 127, 635–674.

Rodriguez-Villalon, A., Brady, S.M., 2019. Single cell RNA sequencing and its promise in reconstructing plant vascular cell lineages. Curr. Opin. Plant Biol. 48, 47–56.

Roetschi, A., Si-Ammour, A., Belbahri, L., Mauch, F., Mauch-Mani, B., 2001. Characterization of an Arabidopsis-Phytophthora pathosystem: Resistance requires a functional pad2 gene and is independent of salicylic acid, ethylene and jasmonic acid signalling. Plant J. 28, 293–305.

Rohila, J.S., Yang, Y., 2007. Rice mitogen-activated protein kinase gene family and its role in biotic and abiotic stress response. J. Integr. Plant Biol. 49, 751–759.

Ron, M., Kajala, K., Pauluzzi, G., Wang, D., Reynoso, M.A., Zumstein, K., Garcha, J., Winte, S., Masson, H., Inagaki, S., Federici, F., Sinh, N., Deal, R.B., Bailey-Serres, J., Brady, S.M., 2014. Hairy root transformation using Agrobacterium rhizogenes as a tool for exploring cell type-specific gene expression and function using tomato as a model. Plant Physiol. 166, 455–469.

Ross, A.F., 1961. Systemic acquired resistance induced by localized virus infections in plants. Virology 14, 340–358.

Roudier, F., Schindelman, G., DeSalle, R., Benfey, P.N., 2002. The COBRA family of putative GPI-anchored proteins in Arabidopsis. A new fellowship in expansion. Plant Physiol. 130, 538–548.

Ruegger, M., Dewey, E., Gray, W.M., Hobbie, L., Turner, J., Estelle, M., 1998. The TIR1 protein of Arabidopsis functions in auxin response and is related to human SKP2 and yeast Grr1p. Genes Dev. 12(2), 198-207.

Ruffe, S., Freixes, S., Balzergue, S., Tillard, P., Jeudy, C., Martin-Magniette, M.L., Van Der Merwe, M.J., Kakar, K., Gouzy, J., Fernie, A.R., Udvardi, M., Salon, C., Gojon, A., Lepetit, M., 2008. Systemic signaling of the plant nitrogen status triggers specific transcriptome responses depending on the nitrogen source in Medicago truncatula. Plant Physiol. 146, 2020–2035.

Ruffel, S., Krouk, G., Ristova, D., Shasha, D., Birnbaum, K.D., Coruzzi, G.M., 2011. Nitrogen economics of root foraging: Transitive closure of the nitrate-cytokinin relay and distinct systemic signaling for N supply vs. demand. Proc. Natl. Acad. Sci. U. S. A. 108, 18524–18529.

Ryu, K.H., Kang, Y.H., Park, Y.H., Hwang, I., Schiefelbein, J., Lee, M.M., 2005. The WEREWOLF MYB protein directly regulates CAPRICE transcription during cell fate specification in the Arabidopsis root epidermis. Development 132, 4765–4775.

Sahu, P.P., Pandey, G., Sharma, N., Puranik, S., Muthamilarasan, M., Prasad, M., 2013. Epigenetic mechanisms of plant stress responses and adaptation. Plant Cell Rep. 32, 1151–1159.

Saijo, Y., Loo, E.P. iian, 2020. Plant immunity in signal integration between biotic and abiotic stress responses. New Phytol. 225, 87–104.

Sakakibara, H., Takei, K., Hirose, N., 2006. Interactions between nitrogen and cytokinin in the regulation of metabolism and development. Trends Plant Sci. 11, 440–448.

Sato, T., Maekawa, S., Yasuda, S., Sonoda, Y., Katoh, E., Ichikawa, T., Nakazawa, M., Seki, M., Shinozaki, K., Matsui, M., Goto, D.B., Ikeda, A., Yamaguchi, J., 2009. CNI1/ATL31, a RING-type ubiquitin ligase that functions in the carbon/nitrogen response for growth phase transition in Arabidopsis seedlings. Plant J. 60, 852–864.

Schäffler, E., Koop, H.U., 1990. Single cell nurse culture of tobacco protoplasts: Physiological analysis of conditioning factors. J. Plant Physiol. 137(1), 95-101.

Schnabel, E., Journet, E.P., De Carvalho-Niebel, F., Duc, G., Frugoli, J., 2005. The Medicago truncatula SUNN gene encodes a CLV1-like leucine-rich repeat receptor kinase that regulates nodule number and root length. Plant Mol. Biol. 58(6), 809-822.

Scholl, R.L., May, S.T., Ware, D.H., 2000. Resources and Opportunities Seed and Molecular Resources for Arabidopsis. Society 124, 1477–1480.

Serrano, M., Coluccia, F., Torres, M., L'Haridon, F., Métraux, J.P., 2014. The cuticle and plant defense to pathogens. Front. Plant Sci. 5, 1–8.

Sevin-Pujol, A., Sicard, M., Rosenberg, C., Auriac, M.C., Lepage, A., Niebel, A., Gough, C., Bensmihen, S., 2017. Development of a GAL4-VP16/UAS trans-activation system for tissue specific expression in Medicago truncatula. PLoS One 12, 1–14.

Shah, N.M., Groves, A.K., Anderson, D.J., 1996. Alternative neural crest cell fates are instructively promoted by TGFβ superfamily members. Cell 85, 331–343.

Shahrezaei, V., Swain, P.S., 2008. The stochastic nature of biochemical networks. Curr. Opin. Biotechnol. 19, 369–374.

Shaikhali, J., Heiber, I., Seidel, T., Ströher, E., Hiltscher, H., Birkmann, S., Dietz, K.J., Baier, M., 2008. The redox-sensitive transcription factor Rap2.4a controls nuclear expression of 2-Cys peroxiredoxin A and other chloroplast antioxidant enzymes. BMC Plant Biol. 8, 1–14.

Shcherbak, I., Millar, N., Robertson, G.P., 2014. Global metaanalysis of the nonlinear response of soil nitrous oxide (N 2O) emissions to fertilizer nitrogen. Proc. Natl. Acad. Sci. U. S. A. 111, 9199–9204.

Singh, A., Soltani, M., 2013. Quantifying intrinsic and extrinsic variability in stochastic gene expression models. PLoS One 8.

Slaughter, A., Daniel, X., Flors, V., Luna, E., Hohn, B., Mauch-Mani, B., 2012. Descendants of primed Arabidopsis plants exhibit resistance to biotic stress. Plant Physiol. 158, 835–843.

Smýkal, P., Coyne, C.J., Ambrose, M.J., Maxted, N., Schaefer, H., Blair, M.W., Berger, J., Greene, S.L., Nelson, M.N., Besharat, N., Vymyslický, T., Toker, C., Saxena, R.K., Roorkiwal, M., Pandey, M.K., Hu, J., Li, Y.H., Wang, L.X., Guo, Y., Qiu, L.J., Redden, R.J., Varshney, R.K., 2015. Legume Crops Phylogeny and Genetic Diversity for Science and Breeding. CRC. Crit. Rev. Plant Sci. 34, 43–104.

Song, Q., Zhang, T., Stelly, D.M., Chen, Z.J., 2017. Epigenomic and functional analyses reveal roles of epialleles in the loss of photoperiod sensitivity during domestication of allotetraploid cottons. Genome Biol. 18, 1–14.

Song, Y., Nolan, K.E., Rose, R.J., 2013. Stable transformation of Medicago truncatula cv. Jemalong for gene analysis using Agrobacterium tumefaciens. Methods Mol.

Biol. 203-214.

Sprent, J.I., 2009. Legume Nodulation: A Global Perspective.

Stagnari, F., Maggio, A., Galieni, A., Pisante, M., 2017. Multiple benefits of legumes for agriculture sustainability: an overview. Chem. Biol. Technol. Agric. 4, 1–13.

Stamp, P., Visser, R., 2012. The twenty-first century, the century of plant breeding. Euphytica 186, 585–591.

Stoeckius, M., Hafemeister, C., Stephenson, W., Houck-Loomis, B., Chattopadhyay, P.K., Swerdlow, H., Satija, R., Smibert, P., 2017. Simultaneous epitope and transcriptome measurement in single cells. Nat. Methods. 14(9), 865-868.

Storkey, J., Macdonald, A.J., Poulton, P.R., Scott, T., Köhler, I.H., Schnyder, H., Goulding, K.W.T., Crawley, M.J., 2015. Grassland biodiversity bounces back from long-term nitrogen addition. Nature. 528(7582), 401-404.

Streeter, J.G., 1985. Nitrate Inhibition of Legume Nodule Growth and Activity. Plant Physiol. 77, 325–328.

Sugano, S., Jiang, C.J., Miyazawa, S.I., Masumoto, C., Yazawa, K., Hayashi, N., Shimono, M., Nakayama, A., Miyao, M., Takatsuji, H., 2010. Role of OsNPR1 in rice defense program as revealed by genome-wide expression analysis. Plant Mol. Biol. 74, 549–562.

Sun, J., Cardoza, V., Mitchell, D.M., Bright, L., Oldroyd, G., Harris, J.M., 2006. Crosstalk between jasmonic acid, ethylene and Nod factor signaling allows integration of diverse inputs for regulation of nodulation. Plant J. 46(6), 961-970.

Swain, P. S., Elowitz, M.B., Siggia, E.D., 2002. Intrinsic and extrinsic contributions to stochasticity in gene expression. Proc. Natl. Acad. Sci. 99, 12795–12800.

Tada, Y., Spoel, S.H., Pajerowska-Mukhtar, K., Mou, Z., Song, J., Wang, C., Zuo, J., Dong, X., 2008. Plant immunity requires conformational charges of NPR1 via S-nitrosylation and thioredoxins. Science. 321(5891), 952-956.

Takahashi, F., Mizoguchi, T., Yoshida, R., Ichimura, K., Shinozaki, K., 2011. Calmodulin-Dependent Activation of MAP Kinase for ROS Homeostasis in Arabidopsis. Mol. Cell 41, 649–660.

Takebe, I., Labib, G., Melchers, G., 1971. Regeneration of whole plants from isolated mesophyll protoplasts of tobacco. Naturwissenschaften 58, 318–320.

Tang, H., Krishnakumar, V., Bidwell, S., Rosen, B., Chan, A., Zhou, S., Gentzbittel, L., Childs, K.L., Yandell, M., Gundlach, H., Mayer, K.F.X., Schwartz, D.C., Town, C.D., 2014. An improved genome release (version Mt4.0) for the model legume Medicago truncatula. BMC Genomics 15, 1–14.

Tegeder, M., Masclaux-Daubresse, C., 2018. Source and sink mechanisms of nitrogen transport and use. New Phytol. 217, 35–53.

Thomma, B.P.H.J., Penninckx, I.A.M.A., Broekaert, W.F., Cammue, B.P.A., 2001. The complexity of disease signaling in Arabidopsis. Curr. Opin. Immunol. 13, 63–68.

Tian, D., Niu, S., 2015. A global analysis of soil acidification caused by nitrogen addition. Environ. Res. Lett. 10.

Tian, H., De Smet, I., Ding, Z., 2014. Shaping a root system: Regulating lateral versus primary root growth. Trends Plant Sci. 19, 426–431.

Tian, Q.Y., Sun, P., Zhang, W.H., 2009. Ethylene is involved in nitrate-dependent root growth and branching in Arabidopsis thaliana. New Phytol. 184(4), 918-931.

Timmers, A.C.J., Auriac, M.C., Truchet, G., 1999. Refined analysis of early symbiotic steps of the Rhizobium-Medicago interaction in relationship with microtubular cytoskeleton rearrangements. Development 126, 3617–3628.

Ton, J., Flors, V., Mauch-Mani, B., 2009. The multifaceted role of ABA in disease resistance. Trends Plant Sci. 14, 310–317.

Torres-Martínez, H.H., Hernández-Herrera, P., Corkidi, G., Dubrovsky, J.G., 2020. From one cell to many: Morphogenetic field of lateral root founder cells in Arabidopsis thaliana is built by gradual recruitment. Proc. Natl. Acad. Sci. U. S. A. 117, 20943–20949.

Toufighi, K., Brady, S.M., Austin, R., Ly, E., Provart, N.J., 2005. The botany array resource: e-Northerns, expression angling, and promoter analyses. Plant J. 43(1), 153-163.

Tsay, Y.F., Schroeder, J.I., Feldmann, K.A., Crawford, N.M., 1993. The herbicide sensitivity gene CHL1 of arabidopsis encodes a nitrate-inducible nitrate

transporter. Cell. 72(5), 705-713.

Tyerman, S.D., Whitehead, L.F., Day, D.A., 1995. A channel-like transporter for NH_4^+ on the symbiotic interface of N_2 fixing plants. Nature. 378(6557), 629-632.

Udall, J.A., Wendel, J.F., 2006. Polyploidy and crop improvement. Crop Sci. 46. S-3

Ullmann-Zeunert, L., Stanton, M.A., Wielsch, N., Bartram, S., Hummert, C., Svatoš, A., Baldwin, I.T., Groten, K., 2013. Quantification of growth-defense trade-offs in a common currency: Nitrogen required for phenolamide biosynthesis is not derived from ribulose-1,5- bisphosphate carboxylase/oxygenase turnover. Plant J. 75, 417–429.

Uroz, S., Courty, P.E., Oger, P., 2019. Plant Symbionts Are Engineers of the Plant-Associated Microbiome. Trends Plant Sci. 24(10), 905-916.

Valentine, A.J., Benedito, V.A., Kang, Y., 2018. Legume Nitrogen Fixation and Soil Abiotic Stress: From Physiology to Genomics and Beyond, Annual Plant Reviews online. 207-248

Van Baarlen, P., Woltering, E.J., Staats, M., Van Kan, J.A.L., 2007. Histochemical and genetic analysis of host and non-host interactions of Arabidopsis with three Botrytis species: An important role for cell death control. Mol. Plant Pathol. 8, 41–54.

Van der Hoorn, R.A.L., Kamoun, S., 2008. From Guard to Decoy: A New Model for Perception of Plant Pathogen Effectors. Plant Cell Online 20, 2009–2017.

Van Spronsen, P.C., Tak, T., Rood, A.M.M., Van Brussel, A.A.N., Kijne, J.W., Boot, K.J.M., 2003. Salicylic acid inhibits indeterminate-type nodulation but not determinate-type nodulation. Mol. Plant-Microbe Interact. 16(1), 83-91.

Venkateswarlu, B., Srinivasarao, C., Ramesh, G., Venkateswarlu, S., Katyal, J.C., 2007. Effects of long-term legume cover crop incorporation on soil organic carbon, microbial biomass, nutrient build-up and grain yields of sorghum/sunflower under rain-fed conditions. Soil Use Manag. 23, 100–107.

Verbelen, J.-P., Cnodder, T. De, Le, J., Vissenberg, K., Baluška, F., 2006. The Root Apex of Arabidopsis thaliana Consists of Four Distinct Zones of Growth Activities . Plant Signal. Behav. 1, 296–304.

Verma, V., Ravindran, P., Kumar, P.P., 2016. Plant hormone-mediated regulation of

stress responses. BMC Plant Biol. 16, 1–10.

Vernié, T., Kim, J., Frances, L., Ding, Y., Sun, J., Guan, D., Niebel, A., Gifford, M.L., de Carvalho-Niebel, F., Oldroyd, G.E.D., 2015. The NIN transcription factor coordinates diverse nodulation programs in different tissues of the medicago truncatula root. Plant Cell 27, 3410–3424.

Vidal, E.A., Araus, V., Lu, C., Parry, G., Green, P.J., Coruzzi, G.M., Gutiérrez, R.A., 2010. Nitrate-responsive miR393/AFB3 regulatory module controls root system architecture in Arabidopsis thaliana. Proc. Natl. Acad. Sci. *107*(9), 4477-4482.

Von Wirén, N., Gazzarrini, S., Gojon, A., Frommer, W.B., 2000. The molecular physiology of ammonium uptake and retrieval. Curr. Opin. Plant Biol. 3, 254–261.

Von Wittgenstein, N.J.J.B., Le, C.H., Hawkins, B.J., Ehlting, J., 2014. Evolutionary classification of ammonium, nitrate, and peptide transporters in land plants. BMC Evol. Biol. 14(1), 1-17.

Waara, S., Glimelius, K., 1995. The potential of somatic hybridization in crop breeding. Euphytica. 85(1), 217-233.

Walch-Liu, P., Ivanov, I.I., Filleur, S., Gan, Y., Remans, T., Forde, B.G., 2006. Nitrogen regulation of root branching. Ann. Bot. 97, 875–881.

Wang, Y.Y., Hsu, P.K., Tsay, Y.F., 2012. Uptake, allocation and signaling of nitrate. Trends Plant Sci. 17, 458–467.

Ward, B.B., 2013. How nitrogen is lost. Science. 341(6144), 352-353.

Ward, W.W., Bokman, S.H., 1982. Reversible Denaturation of Aequorea Green-Fluorescent Protein: Physical Separation and Characterization of the Renatured Protein. Biochemistry 21, 4535–4540.

Wasternack, C., Hause, B., 2013. Jasmonates: Biosynthesis, perception, signal transduction and action in plant stress response, growth and development. An update to the 2007 review in Annals of Botany. Ann. Bot. 111, 1021–1058.

Weber, S., Horn, R., Friedt, W., 1998. User-Developed Protocol : Isolation of plasmid DNA from Agrobacterium using the QIAprep ® Spin Miniprep Kit ; spin

procedure 11–12.

Whalen, M.C., Innes, R.W., Bent, A.F., Staskawicz, B.J., 1991. Identification of Pseudomonas syringae pathogens of Arabidopsis and a bacterial locus determining avirulence on both Arabidopsis and soybean. Plant Cell 3, 49–59.

Wibowo, A., Becker, C., Durr, J., Price, J., Staepen, S., Hilton, S., Putra, H., Papareddy, R., Saintain, Q., Harvey, S., Bending, G.D., Schulze-Lefert, P., Weigel, D., Gutierrez-Marcos, J., 2018. Incomplete reprogramming of cell-specific epigenetic marks during asexual reproduction leads to heritable phenotypic variation in plants. bioRxiv 267955.

Widmann, C., Gibson, S., Jarpe, M.B., Johnson, G.L., 1999. Mitogen-activated protein kinase: Conservation of a three-kinase module from yeast to human. Physiol. Rev. 79(1), 143-180.

Wienkoop, S., Baginsky, S., Weckwerth, W., 2010. Arabidopsis thaliana as a model organism for plant proteome research. J. Proteomics 73, 2239–2248.

Wilmington, S.R., Matouschek, A., 2016. An inducible system for rapid degradation of specific cellular proteins using proteasome adaptors. PLoS One. 11(4), e0152679.

Wilson, C., Tisdell, C., 2001. Why farmers continue to use pesticides despite environmental, health and sustainability costs. Ecol. Econ. 39(3), 449-462.

Winter, D., Vinegar, B., Nahal, H., Ammar, R., Wilson, G. V., Provart, N.J., 2007. An "electronic fluorescent pictograph" Browser for exploring and analyzing large-scale biological data sets. PLoS One. 2(8), e718.

Wirth, J., Chopin, F., Santoni, V., Viennois, G., Tillard, P., Krapp, A., Lejay, L., Daniel-Vedele, F., Gojon, A., 2007. Regulation of root nitrate uptake at the NRT2.1 protein level in Arabidopsis thaliana. J. Biol. Chem. 282(32), 23541-23552.

Wittenberg, J.B., Bergersen, F.J., Appleby, C.A., Turner, G.L., 1974. Facilitated oxygen diffusion. The role of leghemoglobin in nitrogen fixation by bacteroids isolated from soybean root nodules. J. Biol. Chem. 249(13), 4057-4066.

Wong, P.P., 1988. Inhibition of legume nodule formation and n2 fixation by nitrate. CRC. Crit. Rev. Plant Sci. 7, 1–23.

Wu, F.H., Shen, S.C., Lee, L.Y., Lee, S.H., Chan, M.T., Lin, C.S., 2009. Tape-arabidopsis sandwich - A simpler arabidopsis protoplast isolation method. Plant Methods 5, 1–10.

Xie, Q., Frugis, G., Colgan, D., Chua, N.H., 2000. Arabidopsis NAC1 transduces auxin signal downstream of TIR1 to promote lateral root development. Genes Dev. 14(23), 3024-3036.

Xie, Q., Guo, H.S., Dallman, G., Fang, S., Weissman, A.M., Chua, N.H., 2002. SINAT5 promotes ubiquitin-related degradation of NAC1 to attenuate auxin signals. Nature. 419(6903), 167-170.

Xin, X.-F., He, S.Y., 2013. *Pseudomonas syringae* pv. *tomato* DC3000: A Model Pathogen for Probing Disease Susceptibility and Hormone Signaling in Plants. Annu. Rev. Phytopathol. 51, 473–498.

Yang, D.L., Yao, J., Mei, C.S., Tong, X.H., Zeng, L.J., Li, Q., Xiao, L.T., Sun, T.P., Li, J., Deng, X.W., Lee, C.M., Thomashow, M.F., Yang, Y., He, Z., He, S.Y., 2012. Plant hormone jasmonate prioritizes defense over growth by interfering with gibberellin signaling cascade. Proc. Natl. Acad. Sci. 109(19), E1192-E1200.

Yang, J., Xie, X., Xiang, N., Tian, Z.X., Dixon, R., Wang, Y.P., 2018. Polyprotein strategy for stoichiometric assembly of nitrogen fixation components for synthetic biology. Proc. Natl. Acad. Sci. 115(36), E8509-E8517.

Young, N.D., Debellé, F., Oldroyd, G.E.D., Geurts, R., Cannon, S.B., Udvardi, M.K., Benedito, V.A., Mayer, K.F.X., Gouzy, J., Schoof, H., Van De Peer, Y., Proost, S., Cook, D.R., Meyers, B.C., Spannagl, M., Cheung, F., De Mita, S., Krishnakumar, V., Gundlach, H., Zhou, S., Mudge, J., Bharti, A.K., Murray, J.D., Naoumkina, M.A., Rosen, B., Silverstein, K.A.T., Tang, H., Rombauts, S., Zhao, P.X., Zhou, P., Barbe, V., Bardou, P., Bechner, M., Bellec, A., Berger, A., Bergès, H., Bidwell, S., Bisseling, T., Choisne, N., Couloux, A., Denny, R., Deshpande, S., Dai, X., Doyle, J.J., Dudez, A.M., Farmer, A.D., Fouteau, S., Franken, C., Gibelin, C., Gish, J., Goldstein, S., González, A.J., Green, P.J., Hallab, A., Hartog, M., Hua, A., Humphray, S.J., Jeong, D.H., Jing, Y., Jöcker, A., Kenton, S.M., Kim, D.J., Klee, K., Lai, H., Lang, C., Lin, S., MacMil, S.L., Magdelenat, G., Matthews, L., McCorrison, J., Monaghan, E.L., Mun, J.H., Najar, F.Z., Nicholson, C., Noirot, C., O'Bleness, M., Paule, C.R., Poulain, J., Prion, F., Qin, B., Qu, C., Retzel, E.F., Riddle, C., Sallet, E., Samain, S., Samson, N., Sanders, I., Saurat, O., Scarpelli, C., Schiex, T., Segurens, B., Severin, A.J., Sherrier, D.J., Shi, R., Sims, S., Singer, S.R., Sinharoy, S., Sterck, L., Viollet, A., Wang, B.B., Wang, K., Wang, M., Wang, X., Warfsmann, J., Weissenbach, J., White, D.D., White, J.D., Wiley, G.B., Wincker, P., Xing, Y., Yang, L., Yao, Z., Ying, F., Zhai, J., Zhou, L., Zuber, A., Dénarié, J., Dixon, R.A., May, G.D., Schwartz, D.C., Rogers, J., Quétier, F., Town, C.D., Roe, B.A., 2011. The Medicago genome provides insight into the evolution of rhizobial symbioses. Nature 480,

520–524.

Yu, X., Sukumaran, S., Márton, L., 1998. Differential Expression of the Arabidopsis Nia1 and Nia2 Genes: Cytokinin-Induced Nitrate Reductase Activity Is Correlated with Increased Nia1 Transcription and mRNA Levels. Plant Physiol. 116, 1091–1096.

Yu, Z., Boehm, C.R., Hibberd, J.M., Abell, C., Haseloff, J., Burgess, S.J., Reyna-Llorens, I., 2018. Droplet-based microfluidic analysis and screening of single plant cells. PLoS One. 13(5), e0196810.

Zaidi, S.S. e. A., Mukhtar, M.S., Mansoor, S., 2018. Genome Editing: Targeting Susceptibility Genes for Plant Disease Resistance. Trends Biotechnol. 36(9), 898-906.

Zhang, H., Forde, B.G., 1998. An Arabidopsis MADS box gene that controls nutrient-induced changes in root architecture. Science. 279(5349), 407-409.

Zhang, H., Jennings, A., Barlow, P.W., Forde, B.G., 1999. Dual pathways for regulation of root branching by nitrate. Proc. Natl. Acad. Sci. U. S. A. 96, 6529–6534.

Zhang, T., Liu, Y., Yang, T., Zhang, L., Xu, S., Xue, L., An, L., 2006. Diverse signals converge at MAPK cascades in plant. Plant Physiol. Biochem. 44, 274–283.

Zheng, M.S., Takahashi, H., Miyazaki, A., Yamaguchi, K., Kusano, T., 2005. Identification of the cis-acting elements in Arabidopsis thaliana NHL10 promoter responsible for leaf senescence, the hypersensitive response against Cucumber mosaic virus infection, and spermine treatment. Plant Sci. 168, 415–422.

Zhou, Y., Zhu, H., Fu, S., Yao, Q., 2017. Variation in soil microbial community structure associated with different legume species is greater than that associated with different grass species. Front. Microbiol. 8, 1007.

Zhu, T., Wang, X., 2000. Resources and Opportunities Large-Scale Profiling of the Arabidopsis Transcriptome. Society 124, 1472–1476.

Zipfel, C., Robatzek, S., Navarro, L., Oakeley, E.J., Jones, J.D.G., Felix, G., Boller, T., 2004. Bacterial disease resistance in Arabidopsis through flagellin perception. Nature 428, 764–767.